The application of multivariate correlation techniques to vehicle driveability analysis

Pickering, Simon Gideon

Award date:
2005

Awarding institution:
University of Bath

The Application of Multivariate Correlation Techniques to Vehicle Driveability Analysis

Simon Gideon Pickering

A thesis submitted for the degree of Doctor of Philosophy

University of Bath

Department of Mechanical Engineering

October 2005

ProQuest LLC
789 East Eisenhower Parkway
P.O. Box 1346
Ann Arbor, MI 48106-1346

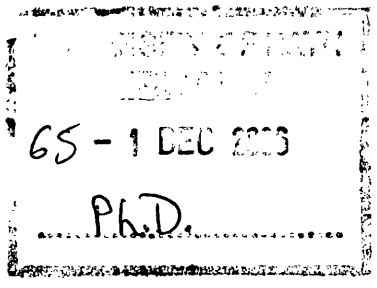
65 - 1 DEC 2003
Ph.D.

i. Table of contents

ii. List of figures

iii. List of tables

iv. Acknowledgements

Dr. C.J. Brace, Prof. N.D. Vaughan, Dr. S. Akehurst for their technical help and support during the project.

V. Rajput for his work on the CADET V12 data acquisition system and vehicle instrumentation. D.R. Blake for his assistance with the test vehicles.

CP Engineering for hardware and software components for the CADET V12 data acquisition system and for their help and support while building and setting up the system

Ricardo Consulting Engineers for the loan of the Prius test vehicle.

RAF Colerne for kindly allowing testing to take place there.

Chris Cochrane, final year Automotive Engineering student, for his help with the initial calibration and testing of the AT Mondeo vehicle.

v. Summary

The aim of the research described in this thesis was to investigate the application of multivariate correlation techniques to driveability analysis. Vehicle driveability is difficult to quantify in an objective sense as it is based on a driver's subjective rating of a vehicle. The ability to predict the subjective driveability rating for a vehicle using only objective metrics such as acceleration, jerk and throttle demand would allow manufacturers to calibrate vehicle powertrains far faster than is presently possible. It would also allow greater scope for vehicle characterisation and allow simultaneous emissions, economy and driveability constraints to be met more easily when performing powertrain calibration.

This thesis presents a methodology for identifying correlations between subjective ratings and objective driveability data. It describes various techniques available to perform multivariate correlations and explains the author's choice to use regression techniques. Computer code used to automate the correlation process is described and the results of using both simple single variable and multivariate regression techniques to analyse longitudinal driveability are presented.

The thesis describes in-vehicle acquisition of subjective and objective driveability data from a Toyota Prius hybrid petrol-electric car and an Automatic Transmission (AT) equipped Ford Mondeo, and the development of a next-generation data acquisition system and its use in testing an AT equipped Ford Mondeo. Two groups, of seven and twelve drivers, tested the Prius and AT Mondeo vehicles respectively. Each driver performed a set of 16 tests. Each test had a specified initial speed and a specified pedal position that the driver would attain in a step fashion after the specified initial speed had been attained. The following objective data were recorded during these tests: vehicle speed, vehicle acceleration, pedal position and engine speed. After each test the driver was asked for their subjective opinion of a range of subjective performance and driveability metrics. These data were then used to establish correlations between subjective and objective longitudinal driveability metrics.

This research has developed the ability to reliably automate the difficult process of producing metrics that describe vehicle driveability characteristics. In particular, automation has been developed for the previously manual tasks of pedal movement, acceleration and gear-shift detection across a range of manoeuvres. This research has shown that driveability predictions can be produced by automated multivariate correlation techniques, even with a relatively small and noisy dataset collected from untrained test-drivers. This research has confirmed the positive correlations between maximum acceleration and driveability rating as well as the negative correlation between maximum initial jerk and driveability rating as found in the scientific literature.

vi. List of abbreviations

Ah	Amp-hours
AT	Automatic Transmission
AMT	Automated Manual Transmission
CAN	Control Area Network – a standard bus configuration and protocol used in automobiles.
CVT	Continuously Variable Transmission
DAQ	Data Acquisition
DC	Direct Current
DOE	Design Of Experiments
ECU	Electronic Control Unit
g	Acceleration due to gravity (approx. 9.81m/s^2).
IC	Internal Combustion
IOL	Ideal operating line
kph	Kilometres per hour
Kbytes	Kilobyte
LS	Least Squares. A curve fitting method
LWS	Least Weighted Squares. A robust least-squares based curve fitting method that is less skewed by outlying data points than the least-squares method.
Mbit	Megabit
MT	Manual Transmission
NaN	Not A Number. Computational representation of a failed calculation
NVH	Noise Vibration Harshness
OBD	On-Board Diagnostics
OEM	Original Equipment Manufacturer
PAS	Power Assisted Steering
R	Correlation Coefficient
rpm	Revolutions per minute. Measure of engine speed
s	Seconds
SVD	Single Value Decomposition
ULEV	Ultra Low Emissions Vehicle
V	Volts

vii. Glossary

Auto-correlation – In this context, this is the description given to the process of determining the correlation produce by testing a regression equation using the data that were used to generate it.

Calibration – The process of populating the data set used by an electronic control unit with values appropriate to give the required system performance.

Colerne – RAF Colerne. Airfield used for vehicle testing.

Driveability – How a vehicle responds to a driver's demands and how its response coincides with their expectations

Driveability calibration – the process of calibrating and tuning a vehicle powertrain (engine and gearbox combination) to produce good driveability.

Driveline shuffle – longitudinal oscillations in the vehicle driveline

Engine speed overflow event – This is the name given to an error produced by the interaction between a poorly calibrated pulse counting system that causes the engine speed to be reported as being lower than it actually is. In this research the error affected some engine speed data. The effect is that once the engine speed rises above a certain value, it overflows, which results in a lower value and then continues moving normally from there. The converse happens once the engine speed falls though the value at which the overflow occurred. This error and its correction are described in Section 5.3.2.4.

Gear Hunting – Repeated and rapid up and down gear-shifts between two gear ratios. This is often caused by poor calibration of the gear-shifting strategy, which causes a down-shift to be triggered as soon as an up-shift occurs and vice versa.

Jerk – rate of change of acceleration. In the context of this research, jerk is specifically the initial rate of change of acceleration, which occurs at the start of a tip-in manoeuvre. The word jerk is often used to describe a negative aspect of performance, such as driveline shunt or poorly timed clutch engagement, which causes oscillatory movements in the vehicle. However, in this research, jerk is the name given to the initial rate of change of

acceleration. This is considered a positive aspect of performance giving an indication of the speed with which the acceleration builds.

Metric – a single measure, which is used to represent a trend or other important event in a large body of data.

Objective measurements – Measurements that are not subject to interpretation and that are measured using instrumentation. These include measurements such as acceleration, vehicle speed and pedal position.

Powertrain – the combination of components that transfer the engine power to the road wheels of a vehicle. This comprises the engine, gearbox and the various drive-shafts.

Quirk – rate of change of jerk (Quadrant Scientific, 1989; Balich, 2004).

Steady state operation – Operation of an engine/powertrain at a constant throttle opening.

Subjective measurements – Measurements that cannot or are not measured using instrumentation, but instead are evaluated by the test driver based on his or her experience of driving the vehicle.

Tip In – A rapid increase in accelerator pedal position.

Tip Out – A rapid reduction in accelerator pedal position.

Traffic crawl – Low speed and small pedal position manoeuvres.

Transient operation – Operation of an engine/powertrain with a varying throttle position.

1 Introduction

Vehicle driveability is difficult to quantify as it is based on a driver's subjective rating of a vehicle's objective performance. The ability to predict the subjective driveability rating for a vehicle using only objective metrics such as acceleration, jerk and throttle demand would allow manufacturers to calibrate vehicle powertrains far faster than is presently possible. It would also allow greater scope for vehicle characterisation and allow simultaneous emissions, economy and driveability constraints to be met more readily when performing powertrain calibration.

The research described in this thesis investigated the use of multivariate correlation techniques for the analysis and prediction of various subjective vehicle driveability ratings. It presents a methodology for identifying correlations between subjective ratings and objective driveability data, describes various techniques available to perform multivariate correlations, and explains the author's choice of regression techniques. Code used to automate the correlation process is described and the results of using both simple single variable and multivariate regression techniques to analyse longitudinal driveability are presented.

The thesis details the in-vehicle acquisition of subjective and objective driveability data from a Toyota Prius hybrid petrol-electric car and the development of a next-generation data acquisition system and its use in testing an AT equipped Ford Mondeo. The data acquired by the author is combined with data collected during a previous research project (Wicke, 2001) to develop a set of automated correlation routines. This data is used as a test set while implementing and testing this correlation code and includes data collected from five vehicles from Wicke's project as well as additional sets of data collected during this project.

The factors influencing the driveability of both CVT and AT equipped vehicles are examined and the thesis reviews the chequered history of CVT powertrain development and looks at how the use of techniques developed in this project may be used to overcome these problems.

Testing the Toyota Prius hybrid petrol-electric vehicle, one of the first production Ultra Low Emissions Vehicles (ULEV), provided additional driveability data with which to test the correlation code while illustrating the strengths and weaknesses of hybrid vehicles. With the projected growth of ULEV, a knowledge and understanding of the technologies involved and their subjective appraisal by drivers opens up further avenues for research.

Multivariate correlation and prediction techniques provide the potential to be used in the optimisation of motor vehicle driveability by being applied at the powertrain design stage to predict driveability during simulation, as well as predicting driveability for test-rig engines and powertrains. These driveability prediction techniques may also be applied to powertrains when integrated into vehicles for in-vehicle calibration. These different areas of application provide a wide scope for the future direction of this research.

1.1 Aims of the research

The overall aim of the research described in this thesis was to investigate the application of multivariate correlation techniques to longitudinal automobile driveability analysis. Multivariate correlation techniques were investigated and a multivariate correlation code was developed with the goal of enabling the prediction of subjective driveability ratings from objective metrics.

In combination with the development of a multivariate correlation code, the data pre-processing, data correction and metric generation tasks associated with the analysis of driveability data were investigated and automated. The goal of this automation was to allow real-time driveability predictions to be made without requiring human intervention. This was carried out to allow the entire process of driveability testing to be performed in a faster and more repeatable fashion.

The subjective rating and objective vehicle driveability data collected during this project along with data available at the University from previous projects were processed to produce objective metrics and analysed using the multivariate techniques developed during this research to determine important correlations between the subjective driveability ratings and objective metrics.

The current research was originally to be a continuation of the work carried out by Wicke (2001). This work was to investigate the driveability prediction and optimisation of a CVT powertrain, using the test data that had been acquired during previous projects at the University, as well as data collected during this research. Unfortunately, due to the loss of use of the experimental CVT vehicle, the project focus was changed to look at powertrain driveability analysis with the goal of using this research as a basis for further optimisation of CVT powertrain driveability. One of the research vehicles that was tested during this research was a AT vehicle which produced a range of gearshifts from good to very poor quality due to the fact that the gearbox had been replaced. Therefore it was decided that gear-shift metrics would be collected from this vehicle in addition to the standard driveability data.

1.2 Summary of chapters

This thesis contains the following chapters:

Chapter 1 contains an introduction to the aims and objectives of the thesis and a summary of the chapter contents.

Chapter 2 introduces the concept of vehicle driveability assessment and presents research that has been carried out in this field. Various aspects of powertrain driveability calibration are introduced including those specific to ATs and CVTs.

Chapter 3 describes the test equipment that was used in this research. This includes the data acquisition (DAQ) equipment that was initially used in this project and the subsequent development and implementation of the new CADET V12 DAQ system to address the shortcomings of the original system and enable future expansion. The vehicle sensors, the test facilities, the vehicles and the test-drivers who took part in this project are described.

Chapter 4 describes the development of the methodology of the testing program, and describes some problems that occurred during the testing stages. The specific driveability testing methods are described, as are the subjective and objective data that were recorded.

Chapter 5 describes the aims and methods of automated metric generation as well as describing the metrics employed in this research. The automated methods used to produce the metric data (for example gearshift detection, pedal movement and acceleration start, and delay time calculation) are described and illustrated. Methods that were implemented to correct or remove poorly calibrated or faulty data are described.

In *Chapter 6,* the application of correlation techniques to driveability is introduced and the possible methods are described. The choice of regression techniques is justified and the various fitting and rating methods for these equations are explained. Outlier detection and other data pre-processing techniques that are required to ensure good correlations are described. The evolution of the regression technique is described from single variable through to the full multivariate techniques. The methods for forming a multivariate equation are evaluated and the reasoning behind the choice of the particular method used in this research is described.

In *Chapter 7,* the subjective and objective metric data are analysed to determine any interesting trends before the correlations are performed. The subjective and objective metrics are correlated with themselves to determine the degree of redundancy in the metrics. The data from the different vehicles, initial speeds and initial pedal positions are analysed. The results of the initial single-variable correlation stages of this project are presented.

Chapter 8 covers the application of the multivariate technique to driveability calibration. This Section introduces possible applications for the multivariate correlation equations that have been generated. These include applying the correlations to achieve vehicle characterisation and test-bed calibration.

Chapter 9 presents the results of the application of the multivariate correlation techniques to the data collected during this and previous work at the University of Bath. The data trends and equation metrics found in the multivariate correlation equations are analysed.

Chapter 10 presents a discussion and commentary on aspects of the research to assist any researcher attempting to implement the results or continue with this avenue of development.

Finally, *Chapter 11* presents the conclusions of the research that has formed the subject of this thesis, along with a discussion of further research that may be carried out to continue this project.

2 Powertrain driveability and calibration

The automotive market place is highly competitive with manufacturers under pressure to develop new vehicles as quickly and cost-effectively as possible and it is during the powertrain development phase that driveability prediction techniques, the subject of this thesis, can play a major role in speeding vehicle development.

The modern motor car has developed so rapidly that even a basic vehicle now has levels of performance and driveability that were available only to the drivers of premium motor cars a decade ago. Drivers have become used to having a wide choice of well developed vehicles available to them and are unwilling to accept poor vehicle driveability and performance, not merely relating to maximum speed or acceleration, but also the behaviour of the vehicle through all of its operating regimens: warm-up, idle, engine start overshoot, tip-ins and pull away to name but a few (List & Schoeggl 1998; Dorey & Martin, 2000).

The majority of the factors affecting a purchase decision may be viewed objectively, and thus comparisons readily made between competing products without the need to drive the vehicle, however it is the subjective driveability performance that must match the expectations of the driver once all the objective considerations have been satisfied.

2.1 Driveability

There are a large number of facets that make up 'vehicle driveability'. The research described in this thesis involved the investigation of longitudinal driveability – that is only those parts of driveability that are related to the powertrain and its performance. Engine calibration and control strategy, and gearshift performance and strategy are aspects of vehicle calibration that directly affect longitudinal driveability. There are other areas of driveability such as engine start-up and warm-up behaviour and handling that are also aspects of 'driveability' (Dorey & Martin, 2000; List & Schoeggl, 1998) but are not within the scope of this project.

Driveability, in all its forms, is a difficult term to define objectively because it depends on the driver's perception of the vehicle and is therefore very much a subjective measure. How a driver perceives the performance and general feeling of the vehicle depends on many factors, including their expectations of the vehicle and situation in which they are driving, the vehicle that they are most used to driving, and previous experience of other vehicles as well as natural driver variation. This may result in different drivers rating the driveability of the same vehicle in different ways depending on their preferences and experience. List and Schoeggl (1998) carried out research into vehicle driveability with the aim of reducing the time required to calibrate the vehicle powertrain. Psychophysical questions were posed as to what a driver is able to feel of vehicle driveability performance, including what objective data (such as acceleration) should be recorded and to what degree of accuracy, how a driver's senses are combined when rating a manoeuvre, and which aspects of a manoeuvre are the most important and how are they weighted.

When collecting data, human psychophysical abilities should be considered, such as what level of different objective measurements (e.g. acceleration, jerk) a driver can actually detect and differentiate between. The manipulation of these factors holds promise for vehicle characterisation. It is known that the human senses can be fooled by specific acceleration profiles, for example this effect is used to make commercial flight simulation using motion simulators feel realistic to pilots (Reid & Nahon, 1988). The use of this information when

performing driveability calibration may enable the production of vehicles that subjectively appear to have better performance that would be assessed in a purely objective sense.

The determination of human sensitivity levels to acceleration and other objective measurements that affect driveability would also enable testing manoeuvres to be targeted to produce human-detectable vehicle responses and would allow the priority of calibrating specific vehicle driveability responses to be weighted according to relative levels of human perception. A large amount of research has been carried out determining human perception levels and measurement techniques for acceleration and velocities by both the military and aerospace industries (e.g. Reid & Nahon, 1988; USAF School of Aerospace Medicine). A large number of medical papers have also been published concerning the use of acceleration perception as a method of measuring the abilities of the vestibular system of the inner ear (e.g. Kingma, 2005). The building industry also has a great interest in the determination of human acceleration perception levels to ensure that tall buildings are not uncomfortable for their occupants. For example, a paper by Berglund (1991) puts this perception threshold at 0.005g. Although not directly related to longitudinal driveability, a number of papers have been published concerning human perceptual response for a variety of automotive related subjects including Diesel engine NVH (Ajovalasit & Giacomin, 2005), clutch actuation (Giacomin & Bretin, 1997), gearshift loads (Giacomin & Mackenzie, 2001) and steer-by-wire perception enhancement (Giacomin, 2005). These are all factors that will affect overall subjective driveability.

Simplistically the spectrum of driveability might be split into two ends of a spectrum of driver expectation: comfort and performance, as illustrated by List & Schoeggl (1998) and Schoeggl et al. (2001). This simplistic view serves to illustrate the point that different people have different expectations as to what constitutes "good driveability". The difference in their expectations means that different vehicles are optimised for different driving styles by making their driveability characteristics suit the target driver. Schoeggl et al. (2001) describe the process of developing a system to be used to deduce a driver's driving style automatically. They used a variety of objective metrics to produce the following metrics for a driver's driving style: sportiness, comfort, aggressiveness, nervousness, alertness, skill, economy and talent. They examined a large number of subjective questionnaires and objective datasets and produced a computer-aided evaluation that they state is able to reproduce the driver evaluations to a high degree of accuracy. The exact methods and metrics that were used are not mentioned in the paper, most probably due to the fact that these papers were written by employees of AVL LIST, a commercial company which sells these products. Dorey et al. (1999, 2000) also mention the fact that there are different

expectations for different classes of vehicle. For example, a typical Mercedes S-class driver (luxury car) would most probably have different driveability expectations to the typical Renault Clio driver (hatchback) or Lotus Elise driver (sports car).

2.1.1 Previous driveability correlation analyses

The research discussed by Dorey et al. (Dorey & Holmes, 1999; Dorey & Martin, 2000) introduces a driveability analysis system and mentions the use of multivariate techniques. These papers, however, show only plots of single objective metrics against single subjective metrics. The research presented in these papers concerns a number of aspects of driveability, one of which is tip-in manoeuvres. In these works a number of objective metrics are used. These are acceleration overshoot, natural frequency, damping ratio, rise rate and rise time. Dorey et al. found that acceleration overshoot and rise rate had a strong effect on the rating of vehicle driveability.

These single variable correlations are similar to those employed by Wicke et al. (1999, 2000) and Wicke (2001) in the analysis of driveability of a mixture of CVT and AT equipped vehicles. Wicke found correlations between objective acceleration delay time (the time between the accelerator pedal depression and vehicle acceleration beginning) and subjective launch feel rating. He also found correlations between objective delay time and subjective performance feel, and objective initial jerk and subjective performance feel.

List and Schoeggl (1998) mention their use of multi-dimensional correlation techniques in their driveability analysis, which is again concerned with a number of driveability manoeuvres amongst which are tip-in manoeuvres. The multi-dimensional techniques were applied to a broad range of vehicle performance metrics in concert with neural networks to simulate a human's subjective reaction. It appears that the main part of the work concerned the use of neural networks rather than regression equations. It should be noted that in a later paper from Schoeggl et al. (2002) it is stated that the values of the subjective metrics had to be limited to those "better than 7" to obtain good overall results for the predictions of the modelling and optimisation that they present. This appears to indicate that it is only the very strong positive trends that show clear correlations.

Crolla et al. (1998) show the use of multivariate regression techniques to the analysis of subjective handling data. They show that mean subjective ratings for drivers with similar skill levels tend to vary. They also show good correlations for the ratings that they performed, however they state that the interpretation of these correlations is unclear.

2.1.2 Driveability rating

Currently, vehicle driveability assessment is carried out by teams of experienced calibration engineers whose subjective opinions of good driveability are used to produce a vehicle calibration that is deemed acceptable. There are issues with this approach. Firstly, the calibrations produced by these engineers are based on their subjective opinions and therefore will have limited repeatability. There are also differences between customers' driveability requirements, which a group of calibration engineers may not be able to reproduce due to their specific training and experiences. This means that they may not repeatably produce optimum calibrations for all of the driving styles that might be necessary.

The calibration engineers and experienced test drivers then drive these test vehicles in a general driving procedure, which tests overall driving aspects, as well as performing set manoeuvres to test specific powertrain responses (Dorey & Martin, 2000). The test drivers and calibration engineers then decide on changes that need to be made to the calibration of the powertrains to improve vehicle driveability. This usually results in the changes being applied to test-rig engines that again attempt to optimise emissions and economy before the engine is returned to the calibration engineer to assess whether the improvement in driveability has been achieved.

This time consuming and costly process is subject to limited repeatability due to the subjective nature of the testing (List & Schoeggl, 1998; Dorey & Holmes, 1999). It also requires skilled calibration engineers and test drivers who are a limited resource as well as the availability of suitable weather conditions (or locations with such conditions) in which to perform climate-specific calibration.

Each driveability aspect is given a rating, often on a scale from 0 to 10 (List & Schoeggl, 1998. Dorey & Holmes, 1999), that denotes how good or bad a certain aspect seemed to the driver. It should be noted that in some cases, such as in the paper by Schoeggl et al. (2001), the driveability scale appears to rate whether negative aspects are noticed by the vehicle driver, taking no account of positive effects that may be produced by particular aspects of the vehicle calibration. This is based on List and Schoeggl's (1998) finding that the weighting of negative aspects is greater than for positive aspects when drivers consider vehicle driveability.

Inevitably, given the human factor, the determination of a subjective rating is prone to scatter even with just one driver, let alone with different groups of drivers, and this makes the task of developing reliable correlation methods very difficult. In a research context, a smaller

number of drivers with similar driving backgrounds and experiences may be used to reduce the scatter in the collected data. This can facilitate the establishment of an effective testing methodology and more easily determine possible underlying trends that should be studied in testing performed by representative drivers.

This requires the development of automated driveability prediction techniques, which have been investigated by a number of researchers (List & Schoeggl, 1998; Dorey & Holmes, 1999; Wicke et al., 1999). Being able to quantify driveability objectively offers the ability to set driveability targets in the same way as targets for fuel consumption and emissions production are currently set.

Although general driveability prediction for calibration would produce large cost and time benefits when applied early in the calibration process, it is also envisioned that these techniques could be applied later in the process to perform vehicle characterisation and fine-tuning for more specific manoeuvres. Manufacturers' vehicles are often calibrated to produce specific transient powertrain characteristics for particular vehicle classes and markets (Dorey & Martin, 2000), whether this is by design or due to the small number of test-driver/calibration engineers, the form of these traits and characteristics could be captured and then applied to vehicles automatically. The copying of driveability characteristics is not only open to a single manufacturer – it is equally possible that competing manufacturers could characterise the traits of competitors' vehicles that have been found to produce good driveability ratings.

2.1.3 Driveability test selection and data collection

Due to the wide variety of aspects of driveability there are many ways in which to measure a vehicle's driveability. Dorey & Holmes (1999) and Dorey & Martin (2000) describe the methods they used to perform some of their driveability testing. Some of the tests that they performed were concerned with 'engine start' driveability and engine idle response due to accessory loads (power assisted steering (PAS), and air-conditioning systems). Of more interest to this project were their general driveability tests, which consisted of the drivers performing a variety of manoeuvres including tip-in and back-out manoeuvres. For these tests, acceleration 'jolts' (overshoot) and oscillations were measured.

Jansz et al. (1999), who were performing longitudinal acceleration calibration, performed a variety of tip-ins manoeuvres from which they measured and tried to minimise acceleration overshoot and oscillations to improve the driveability of the Ford Focus.

The papers from Dorey et al. (1999, 2000) and Jansz et al. (1999) do not mention the number of drivers or test repetitions that were performed. List and Schoeggl (1998) do state that around 250 test results were used in the training of their neural network system, however they do not mention whether these tests were carried out by the same, or different drivers. In their 2001 paper, Schoeggl et al. were able to collect a vast amount of data by situating a driving simulator at a regional exhibition. They collected data from approximately 13,000 visitors, whom it can be assumed were not highly trained.

Objective and subjective data collection techniques have also been applied to vehicle handling research since the 1990s. Research by Chen et al. (1997) on the collection of vehicle handling data used eight trained drivers to perform the testing. Farrer (1993) deals with the establishment of an objective measurement technique for on-centre handling quality. Whitehead et al. (1998) present a case study of how subjective data acquisition was performed for a research project correlating subjective driver ratings with objective vehicle handling data. One of the aspects discussed in these papers is the size of the test panel and whether a technical background is advantageous or not. Ideally there should be large numbers of drivers with a range of ages, skill levels and vehicle handling backgrounds, however, due to the technical nature of these projects and time constraints, they used six (Farrer) and eight (Whitehead) test drivers respectively. All of these drivers had a technical background, which was required due to the demands of carrying out the handling tests while considering the questionnaire.

2.1.4 Driveability metric selection

The subjective rating data provided by test drivers are used in conjunction with objective data that are simultaneously recorded during the test. The typical format of subjective and objective data sets is very different meaning that the data sets must be processed to allow a correlation analysis.

2.1.4.1 Subjective metrics

Obtaining useful subjective ranking data can be difficult because of its subjective nature. A significant amount of research has been carried out on vehicle handling, using a variety of rating scales (Weir & DiMarco, 1978; Sano et al. 1980; Farrer, 1994; Chen et al., 1997). These scales range from having five to 10 increments, with a variety of descriptive labels used to help the drivers decide on the appropriate rating. Crolla et al. from the University of Leeds have published a number of papers (1997, 1998, 2000) describing methods of performing subjective and objective vehicle handling assessment. Although driveability in

these reports refers to longitudinal aspects, their methods have some bearing on the acquisition of subjective data in general.

For some of their testing, a vehicle with adjustable handling calibration was ranked against a control vehicle in a relative rather than absolute fashion. The adoption of such a testing scheme for longitudinal driveability should reduce the effect of a test driver's previous driving experience on their ranking of the test vehicle.

Bergman (1973) notes the difficulties of getting drivers to use the full range of a rating scale, and also that drivers with similar skill levels may rate a vehicle differently. Chen et al. (1997) and Crolla et al. (1998) discuss the advantages and disadvantages of various different questionnaire designs. They discuss the fact that getting drivers to use the full range of a rating scale is difficult; that the use of adjectival ratings (e.g. good, better, worse) rather than, or in addition to, numeric ratings is easier for test drivers to understand and that despite drivers having similar skill levels, they often rate a given manoeuvre differently. This latter point appears to be related to the fact that different drivers may like different aspects of vehicle driveability. Chen (Chen et al., 1997) also notes the fact that sometimes drivers were unable to answer a question, and therefore a "Don't know" answer was available during his testing to avoid forcing a choice that might obscure trends in the existing data. He also notes that the use of trained test drivers in his testing was advantageous – that the drivers were used to performing testing and answering questionnaires objectively – but also that it may have disadvantages if the drivers' training and experiences mean that they evaluate handling differently to the general populace.

Deacon's (1996) and Wicke's (2001) subjective data acquisition methods were somewhat different in that the test drivers had to rate each vehicle in an absolute sense with no comparison vehicle available against which the drivers could 'calibrate' their assessments. Work by Deacon (1996) and then Wicke (2001) developed the following subjective metrics:

- Initial jerk rating
- Acceleration progression rating
- Overall smoothness rating
- Engine delay rating
- Vehicle delay rating
- Overall driveability rating

Schoeggl et al. (2001; 2002) also list a number of subjective metrics; these include:

- Overall driveability rating
- Engine start, warm up and idle behaviour ratings
- Ratings for driving conditions including tip-ins and tip-outs
- Pull away rating
- Gear shift rating
- Noise and vibration ratings

2.1.4.2 Objective metric selection

The objective data are usually a time-based recording of a number of channels describing the vehicle response and these usually correspond to a single-figure rating or set of single-figure ratings that signify the driver's evaluation of the vehicle. Therefore, for correlation analysis, the objective data are often processed to produce metrics that characterise the objective performance in more succinct form. For example, the acceleration response of the vehicle could potentially be represented by a single figure for peak acceleration.

The selection and calculation of driveability metrics is a very important part of correlation analysis. A number of researchers have investigated aspects of driveability. List and Schoeggl (1998) and Dorey and Holmes (1999) investigated tip-in behaviour of vehicles with automatic and manual transmissions respectively. These papers concluded that vehicle acceleration related driveability metrics were the most influential on driveability assessment.

List and Schoeggl (1998) presented an analysis of the Fourier transform of acceleration data from a typical tip-in test as part of the driveability analysis research they carried out. They stated that only a small part of the acceleration frequency spectrum affects the subjective assessment. They do not give any quantitative figures, however it can be seen that these are low frequency components. They also stated that the subjective rating for a given acceleration jerking (the peak to peak size of the first acceleration oscillation) has more affect the smaller the overall acceleration, this may either be interpreted as the driver rating the size of the acceleration oscillations relative to the overall acceleration, or that the later high acceleration is positively weighted more heavily than the negative weighting for the initial oscillatory behaviour.

The research discussed by Dorey et al. (Dorey & Holmes, 1999; Dorey & Martin, 2000) concerns a number of aspects of driveability, one of which was tip-in manoeuvres. In these works a number of objective metrics were used. These were acceleration overshoot, natural

frequency, damping ratio, rise rate and rise time. Dorey et al. found that acceleration overshoot and rise rate both had a negative correlation with the rating of vehicle driveability.

Mo et al. (1996) identified shuffle, acceleration oscillations after an accelerator pedal change, as being important driveability metrics. Their research was concerned with reducing this shuffle using powertrain control. A paper by Balfour et al. (2000) shows similar research, looking at reducing acceleration oscillations in Diesel engine vehicles. Another paper by Karlsson and Jacobsson (2000) looks at engine and driveline modelling with a focus on simulation and optimisation of tip-in events. Their simulation looks at methods for smoothing driveline torque to produce fewer acceleration oscillations and a smaller peak acceleration (at the first oscillation).

Significant driveability research related to CVT vehicles has also been carried out. A PhD project carried out by Deacon (1996), investigated the control of a diesel powered (Torotrak) toroidal traction CVT equipped passenger car. As part of this project, driveability requirements were investigated and key areas of CVT driveability were highlighted through driveability appraisals and questionnaires. This work and other intermediate papers (Dorey and Martin, 2000) indicate the use of the following metrics in the analysis of longitudinal acceleration.

- Acceleration response overshoot – the size of initial acceleration oscillation above the mean acceleration response after a tip-in manoeuvre
- Rise rate – the rate of change of acceleration during a tip-in manoeuvre
- Damping during the decay of acceleration oscillations after an tip-in manoeuvre

A continuation PhD project (Wicke, 2001) investigated integration and control aspects of CVT vehicles. This project used single-variable driveability correlations to assess how different powertrain characteristics affected the CVT vehicle's driveability. Wicke et al. (1999) showed that simple correlations exist between mean subjective driveability evaluations and mean objective performance metrics for a set of vehicles, highlighting the following metrics as having important links to the evaluation of driveability:

- Acceleration delay time
- Initial and maximum acceleration
- Initial and maximum jerk (rate of change of acceleration)

Research by Schoeggl et al. (2001) developed almost 300 input objective metrics for a neural network driveability prediction system. They mention a number of these objective metrics in their paper, however they give no explanation of their exact meaning. The objective metrics that they mention are:

- Tip-in delay
- Tip-in jerks
- Gearshift engine speed decrease
- Cruise controllability
- Engine start duration

They note that some of the objective metrics have a positive effect, while others are neutral or negative. In a later paper, Schoeggl et al. (2001) concentrated on the following objective metrics in the evaluation of tip-in manoeuvres:

- Kick (the size of the initial acceleration oscillation)
- Jerks (The size and number of acceleration oscillations)
- Response delay (delay between the pedal input and a threshold acceleration that was considered to be detectable by a driver)

It should be noted that Schoeggl et al. (2001), Dorey and Holmes (1999) and Dorey and Martin (2000) found that high initial acceleration oscillation or acceleration rise rate was an aspect of tip-in manoeuvres that produced a negative effect. This is in contrast to the findings of Wicke et al. (1999) and Wicke (2001). However, it should be noted that Wicke's definition of jerk differs from that of the other mentioned authors. Wicke's definition was for the average rate of change of acceleration over the initial portion of the test while the other authors were measuring the size of the initial acceleration oscillation or the rise rate associated with this. Wicke's metric is therefore more closely related to the overall value of acceleration during the test rather than any undesirable spikes that may have occurred.

2.2 Powertrain calibration

Driveability must be taken into account during the calibration of a vehicle powertrain even though other objective issues such as fuel economy and emission control may assume a higher priority. The need to improve fuel economy and the introduction of ever more stringent limits on the emissions of NOx and CO makes emission control one of the most, if not the most, important factor in vehicle development today (Pfalzgraf et al., 2001).

The drive for efficiency and performance in the automotive sector has resulted in increasingly sophisticated engine and gearbox control systems leading to the adoption of drive-by-wire throttle systems where the driver is no longer in direct control of the engine. The driver instructs the computer via the accelerator as to the performance required and the computer optimises how to deliver it (List & Schoeggl, 1998). The resulting increase in component and system complexity has increased the number of electronic maps and tables in the system, all of which require calibration to optimise emissions, economy and driveability.

Electronic control is now very widely employed in all aspects of powertrain control. These areas include ignition timing, pedal mapping and throttle control, lambda control, variable valve timing and gearshift strategy and timings. A number of Electronic Control Units (ECUs) are required to control and coordinate these various aspects of the powertrain to ensure that the vehicle exhibits appropriate responses to driver input as well as ensuring that emissions and economy requirements are met.

The computer code that controls the powertrain is referred to as the control strategy. The complexities of the many variables in the powertrain system, as well as the requirements to balance economy, emissions and driveability result in a complex piece of software whose parameters require extensive calibration to produce optimum behaviour.

Calibration is the process of determining suitable values for the data maps and parameters that make up the strategy, controlling how the powertrain responds in any given situation (Kämmer et al., 2003). Although some aspects of calibration are relatively generic, specific vehicle factors (such as weight and the type of driving style for which it is being calibrated – e.g. smooth and relaxed, aggressive and sporty, etc.) make a large difference to the final tuning stages of a vehicle's calibration.

The process of calibration is a time consuming and labour intensive part of the production and the continual development of modern vehicle powertrain technology (Dorey & Martin, 2000). The introduction of new lean burn engine technology and AMT and CVT gearboxes, will produce yet more complex powertrain control strategies (Lumsden et al., 2004). An outline of the various stages involved in a typical vehicle powertrain calibration process is shown in Figure 2-1.

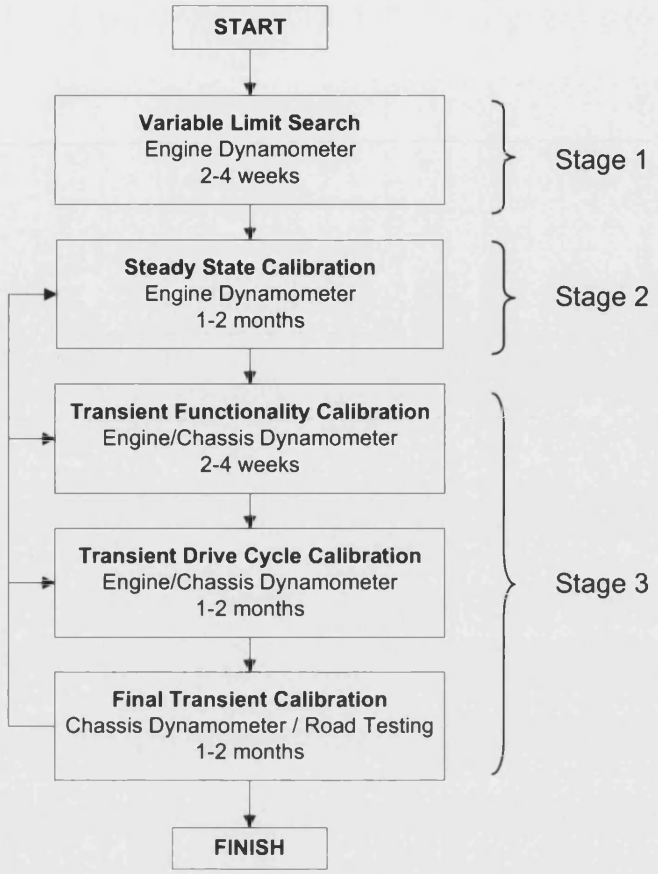

Figure 2-1 - Calibration Flowchart (adapted from Dunne, 2005)

The first stage of the process, the *Variable Limit Search,* identifies safe operating ranges for the variable that is to be calibrated to avoid damaging the engine during the subsequent automated calibration process. Having established safe limits for the calibration variables, the second and third stages of the calibration process are performed using an engine dynamometer (test-bed). These sections consist of testing and populating various data maps and parameters within the control strategy to satisfy fuel economy and emissions constraints. The second stage deals with optimising the calibration for steady-state operation, while the third stage optimises calibration for transient operation. The second stage and especially the subsections of the third stage of the calibration process are often carried out iteratively as changes in one part of the calibration affect other parts.

Although steady-state calibration has been at least partially automated for some time (Hochschwarzer et al., 1992) and is being constantly improved due to more complex engine and powertrain designs (e.g. Stuhler et al., 2002), the current state of the art in the automotive industry is for control strategy calibration to be performed on a transient engine test-bed to optimise fuel economy and emissions during the very important (for the driver)

and more realistic transient manoeuvres. A number of groups including Ricardo Consulting Engineers (Dorey et al., 2001) and the University of Bath's Powertrain and Vehicle Research Unit (McNicol et al., 2004) are engaged in producing accurate transient powertrain facilities that are able to reproduce the same effects as are seen in a real vehicle. The aim of automated calibration systems is to enable the bulk of the calibration of dynamic aspects of powertrain control strategy to be performed using a dynamic test-rig. This reduces the requirement for time-consuming and expensive chassis dynamometer and vehicle testing as well as being less labour intensive than current manual test-rig calibration methods. The adoption of automated methods also offers the potential to improve the optimisation and consistency of the calibration.

The imposition of absolute emission output standards results in driveability calibration being involved in a trade-off between these and other factors (List & Schoeggl, 1998). It should be noted that the economy and emissions constraints that have historically been optimised on powertrain test-rigs are often mutually competitive. Therefore the addition of driveability constraints requires no major change to the calibration optimisation processes. The addition of driveability constraints to automated transient-event calibration would enable driveability calibration to be addressed earlier in the calibration process, resulting in cost and time benefits. However, to produce driveability constraints, either driveability expert knowledge or real-time driveability prediction systems must be implemented. Such systems are in development by Ricardo Consulting Engineers (Dorey & Martin, 2000) and AVL LIST (Schoeggl et al., 2001) and are also the focus of this thesis.

2.2.1 CVT calibration and driveability

The current research was originally to be a continuation of the work carried out by Wicke (2001). This work was to investigate the driveability prediction and optimisation of a CVT powertrain, using the test data that had been acquired during previous projects at the University, as well as data collected during this research. Unfortunately, due to the loss of use of the experimental CVT vehicle, the project focus was changed to look at powertrain driveability analysis with the goal of using this research as a basis for further optimisation of CVT powertrain driveability.

The Continuously Variable Transmission (CVT) has much to offer in motor vehicle applications but has to date received limited acceptance, the complex engineering and low production volume resulting in a high cost transmission with unusual driving characteristics offering little perceived benefit to the driver (Brace et al., 1999a).

The Continuously Variable Transmission (CVT), unlike a conventional stepped ratio gearbox, which has a number of fixed ratios, is able to change its effective ratio to any point within its ratio range. This ability allows the CVT ratio to be matched to the engine speed and load to produce combinations of good driveability, good emissions and good fuel economy. The use of a CVT is therefore seen as a potential solution to the ever more stringent emission regulations when coupled with modern control systems able to link CVT and engine control. However, familiarity, on the part of the driver, with the behaviour and performance of conventional AT gearboxes has resulted in the driveability standards required for a CVT being difficult to achieve while still maximising the strengths of the CVT. This is partly because of the unusual lack of a link between engine and road speeds, and also because the maximum efficiency engine operating conditions often leave little or no torque reserve with which to accelerate the vehicle should the driver need to (Brace et al., 1999a).

A study carried out in the early 1990s by Thompson and Lipman (1992) concluded that although the CVT promised benefits in the areas of performance, economy and emissions, production versions were often unable to deliver better performance and economy than a comparable manual gearbox. The problems with these early CVT cars were attributed to a combination of factors including the increased size and weight of the CVT and its ancillary components, incorrect efficiency predictions and non-optimised control strategies. Despite an initial lack of faith in the CVT, there are a large number of automobile manufacturers who now produce CVT equipped small to medium sized passenger cars and SUVs, many as part of hybrid electric systems.

Although not all CVTs are as efficient as ATs or MTs throughout their operating ranges, they are still generally able to produce better overall powertrain efficiencies than fixed ratio transmissions. This is because the powertrain controller strategy can be optimised to keep the engine at its most efficient operating speed for a given torque requirement. This is obviously not possible with AT or MT vehicles, which must vary their engine speeds depending on the vehicle speed and selected gear ratio. Experimental fuel economy improvements of up to 20% have been reported with the use of a CVT (Takiyama & Morita, 1996; Hendriks, 1993).

A paper by Kluger and Fussner (1997) provides approximate efficiencies for various types of vehicle transmission. These figures are shown in Table 2-1 below.

Table 2-1 - CVT efficiencies from Kluger and Fussner (1997)

Transmission Type	Approximate Efficiency
Manual transmission	97%
Automatic Transmission	80-86%
Belt driven CVTs:	
Steel	90-95%
Rubber	90-97%
Traction CVTs:	
Toroidal	70-94%
Nutating	75-96%
Epicyclic CVTs	85-93%

Akehurst (2001) showed that belt-drive CVTs in fact have higher efficiencies than MTs at high speeds where their efficiencies increase due to their improved ratio range but have poor efficiencies at low speed and under low load conditions. Therefore, the figures in Table 2-1 should be considered the optimum for each transmission type, running at their own optimum operating conditions. This also gives an indication of the benefits that might be gained by using specific strategies to control the differing transmission types.

The ability to operate a vehicle's engine within specified speed bounds also allows powertrain noise, vibration and harshness (NVH) to be reduced. This offers opportunities for the use of the CVT in luxury cars, where this reduction of NVH, combined with the lack of jerking produced by gearshifts, would produce a very smooth driving experience. The Audi A6 Multitronic is a perfect example of a luxury car that benefits from a CVT (Goppelt, 2000). It should also be noted that the CVT used in this vehicle employs a chain CVT because of the large amount of torque that must be handled.

The altering of engine speed and load characteristics allows different harmful emissions to be reduced. Unfortunately, the operating regimes required to reduce different types of emissions are often at odds with one another. Despite these constraints, Torotrak claim harmful emissions reductions of up to 30% (Wicke, 2001). Audi claim a 10% improvement in fuel consumption using their Multitronic CVT when compared with a 5-speed AT and a marginal improvement over their 5-speed manual gearbox (Kimberley, 1999). These reductions are due to the ability to run the vehicle's engine at a speed and load that reduces the overall fuel consumption and emissions production. This is illustrated in Figure 2-2 which shows an engine map of the type which allows an adaptive CVT powertrain controller to select the best engine speed for a given torque requirement, taking into account power requirements and fuel consumption goals.

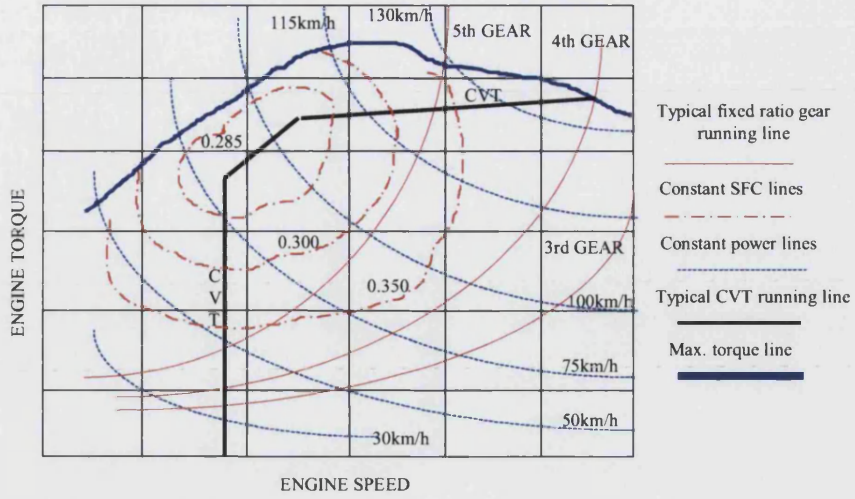

Figure 2-2 - A typical CVT driving strategy map for fuel economy

(from Akehurst, 2001)

More complex maps than this one would be used in reality, also taking into account the amounts of harmful emissions produced by various engine torque and speed combinations as well as considering driveability aspects (Wicke et al., 2000).

2.2.1.1 CVT Driveability aspects

Minimising fuel economy and various emissions as well as improving driveability are all factors in the design of CVT powertrain control strategies, and each of these factors requires a different operating strategy to achieve its optimum and it is this problem that has made the design of CVT control strategies so problematic (Brace et al. 1999b). It is only relatively recently that advances in multivariate optimisation, simulation and various other computerised techniques such as genetic algorithms (GA), fuzzy logic (Deacon et al., 1999), and neural networks (Brace et al., 1999) have made the design of control strategies an economical prospect.

Vehicle driveability in general is a field that has not been thoroughly explored in the case of the CVT, receiving, until quite recently, little attention due to the relative lack of interest in this type of transmission for automotive applications. The advances made in CVT design have resulted in renewed research now taking place into driveability criteria of CVT vehicles (Field & Burke, 2005; Patel et al., 2005; Ohashi et al., 2005; Pick et al., 2005; Schmizu et al., 2006).

As the engine in CVT powertrains can be controlled to stay within a narrow range of speeds, it is possible to design a transient strategy that, for example, operates the engine in areas of high torque during these transients to provide good driveability and powertrain response. Unfortunately, the goal of good economy and emissions cannot easily be achieved at the same time as good driveability, so the powertrain designer, and possibly the controller itself in real-time, must decide which are the most important and weight them accordingly or adaptively.

Research has been performed to determine the driveability characteristics of a number of CVT vehicles (Wicke et al., 1999; Wicke et al., 2000; Wicke, 2001). Subjective driveability rating and objective data acquisition was performed on six different CVT vehicles using approximately 12 test drivers for each vehicle. This study found that high initial accelerations and short acceleration delay times produced positive subjective launch feel ratings. Delay time and initial acceleration were also found to be the most influential metrics in the subjective 'overall driveability feel' rating, but it was also affected by what is called 'jerk', which is defined here as the initial rate of change of acceleration.

The feeling of driving a CVT vehicle is somewhat different to that of driving a vehicle with a conventional AT. The main issue is the apparent lack of a connection between the engine speed and the vehicle speed over the entire engine speed range and is an effect that many drivers find disconcerting, especially when trying to accelerate as the engine speed will often drop part way through the manoeuvre even though the vehicle speed is increasing. This drop in engine speed is caused by the CVT control strategy returning the engine to its most efficient operating speed once the initial high acceleration phase at the start of the manoeuvre is complete. Though this does not signal a drop in performance as it would in a vehicle with a conventional AT transmission it can be misinterpreted by the driver as such. These differences between what a driver expects, and what a CVT equipped car actually delivers, are a major factor in the slow uptake of CVTs and further research into the effects of CVT control strategies and drivers' perceptions of CVT vehicle driveability are required.

2.2.2 Real-time powertrain calibration modification

Sawamura et al. (1998) published a paper describing the development of an integrated powertrain control system for a vehicle with an AT. Rather than determining the driver's driving style, the controller uses fuzzy logic to decide on the current physical driving conditions (traffic congestion, traffic speed and road inclination) as well as predicting the driver's intentions (using vehicle acceleration, noise generation and accelerator pedal position and speed). This information is used to alter the shift-scheduling and electronic

throttle mapping control to produce better driveability. Takada et al. (1996) published a paper detailing their investigation of accelerator pedal sensitivity. They detail two methods of changing the sensitivity of a drive-by-wire accelerator using Feed Forward or Feed Back control, which could be used to alter the pedal torque map in real time, rather than needing to pre-calculate different maps.

In a number of more recent papers Schoeggl et al. (2001) and Schoeggl and Ramschak, (2000) have shown research on controllers which allow the driveability characteristics of a vehicle to be adjusted in real-time to match the driving style of its driver as interpreted by the controller. This powertrain controller rates various behavioural aspects of its driver, and then alters its calibration to produce better driveability. The controller first uses a fuzzy logic system to decide whether the driver has changed his or her driving behaviour. It then uses a neural network to assign a rating to its driver's driving style for each of the following categories:

- Sportiness
- Economy
- Comfort
- Aggressiveness
- Nervousness
- Talent/Ability
- Skill level

The combination of these scores is then used to determine how to change the powertrain calibration. It is not explained how the vehicle calibration is altered; however it is clear that the main changes are made to the accelerator pedal torque demand map. Whether these changes are calculated "in real-time", or are stored in a look-up table, is not known, although the use of pre-compiled look-up tables is most probable.

Although not strictly real-time, Dorey and Martin (2000) outline an approach to in-vehicle data acquisition for use in "on the spot" driveability calibration, which allows the latter stages of vehicle calibration to be carried out more effectively.

3 Description of the test facilities and equipment

This section starts by describing the data acquisition equipment used in the initial testing carried out during this project. This is followed by a description of the development of a new system that was used for later testing and the sensors and other equipment that were used to record the objective data for this project. The test facilities, existing test data and new test vehicles are then described. This is followed by a description and categorisation of the test-drivers who took part in the project.

3.1 Data Acquisition

A data acquisition system called DIS-Drive (Ricardo Consulting Engineers Ltd., 1995; Ross-Martin & Pendlebury, 1997) was in use at the University of Bath having been used by Wicke to collect the test data for his PhD project, and this was the system initially used by the author for the testing of the Toyota Prius. A number of limitations were found with the DIS-drive system during the author's initial testing, namely the difficulties of installing and calibrating the system, as well as the limited number of channels that were available with which to record data. Therefore a decision was made to develop a more flexible and advanced system using CP Cadet V12 (CP Engineering, 2000 & 2001) to overcome these limitations. The new system was required to allow an increase in the number of channels which could be recorded, to allow variable acquisition rates, and to permit future expansion for other projects. High-speed in-vehicle data acquisition for in-cylinder pressure testing is an example of a potential project that would require the use of this advanced system. Following the development of this new system, it was subsequently used in the testing of the AT Mondeo test vehicle.

3.1.1 DIS-Drive and EMPS - A portable data acquisition system

The DIS-drive data acquisition system was originally developed so that hired vehicles used during Wicke's PhD project (2001) could be equipped with sensors as quickly and as non-invasively as possible. To equip any vehicle with the system (including the installation and connection of all transducers in the vehicle) usually took about two days, allowing the rigging and testing to be carried out in relatively short and therefore inexpensive period of time. The DIS-Drive data acquisition system was developed on top of an standard University data acquisition and control rapid prototyping system called EMPS.

The original function of the EMPS software was as an engine calibration and management prototyping software system, with additional features that mean it could also be used as a

data acquisition system. The EMPS program allowed easy calibration of each variable that was to be acquired; unfortunately, this calibration had to be performed each time the data acquisition system was used making the setup process somewhat laborious.

When used in a vehicle, the program was run on a laptop computer which communicated with the acquisition system via a CAN bus and RS-232 serial link. The serial link was used to control the acquisition system while the CAN bus was used to pass recorded data between the acquisition system and laptop. The system was able to acquire data on up to *eight* channels in parallel and to display the data on the laptop in real-time. All of the data acquired with this system were logged at *100Hz.*

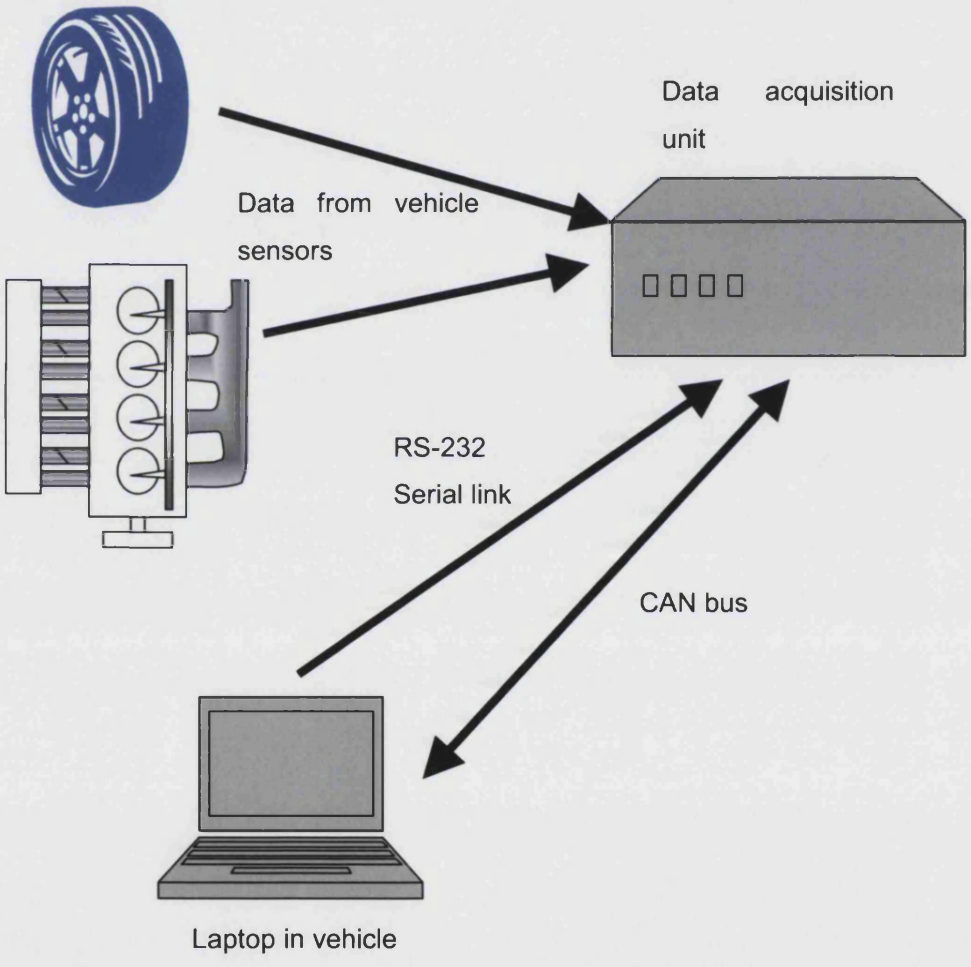

Figure 3-1 – DIS-Drive/EMPS data acquisition system diagram

The program was modified for the driveability research to include the capability to record subjective ratings and comments at the end of each test run. This allowed the test drivers to

fill in the rating questionnaire on the laptop and to comment on each test manoeuvre immediately after it had been performed.

Table 3-1 - DIS-Drive/EMPS system information

Dimensions (width x length x height)	194 x 138 x 66 mm
Mass	1.08 kg
Maximum bus data transfer rate	1 Mbit/s
Maximum data acquisition rate	100 Hz
Maximum number of data acquisition channels	8 Channels.
Channel types (AD/DA bits)	Speed channels at 16bits/channel Position channels at 10bits/channel Pressure channels at 10bits/channel
Battery duration	Directly connected to vehicle 12 V system
Cost	approx £10,000

3.1.2 Development and use of CP Cadet V12 system for data acquisition

As part of the research described in this thesis, it was decided to develop and implement a more modern, flexible and easily useable in-vehicle data acquisition system. Systems such as that described by Steiner (2005) allow many vehicle performance parameters to be recorded from ECU data to in-cylinder pressures. This large amount of data, which could otherwise only be recorded on a test-bed, allows accurate and realistic data to be recorded in on-road driving. Although the goals of this project did not require this level of instrumentation, it was decided that a system should be developed which would be able to be easily extended to encompass ECU and in-cylinder data acquisition. Therefore it was decided to modify and use the CP Cadet V12 test-cell control and data acquisition system (CP Engineering, 2000 & 2001) to perform the data acquisition. This system was chosen as it was tried and tested, having been used for a number of years within the automotive department at the university to control powertrain test-cells.

CP Engineering's CADET V12 system runs on personal computers (PCs) using the Windows NT operating system (support has since been extended to include Windows XP and Windows 2000). It is fully configurable and customisable using the Microsoft Visual Basic programming language.

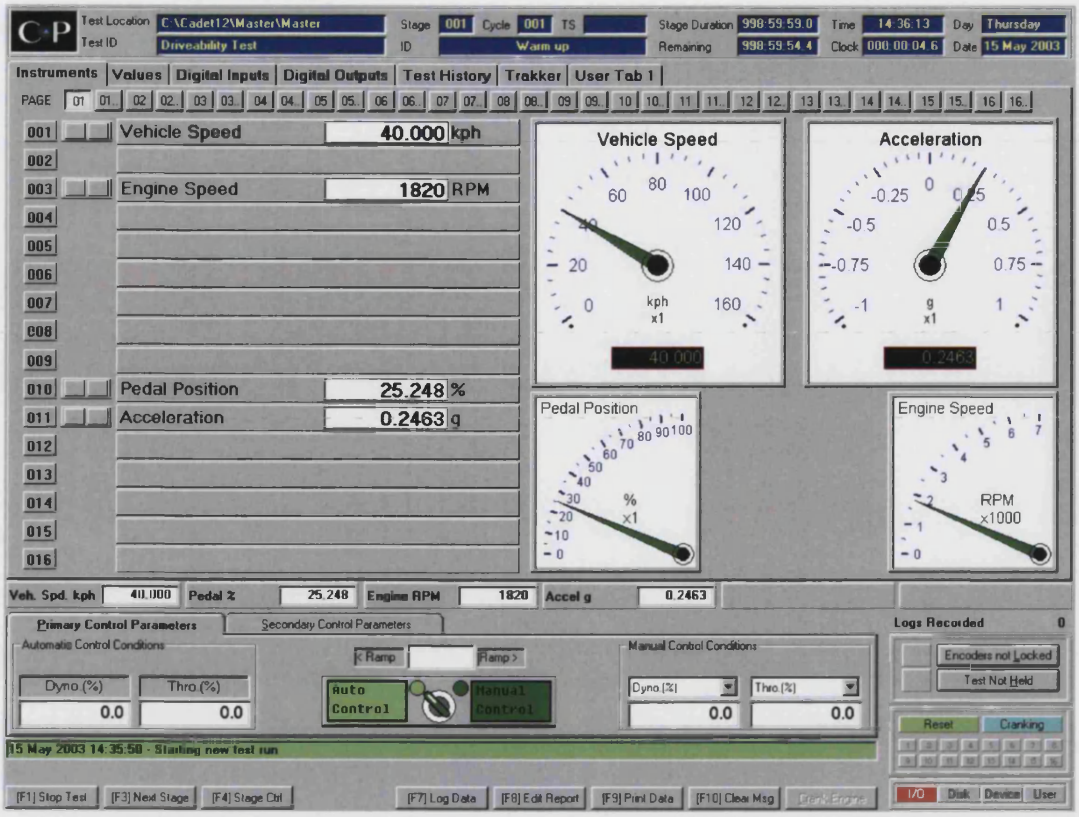

Figure 3-2 - CADET V12 interface: during testing

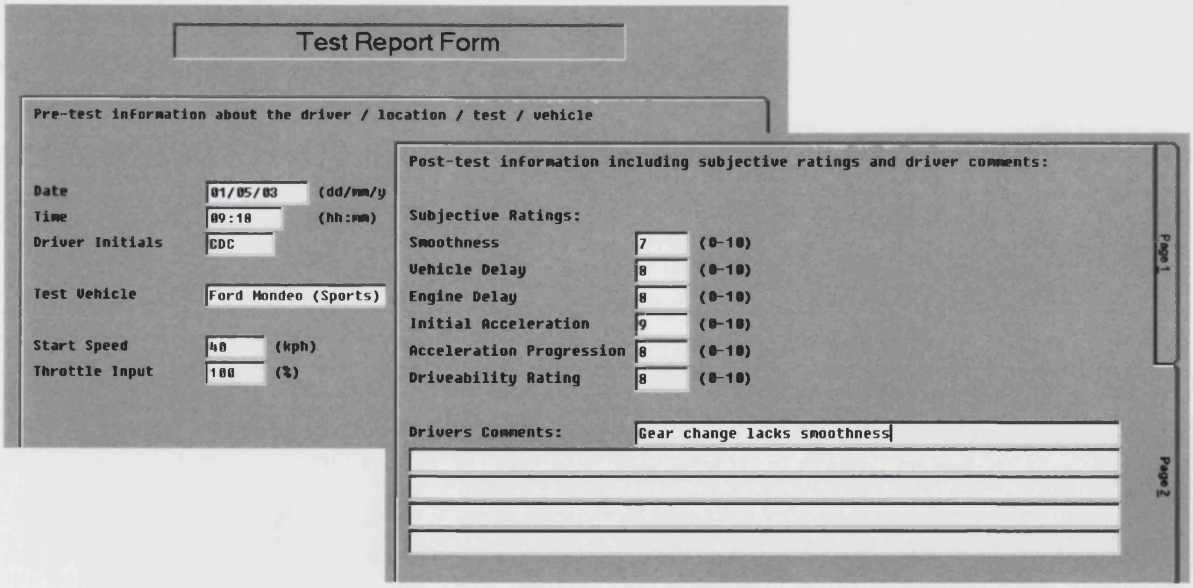

Figure 3-3 – CADET V12 interface: post testing subjective metric recording

The relatively simple task of performing data acquisition may not require the use of this level of technology but there were a number of reasons for making this choice:

- The extensibility of the system – allowing the system to interface with multiple different data acquisition cards of differing types and speeds which would allow many channels to be recorded at different rates and levels of accuracy as well as allowing very high-speed in-vehicle data acquisition for in-cylinder pressure testing.
- The ease of setup due to the standardised CADET acquisition cards which were already available at the university.
- Familiarity with the use and setup of the system due to its use in the department for a number of years.
- The convenience of built-in data viewing and analysis tools – for example the 'Trakker' feature, which visualises the recorded test-data in real time (see Figure 3-4). This feature is useful for the detection of poorly calibrated channels and sensor failures.

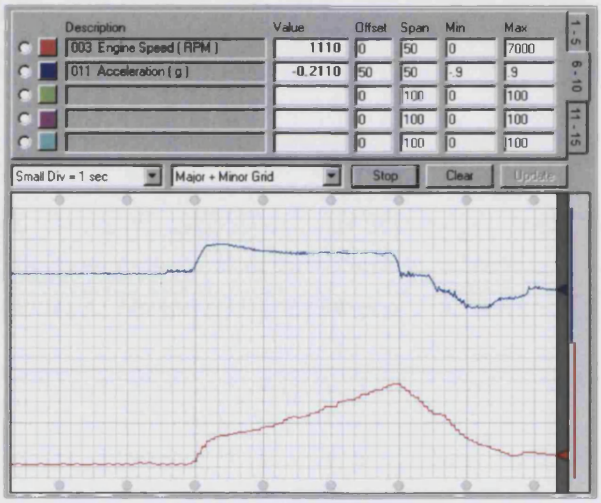

Figure 3-4 - Cadet V12 'Trakker' window - real-time data visualisation

On the negative side, there were a number of problems with setting-up the system:

- System complexity and software setup time considering the basic use to which it would be put.
- Computer hardware requirements.
- The fact that this was the first in-vehicle system that had been commissioned using the CADET software. This meant that it took longer to debug some problems that were encountered while setting up the system than had been envisioned.

The basic CP Cadet V12 system consists of a computer attached to a custom card-rack (see Figure 3-5) in which various types of acquisition/output cards are located. The CADET

system communicates with the card rack through a mixture of serial and parallel communications.

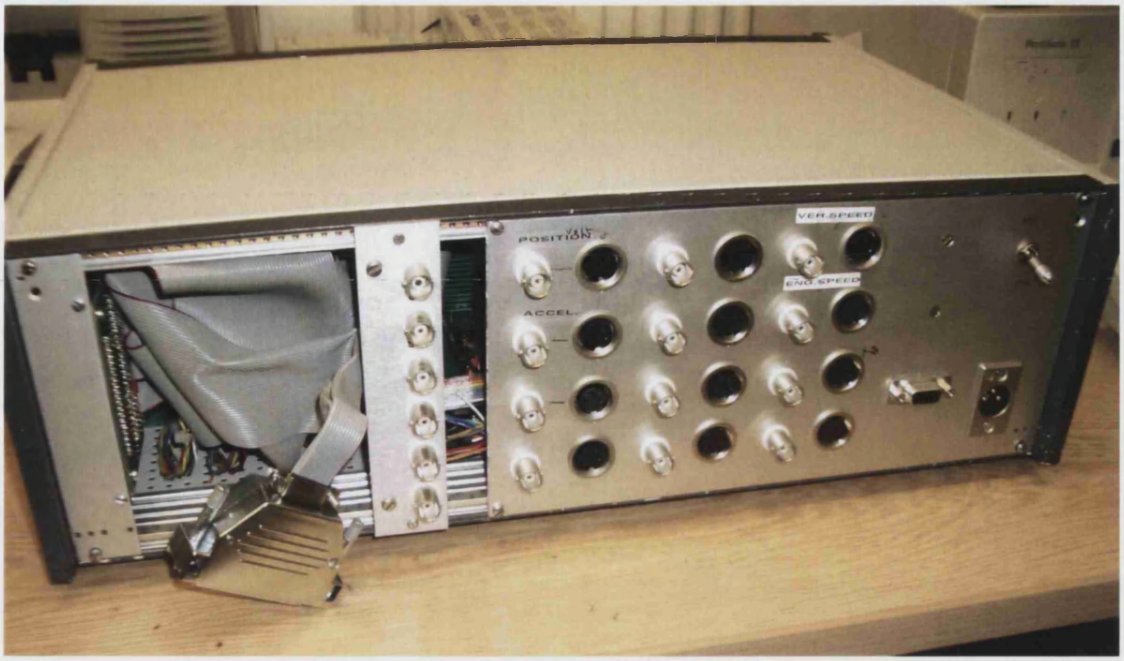

Figure 3-5 - CADET V12 system portable card-rack

The initial plan had been to run the entire CADET V12 system (henceforth referred to as CADET) on a laptop computer; unfortunately a number of compatibility problems were discovered:

- CADET is not normally run solely through single serial connections; it was found that although it was possible to communicate with the card-rack, the data transfer rate was limited to approximately 20Hz. This recording-rate was not acceptable for transient events with an expected bandwidth of around 5Hz because of the danger of aliasing.

- To increase the transfer rate (and allow the card-rack to perform to the full specification on the cards it contained – up to 320Hz), two serial ports would be required; unfortunately most laptop computers only have one serial port and many now have no serial ports at all, having replaced them with the increasingly ubiquitous USB. Unfortunately, CADET is not yet able to communicate through USB or Ethernet network connections.

- Therefore a secondary serial port was required – for a laptop computer the options are to use a pc-card or USB serial adaptor. No pc-card serial adaptors could be found which were supported by Windows NT. USB serial adaptors were available, however USB is not well supported on Windows NT and no drivers could be found.

- CADET was untested on anything but Windows NT 4 computers before this project began, however it was in development for Windows XP (which supports USB) and a copy of the developmental program was obtained. It was eventually discovered that due to the low-level nature of CADET's communication with the serial port (due to the real-time nature of the communications) a USB or pc-card adaptor could not be used without major changes to the CADET serial driver handling. It was therefore decided to use a desktop computer to communicate with the card-rack.

The desktop computer was fitted with two serial ports and a specialised parallel port card (allowing even greater data-rates to be transferred – looking forwards to possible in-cylinder data acquisition). To power the desktop computer, a 12V DC to 240V AC power inverter was used, powered by a dedicated battery located in the boot of the test vehicle along with the desktop computer itself.

Initially the system had been used employing keyboard/mouse and screen extension cables, however it was found that it was inconvenient for the author to use the keyboard as the LCD screen was too large to be affixed firmly to the test vehicle's dashboard and therefore had to be partially supported.

A laptop was far easier to use and had the added advantage that it significantly reduced the drain on the desktop computer's dedicated (non-charging) battery by not requiring it to power an LCD monitor constantly. The laptop computer was attached to the 12V cigar lighter in the cabin to draw power directly. The desktop computer was controlled from inside the vehicle using the laptop computer, which displayed the desktop's screen using the Symantec pcAnywhere package transmitted via an Ethernet link. The monitor (unpowered), keyboard and mouse were retained with the Cadet computer to allow debugging of any possible communications problems.

Figure 3-6 - System in-vehicle

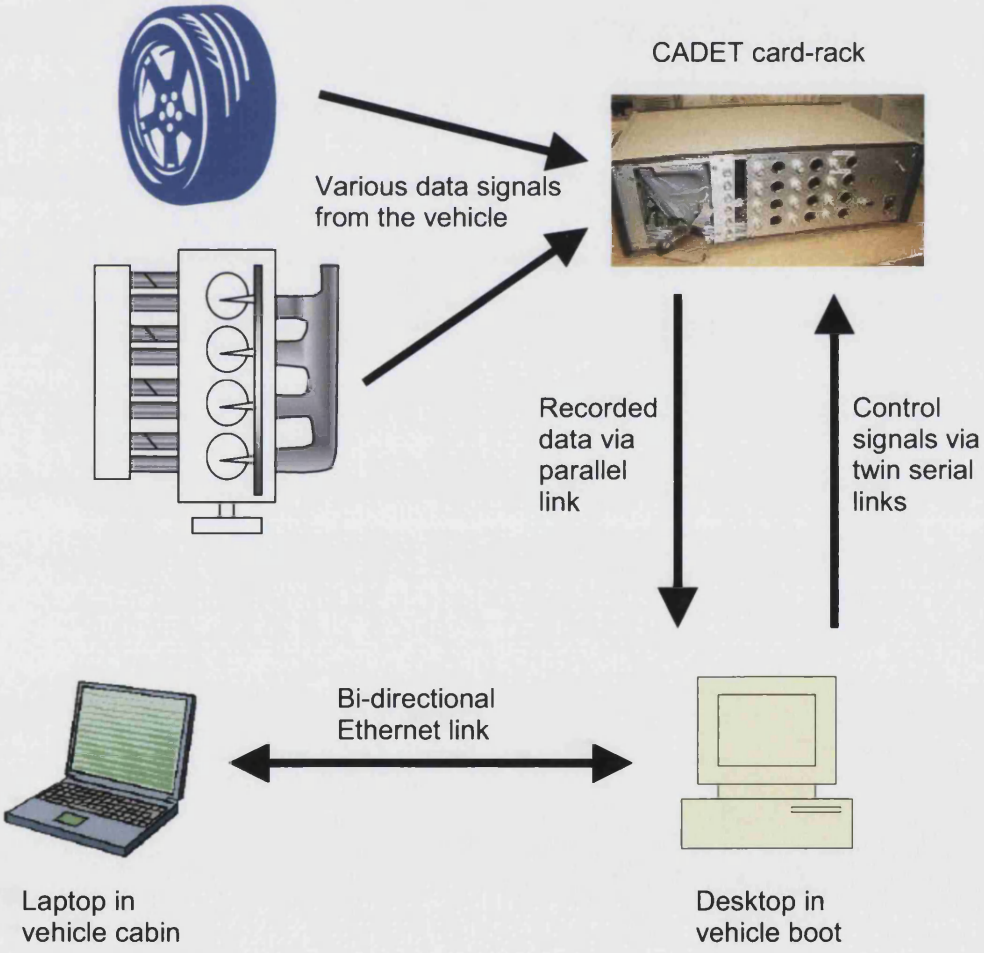

Figure 3-7 - CADET V12 data acquisition system diagram

Battery life was found to be approximately 1.5 hours enabling two or three sets of tests to be performed with a given battery. Therefore, two batteries were normally used and swapped during the course of testing.

Table 3-2 – CADET V12 system information

Dimensions (width x length x height)	450 x 305 x 160 mm
Mass	3.00 kg
Maximum bus transfer rate	1 Mbit/s
Maximum data acquisition rate	Dependant on hardware setup: 80 Hz for this work.
Maximum number of data acquisition channels	Dependant on hardware setup: 1 slot required for communications card (DL-INT-02). 3 slots used for DAQ cards (see below). 6 slots remaining for further DAQ cards. Further card racks can be linked into this one using the same power and communications cards.
Channel types (AD/DA bits)	1x frequency measurement card (DL-MSS-04): 4 frequency channels (up to 614.4 kHz clock, 16 bit counter). 2x voltage measurement cards (DL-VAD-09): 4 A/D channels per card, 80Hz at 11 bits/channel.
Battery duration	1.5 hours per 12V, 45Ah battery
Cost	Software: approx. £5,000 Each DAQ/comm. card: approx. £350

3.2 Recording equipment

The types of sensor used to record each variable varied from vehicle to vehicle depending on what could be easily fitted without requiring invasive changes to the vehicles.

The data recorded during this work were pedal position, engine speed, vehicle speed and vehicle acceleration. These data were chosen as they represent both the longitudinal behaviour of the vehicle (vehicle speed and acceleration) as well as the driver's demands (pedal position) and the engine response (engine speed). These channels provide the data to generate the acceleration and delay time related objective metrics that have been found to be important in longitudinal driveability analysis (List & Schoeggl, 1998; Dorey and Holmes,1999; Wicke et al., 2000; Schoeggl et al., 2001), as well as allowing the particular driving conditions (i.e. vehicle speed, pedal demand, engine speed and therefore gear-ratio) to be determined. The experimental sensor setups are described below:

3.2.1 Pedal position

For the CVT Ford Mondeo and the Vauxhall Omega, a linear potentiometer was attached to an accessible section of the accelerator cable within the engine compartment. For the Prius

and BMW a potentiometer was installed in the driver's foot well directly measuring the movement at the pedal itself. The potentiometer specification is given in Table 3-3, below.

Table 3-3 – Pedal position sensor specification

Sensor type	Penny and Giles linear displacement sensor (DC-DC potentiometer) SLS-130
Stroke length	75 mm with spring return
Resistance	3 kΩ
Supply voltage	5V
Linearity	±0.15%
Hysteresis	0.01mm

A diagram of the pedal position sensor attachment location is shown in Figure 3-8, below.

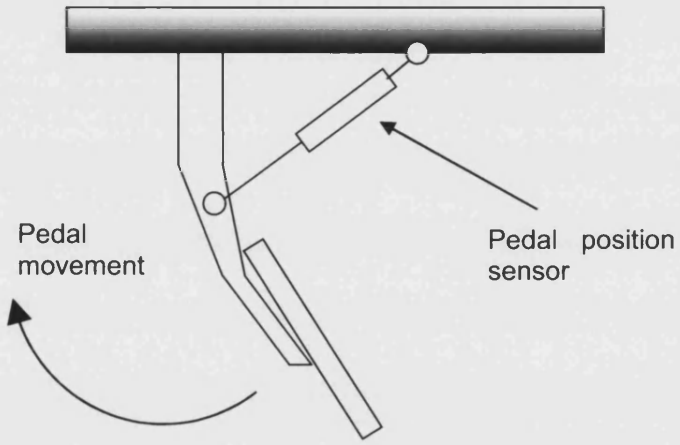

Figure 3-8 – Pedal position sensor location

For the AT Mondeo a number of methods were considered, in the hope of avoiding the use of a potentiometer mounted in the foot well as these are prone to disturbance by drivers getting in and out of the vehicle, which means they require frequent recalibration.

It was initially hoped that the pedal position could be read directly in the engine bay using the pedal position sensor in the throttle housing – unfortunately, it was not possible to obtain a feed from this sensor without risking damaging it. After attempting to mount a potentiometer inside the engine bay to measure the cable movement but finding that there was insufficient space, it was eventually decided to mount the potentiometer inside the driver's foot well but in a more protected location than that used on the Prius.

The pedal position sensor was calibrated using two data points: full and zero depression of the pedal position. For the testing of the Toyota Prius and AT Ford Mondeo the drivers were allowed to perform practice runs in the vehicle using a visual pedal position indicator. This indicator was provided as drivers had commented during preliminary testing that they had

found it difficult to judge pedal position accurately. For the actual testing the drivers were told to ignore the pedal position indicator so that they could concentrate on the driveability aspects about which they would be questioned.

Figure 3-9 - Visual pedal-position indicator

3.2.2 Vehicle acceleration

The same accelerometer was used for all the test vehicles both in the current research and also in Wicke's testing. The specification of this sensor is shown in Table 3-4, below.

Table 3-4 – Accelerometer sensor specification

Sensor type	Bosch 0-265-005-109 Spring-mass, single-axis, Hall-effect acceleration sensor
Range	-1.0 to 1.0g
Output Voltage	0.96 to 4.38 V
Linearity	Linear between +0.9g and -0.9g
Accuracy	± 225mV corresponding to 0.12g

The acceleration sensor was attached to a horizontally-mounted metal plate to ensure that it was easy to mount and that it would remain horizontal once fitted. For Wicke's testing this plate was fitted beneath the driver's seat between the seat rails, but during the current project it was found that the test-drivers often wanted to adjust the seat and therefore the plate was fitted in the same manner beneath the passenger's seat, which always remained in the same position to avoid the sensor being moved out of alignment. The exact horizontal positioning was determined by adjusting the positioning of the sensor mounting plate under the seat rails until the output of the sensor indicated zero acceleration.

The accelerometer used a single-axis Hall-effect sensor to pick up the forces acting on a mass-spring-damper system from which the longitudinal vehicle acceleration was derived. The acceleration sensor provided a linear signal and thus could be calibrated by means of two distinct data points: holding the sensor vertically provided a signal with a value of gravitational acceleration (g), and holding it horizontally provided a zero g signal.

Figure 3-10 - Accelerometer mounted beneath passenger-seat

As the sensor was a single axis accelerometer and the mounting plate was firmly mounted parallel to the line of acceleration, the mounting and plate stiffnesses and any resonant frequencies produced negligible effects on the output from the sensor.

3.2.3 Vehicle speed

An optical encoding speed transducer was attached to the wheel hub of one of the road wheels by a retaining device that had to be fabricated for each vehicle. The sensor measured the speed of rotation of the wheel producing a signal proportional to the vehicle speed. The specification of this sensor is shown in Table 3-5, below.

Table 3-5 – Vehicle speed sensor specification

Sensor type	Leine & Linde incremental encoder 530
Range	0-6000 rpm
Measuring steps	1600/revolution
Output	RS-422, TTL

Calibration of this signal was performed either by comparing this signal to the speed signal from the rolling road or by calibration against the vehicle's speedometer which itself was

checked by measuring the time taken for the vehicle to travel a set distance at a given indicated speed.

The speed encoder, due to the construction of the wiring loom, was attached to the centre of one of the front wheels for the testing of the Prius. This was not completely satisfactory as the application of steering lock when turning around within the confines of the airfield taxiway could result in the cabling either being over stretched or caught against the front wheel, detaching the sensor from the wheel hub.

However when testing the AT Mondeo the loom was extended so that the sensor could be attached to one of the rear wheels. This eliminated not only the sensor detachment problem that had occurred while testing the Prius but also the possibility of wheel-spin adversely affecting the vehicle speed measurement.

The pulse encoder chosen for this application produced 1600 pulses per revolution. The circumference of the AT Mondeo's wheel was measured to be approximately 1.8m meaning that a single pulse would produce a minimum measurable distance of 1.8/1600 = 0.001125m. At a sampling frequency of 80Hz this results in a minimum measurable speed of 0.09m/s = 0.324 kph.

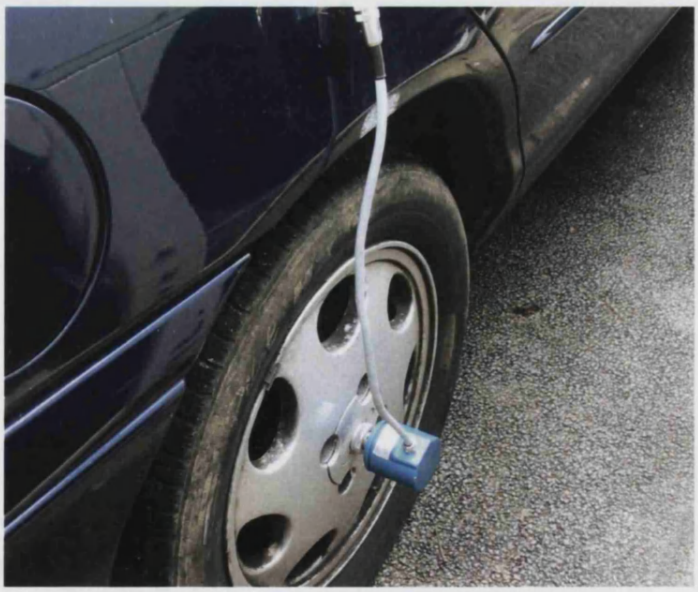

Figure 3-11 - Vehicle speed sensor attachment

3.2.4 Engine speed

The engine speed data collected by Wicke were collected in a variety of ways depending on the vehicle being tested. The first, and least troublesome of these, was to directly access the vehicle's engine control data bus and read the engine speed directly from the ECU. This method produces the best data as it is updated at high frequency (typically 16ms period (Ricardo Consulting Engineers Ltd., 1995)) and is already in a calibrated digital form, making further processing unnecessary. However decoding this digital data can be difficult, and for many vehicles, the data bus connector and protocols are unknown or require very expensive equipment making the use of this technique unfeasible if not impossible. This technique was used to acquire the data from the Torotrak Mondeo as its engine and powertrain buses were connected to a dSpace controller allowing easy access to these data.

For the remainder of Wicke's vehicles and for the Prius, a standard inductive transducer was used for the measurement of the engine speed signal. The transducer was clipped around the injection or spark leads where it measured the current flowing though the cables during injection or ignition firings respectively. The inductive sensor was supplied as part of Gunson's Timestrobe RPM Inductive Xenon Timing Light with clip-on ignition pickup.

However, this engine speed measurement method failed to record the engine speed signal of the BMW for low engine speeds and would not work for the AT Mondeo at any engine speed. The cause of the problem with the BMW is that the engine control strategy employs multiple spark generation during different engine speed regions and especially at the beginning of transients. This meant that the BMW engine speeds recorded by Wicke contain a variety of errors that have had to be corrected before the data could be used for metric generation (see Section 5.3.2).

The AT Mondeo problem was due to the sensor not being able to pick up a reliable signal through the shielded spark-plug leads. It should also be noted that this technique would only provide one signal for every two revolutions of the engine, which would produce either a low granularity output or a low update rate. Using a similar signal from the alternator was considered (which would provide one signal per revolution) however this was still not considered to be accurate enough.

The cabling from the flywheel sensor used by the ECU was found and spliced into, and although the signal was clear on an oscilloscope, the current drawn by the DAQ equipment was too much and caused the sensor's signal to the ECU to fail and the engine to therefore shutdown even with the use of a custom high-impedance DAQ circuit.

Due to these problems, it was decided to use a magnetic pickup sensor instead to perform pulse counting on a rotating component. The sensor was situated to detect the teeth on one of the camshaft sprockets. It should be noted that this did require invasive installation and therefore could not have easily been used on a hired vehicle. The specification of this sensor is shown in Table 3-6, below.

Table 3-6 – Engine speed sensor specification

Sensor type	RS 304-166 magnetic pickup sensor
Output	10V
Positioning	Air gap of 2.5mm is normal

Figure 3-12 shows the positioning of these sensors.

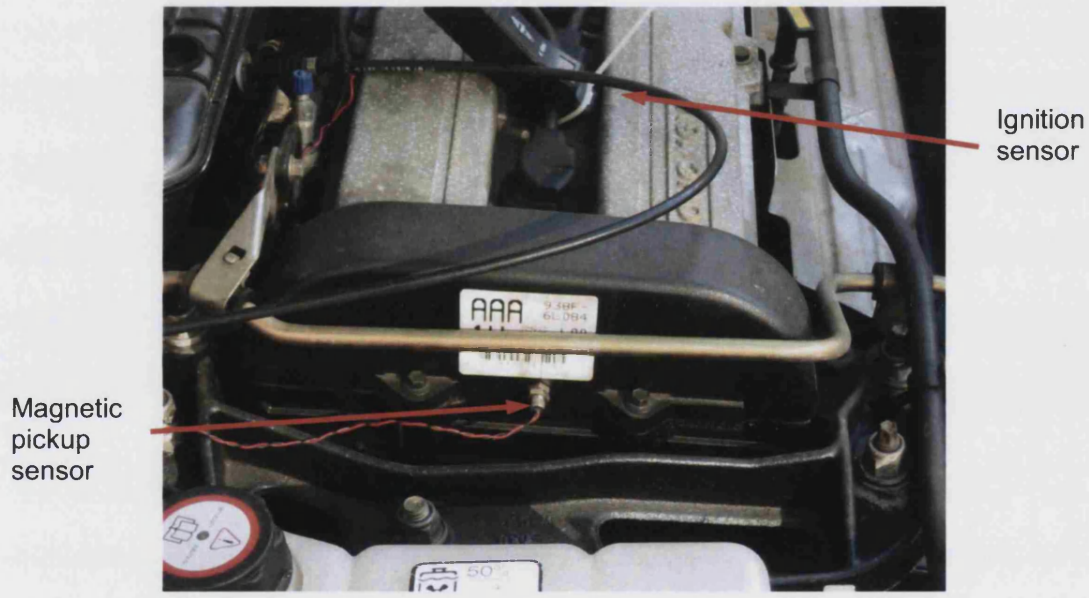

Figure 3-12 - Engine speed sensor placement

To resolve the conflict between ensuring sufficiently fast updates whilst returning accurate readings the sampling time used in the frequency acquisition card's pulse counter had to be carefully chosen. A short sampling time gives a rapid update but will result in poor resolution at low shaft speeds as the number of targets (teeth) passing the sensor during the sampling time will be small. Only integer numbers of teeth can be detected, so the number of teeth passing the sensor per sampling interval defines the resolution of the measurement. As there were 40 teeth on the camshaft sprocket, which was rotating at ½ the crankshaft, speed, it was decided to employ a sampling rate of 10Hz.

Therefore:

Crankshaft rotation per tooth = 2 x 360° / 40 teeth
= 18° / tooth

Sampling rate = 10Hz, therefore at the lowest accurate sampling rate of 1 tooth/sample = 10 teeth/s:

Minimum measurable rotation = 18° / tooth x 10 teeth/s
= 180° / s

Converting into revolutions per minute, this produces a minimum step size of:

Minimum engine speed step size = 180° / s x 60s / 360°
= 30 rev/min

This minimum detectable engine speed difference and the 10Hz update rate were deemed sufficient for the needs of the testing.

3.2.5 Current

For the testing of the Prius an additional channel was used to record the charging current from the generator to the battery using a current transducer. The specification of this transducer is shown in Table 3-7, below.

Table 3-7 – Current transducer specification

Sensor type	LEM HT200-SRUD
Current measuring range	±0 to 200A
Linearity	±0.5%
Accuracy	±1%

It had been planned to record both the generator to battery and battery to motor currents, allowing the various electric motor operating regimens to be distinguished, however only one current could be recorded due to the lack of available current clamps and the inability to acquire more within the constrained time for which the test vehicle was available on loan from Ricardo Consulting Engineers. These data were therefore not used during this research.

3.3 Test facilities

The vehicle testing during this project and during Wicke's project was carried out at RAF Colerne airfield. Colerne airfield lies approximately 5 miles to the Northeast of Bath, which was convenient for testing. The University of Bath's Mechanical Engineering department has an understanding with Colerne allowing the use of part of one of the taxiways for vehicle

testing. Although Colerne is an operational military establishment, it has a very low number of incoming and out-going flights meaning that such testing was possible.

The tests were carried out along a section of the perimeter taxiway around 1500m long and 10m wide. This was long enough to carry out a single 60Kph start-speed test (due to the requirement to achieve steady-state conditions at 60Kph before starting the test), or a number of lower start-speed tests.

Figure 3-13 - Colerne Airfield (Ingham, 2005)

Figure 3-14 – Aerial view of Colerne airfield with region used for testing indicated in blue (Multimap, 2005)

3.4 Existing test data

As part of Wicke's PhD project, data were collected from a number of vehicles, which are described in Table 3-8.

Table 3-8 - Vehicles tested by Wicke (2001)

Manufacturer:	**Rover**	**Ford**	**Vauxhall**	**BMW**
Model:	**216Si**	**Mondeo 2.0i**	**Omega 2.0**	**323Ci**
Category:	hatchback	saloon	saloon	coupe
Engine:	16V In-line 4 cylinder petrol	16V In-line 4 cylinder petrol	16V In-line 4 cylinder petrol	24V In-line 6 cylinder petrol
Cylinder vol(cm^3):	1590	1988	1998	2494
Max Power kW:	82kW @ 6000rev/min	96 kW @ 5700rev/min	100 kW @ 5600rev/min	125 kW @ 5500rev/min
Max. Torque:	145Nm @ 3000rev/min	176Nm @3700rev/min	185Nm @ 4000rev/min	245Nm @ 3500rev/min
Drive:	Front	Front	Rear	Rear
Curb weight:	1025kg	1328kg	1430kg	1410kg
Transmission:	CVT (van Doorne's Transmissie)	CVT (Torotrak experimental)	AT (4 speed)	AT (5 speed)
0-100kph time:	9.9s	9.9s	9.3s	9s
top speed /kph:	190	206	210	230
Number of test drivers:	12	13	14	18

Wicke's test drivers performed a series of tests whose initial speeds, pedal positions and methodology were similar to those employed in the current project as described in Section 4.1. It should be noted that no test data from the Rover 216Si were used in this project as they were poorly scaled and contained a significant number of errors (caused by faulty recording equipment) which makes automated processing difficult.

3.5 New test vehicles

Two additional vehicles were tested during the course of the current project. These are described in Table 3-9 below.

Table 3-9 – Test vehicle descriptions

Manufacturer:	**Toyota**	**Ford**
Model:	**Prius**	**Mondeo 2.0i**
Category:	saloon	saloon
Engine:	16V In-line 4 cylinder petrol + electric motor	16V In-line 4 cylinder petrol
Cylinder volume (cm^3):	1496	1988
Max Power (kW):	43kW @ 4,000 rev/min + 30kW @ 940-2000 rev/min	96 kW @ 5700rev/min
Max. Torque (Nm):	102Nm @ 4,000 rev/min + 311Nm @ 0-940 rev/min	176Nm @3700rev/min
Drive:	Front	Front
Curb weight:	1255kg	1328kg
Transmission:	IVT (planetary gearbox with IC engine and electric motor)	AT (4 speed)
0-100kph time:	11.9s	9.9s
top speed (kph):	162	206
Number of test drivers:	7	12

The AT Mondeo vehicle was tested using two different AT operating modes – economy and sports. These operating modes alter the behaviour of the AT gearshift points. Therefore, the data collected from the two operating modes are considered as coming from separate vehicle types.

Table 3-10 - Test vehicle power and torque to weight values

Manufacturer:	**Rover**	**Ford**	**Vauxhall**	**BMW**	**Toyota**	**Ford**
Model:	**216Si**	**Mondeo 2.0i**	**Omega 2.0**	**323Ci**	**Prius**	**Mondeo 2.0i**
Power to weight (kW/tonne)	*80.0*	*72.3*	*70.0*	*88.7*	*58.2 **	*72.3*
Torque to weight (Nm/tonne)	*141.5*	*132.5*	*129.4*	*173.8*	*329.1 **	*132.5*

Table 3-10 summarises the power to weight and torque to weight values for these vehicles (* the figures for the Toyota Prius are for the situation where both the IC engine and electric motor are producing their maximum powers/torques).

3.5.1 Toyota Prius

The Toyota Prius is a four-door saloon car and is one of the first petrol-electric hybrid vehicles to be sold in the UK. It has been on sale in Japan since late 1997. The Prius that was tested at the University of Bath was a Japanese market car on loan from its owners, Ricardo Consulting Engineers.

The Japanese car which was tested featured a 43kW, dual-overhead camshaft (DOHC), 16-valve, inline four-cylinder 1.5 litre petrol IC engine with variable intake valve timing producing 102Nm of torque. The engine runs a modified Atkinson cycle (Heywood, 1988) giving it a long power stroke and high expansion ratio thereby reducing pumping losses (Sasaki, 1998). The engine is limited to 4000 rev/min allowing lighter components to be used with the emphasis on fuel economy. The electric part of the hybrid system consists of an electric motor producing 30kW from 940-2000 rev/min with a maximum torque of 311Nm from 0-940 rev/min. Power for the electric motor is supplied by a battery pack directly behind the rear seat. The battery pack contains 240 individual nickel-metal hydride cells supplying 288V DC with an approximate capacity of 6.5Ah (1.8kWh).

The IC engine is coupled to the electric motor/generator combination via a planetary gearbox (in fact there are two motor/generator assemblies, which are used in combination to produce motive power, regenerative braking and battery charging charge the battery from the IC engine). This system allows the Prius to operate in a variety of modes depending on the driving conditions and vehicle requirements. These modes are as follows:

- Electric motor powers wheels; IC engine is switched off or charges battery – low speed/load operation.
- Electric motor powers wheels; IC engine powers wheels (and can also charge battery) – high (or medium) load operation.
- Electric motor produces regenerative braking; IC engine is switched off or charges battery – braking.
- Electric motor is switched off (low battery); IC engine powers wheels – low battery, high load mode
- Electric motor is switched off (low battery); IC engine powers wheels and charges battery – low battery mode.

3.5.2 Ford Mondeo

The Ford Mondeo test vehicle was a standard 1996 Ghia model 2.0l 4-speed automatic which had its standard engine and transmission replaced with a CVT unit as part of another project and then had a new engine and AT gearbox fitted (from an identical vehicle). Although the vehicle had been re-registered and passed as fit for road-use, it exhibited undesirable shifting behaviour at certain speed and pedal position combinations, which made the gear-shifts very jerky and resulted in gear hunting. It was therefore hoped that this range shifting behaviours would produce a wide range of driveability evaluations from the test drivers.

3.6 Test drivers

The drivers who carried out the testing in the current project were all engineers – staff and postgraduate students from the Department of Mechanical Engineering at the University of Bath. Some of these test drivers also took part in Wicke's testing which provided the opportunity to evaluate trends in their responses. Wicke's test drivers were also all engineers, both employees of the company sponsoring his work, as well as staff and postgraduate students from the department.

It is accepted that drivers fall into a number of different groups that are characterised by facets of their driving style as shown by Schoeggl et al. (2001). It is expected that a variety of different driving styles will be represented by the test drivers who took part in this project and the preceding project. It should be noted that these drivers were, by necessity of availability and time, not a representative cross-section of the population in terms of their gender and ages – all but one were male (one of Wicke's drivers was female) and all were engineers. The fact that the drivers were all engineers may make them more able to understand and analyse the vehicle behaviour due to their familiarity with engineering principals and their training to report events in an objective manner. There is no published data available which categorises drivers' driveability preferences for different combinations of age, gender, profession or any other differentiating factor, however it is accepted that there are in fact differences (List & Schoeggl, 1998). Such categorisation data could usefully be produced by analysing the characteristics of drivers who privately own/drive/buy certain types of vehicle, after correcting for spurious effect such as vehicle price, prestige value, and availability.

Table 3-12 contains the results of a questionnaire (shown in Table 3-11) filled out by the test drivers who took part in this project. This data were collected to assess the range of driving

experience which individual drivers possessed. These data were not used in the later analysis but were included for completeness.

Table 3-11 - Driver information questionnaire

Question
Driver's initials
Driver's gender
Driver's age
Driver's current car(s)
Driver's experience – number of cars driven
Driver's experience – range of cars driven

Table 3-12 - Driver questionnaire results

Driver	Gender	Age	Current car(s)	Experience - number of cars driven	Experience - types of cars driven
LJN	M	25	Renault Clio 1.2 & Toyota MR2 1.8	8	mini -> Peugeot estate, Toyota mr2
ACM	M	25	Peugeot 106 1.1	10	2.0l saloon cars, SUVs
PJN	M	25	Subaru Impreza 2.0	10	Vauxhall Corsa 1.2, Skodia Fabia 1.3, minibus, transits, VW Bora 2.0, Vauxhall Astra 1.3
CJB	M	35	Nissan Primera 1.6 & Ford Galaxy 1.9TDi	50	Tractors to sports; Lotus Elise, Ford Expedition, Mini Pickup, BMW 325, MPVs, etc.
MCW	M	25	Ford Escort 1.4l 5spd	4	VW Passat TDI 130ps, Ford Sierra 1.8GLX auto, Vauxhall Vivano 1.9TDi Van
MDG	M	27	VW Golf GTi 8v	6	1.0l Ford Fiesta, Vauxhall Nova SR, 4l Jeep Grand Cherokee, Ford Escort, Citroen Picasso
HHP	M	25	Mitsubishi Galant 2.0	10	Fiat Punto 1.2, 800cc -> SUV, Nissan 280
CDB	M	24	Vauxhall Cavalier 1.4	7	Toyota MR2 - MG metro 950
AC	M	39	Ford Fiesta 1.8TDi & Audi TT 180ps & Ford Focus 2.0	12	Ford Transit vans -> Audi TT
SGP	M	25	Renault Clio RSi 1.8i	50	Renault 5 1.1, Clio RSi 1.8, BMWs: 328Ci, 535i, Jeep 4x4s, VW Passat TDi
RSW	M	28	Peugeot 205 Dturbo	10	VW Polo 1.3 -> Audi S3, Diesels, naturally aspirated and turbo-charged from 1.5 to 2.4L
DMH	M	27	Citroen AX 1.0	20	Austin Allegro, Morris Ital, Ford Fiesta, BMW 318i

4 Methodology of the driveability testing

The tests used to analyse the drivability of a vehicle cover a range of manoeuvres experienced during the routine operation of the vehicle such as a tip in, a gearshift or pulling away from rest. However many of these aspects of vehicle drivability are normally given no thought by the driver in the normal course of operating the vehicle.

Current drivability testing employs a number of test drivers to drive a selection of pre-defined tests in a given vehicle, who then subjectively rate the vehicle for each individual test covering a range of characteristics such as smoothness, delay and initial acceleration.

The approach used by List and Schoeggl (1998) to subjective testing was to investigate a set of driveability criteria, such as subjective evaluations of gear-shift, engine start and idle quality, collected from test drivers interviewed during and subsequent to test driving. They found that more criteria were reported when the interview was conducted during testing than if it were carried out after the test. They also found that the more experienced the tester the greater the number of criteria that would be evaluated both during and after the test. Also the greater the problems exhibited by the vehicle the larger the number of criteria identified by the driver with a higher rating being directed towards the negative aspects of the drivability at the expense of positive aspects.

Vehicle calibration involves a far more comprehensive analysis of the behaviour of the vehicle extending beyond those criteria used during drivability testing, requiring both objective and subjective rating of the vehicle. These include the testing of engine start behaviour, engine idle characteristics and engine response in neutral.

The measurement of objective data is referred to in the papers by List and Schoeggl (1998) and Schoeggl et al. (2001), which consider how a driver's mind may be modelled by a computer, and asks the question 'What do humans feel?' The researchers used vehicle speed as detected by human sight, engine speed as detected by human hearing, acceleration detected by being 'pushed back in the seat' and pedal position being the only driver input considered.

4.1 Test program

The approach taken was similar to that taken by Wicke (2001). Objective data were obtained during test drives after which the driver would be asked for their subjective opinion of various

subjective performance and driveability metrics. These objective data were obtained using data acquisition hardware linked to a laptop computer on board the vehicle as described in Section 3.1. The laptop computer was then used to record the driver's subjective ratings and any comments made at the completion of the test.

Each test driver performed a set of 16 tests shown in Table 4-1; each of these tests was performed once. Each test had a specified initial speed and a specified pedal position that the driver would attain in a step fashion after the specified initial speed had been attained..

Table 4-1 - Test descriptions

Test Number	Initial Vehicle Speed (km/h)	Desired Pedal Pos'n (% of full travel)
1	0	25
2	0	50
3	0	75
4	0	100
5	2	25
6	2	50
7	2	75
8	2	100
9	12	25
10	12	50
11	12	75
12	12	100
13	40	75
14	40	100
15	60	75
16	60	100

The starting speeds of 40 km/h and 60 km/h were only assessed using 75% and 100% pedal positions as the pedal position needed to maintain the initial speed was often more than 50%, the lower pedal positions being impossible to achieve while maintaining a steady speed for the start of the test.

The test drivers were asked to drive steadily at the required initial speed (as indicated in Table 4-1), then to signal the author, who always sat in the front passenger seat, that they were ready. The DAQ equipment would then be started to record steady state data for approximately two seconds, then the driver would be signalled to perform the test by moving

the accelerator pedal to the required position. For the testing performed in the Mondeo AT vehicle, a gauge was fitted on the dashboard indicating the pedal position to help the drivers.

The set of tests used in this project, as described in Table 4-1, were chosen to be similar to the data recorded during Wicke's project, allowing both sets of data to be used together, to provide a range of different driving conditions for which the vehicle could be rated. It can be seen that there are 16 combinations of initial speed and pedal position demand, therefore different test combinations are assigned to a *driving condition* category, which means that a smaller number of subsets containing more data can be analysed.

Three driving condition categories were initially used for this project. These were based on the categories that Wicke used in his project, which are described in the table below from his thesis:

Table 4-2 - Wicke's definitions of driving condition categories (adapted from Wicke 2001)

Launch Feel	The tests in this category involved starting from rest with different but mainly large pedal movements.
Traffic Crawl	The starting velocity of the tests in this category are low (*3, 12* and *40 kph*) but more importantly, the pedal movements are low (below *25%* of the total pedal travel)
Overall Performance Feel	In this category, the drivers expected the cars to provide maximum performance quickly, e.g. when joining a motorway or overtaking another vehicle. The pedal position is always depressed half way or to its maximum position. The starting velocities of this driveability category were *12, 40* and *60kph*.

These categories were initially tested, however it was decided that the number of categories should be expanded to include additional driving conditions if possible. Therefore the driving condition categories shown in Table 4-3 below were tested.

Table 4-3 -Definition of the driving condition categories

Pull away	This category simulates a normal pull away manoeuvre. The tests in this category all start from rest (0Kph) and have small pedal movements of 25% and 50%.
Launch Feel	This category simulates a fast pull away manoeuvre. The tests in this category all start from rest (0Kph) and have large pedal movements of 75% and 100%.
Traffic Crawl	This category simulates driving in heavy traffic. The initial speeds of the tests in this category are low to medium (*2, 12* and *40 kph*) and have small pedal movements (*25%* of pedal travel)
Town Driving	This category simulates the range of speeds and pedal positions that might be expected while driving in town. The initial speeds of the tests in this category are low to medium (*2, 12* and *40 kph*) and have small to medium pedal movements (*25% and 50%* of pedal travel)
High speed driving/ overtaking	This category simulates high speed driving which might include joining motorways and overtaking manoeuvres. The pedal position is always 75% or 100% of its maximum travel. The starting velocities of this driveability category were *40* and *60kph.*
Overall Performance Feel	This category attempts to capture all of the performance tests that might occur across a range of driving conditions. The pedal position is always depressed to 75% or 100% of its maximum travel. The starting velocities of this driveability category were *12, 40* and *60kph.*

It was found that some of these categories produced only small correlations (R^2< 0.3. See section 6.6.3 for a definition of the correlation size).Therefore, a smaller set of three categories was chosen. These are shown in Table 4-4. These categories are similar to those used by Wicke. The *Traffic Crawl* category was expanded to include larger pedal movements, which made it a *Traffic Driving* category. This decision was taken both because it was found that the low pedal movement results showed significant scatter that made producing correlations difficult and also because, while Wicke was interested specifically in outliers in the small pedal position data as he was looking to improve CVT shift-quality, this project is focused on the evaluation of driveability using multivariate techniques which requires a consistent body of data from which trends can be obtained.

Previous research has used similar types of categorical grouping of driveability test data. List and Schoeggl (1998), Schoeggl and Ramschak (200) and Schoeggl et al. (2001) list the following driveability/operation modes amongst others:

- Cruising
- Normal driving
- Acceleration/performance
- Tip-ins
- Drive away
- Gear shift

It should be noted that they say each of these driving modes contains further, more precisely defined driving conditions, however they do not state what these are. Dorey and Holmes (1999) used a range of test conditions for their testing. These include:

- Pull away
- Tip-in (city driving)
- Tip-in (highway driving)
- Acceleration from low to high speeds
- Gearshifts

They do not give any more information about the specific tip-in sizes, or relevant vehicle speeds. Dorey and Martin (2000) used a range of driving manoeuvres for their research, these included:

- Light throttle pull-away
- One third (pedal position) tip-in and acceleration to 30 km/hr

They also describe the analysis of tip-in events and Wide Open Throttle (WOT) acceleration responses at a range of engine speeds in 2nd gear.

It should be noted that the range of categories that were chosen and used in this research did not attempt to cover the full range of driving conditions. These category areas were identified as useful areas of driveability to investigate after consulting the literature and assessing the testing data already available at the University. It should also be noted that due to the financial and time limitations of the research, the full range of pedal positions and speeds contained in the categories could not be covered. A subset of manoeuvres incorporating a range of large and small pedal movements at high and low vehicle speeds was chosen for the purposes of validating the approach used. A practical calibration exercise would require a larger range of manoeuvres to be included to cover all possible

driving situations. The driving condition categories that were used for this project are shown in the table below:

Table 4-4 -Definition of the driving condition categories

Launch Feel	The tests in this category all start from rest (0Kph) and have large pedal positions of 75% and 100%.
Traffic Crawl (Town driving)	The initial speeds of the tests in this category are low to medium (*2, 12* and *40 kph*) and the pedal positions are small to medium (*25% to 50%* of pedal travel)
Overall Performance Feel	This category produces manoeuvres where the drivers require maximum performance very quickly. For example when acceleration to join a motorway or when overtaking another vehicle. Pedal position is always 75% or 100%. The starting velocities of this driveability category were *40* and *60kph.*

After each test, the drivers filled out a questionnaire, shown in Table 4-5, describing the driveability aspects of the vehicle for the manoeuvre that was carried out. This process is described in Section 4.2.

4.1.1 Testing difficulties

A number of issues were noted while performing the testing and data acquisition. These are explained in the following sections.

4.1.1.1 Driver pedal/speed accuracy

An issue that affected some drivers was not being able to attain the correct pedal position or vehicle speed and this did not improve even after a number of practice-runs. This problem affected the Prius during its initial testing, as there was no visual indication of the pedal position available for the driver to refer to. In the main testing of the Prius and the AT Mondeo, a visual pedal position indicator was provided for the drivers to use. This indicator improved the pedal position accuracy as can be seen in Section 7.1.

The pedal/speed inaccuracy is troublesome purely from the point of view that the driver is driving at a speed/pedal position other than that which they think they are using – the speed errors are relatively small with a mean error of 2kph (see Figure 7-11) and the driver can see outside and hence judge their speed so this is really not an important issue. The pedal position errors are more important as they are significantly larger (see Figure 7-12) which could give the driver a false impression of the vehicle's performance. However this does not

cause any issues for the analysis as the actual speeds/pedal positions are recorded and used during the analysis rather than the test speeds/pedal positions.

It was also seen that sometimes drivers performed a series of steps in their pedal input, rather than a single step or ramp input. This generally happened as they realised that they had not depressed the pedal sufficiently. Figure 4-1 shows a pedal position trace containing steps. In this test the target input was 50%. It can be seen that the eventual level reached by the driver was 46%, and this was achieved in a number of steps.

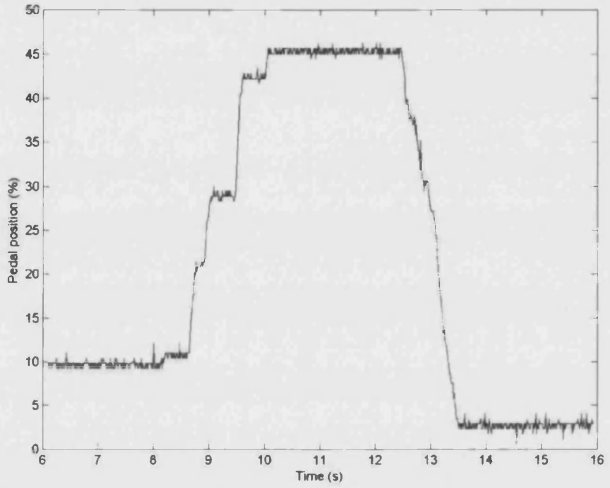

Figure 4-1 - Pedal position steps

Provided the steps are performed sufficiently quickly, the test can be considered to be a slow application as opposed to a step input. However, the fact that there are steps means that the automatic pedal position detection code has to be quite sophisticated to differentiate between the start of the manoeuvre and the flat regions during the steps (see Section 5.3.4.1 for more details).

Similarly, on some occasions, drivers pressed the pedal too much and then after realising that they had overshot the required test position, they lifted off. This trend seemed to affect drivers of vehicles without a visual pedal position indication and even some of those with this aid tended to overshoot the desired pedal position. This may be because the drivers had misjudged the amount of force required or the speed at which to move the pedal rather than having misjudged the amount to move it. This effect can be seen in Figure 4-2, in which the driver has initially overshot the target pedal position of 50%, before attaining a level of approximately 52% for the remainder of the test.

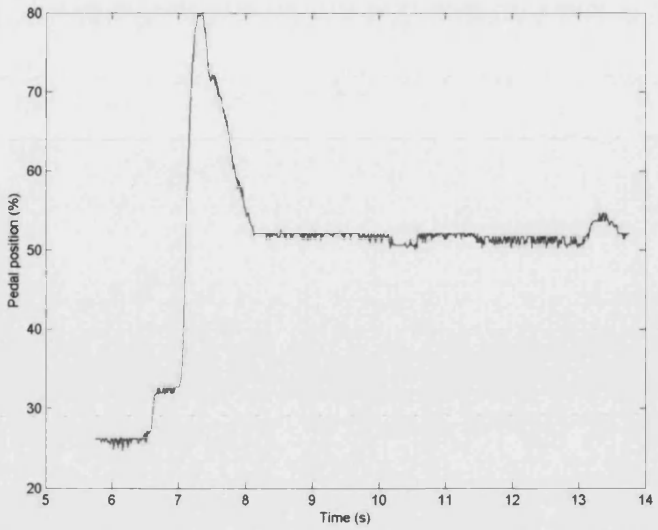

Figure 4-2 - Pedal position overshoot

This will almost certainly have an effect on the way the vehicle is then rated as the driver will have experienced an initial acceleration for a larger pedal input than was expected, followed by the reduction as they realised their mistake. The difference in accelerations between the overshoot and lift-off positions will contrast with one another and may alter the driver's rating.

Both of these pedal adjustments tended to occur more frequently in the vehicles without a visual pedal position indicator. It is therefore the author's recommendation that in future research the driver is allowed to perform a number of test-drives to obtain a feel for the pedal position using the pedal position indicator rather than using feedback from the test supervisor as was the case in those vehicles without the indicator. Using the pedal position indicator during a test is not recommended as in this case the driver is concentrating on the indicator rather than the vehicle performance. In this research the drivers were allowed to familiarise themselves with the pedal position before each test and were then instructed to ignore the indicator during the test.

There is little indication from the literature as to how commercial companies achieve accuracy when performing tip-ins to a given pedal position level. In fact, although there is literature showing that these manoeuvres are performed (e.g. Dorey & Martin, 2000), there is no indication of how the exact sizes of the tip-in events are controlled, or whether they need to be controlled for the tests which are being performed.

4.2 *Subjective test data*

4.2.1 Subjective metrics

It was decided that for this project the same subjective metrics would be collected as were collected by Wicke for his PhD project (2001). His choice of metrics was in turn influenced by those collected by Deacon (1996) for his PhD project. This choice was taken to enable the data collected by Wicke to be used in this project and because these metrics appear to offer a useful assessment of longitudinal driveability characteristics.

A small amount of introductory training was given to the test drivers before they started to drive the vehicles. This consisted of a written description of which tests were to be performed and which aspects had to be assessed (Table 4-5). The test drivers then had the opportunity to test drive the vehicle for a short period of time (usually 5 to 10 min) to get used to it and to have the opportunity to perform different pedal position inputs with feedback on their pedal position accuracy. Immediately after each test, with the car stationary and engine at idle, the driver answered a verbal questionnaire (the questions which were asked are shown in Table 4-6 and the driver was reminded of the rating scale as each question was asked) asking them to rate the car's performance in various categories. This questionnaire was originally developed by Wicke for testing carried out during his PhD (Wicke, 2001).

Table 4-5 – Description of subjective metrics

Subjective metrics	Description
Smoothness:	Smoothness is the absence of unwelcome discontinuities or disturbing vibrations (e.g. caused by load reversals or stiction) in the driveline over the whole time of the manoeuvre until shortly before the pedal is released again. The smoother the ride, the higher the assessment should be. If it was not thought to be smooth, the driver has the opportunity to comment on the source of the vibrations.
Engine Delay:	Time between a first change in pedal position and a first noticeable change in the engine speed. A high mark should be given, if the engine delay time was felt as being appropriate. If it was not thought to be appropriate, the driver has the opportunity to comment whether it was too long a delay or too short a delay.
Vehicle delay:	Time between a first change in pedal position and a first noticeable change in the vehicle speed. A high mark should be given, if the vehicle delay time was felt as being appropriate, but note that this depends on the driving situation. If it was not thought to be appropriate, the driver has the

	opportunity to comment whether it was too high a delay or too short a delay.
Jerk (as in performance feel):	This aspect assesses the sensation felt by the driver - after the vehicle delay - of the initial change in acceleration (initial push back in the seat). This change occurs in a narrow time window of up to half or one second. A high mark should be given, if the jerk was felt as being appropriate, but note that this again depends on the driving situation. If not, the driver has the opportunity to comment whether it was too big or too little a jerk.
Acceleration feel/progression:	The sensation felt by the driver of the vehicle response to an increase in pedal position over about a 5 second time period. The time period starts after the vehicle delay, when the acceleration can be felt for the first time and ends before the driver releases the pedal. A high mark should be given, if the acceleration was felt as being appropriate, which again depends on the driving situation. If it was not thought to be right, the driver has the opportunity to comment whether it was too low or too high an acceleration.
Overall driveability feel:	All aspects mentioned earlier should be included into this category as a single mark. Confidence in controlling the vehicle and predictability of vehicle responses should lead to a high assessment.

Table 4-6 –Subjective metric questionnaire

Subjective metric	**Rating (Driver complaint = 1, excellent = 10)**
Smoothness rating	
Engine delay rating	
Vehicle delay rating	
Jerk (as in performance feel) rating	
Acceleration feel/progression rating	
Overall driveability feel rating	

By collecting identical subjective metrics and objective data, comparisons can be drawn between the data collected in this project and that collected by Wicke (2001).

Some additional subjective metrics were collected during the testing of the AT Mondeo vehicle, to focus on specific areas of interest for AT equipped test-vehicles. Due to the variability of the quality of the vehicle's shift behaviour, it was decided that these additional subjective metrics might produce useful range of subjective driveability evaluations. Subjective metrics were collected for all tests in which a gearshift (or shifts) occurred. The description sheet and questionnaire used for to collect these data are shown in Table 4-7 and Table 4-8. These subjective metrics are listed below:

- Kick down smoothness
- Up shift smoothness
- Up shift timing
- Gearbox response

Table 4-7 - Gear-shift metric descriptions

Driveability Value	Description
Kick down smoothness	The quality (speed, smoothness) of the initial gear down-shift
Up shift smoothness	The quality (smoothness) of the first gear up-shift
Up shift timing	Rate whether the gear up-shift occurred too early or too late (both poor ratings) or at the appropriate time.
Gearbox response	Overall rating of the gearbox performance. This encompasses gear up- and down-shifts, including the timing, smoothness and speed of these shifts.

Table 4-8 – Gear-shift questionnaire

Question	Rating (Driver complaint = 1, excellent = 10)
Kick down smoothness rating	
Up shift smoothness rating	
Up shift timing rating	
Gearbox response rating	

It should be noted that it was found that this number of ratings was sometimes difficult for some of the untrained (or not highly trained) drivers to concentrate on and remember over the course of a test. In fact on some occasions the drivers were forced to repeat a test (the data for the original was discarded) so that they could concentrate better on particular details and they were also encouraged to verbalise their thoughts as they were carrying out the test to both help them to remember and also so the author could record and repeat this to them should they need to be reminded while answering the questionnaire.

4.2.1.1 Rating scale

Wicke's research was based on the optimisation of a poorly calibrated CVT transmission's control strategy so therefore he focused his subjective questionnaire on determining how bad the faults were in the vehicle's driveability.

This is a valid approach when the test vehicle is poorly calibrated, and when the test drivers know the nature of the faults they are rating. In this project, production vehicles were being tested and therefore it was decided that this fault-based rating system would be of less use as these vehicles should be relatively fault-free and driveable. The value of applying an automated driveability system to these vehicles is to optimise their driveability (to make what is adequate better), to focus the calibration for a particular class of driver (i.e. sporty or relaxed/comfortable, etc.) or to emulate specific driveability quirks and features which might be desirable characteristics of other manufacturers' vehicles.

Therefore, although the same subjective metrics were recorded to enable comparisons between the data collected in this project and that collected by Wicke, the rating system was changed to eliminating some of Wicke's categories at the lower end of his scale. This resulted in a rating scale from 0 to 10. This increased the granularity of the scale and should make the ratings more reliable and easier to understand for untrained test drivers (Friedenberg, 1995, p.120; Thorndike et al., 1991).

Wicke's rating scale was originally designed by Deacon in collaboration with his industrial collaborator, the Ford Motor Company (Deacon, 1996). This rating scale is an interval scale (Torgerson, 1958, p31). The drivers answering this questionnaire were not supplied with the descriptive labels, which are shown in Table 4-9, while they filled out the questionnaire. Instead, they were given the descriptions and the limits of the scale: Production reject – poor = 1, and excellent = 10, and asked to choose a score between these limits. The labels attempt to describe the ratings typically assigned to certain performance traits and the class of driver able typically to detect the behaviour in question (Deacon 1996). Table 4-9 shows Wicke's rating method:

Table 4-9 – Wicke's subjective metric rating scheme

<table>
<tr><th>Rating Index</th><th>Evaluation</th><th>Condition noted by</th></tr>
<tr><td>1</td><td rowspan="3">Production reject – poor</td><td>All drivers</td></tr>
<tr><td>2</td><td rowspan="3">Average drivers</td></tr>
<tr><td>3</td></tr>
<tr><td>4</td><td>Driver complaint</td></tr>
<tr><td>5</td><td>Borderline</td><td rowspan="4">Critical drivers</td></tr>
<tr><td>6</td><td>Barely acceptable</td></tr>
<tr><td>7</td><td>Fair</td></tr>
<tr><td>8</td><td>Good</td></tr>
<tr><td>9</td><td>Very good</td><td>Trained observer</td></tr>
<tr><td>10</td><td>Excellent</td><td>Not perceptible</td></tr>
</table>

It should be noted that ratings from one to three are classified as 'Production reject - poor. This wide-ranging scale was required as Wicke was testing a developmental vehicle, which

did stray into this region of the driveability envelope; however, the vehicles that were tested as part of the current project were all production standard, and would therefore not appear in this region of the rating scale. This problem was noted by Bergman (1973) in his paper evaluating vehicle handling. He notes that only the top part of a 10 point scale which encompasses all possible handling evaluations, from a minimum conceivable level of handling to that of perfect handling, would generally be used when testing for production vehicles. This is because vehicles scoring less than a value of 5 would not be acceptable for production. His solution was to use a 10 point scale, but only ranging over the handling performance that is expected from production vehicles. It is for this reason that the scale was altered in this research. The 'evaluation' and 'condition noted by' descriptions are included to predict how they relate to Table 4-9, but were not made available to the drivers. Table 4-10 shows the rating method used in this research:

Table 4-10 – Current project's subjective metric rating scheme

<table>
<tr><th>Rating Index</th><th>Evaluation</th><th>Condition noted by</th></tr>
<tr><td>1</td><td>Driver complaint</td><td>Average drivers</td></tr>
<tr><td>2</td><td rowspan="2">Barely acceptable</td><td rowspan="7">Critical drivers</td></tr>
<tr><td>3</td></tr>
<tr><td>4</td><td>Borderline</td></tr>
<tr><td>5</td><td rowspan="2">Fair</td></tr>
<tr><td>6</td></tr>
<tr><td>7</td><td rowspan="2">Good</td></tr>
<tr><td>8</td></tr>
<tr><td>9</td><td>Very good</td><td>Trained observer</td></tr>
<tr><td>10</td><td>Excellent</td><td>Not perceptible</td></tr>
</table>

The rating scale used in this project was also designed as an interval scale which can be mapped directly onto the scale used by Wicke to enable the data collected in both projects to be compared. The drivers were not supplied with the descriptive labels shown in Table 4-10 while they filled in the questionnaire. Instead, they were given the descriptions of the limits of the scale: Driver complaint = 1 and excellent = 10, and were asked to choose a score between these limits.

The data collected during this project are automatically mapped onto Wicke's rating scale when compared with the data he collected, ensuring that the full range of data can be used (this is possible as his scale is the broader). For comparisons carried out solely using the new subjective metrics the scale is not altered. This has no effect on the analysis of the data.

The mapping was performed using the following algorithm:

$$Rating_{old\_scale} = \left(Rating_{new\_scale} - 1\right) \times \frac{6}{9} + 4$$

This transforms the readings in the following way:

Table 4-11- Subjective metric conversions

Rating Value - new method	Rating Value - old method
10	10
9	9.33
8	8.67
7	8
6	7.33
5	6.67
4	6
3	5.33
2	4.67
1	4

Chen (Chen et al., 1997) noted the fact that sometimes drivers were unable to answer a question, and he therefore included a "Don't know" answer for the drivers to avoid forcing an answer that is not correct. The same scheme was considered for this project, however it was decided that due to the small number of test drivers, the driver would be allowed to repeat a test (the original test data were completely discarded and the driver was told to read the questionnaire descriptions to refresh their memory) if they were not able to rate any of the subjective aspects to ensure that as much useful data as possible could be recorded.

4.3 Objective test data

The following objective data were recorded during each test:

- Vehicle acceleration
- Vehicle speed
- Engine speed
- Accelerator pedal position
- Elapsed test time

These data were recorded at a frequency of 100Hz during the testing of the Prius and at a frequency of 80Hz during the testing of the AT Mondeo due to differences in the data acquisition equipment. The reduction in data acquisition frequency was acceptable as the frequency components of interest have a frequency of 5Hz or lower (graphs showing the power spectral density functions for a typical set of test data are shown in Appendix XI) and additionally the CADET data acquisition hardware contained anti-aliasing filters (CP Engineering, 2001).

The test equipment used to record the Prius data was limited to recording 12s of data, however the CADET 12 system developed during this project was able to perform continuous recording allowing longer accelerations to be performed. Despite this ability, the length of the taxiway on which the testing was performed (see Section 3.3) meant that the majority of tests lasted less than 20s.

Although other groups have included additional objective data, for example Dorey and Martin (2000) note that they additionally record manifold pressure, mass airflow, fuel pulse width, ignition timing and exhaust air fuel ratio, due to the limitations of time and hardware available to instrument vehicles it was not possible to capture these additional data. The one exception is manifold pressure. This was recorded for the Prius test vehicle, however Wicke found no correlations with manifold pressure and therefore did not record it for the Omega and BMW vehicles. Therefore, with manifold pressure data available for only half of the test vehicles, it was decided to exclude it from further analysis.

5 Metric generation

5.1 Aims of automated metric generation

There were two main aims in designing and implementing a system that automates the metric generation process: The first was to make development easier and faster by reducing the amount of manual data manipulation that is required. For example, Wicke (2001) was forced to calculate his metrics manually as well as having to perform re-calibration and data reconstruction tasks. The second aim was to make the process sufficiently robust and easily enough deployed to be used in real-time vehicle testing.

5.2 The automation of metric generation

The analysis of large amounts of data requires that as much as possible of the process is automated enabling it to be performed quickly and, reliably with repeatability and accuracy. Therefore an aim of the current project has been the automating of both the processing of raw data files (from vehicle data acquisition for example), and the analysis and correlation of the data in these files together with subjective ratings so that the user is simply presented with the list of correlation results. The *MATLAB* programming language, version 6.5, from *The Mathworks Inc.* has been used throughout this project for all data processing and presentation tasks including data correction, metric generation and correlation generation and analysis (Mathworks Inc., 2002). The choice to use *MATLAB* was made due to its efficient matrix and vector data handling structure and its availability at the University.

Although implementing the automation was initially a time-consuming process, it has been beneficial as it is now possible to very quickly add or remove metrics and to make alterations to their method of calculation and then re-calculate the correlation equations. Additionally, the automation makes it very simple to add new test data with only minor adjustments to allow for file format differences and differences in data calibration.

One of the major problems with automated data processing is that it can be difficult to identify faulty data and once processed this faulty data can seriously affect the results of an investigation. To ensure that sensor calibration drift as well as faulty sensor equipment did not adversely affect the results, a routine was developed to analyse the recorded objective data before it is processed to produce correlations to ensure that the data do not contain errors (this analysis is described in Section 5.3.2). If the data are found to be faulty, they are automatically re-calibrated, re-generated or replaced using other data which have not been

found to be faulty. The calibration of the objective data is first checked for both accelerator and pedal position offsets and if necessary adjusted without user intervention.

If all of these steps fail, the faulty data are excluded from the data processing and a warning is issued so that the tester can, if required, ascertain what the problem was after the processing has been completed.

5.3 *Extraction of driveability metrics*

It was decided to extract representative metrics from the time series data in order to reduce the amount of data that needed to be recorded, stored and processed. This was carried out after each driver had finished their complete set of tests. The use of metrics reduces processing time (due to the reduced amount of data that must be processed) and produces more easily understood correlation equations.

Figure 5-1 shows some typical time series data recorded during testing of the AT Mondeo vehicle (economy mode). After these data are recorded, they are processed to produce the objective metrics.

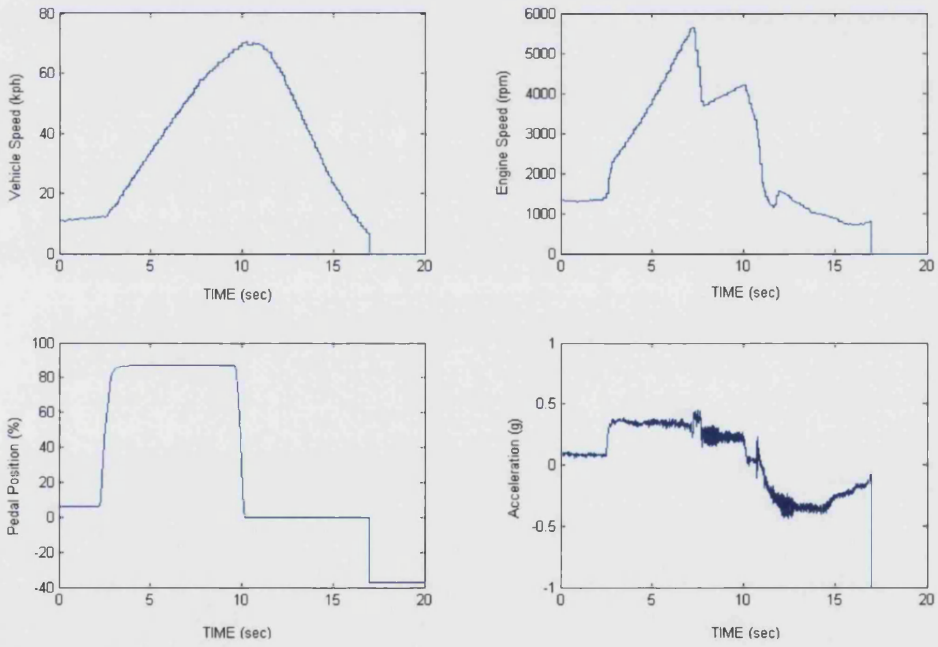

Figure 5-1 – Example time domain data from AT Mondeo (economy mode)

This process can be applied to the time series data from a single test, for example to allow real-time testing, or to entire sets of previously recorded data. In either case, the process is

completely automated by the code developed during this project allowing the operator to concentrate on analysis rather than the processing itself.

The analysis of the time series data and the generation of the metrics requires approximately one second per set of test data, so it is possible to implement metric generation as part of a continuous testing scheme where a manoeuvre is carried out and the time series data is recorded, then as soon as the manoeuvre is finished, the metrics are generated and could be analysed immediately after the manoeuvre. This approach was partially tested during this project by analysing the entire data set for an on-road driving session at the end of the test session. It was found that major manoeuvre types could easily be detected automatically, however it was difficult for the driver to evaluate any given part of the driving session. Therefore, the use of driver commentary was investigated (whereby the driver evaluates each manoeuvre or any significant driveability events as they occur in a continuous verbal commentary). Unfortunately, the lack of monetary funds in the current project meant that only 2 test drivers could be insured to drive the test AT Mondeo vehicle on public roads, and therefore this approach was abandoned after these initial tests on the grounds that there would be insufficient data available. It should be noted that this approach does hold promise for obtaining data in real-world conditions and as such is a promising area of research that is being actively pursued (Baker et al., 2006).

The 35 driveability metrics, which are described in Section 5.4, were automatically calculated using the data within the time series data files. The choice and calculation of the metrics could be easily altered or added to, due to the modular nature of the code. The code automatically processed the results from a complete set of test runs (i.e. all the tests performed by one driver) and output a separate data file for each test containing the calculated metrics and subjective ratings.

This procedure was developed to be generic. The system of generating metrics separately from the correlation generation code means that data from different DAQ systems (with different sampling rates and calibrations for example) can still be used with the correlation code. This has been shown in this research, where data from two separate systems in different formats has been combined and processed together.

As an example demonstrating the procedure, a selection of generated objective metrics for an acceleration demand or "tip-in" manoeuvre is listed below:

- Maximum vehicle acceleration
- Initial jerk
- Delay time (between pedal movement and start of acceleration)

Figure 5-2 shows a graph of vehicle acceleration and pedal position against time. The initial pedal movement, initial vehicle acceleration and maximum acceleration point are labelled. These times and magnitudes are automatically determined by the code and are used to generate driveability metrics. It should be noted that this list is not exhaustive and that other times and magnitudes are also calculated and used to generate other metrics. The delay time is calculated from the difference between the initial acceleration and initial pedal movement times. The initial jerk is calculated from the gradient of the acceleration over the first second of the test.

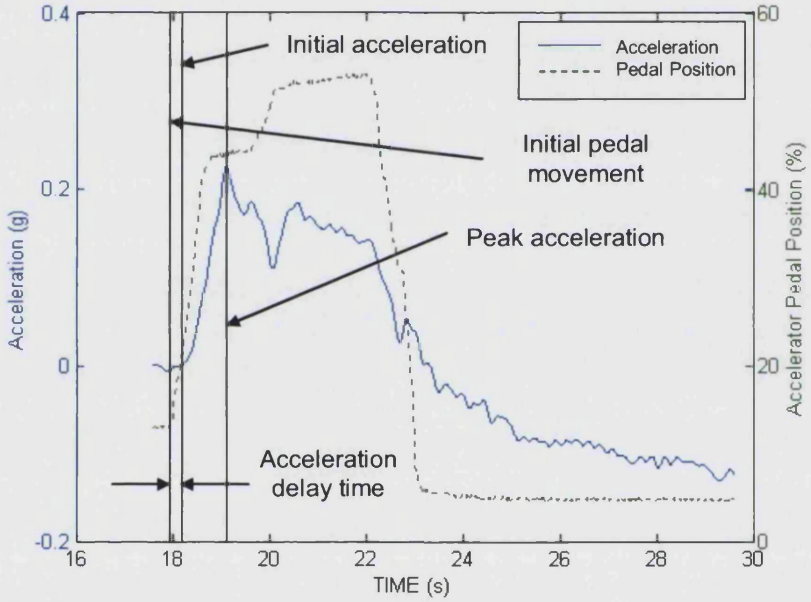

Figure 5-2 - Delay time calculation

Objective metric	Value
Peak vehicle acceleration	0.226g
Initial jerk	0.305g/s
Delay time (between pedal movement and start of acceleration)	0.271s

The driveability data used in this research were originally recorded to determine those aspects of AT performance that drivers liked, so that these could be applied to an experimental CVT (Wicke et al. 1999; Wicke, 2001). Wicke's recorded data include both gearshifts and kick-downs. Since gearshift quality is a very important aspect of driveability for both ATs and the newer Automatic Manual Transmissions (AMTs) these aspects have

been rated and interpreted for the AT Mondeo vehicle tested during this project as a first step in establishing whether these events could be automatically evaluated.

5.3.1 Choice of metrics

Initially a large number of metrics were used to test that the system worked correctly. However it was soon realised that the use of large numbers of metrics can result in the correlation generation phase taking a long time. Additionally, for noisy or small sets of data, there is the possibility of an uncorrelated variable randomly producing a correlation and therefore being added to the equation. By reducing the number of extraneous metrics used in the correlation generation, this chance is reduced.

The original metrics were therefore removed if they did not show any correlation with the recorded subjective metrics (i.e. these metrics did not appear in any of the correlation equations), leaving only those that did show a correlation.

It should be noted that some of the last metrics that were removed had relatively high partial correlations and high occurrence frequencies. They were removed from the set because they represented averages that could not characterise the manoeuvres from which they were generated. Two examples of this kind of metric are: *aAverageSpeed*, the average vehicle speed over the course of the test; *aAveragePedalPosition*, the average pedal position over the course of the test. Although these variables were often found in the correlation equations, their physical meaning is not useful for either prediction or modelling of powertrain performance without knowing more about the test type. As both are averages, the data from which they come can behave in a range of ways that cannot be differentiated simply using these metrics.

In the case of *aAverageSpeed*, other metrics such as initial speed, acceleration and deceleration rates and maximum speed are needed in addition to the average speed to characterise the test in a useful manner. It was therefore decided to remove these metrics despite their apparent correlation (see Section 6.4.4).

Other more complex metrics were developed based on expert-knowledge of the type of effects that might affect people's ratings. The metrics fell into the following categories:

- Vehicle speed based (e.g. max speed)
- Acceleration and Jerk based (e.g. max Jerk)
- Engine speed based (e.g. max engine speed)
- Pedal position based (e.g. rate of change of pedal position)
- Time based (e.g. delay time)

A number of papers, for example those by Dorey and Martin (2000) and Jansz et al. (1999), highlighted acceleration overshoot and oscillations as important metrics in vehicle driveability. Attempts were made to develop metrics to measure these effects, however the very noisy acceleration data in combination with the range of test manoeuvres whose data were included made the automation of this process highly error-prone and therefore these metrics were excluded from the analysis.

5.3.1.1 Gear-shift metrics

The driveability aspects of conventional automatic gearbox powertrains are well established and mainly relate to the characteristics of the engine while driving in a single gear. The majority of papers relating to AT driveability are concerned with gearshift quality, start from rest feel or vehicle behaviour during tip-ins.

Küçükay (1995), has investigated the shift quality of automatic transmissions and identified the following objective metrics as the most influential to driveability (listed in order of importance):

- Magnitude of vehicle acceleration
- Noise inside the vehicle
- Vehicle responsiveness (in terms of both delay time and acceleration)
- Frequency of gear changes

Schwab (1994) looked at the correlations between a number of objective metrics and subjective shift quality in an attempt to develop a gearshift quality metric. He found correlations with the following objective metrics:

- Peak-to-peak amplitude of acceleration (after filtering)
- Peak-to-peak jerk
- Maximum average engine power
- 10-14 Hz frequency content (vehicle body and suspension resonances)

5.3.1.2 Other significant metrics

There are many factors that may have an effect on the drivers' rating of vehicle driveability and which would ideally be ignored by the vehicle test drivers, however due to the subjective nature of people's evaluations these may need to be considered and standardised. These factors include the following:

Vehicle expectations

A major part of this would be related to the vehicle manufacturer/make due to connotations associated with the style/class/expense of the vehicle. This is itself a very subjective classification and although not directly related to driveability analysis, it will have an effect on drivers' ratings which it would be difficult to overcome without using a single vehicle for which the powertrain calibration could be altered to simulate different vehicles' driveability characteristics.

There are a variety of subjective factors that could be considered here:

- Vehicle marque (may set expectations due to the known quality of the marque as well as set expectations of the vehicle's performance and behaviour)
- Vehicle exterior exhibiting sporty accessories (leading to expectations of the vehicle's performance and behaviour)
- Vehicle interior bias towards a sporting or luxury feel (e.g. sports seats) (again leading to expectations of the vehicle's performance and behaviour)
- The quality and feel of the controls operated by the driver (raising expectations due to the overall 'quality feel' of the vehicle)
- Seat quality/positioning (this will affect how the driver enjoys driving the vehicle and therefore may affect their ratings)
- The firmness of the suspension and the non-longitudinal handling (this relates to the bias between sporty or luxury as well as to how comfortable the driver finds driving the vehicle)

A number of these factors are classified by the J.D. Power Survey (J.D. Power, 2005). The metrics which they use are listed below:

- Mechanical quality
- Interior quality
- Exterior quality
- Service experience
- Performance
- Interior comfort
- Style
- Ownership costs

Unfortunately, some vehicle types tested are not available in the survey data. It should also be noted that the J.D. Power survey classifies vehicles into broad swathes (e.g. The closest classification for the *BMW 323Ci* is under *BMW 3 Series*, which comprises a range of six engine sizes and types (petrol and Diesel) and three different interior trim levels. In addition, the *BMW 3 Series* could potentially classify three different body styles – coupe, saloon and estate, the majority of which have differing specification in terms of standard equipment and suspension setup, to the vehicle that was tested).

One aspect of the J.D. Power survey that may be applicable is the Nameplate Index Ranking. This is a ranking of the overall appeal of a given manufacturer's vehicles. These data are also from the USA, meaning that the class expectations may well be different to those in this country, however it may provide some indication of the overall appeal of the different vehicles. The rankings are shown in Table 5-1, below.

Table 5-1 - 2005 APEAL Nameplate Index Ranking

Manufacturer	Ranking (1000 point scale)
BMW	898
Toyota	857
Industry average	855
Ford	848
Chevrolet (Vauxhall)	838

Two conclusions can be drawn: Firstly that both BMW and Toyota are seen as being above average, while both Ford and Chevrolet are seen as below average. Secondly, BMW's ranking is significantly removed from and higher than those of the other manufacturers'.

Sound quality

For sporty vehicles, the presence of engine/exhaust noise may be expected. The converse is also true, in that for luxury vehicles engine/exhaust noise is not wanted, however there is some overlap for certain driving conditions with both vehicles that will either positively or

negatively influence the overall subjective rating of a given vehicle. (Autocar, 2002; Schoeggl et al., 2001).

Refinement and Noise/Vibration/Harshness (NVH)

One less subjective measure, is that of refinement and NVH. This is generally classified by experienced test drivers, however it would be useful to develop metrics to accurately classify a vehicle's NVH score. This would enable calibration engineers to test how drivers react to levels of NVH under certain operating conditions – e.g. at idle, full acceleration, etc. This would allow calibration engineers to focus on the particular operating regimens when NVH is most noticeable.

Table 5-2, below, shows some possible subjective and objective factors that may influence the test drivers' scores for the subjective metrics that were used in this research.

Table 5-2 – Subjective and objective factors affecting the recorded subjective metrics

Subjective metric	Possible subjective factors	Possible objective factors
Smoothness	Quiet cabin; comfortable seats and suspension; linear pedal-torque mapping (no sudden bursts of power)	Smooth transitions/pickup of engine speed; engine refinement (in terms of the decay rate, and transient fuelling behaviour)
Engine Delay	Engine speed decay rate (though this is in the opposite sense, it would add to the overall impression). Engine torque – this will alter how quickly the engine will accelerate and indicate a delay to the driver	Accelerator pedal to throttle mapping; inlet manifold volume and transient fuelling strategy (and therefore engine acceleration); accelerator pedal slack.
Vehicle Delay	Engine delay; suspension hardness; seat hardness; possibly steering wheel feel/sharpness.	Driveline wind-up/play; gearbox ratios and shift-times (for AT). CVT strategy.
Init accel - Jerk	Engine and vehicle delays; suspension hardness; engine noise; engine/exhaust noise	Engine delay; pedal mapping
Accel prog - Acceleration	Engine/exhaust noise; suspension/seat firmness	Pedal mapping; engine map (torque/power map); outright performance of vehicle.
Performance - Driveability	Vehicle marque	Mixture of factors affecting the other metrics, with the emphasis shifting depending on the driver type (e.g. a 'sporty' driver may be more affected by the accelerative abilities, with a more 'relaxed' driver more affected by the smoothness and delays).

5.3.2 Automated data verification and replacement

Although a small number of sensor failures are to be expected, meaning that such tests could therefore generally be ignored, it was found that the test data collected by Wicke contained many sensor failures and poorly calibrated data sets. As these test data are an important and valuable set of data it was decided that an automatic system would be implemented to detect these errors and to correct them where possible.

As around 1 Kbytes of data, or about 500 readings, were generated each second during the tests, it was necessary to automatically check each stream of data to ensure that it was valid (not off-scale due to a sensor drop-out or poor calibration, poorly calibrated producing inaccurate values–this can be very difficult to detect, or constant value due to a sensor failure) before it was processed and used to produce metrics.

Detecting the following error conditions is the main goal of this process:

- Sensor/conditioning dropouts or poor calibration– indicated by off-scale high/low values.
- Sensor failure – indicated by a constant value for the returned data
- Poor calibration – this is difficult to detect automatically and must be handled on a per-channel basis. It is indicated by data that exceed the ranges and magnitudes expected for a given channel for a given manoeuvre.

Sensor dropout and failure can be detected in one of two ways (depending on the sensor and conditioning equipment setup). A faulty sensor will either start producing constant value data, or go off-scale low or high. Both of these effects are relatively easy to detect automatically.

Poor calibration is more difficult to detect as the data can be of the right order of magnitude, with only a small relative error. In the easiest case since it can be seen that the returned data moves off-scale, then returns – this is indicative of either poor calibration, or a temporary sensor drop-out and will normally be handled as if the entire data stream were faulty (as it is not possible to recover the data which was off-scale).

Errors caused by poor calibration, which do not go off-scale, are detected by assuming that the sensor calibration remained constant for a given set of tests (the tests are demarcated by their names or time-stamps and generally encompass all of the test performed by a single driver), and determining whether the various sensor values agree with initial test conditions – for example start-from-rest tests should have an initial speed of 0kph, an initial acceleration

of 0g and an initial pedal position of 0%. Meanwhile 100% tests will have a maximum pedal position of 100%.

Other poorly or un-calibrated data are easier to detect, often because the returned data is of the wrong magnitude (e.g. a 16-bit integer value being returned rather than an acceleration in multiples of 'g') or is significantly outside the expected range for a given variable. It is sometimes possible to automatically re-scale this data using the above criteria to provide a baseline (e.g. start from rest will have 0 kph, 0% pedal and 0g acceleration), though otherwise the data is marked as bad, and replaced if possible (if it is not possible to replace the data, it is automatically excluded).

Although these checks are not perfect, they do detect the vast majority of poorly calibrated tests, which, in many cases, can then have their data automatically re-generated using other recorded metrics as a basis. Each set of data is automatically validated using this methodology to determine whether any data are missing or invalid before being used to generate metrics.

5.3.2.1 Vehicle speed validation and replacement (from acceleration)

The first check determines whether the vehicle speed data is all a constant value, which indicates a faulty sensor. The data are then checked to look for readings which show a speed of >140Kph or <0Kph. If more than a second (non-consecutive) of either type of data is found then the data is marked as faulty, if values outside these bounds are found but of less than one second total duration, these data are replaced by the averaged value of their neighbours.

If the vehicle speed data are found to be faulty, they are replaced by integrating the vehicle acceleration with a suitable factor determined for each vehicle. The initial speed is determined from the test type and the point at which to start the integration process is determined by assuming zero acceleration at the point just before pedal movement begins (this is part of the acceleration normalisation/correction procedure – see Section 5.3.2.2)

5.3.2.1.1 *Poor vehicle speed sensor calibration*

Figure 5-3 presents a set of data from Wicke's project that suffers from poor sensor calibration. This can clearly be seen from the value of the recorded vehicle speed data as seen in the data collected from the CVT Mondeo vehicle shown in Figure 5-3 below.

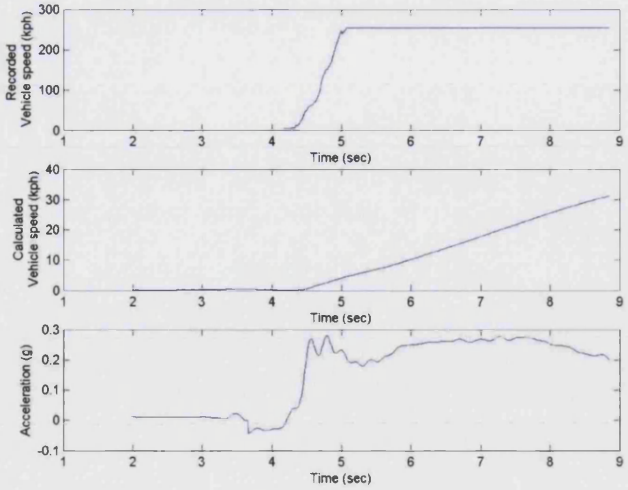

Figure 5-3 – Torotrak Mondeo data

The recorded data is incorrect as vehicle speed ramping from 0 to 255kph in one second is not physically possible, and in fact the maximum speed of 255 is an indication that the data has gone off-scale high (this is the maximum value of an 8bit number: 2^8-1). Therefore the vehicle speed data is regenerated from the acceleration data (assuming it is itself deemed to be valid by checking that it is non-constant and does not exceed the maximum range set at ±1g).

Figure 5-4 shows the vehicle speed data calculated from the vehicle acceleration with the recorded data re-scaled and plotted on the same axes. It can be seen that there is good agreement between the two sets of data until the recorded data reaches a constant value of approximately 5kph. It was as this point that the poor calibration caused its movement off-scale while being recorded.

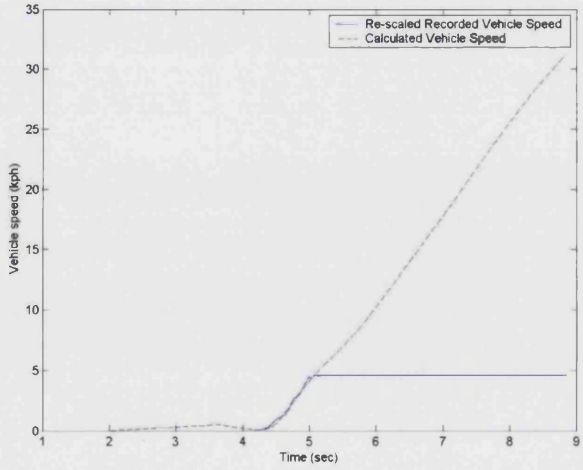

Figure 5-4 – Poorly calibrated data regenerated: Torotrak Mondeo data

To validate this method of vehicle speed re-generation a number of tests were performed comparing the generated data with non-faulty vehicle speed data. These figures can be seen in Appendix VII. It was found that the majority of the re-generated vehicle speed traces had good accuracy (less than 5% error between the re-generated and actual speeds) with only a small number with larger errors. Despite the presence of some inaccuracy in the re-generation method, it was decided that as even the largest inaccuracies were only around 10% of the actual speed this was sufficiently accurate, and without the use of this re-generation technique, a large proportion of Wicke's data would be unusable.

5.3.2.1.2 Blocky signal

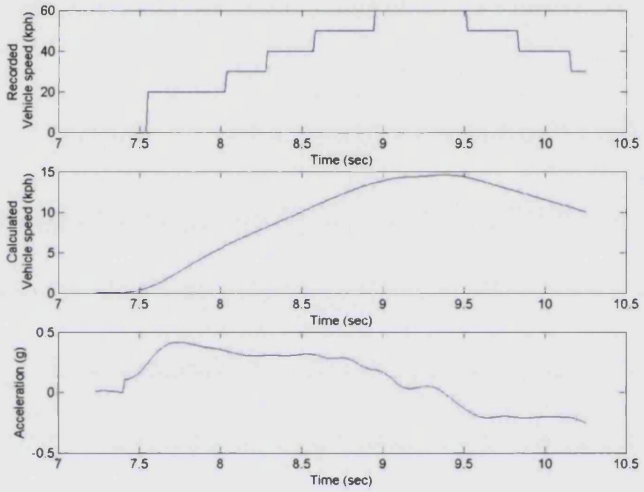

Figure 5-5 – Blocky signal

Figure 5-5 shows a combination of poor calibration and a blocky, low frequency signal. The blockiness of the signal is caused by a low update rate, which indicates a poor choice of speed encoder pulse-counter.

5.3.2.1.3 Faulty vehicle speed sensor

Figure 5-6 shows what looks like random noise in the recorded vehicle speed data while Figure 5-7 and Figure 5-8 show less random but equally faulty data.

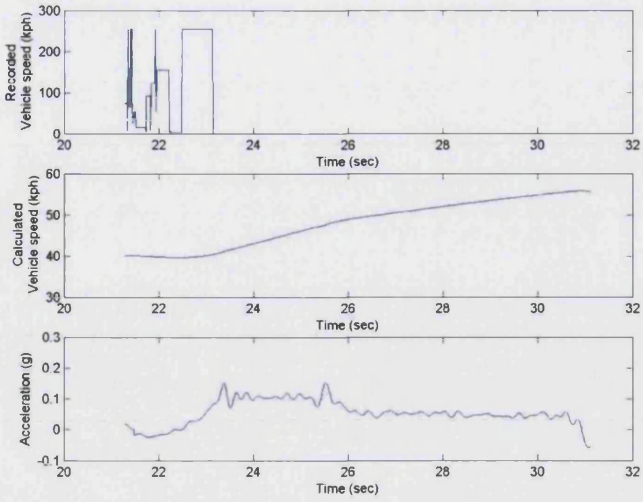

Figure 5-6 – Blocky signal

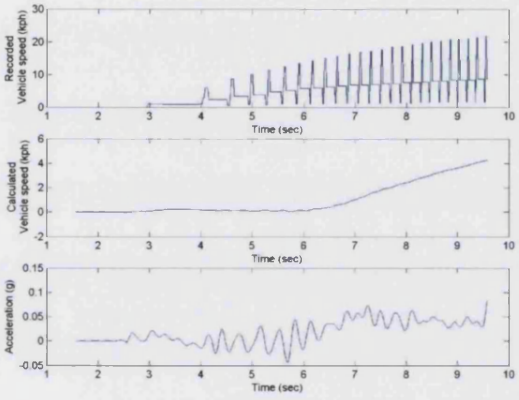

Figure 5-7 – Faulty vehicle speed sensor

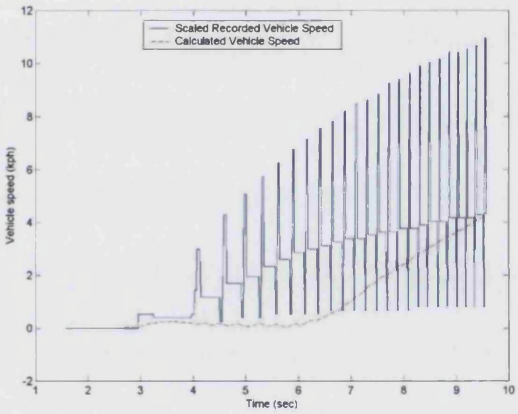

Figure 5-8 – Faulty vehicle speed sensor

These are all characteristics of the failure of the speed encoder (which Wicke noted had happened for some of his tests due to water ingress). These data must be detected and replaced.

Another issue encountered was that of a continuously faulty sensor, however this can be easily detected due to its constant value, and is re-generated using the recorded acceleration data as for the other types of faulty data.

5.3.2.2 Acceleration data validation and replacement

As the majority of the acceleration data were found to be valid with no dropouts, or sensor failures, though sometimes with an offset or poor scaling, it was decided that it was not necessary to try to automatically replace defective acceleration data. Although replacing the

data using vehicle speed data is possible, there would be a number of problems with doing this. Firstly there are a very high number of vehicle speed failures or poor calibrations in the data set that was recorded by Wicke with the old DAQ equipment. These tests would not be able to have their acceleration data re-generated. Secondly, due to the manner in which the speed sensor works (pulse counting), its accuracy at low speeds is limited. This would make the acceleration date generated at low speeds inaccurate and would preclude a useful measure of the acceleration delay time.

The acceleration data for some tests (namely the Prius tests) were found to contain high frequency noise due to the accelerometer type and its calibration, therefore these data were smoothed to remove these effects otherwise the automated analysis becomes difficult due to the myriad oscillations and gradient changes. Computational smoothing was carried out on the data using a window-based digital finite-duration response filter provided by the MATLAB programming environment (function name: *fir1*). To prevent any phase distortion, the data set was filtered in both the forward and reverse directions (function name: *filtfilt*). The filter was chosen to be a low-pass type as the high frequency oscillations were to be removed. The exact filter parameters were chosen by testing a variety of filter orders and cut-off frequencies and observing the resultant smoothed data. The eventual parameters were an effective order of 200, and a cut off frequency of 5Hz.

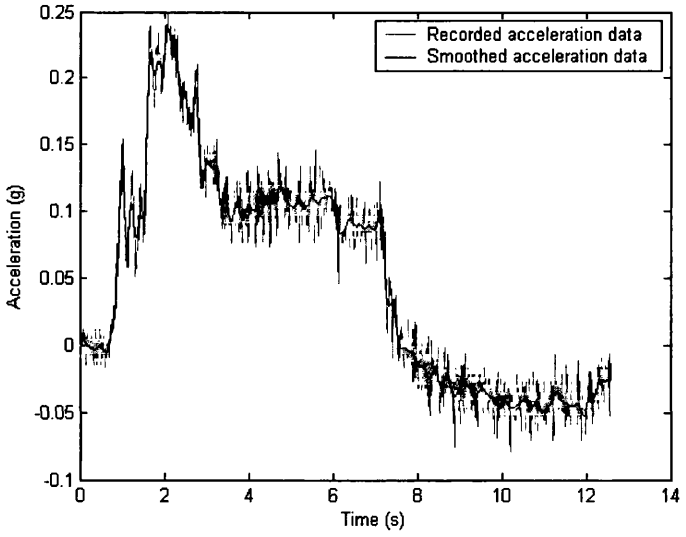

Figure 5-9 - Metric generation: acceleration smoothing

The difference between the smoothed and raw data can be seen in Figure 5-9, above.

5.3.2.3 *Removing non-valid data at the end of tests (for CADET DAQ system)*

When performing a test using the CADET-based system, the test was stopped in two stages – firstly the recording equipment was switched-off programmatically and then the test session was stopped on the computer and the data were saved to disk. The process of stopping the recording of the objective data was carried out as the test-driver brought the vehicle to a stop and the subjective data were recorded with the vehicle at idle. In the time between the recording equipment being switched-off and the test session being closed, data continued to be recorded on all the channels but with an off-scale low value (as this is what was returned from the now inactivated sensors). These data must therefore be detected and removed otherwise they will interfere with the automatic generation of various metrics (especially those which involve minimums, means and gradients).

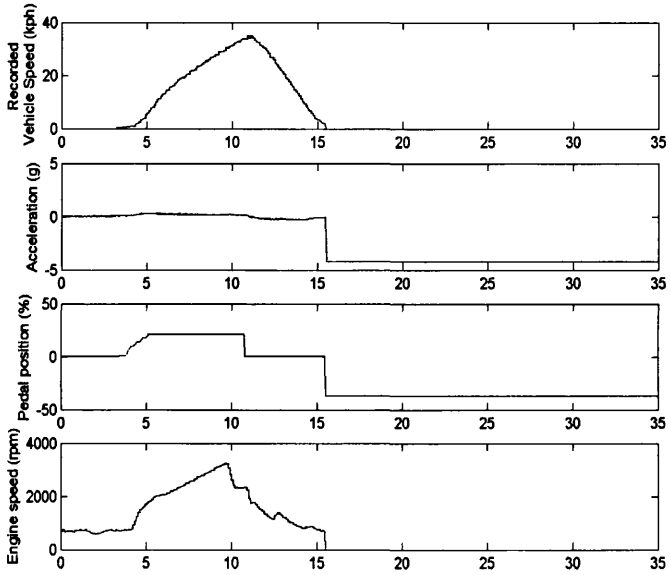

Figure 5-10 - End of test data drop-outs

Figure 5-10 shows this effect on the vehicle speed, acceleration, pedal position and engine speed data. The data shown in red (starting just after 15s) is the off-scale low data recorded after the test has finished but before the DAQ system has been shutdown.

5.3.2.4 *Engine speed data drop-outs and overflow correction*

Some of the engine data collected by Wicke in his PhD project suffers from corruption caused by the dual effects of malfunctioning engine speed sensors and an interaction of the acquisition and the pulse encoder counting frequencies. The malfunctioning engine speed sensors cause spikes or 'drop-outs' in the engine speed data as seen in Figure 5-11 below.

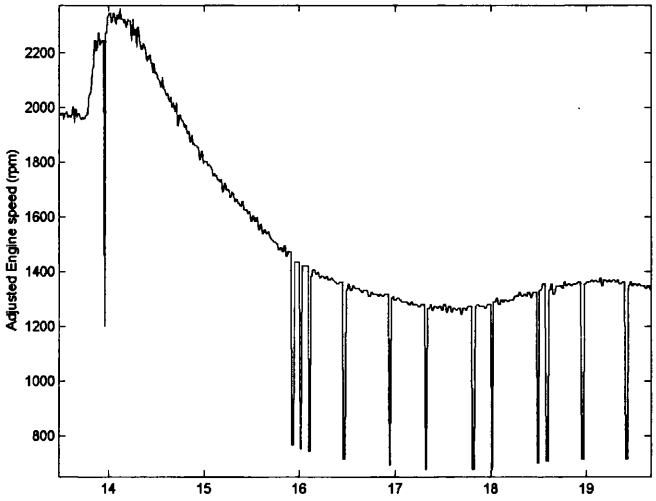

Figure 5-11 – Engine speed data drop-outs

The data acquisition and pulse encoder frequency interaction for the parameters chosen for Wicke's testing causes an interesting, and difficult to detect, effect in the data. This effect is that once the engine speed rises above a value of about 3450 rpm the sensor data appears to move to a value of 1780 rpm and then continues moving normally from there (this can be see in Figure 5-12 below – note that the high frequency oscillations seen on the right-hand side of this figure may also be related to this effect) – the opposite is also true, in that as the engine speed falls and passes though a true value of 3450 rpm (shown as 1780 rpm as the data have already overflowed), it jumps up to about 3450 rpm and the indicated and true engine speeds once again match. It should be noted that the transition points can stray somewhat from these figures, and that the transition is not normally a direct movement. The transition tends to take a number of time steps to happen and/or there are a number of high frequency oscillations before it stabilises at its new level.

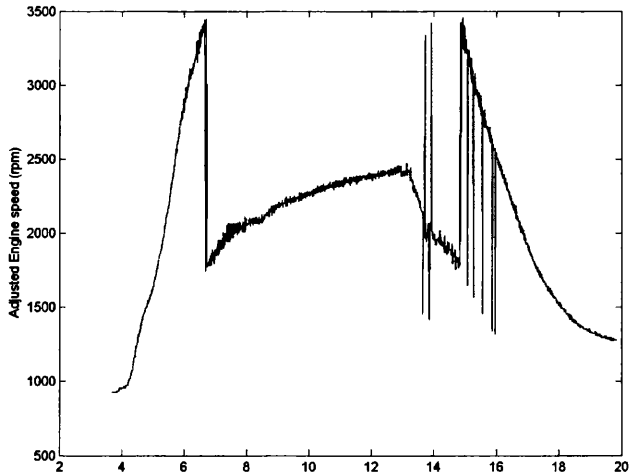

Figure 5-12 - Engine speed data overflow

This behaviour is believed to be caused by a combination of the sampling rate of the DAQ equipment and the pulse rate of the speed encoder itself. As some of the engine speed data were recorded using an inductive sensor on an engine injection lead, another possibility is that multiple pulses are employed over part of the engines speed range, confusing the sensor calibration. To overcome this type of problem for the testing in the current project a higher sampling rate and higher accuracy. (more pulses per revolution) encoder were employed. This consisted of a Hall-effect sensor and pulse counter which were used to count the teeth on the cam-shaft sprocket (see Section 3.2.4 for a description of the engine speed acquisition system).

However the data that Wicke recorded were still valuable and could be salvaged with some care. The approximate transition speed was found, after some analysis of the data trends, and then the metric generation code was programmed to deal with this overflow error and the occurrence of dropouts. The correction code worked using a number of steps to eliminate both dropouts and spikes and to move the offset data back to its correct position. The first stage looks for instantaneous (that is lasting only one time-step) drops or spikes with a magnitude greater than 800rpm. This threshold value was chosen as it was sufficient to detect the drop outs while still being safe from detecting false positives as it is not physically possible to achieve this kind of engine speed change ~ 800rpm in 1/100th of a second. Any drops or spikes that occur over a single time-step and then return to within 10% of the original value are simply removed by substituting the erroneous value with the mean of the two surrounding values.

In Wicke's data, there were, however, many dropouts that lasted more than one time-step as seen in Figure 5-13.

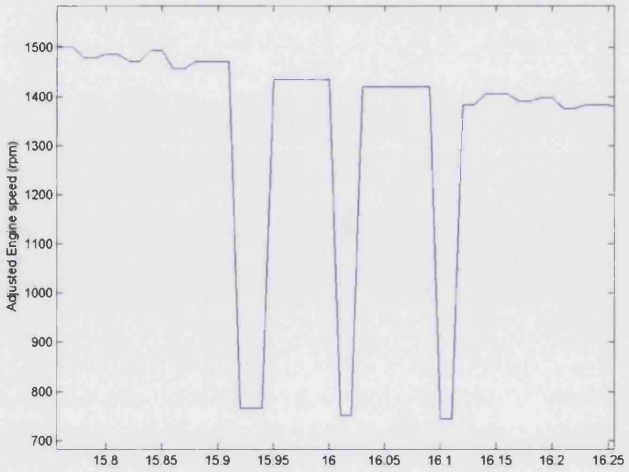

Figure 5-13 - Variable length drop-outs

Many of the dropout events also had descents or rises which were not instantaneous but instead lasted for a number of time-steps as seen in Figure 5-14. These often contained both steps and high frequency oscillations, which made the analysis even more difficult.

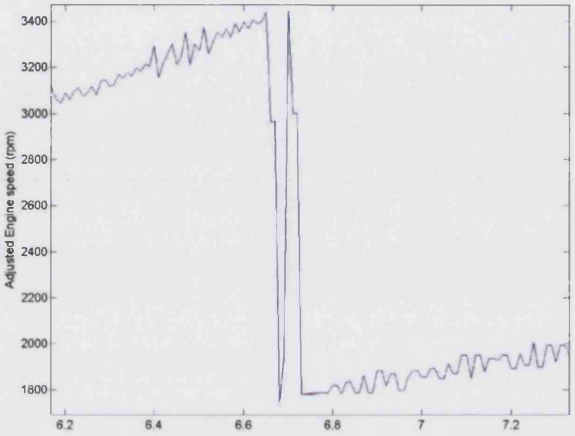

Figure 5-14 - Steps and oscillations

In the next stage, both stepped and long-lasting drop-outs/peaks are detected and removed, and any engine speed over-flows are detected and removed. The first stage is to look for instantaneous drops or peaks with magnitudes of at least 250rpm. These are measured against the mean of the previous 10 values and must last more than one time-step to ensure that stepped spikes are also detected correctly, are flagged and are processed further. After each spike, the remainder of the data are processed to determine the exact point at which their value returns to within 10% of the pre-drop/spike value. Once this value had been found the post-drop/spike value is found by calculating the median of the 10 samples after the initial drop/spike itself. This step is performed to remove the effect of stepped drops/spikes and oscillations. The difference between this post-drop/spike value and the original value is used to decide whether to treat the current artefact as a drop-out/spike or as an engine speed overflow. It should be noted that in some of the test data processed as part of this project, the test ended before the engine speed data overflow could return to normal. These tests are also handled by the code described above if no return to the original pre-drop-out value can be found .

If the event is found to have a magnitude of less than 1500rpm, it is treated as a drop-out/spike. As the majority of these multiple time-step drop-outs/spikes tend to be of very short duration, the erroneous data are simply replaced by fitting a straight line between the two values surrounding the erroneous data points.

If the event is found to have a magnitude greater than 1500rpm, it is treated as an engine speed overflow and the affected data are simply adjusted by the difference between the good value and the post overflow value.

Figure 5-15 and Figure 5-17 show the engine speed data plotted against time for two different tests that required adjustments. In both figures, the top-most graph shows the initial data, the middle graph shows the data after any single time-step drop-out/spikes have been corrected, and the bottom-most graph shows the final result of the data processing after multiple time-step drop-outs/spikes and engine speed overflow has been corrected. Figure 5-16 and Figure 5-18 show the same data on the same axes so that the changes can be better compared.

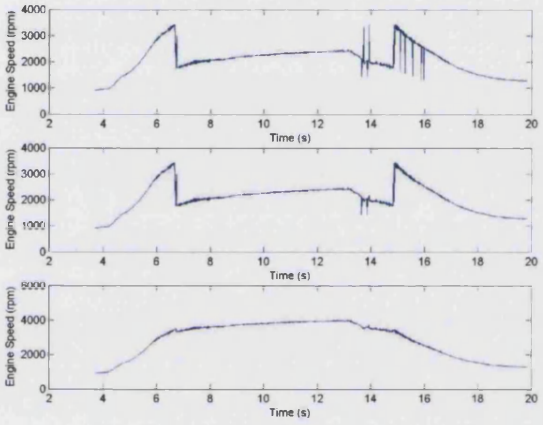

Figure 5-15 - Engine speed data correction: Example 1, split figures

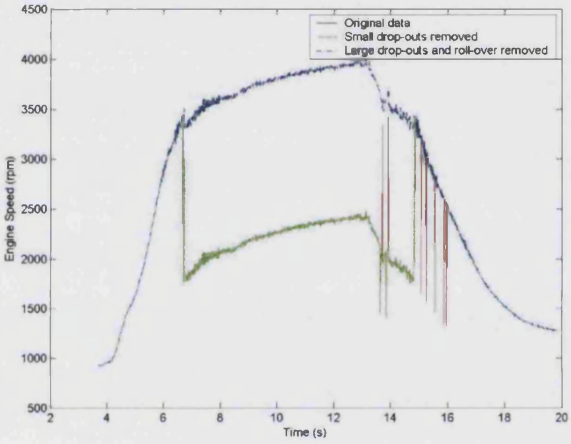

Figure 5-16 - Engine speed data correction: Example 1, combined figures

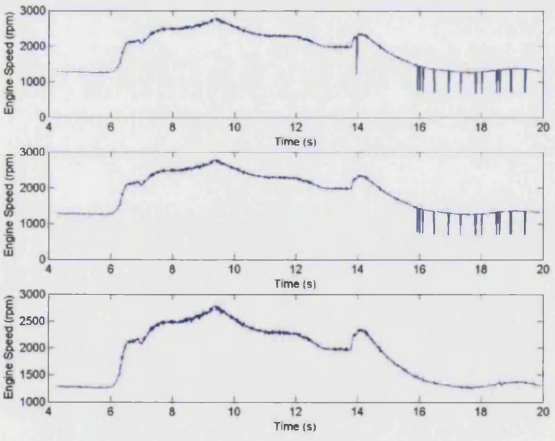

Figure 5-17 - Engine speed data correction: Example 2, split figures

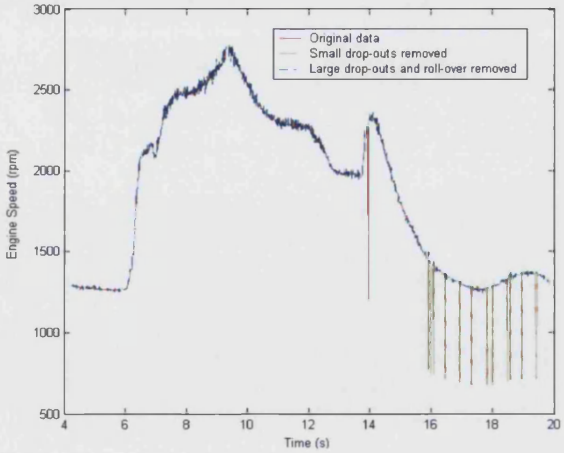

Figure 5-18 - Engine speed data correction: Example 2, combined figures

5.3.3 Automatic data re-calibration

Automatic re-calibration is carried out on data which passes the validation tests but which has been found to have suspect values that indicate a possible mis-calibration or drift of the data acquisition sensors' values.

The re-calibration is performed to allow for drift or small errors in the sensor calibration between tests. In this project, the re-calibration has been performed on acceleration and pedal position data as their values can be corroborated using other sensor data. It would also be possible to perform this automatic re-calibration on other variables as long as the test type or test data provide sufficient information to establish the correct gain and offset for the data.

5.3.3.1 Pedal position data

The pedal position scaling and offsetting is determined by examining the difference between the 0kph start speed values for pedal position (as these will have an initial 0% pedal position) and those for the 100% demand position tests (which should have a maximum value of 100%). The pedal position values for all tests in a given testing session (that is the series of tests performed on a given vehicle by a given driver) are automatically offset and re-scaled to take account of the maximum and minimum values recorded during that session.

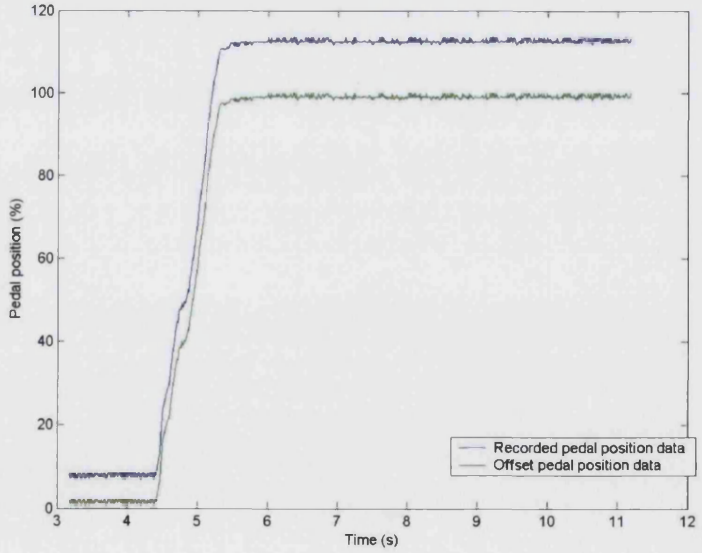

Figure 5-19 - Pedal position data offsetting and scaling

Pedal position sensor errors are also detected by looking for tests which contain only constant value data. In these cases there is no way of determining the actual pedal movement and these tests are therefore excluded from further testing.

5.3.3.2 Acceleration data

The acceleration data are then checked to see if they require offsetting. This is determined on a per-driver basis (it is assumed that the accelerometer position will remain constant over the comparatively short testing period). The zero-acceleration position is determined by looking at the value of the accelerometer before the manoeuvre is started (itself determined by looking at the pedal movement) for tests with an initial speed of 0Kph. The entire set of data for a given driver is adjusted depending on the offset determined from this calculation. This is necessary as during Wicke's testing the accelerometer was mounted beneath the driver's seat, which meant that it was disturbed by the test-drivers, when adjusting the seat. These disturbances resulting in a tilting of the accelerometer's position which changed not only the zero position but also, due to the change in angle, the scaling of the acceleration. This can then be overcome and accounted for by determining the angle at which the accelerometer was lying (from the offset, knowing the vertical acceleration due to gravity).

If the acceleration data are now found to exceed imposed limits (1g – this limit is applied to the smoothed acceleration) after the adjustments, the data are assumed to be poorly calibrated and the test is rejected and excluded from further use.

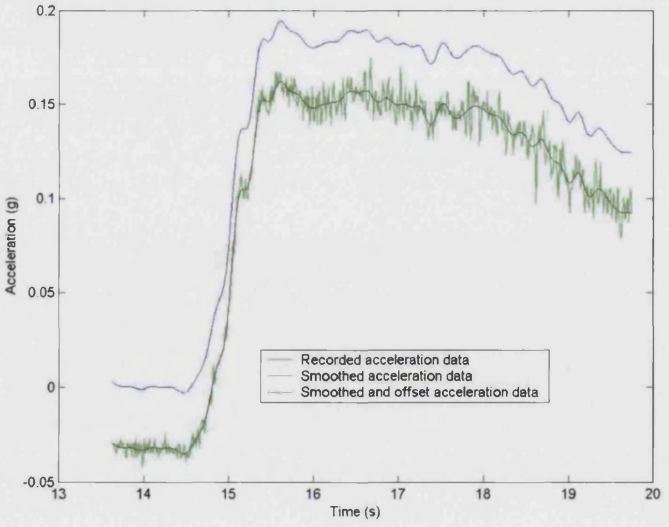

Figure 5-20 – Comparison of original and smoothed and offset acceleration data

5.3.4 Automated event detection

A number of self-explanatory calculations are performed on the time series data, or parts thereof, in the course of the metric generation process. These include the calculation of maximum, minimum and mean values, ranges and differentials, and combinations of the above. Some additional calculations must also be performed to extract more complex information from the time series data. These are explained in more detail in the next sections.

5.3.4.1 Manoeuvre start detection (for delay time calculation)

One of the metrics that Wicke found to be of great importance was the time delay between a driver's pedal demand and the vehicle's response. To accurately measure this delay the precise instant at which the pedal is depressed and the time at which the vehicle starts to accelerate must be determined, as these are the input and response that the driver is rating.

The initial pedal movement is used to determine the beginning of the delay time, however there was a choice of using the vehicle speed or acceleration data to determine the end of the delay time. Initially, the end of the delay time was determined by looking for an increase in the vehicle speed; however, the majority of the tests were carried out with the vehicle initially moving in a quasi-steady-state condition and although ideally the driver would control the vehicle to maintain a steady state condition, this was not generally possible due to driver ability and reaction-time limitations.

The fact that the vehicle speed was not constant before the start of the tests makes using this technique to determine the exact manoeuvre start point difficult to ascertain with the required degree of accuracy. In addition, some of the manoeuvres required only small pedal inputs and therefore very gentle acceleration, this meant that the vehicle speed increased quite gradually, making the accurate determination of its start point very difficult.

It was because of this that the focus switched to the analysis of the acceleration data, which had the advantage of being very sensitive, but had the associated disadvantage of containing a significant amount of noise. The acceleration data were even more noisy in the 'steady-state' region before each test than the vehicle speed data, for the same reason as was explained above. However, the high sensitivity of the acceleration data made it possible to determine the start point of an acceleration ramping far more accurately than was possible with the vehicle speed data after smoothing the data.

5.3.4.1.1 Acceleration start detection

To determine the exact start point a threshold technique was initially employed whereby the start point was determined by looking for the point at which the value of the data exceeded a pre-set threshold. However, it was found that due to the noisiness of the pre-manoeuvre 'steady-state' acceleration data a large threshold was required to avoid the false detection of the start point. This in turn added a variable length artificial delay to the returned acceleration start time.

Therefore a more complex method was developed by the author to both ignore the significant 'steady-state' noise and also accurately determine the start of any ramping once it had been discovered. This technique involves looking for the point at which the acceleration exceeds a threshold value; smoothing and rolling averaging are performed to reduce the amount of high frequency noise in the acceleration data making it easier to determine direction trends. The start point of the acceleration is found by working back towards the start of the test from the point at which the threshold was exceeded using a flexible gradient following technique developed by the author. This technique follows the gradient but avoids local minima. This technique was inspired by the method of steepest descent (Arfken, 2001) and simulated annealing algorithms (Kirkpatrick, 1983). As the acceleration data tend to be inherently noisy, they require smoothing and averaging to remove/reduce this noise; however this significantly reduces the sharpness of the data values and therefore the accuracy the with which the data can be analysed. Therefore, to determine the start position more accurately once its general position has been found, a technique was developed which used threshold values for the first and second differentials of acceleration to determine the precise start time.

This technique proceeds as follows. The acceleration data are analysed time-step by time-step from the point at which the pedal movement starts until the end of the valid test data. The pedal position data are less noisy than the acceleration data and therefore the start of pedal movement is calculated first. As the start of vehicle acceleration must occur after the pedal movement, this value can be used to reduce the amount of the 'steady-state' acceleration data that must be analysed.

If the value of the current data point is less than a pre-set threshold value (50% of the maximum value of the acceleration data from the start of the pedal movement to the maximum detected during the test), then the point is ignored and the next point is

considered. If the value of the current data point does exceed the threshold, then the acceleration start time is definitely before this point and the process of finding it begins. Example acceleration data can be seen in Figure 5-21, where the horizontal line is the threshold. It should be noted that the use of such a large threshold value avoids picking up any acceleration oscillations that may occur during the 'steady-state' period before the start of the test.

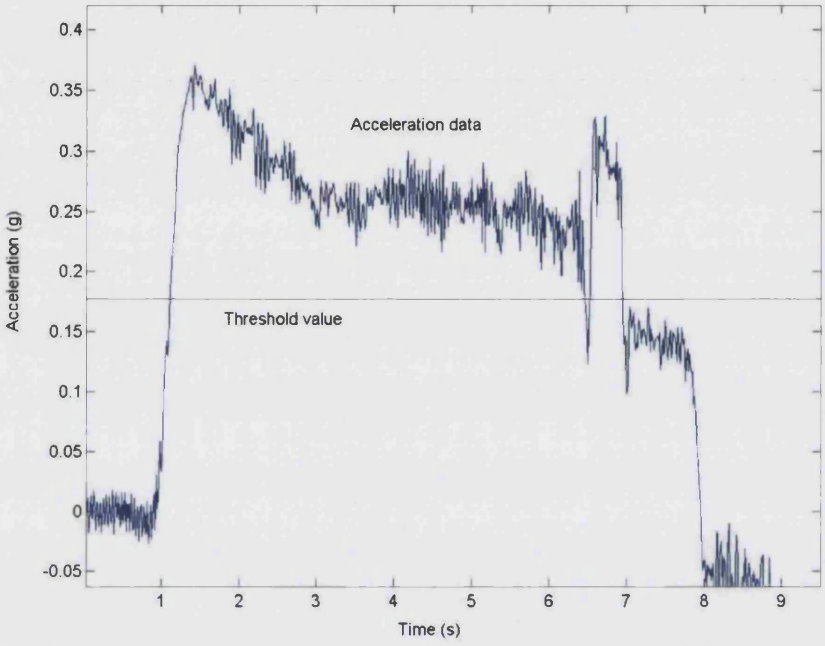

Figure 5-21 – Acceleration threshold point

The acceleration data are smoothed to remove frequency components above 5Hz as explained in Section 5.3.2.2 and the code starts moving back from the point at which the threshold was exceeded towards the pedal start point (towards the start of the data). If any points are found where the gradient of the acceleration is constant (over two time-steps), indicating that the constant speed region may have been reached, or where the gradient becomes negative, this may indicate the start of the vehicle acceleration.

One of these gradient changes can be seen in Figure 5-22 and Figure 5-23 below. These figures show the original acceleration data and the smoothed data respectively. The horizontal red line indicates the acceleration threshold value.

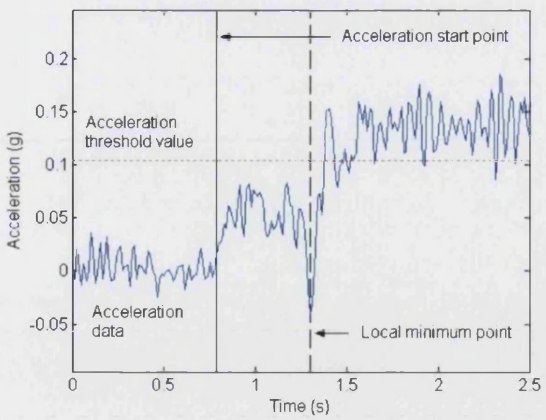

Figure 5-22 – Acceleration gradient check

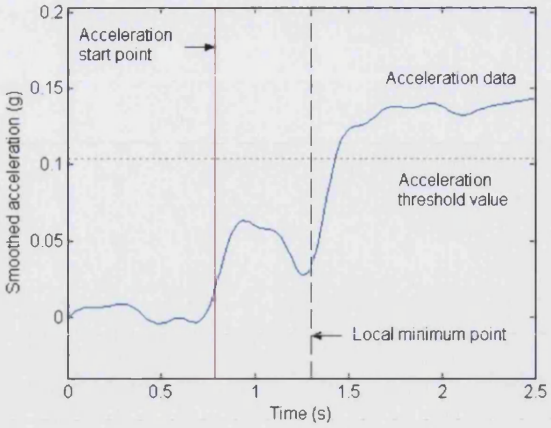

Figure 5-23 – Acceleration gradient check (smoothed acceleration)

This point of intersection between the acceleration threshold and the acceleration data is where the process starts. Moving from this point towards the start of the data (to the left), the yellow vertical line indicates the point at which the code has detected a change in gradient from negative to positive. The code then determines whether this is in fact a local minimum, which should be ignored. This is achieved by looking to see whether the difference between the current value and the value at the pedal movement time is less than the approximate 0.04g noise level of the acceleration data. If it is within this noise threshold then the current time is assumed to be the start of the acceleration.

If it is greater than this noise level, the code attempts to move out of the local minimum point by continuing moving back towards the start of the test until the difference between the current acceleration value and that, which was detected at the point of the gradient change, is more than 0.01g. This is performed to ensure that any small perturbations in the local minimum region are ignored. Once a new point that matches these criteria has been found, the code continues moving towards the start of the data again looking for zero or negative gradients. If no point is found, or if the current point is within the noise level, then it is returned as the acceleration start point.

5.3.4.1.2 Pedal movement start detection

The time at which the pedal movement begins is detected by looking for movement beyond a threshold in the pedal position.

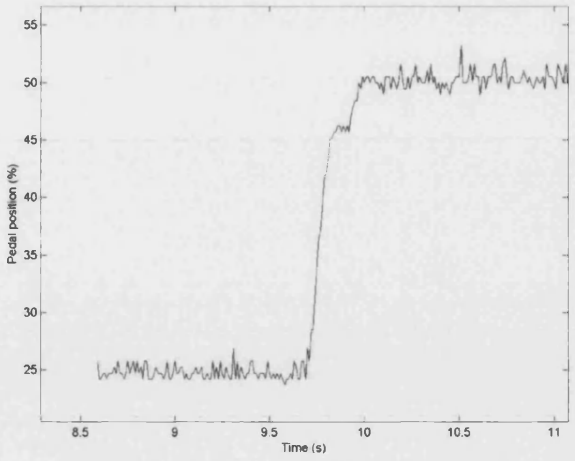

Figure 5-24 – Noisy pedal position data

As the pedal data is inherently noisy (as can be seen in Figure 5-24) due to driver positioning error and jitter in the recording equipment, smoothing and a relatively large threshold value are used to eliminate false detections of the initial pedal movement. This, however, means that the position at which the pedal movement is detected is made a relatively long period after the movement begins. Therefore, after the movement is detected, a process of refining the exact start point is employed. This entire process is made more difficult by a feature of some drivers' pedal movements whereby they make the movement in a number of steps. This means that a simple gradient following scheme can easy confuse one of these steps for the steady-state period preceding the pedal movement. Therefore a complex gradient following system was implemented with a degree of flexibility allowing it to move beyond these stepped regions and test whether they represent a false pre-manoeuvre steady-state region.

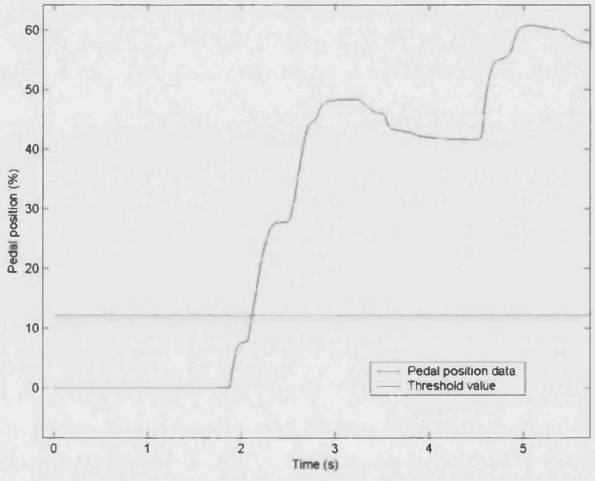

Figure 5-25 – Pedal position data

In the complex gradient following system the pedal position data are analysed time-step by time-step from the start of the test until the end of the valid test data. If the value of the current data point is less than a pre-set threshold value (20% of the maximum range of the pedal position data over the test), then the point is ignored and the next point is considered. If the value of the current data point does exceed the threshold, then the point at which the pedal was moved is definitely before this point in the test and the process of finding it begins. Figure 5-25 shows the pedal position data with the horizontal line showing the 20% threshold.

The use of a large threshold value avoids picking up any pedal position noise or driver jitter that may occur during the 'steady-state' period before the start of the test.

The code then moves through the data from the threshold position towards the start of the test looking for the first point at which the data either stays constant or starts to increase rather than decrease (as this is a tip-in event, moving backwards through the data the gradient should remain negative).

In Figure 5-26, below, the vertical green line shows one of these detected changes in the pedal position gradient.

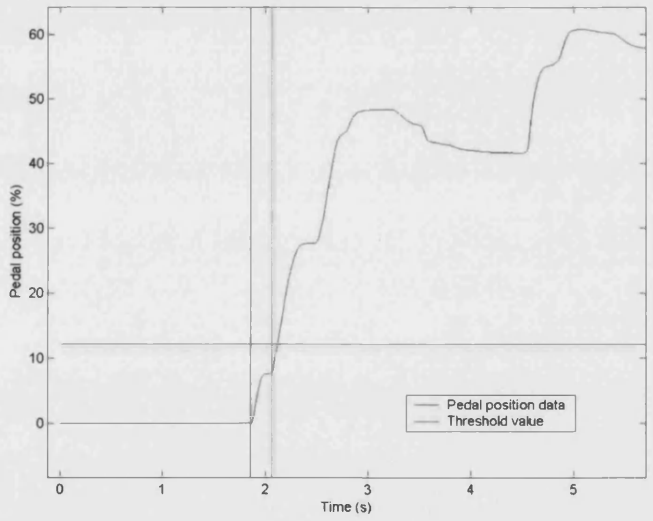

Figure 5-26 – Pedal position with step detected

Once such a point is found, it is checked to ensure that is not simply a step in the pedal ramping. This is achieved by smoothing the pedal position data and then determining whether the difference between the pedal position value at the current position and that at

the start of the test is less than 4% of the overall range. If this difference is less than 4%, it is assumed that this is the pre-pedal movement region. If it is in fact greater than 4%, it is assumed that this is simply a step in the pedal movement and the start of the next descent is found by moving backwards until a region that is 4% of the pedal position range less than the pedal position value at the start of the step is found. This process continues until the bottom of the pedal ramping is found.

Once the bottom of the pedal ramping is detected, a final test is performed to ensure that the starting position is as accurate as possible. A moving average (averaging two points either side of the current position) of the pedal position is calculated between the current time and a point 0.25 of a second earlier in the test data. The code moves from the current location towards the start of the rolling-averaged pedal data looking for a point where the current pedal position moves within 2% (absolute) of the value at the previously detected start of the pedal movement. This point is then returned as the start of the pedal movement. This final check ensures that the smearing effect of the pedal position smoothing is eliminated. The final check only takes place over 0.25 of a second as this was found to be sufficiently large to account for any errors created by the smoothing.

5.3.4.2 Gear-shift event detection

As the AT Mondeo's automatic transmission was retrofitted (replacing an experimental CVT unit) and was consequently not well calibrated, exhibiting hunting and jerky gearshifts, it was decided that it would be interesting to investigate gearshift ratings in addition to the standard driveability ratings. Gearshift data were therefore collected for the AT Mondeo vehicle (in both economy and sports mode).

The detection of gearshift events is a definite requirement for continuous testing. Even if the gearshift is not to be rated itself, the fact that it has occurred must be noted as it interrupts the flow of power through the powertrain; therefore the fact that automatic gearshift detection code was developed is a necessary step toward implementing continuous driveability testing even without the analysis of gear shift ratings. The ability to detect the factors that affect gearshift ratings is also a necessary process to enable better calibration of CVT and AMT shift strategies.

Although the automatic detection of a gearshift event is relatively straightforward for a manual gearbox vehicle, the code need merely to monitor the ratio of vehicle speed to engine speed and detect steps in this, for an AT vehicle, which uses a torque converter, the

process is more difficult as the torque converter means that this ratio does not necessarily exhibit step changes, especially at low vehicle speeds before the torque converter is locked.

All of the gearshifts are detected in a given manoeuvre and their start and end offsets are returned along with a flag indicating whether they are up- or down-shifts. Figure 5-27 shows the engine speed trace from a test including a gear up-shift.

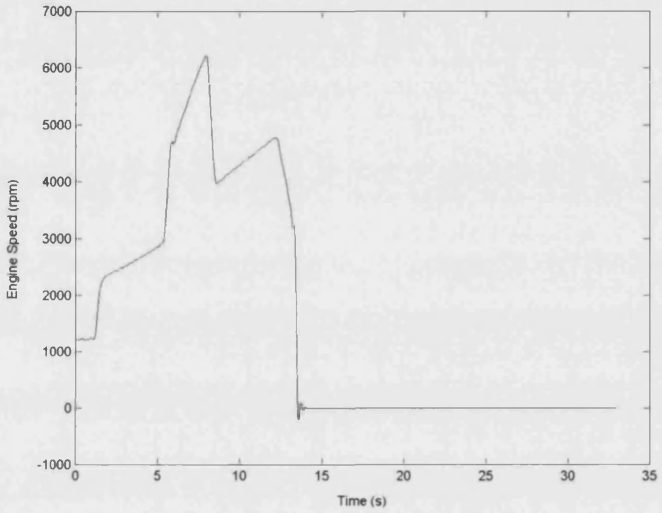

Figure 5-27 – Engine speed trace

A gearshift event is associated with a sharp change in the engine speed gradient over time (engine angular acceleration). This feature is used to determine the location of the gearshifts. The engine speed data are first pre-processed to remove any data point dropouts or overflow events (see Section 5.3.2.4) and then the data are smoothed (as explained in Section 5.3.2.2) to remove frequency components above 5Hz in the engine speed data.

As gearshifts produce a change in engine speed, an engine angular acceleration spike were produced in the data and could therefore be detected. Negative engine angular acceleration indicates that a downshift has occurred while positive engine angular acceleration indicates an up-shift.

The gearshift data were therefore analysed time-step by time-step from 0.5 second after the start of the test until the end of the valid test data. The first 0.5 seconds of the vehicle data were not analysed to ensure that no engine speed fluctuations produced as the data acquisition starts were captured and misinterpreted.

If the absolute engine angular acceleration (calculated from the engine speed data) was found to reach or exceed 1.5 times the engine speed gradient's overall standard deviation, this indicates that a gearshift was underway. This value was chosen experimentally to detect the very fast change in engine speed, associated with the gearshift, without accidentally detecting over-run or lift-off engine speed changes or fast (low vehicle speed) engine acceleration. Figure 5-28, below, shows a diagram of the engine speed gradient. The standard deviation and standard deviation x 1.5 threshold are indicated by light and dark blue horizontal lines respectively.

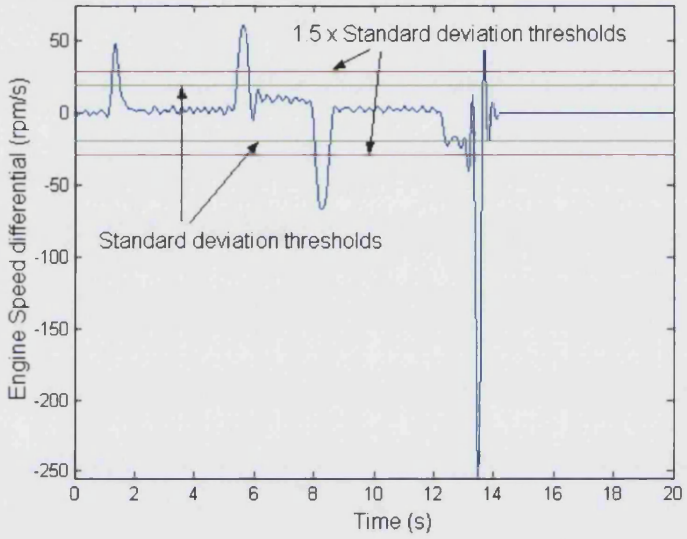

Figure 5-28 – Differential of engine speed

The data points surrounding the current point are then tested to determine whether the current location is on an up or down slope and whether the overall acceleration spike indicates an up or down shift.

A number of checks are then performed to ensure that it is only real gearshifts that are recognised. First, any gearshift events in the last 2 seconds of the test are rejected. This check is performed to stop torque converter slip events as the vehicle stops from being accidentally recognised as gearshift events. To eliminate any other false gearshifts associated with changes in the effective gear ratio created by the torque converter, any gearshift events that occur within 0.5 second of one another are merged together. Figure 5-29 shows a diagram of the gear ratio (engine speed/vehicle speed). The detected gearshift events are highlighted.

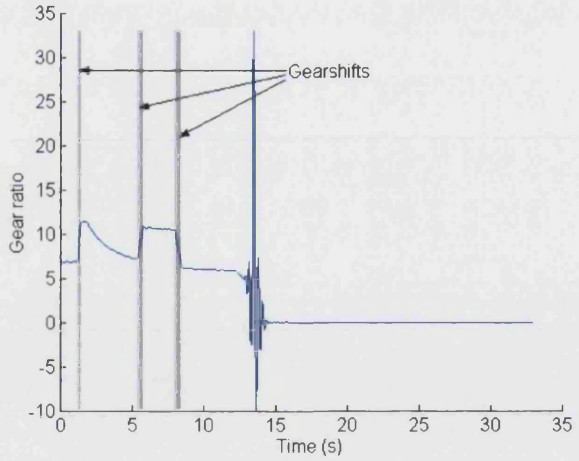

Figure 5-29 – Engine speed/vehicle speed ratio

It can be seen that the gradient does not remain constant between gearshift manoeuvres as it would with an MT or AMT equipped vehicle. This is due to (designed) slippage in the torque converter, which has not been locked due to the low vehicle speed. This effect makes the detection of gearshifts more difficult for AT vehicles and is the reason why changes in the engine speed acceleration are used, rather than the simpler gear ratio, to determine gearshift points.

An additional test is performed to eliminate any accidental gearshift detections caused by the fast change in engine speed which happens when the engine is switched off. Any gear-shift events which appear to have an engine speed of less than or equal to 100 rpm at the end of the shift are removed as these are simply artefacts caused by the large change in engine speed if the vehicle ignition is switched off while data acquisition is underway.

The result is reliable gearshift detection as is shown in Figure 5-30

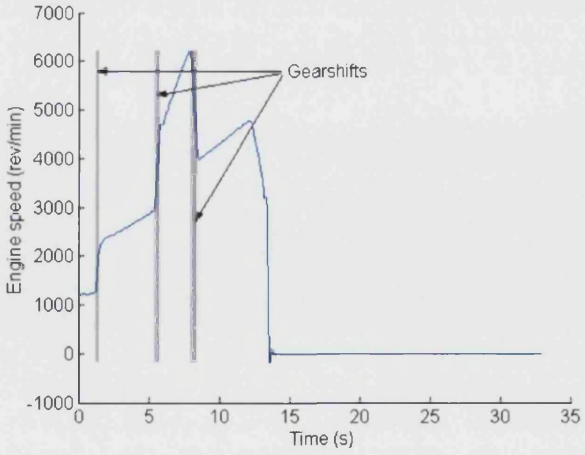

Figure 5-30 – Smoothed engine speed with gearshift events highlighted

5.4 List of metrics

Two sets of metrics were used for the main testing. A full set, and one containing just delay times, acceleration and jerk metrics for direct comparison with Wicke's findings.

Some additional objective metrics were collected to perform the analysis of the gearshifts; however these were only used when analysing the gearshift-related subjective metrics (see Section 4.2.1). These additional objective metrics are described below (see Section 5.4.1.1).

5.4.1 Longitudinal driveability objective metric descriptions

aInitialSpeed

Test vehicle speed at the start of the test. This is the mean value of the vehicle speed data for the first 0.25s at the start of the test.

aDesiredStartSpeed

The vehicle speed that the driver was asked to attain before starting the test. This is determined from the test type. This is recorded test data for the testing of the AT Mondeo and Prius and automatically determined from the data file names for Wicke's data.

aMaxSpeed

This is the maximum speed that occurred during the test. This always occurs at the end of the test just before the driver starts braking. This is a simple maximum over the range between the start of pedal movement and the end of the test.

aChangeInSpeed

Difference between the initial speed and the maximum speed (difference between aMaxSpeed and aInitialSpeed).

aInitialPedalPosn

The pedal position at the start of the test (during the steady state stage just before acceleration begins). Mean position of accelerator pedal over the first 0.25s of the test.

aMaxPedalPosition

The maximum position of the accelerator pedal. Maximum position between the start of pedal movement and the end of the test.

aDesiredPedalPosition

The accelerator pedal position that the driver was asked to attain for the test. This is determined from the test type. This is recorded test data for the testing of the AT Mondeo and Prius and automatically determined from the data file names for Wicke's data.

aRateOfChangeOfPedalPosition

Rate at which the pedal is moved from its initial position to the desired position for the test. Differential of the pedal position between the start of movement and reaching the maximum position.

aMaxAccel

Maximum acceleration between the start of the vehicle acceleration and the point of maximum speed (which is the end of the accelerative phase).

aAverageAccelToMaxAccel

Mean acceleration from the start of the manoeuvre to the point of maximum vehicle acceleration.

aAverageAccelToMaxSpeed

Average acceleration over the course of the acceleration phase of the test. Mean acceleration from the start of vehicle acceleration to the point of maximum vehicle speed.

AccelDelayTime

Time between start of pedal movement and start of vehicle acceleration.

aAccelGradient

Rate of change of acceleration over the first 4 seconds of the test or until the maximum vehicle speed is reached (in case the manoeuvre takes less than 4 seconds).

aInitialJerk

Average jerk over the first second after the initial pedal movement is detected.

aMaximumJerk

Maximum jerk between the start of the vehicle acceleration and the point of maximum acceleration.

aAverageJerk

This is the average jerk during the vehicle acceleration. Mean jerk from the point of initial acceleration to the point at which positive vehicle acceleration stops.

aInitialQuirk

Average quirk over the first second after the initial pedal movement is detected.

aMaximumQuirk

Maximum quirk between the start of the vehicle acceleration and the point of maximum speed (which is the end of the accelerative phase).

aAverageQuirk

This is the average quirk during the vehicle acceleration. Mean quirk from the point of initial acceleration to the point at which positive vehicle acceleration stops.

aMaxEngSpeed

Maximum engine speed between the start of pedal movement and the end of the test.

aDeltaEngSpd2MaxSpeed

Difference in the engine speed detected at the following times in the test: time of the start of vehicle acceleration and the time at which vehicle maximum speed occurs.

aDeltaEngSpd2MaxAccel

Difference in the engine speed detected at the following times in the test: time of the start of vehicle acceleration and the time at which vehicle maximum acceleration occurs.

aEngSpdAtMaxVSpeed

The engine speed when the maximum vehicle speed is reached.

Of this set of metrics, the following are used in the acceleration and jerk subset:

- aMaxAccel
- aAverageAccelToMaxAccel
- aAverageAccelToMaxSpeed
- AccelDelayTime
- aAccelGradient
- aInitialJerk
- aMaximumJerk
- aAverageJerk

This subset was selected to produce correlation equations that could be compared with Wicke's finding that jerk and delay time were correlated with vehicle driveability (Wicke et al. 2000; Wicke, 2001).

5.4.1.1 Gearshift objective metrics

The same full set of objective metrics was used as described in Section 5.4.1. In addition to these metrics, some that were more specific to the gearshift manoeuvre itself were also included.

Up/DownshiftJerk

The jerk caused by the difference in acceleration before and after a gearshift event. This change in acceleration, and consequently jerk, occurs as the vehicle accelerates or decelerates (depending on the shift direction) during the gearshift as the current gear is disengaged and then accelerates or decelerates (again depending on the shift direction) as the new gear is engaged the flow of power continues.

As an example, when performing an up shift during hard acceleration, the vehicle will decelerate as the current gear is disengaged, then will accelerate again as the new gear is engaged. The Initial deceleration will depend on the effective inertia of the vehicle (related to mass and wind resistance) and the exact method by which the throttle is lifted, while the post-gear-engagement acceleration will depend on the gear ratio, engine speed and throttle position and the application of the throttle as the gear is engaged.

Up/DownshiftPreJerk

This is the jerk caused by the disengagement of the gear. This is the first half of the *Up/DownshiftJerk* metric.

Up/DownshiftPostJerk

This is the jerk caused by the re-engagement of the new gear. This is the second half of the *Up/DownshiftJerk* metric.

Up/DownshiftAccelDiff1

This is the difference in acceleration across the gearshift. It is calculated from the difference of the accelerations at the exact start and end points of the gearshift (this means before and after any jerk changes caused by the gear engagement/disengagement).

Up/DownshiftAccelDiff2

This is similar to *DownshiftAccelDiff1* above but instead of using the instantaneous acceleration at the start and end of the gearshift event, the two accelerations are averaged over $1/20^{th}$ of a second before and after the gearshift.

Up/DownshiftDelay

This is the time taken to perform the gearshift.

Up/DownshiftPreAccelInst

This is the instantaneous acceleration at the beginning of the gearshift event.

Up/DownshiftPostAccelInst

This is the instantaneous acceleration at the end of the gearshift event.

Up/DownshiftPreAccelAvg

This is the average acceleration for the $1/10^{th}$ of a second before the start of the gearshift event.

Up/DownshiftPostAccelAvg

This is the average acceleration for the $1/10^{th}$ of a second after the end of the gearshift event.

Up/DownshiftPreEngSpd

This is the engine speed at the beginning of the gearshift event.

Up/DownshiftPostEngSpd

This is the engine speed at the end of the gearshift event.

6 Correlation generation

There are a number of multivariate approaches that can be applied to analysing the correlations between subjective ratings and metrics representing objective data. The research described in this thesis intended to investigate the correlations between a driver's subjective perception of a vehicle's performance and the objective measurements taken experimentally from the same vehicle. The research focused on the longitudinal driveability characteristics associated with the driver's feel of vehicle response rather than those involving driveline vibrations or other factors, which may affect the subjective assessment, such as start-up behaviour.

This analysis includes driveability data sets from CVT and AT vehicles, however the research could also be extended to include some aspects of MT vehicle driveability. The testing of the Toyota Prius provided more driveability data from a vehicle with an unusual transmission. Some may consider the number of different vehicle transmissions a hindrance; but it allowed more general driveability trends, which are not simply related to the type of gearbox, to show through in the analysis.

6.1 Application of correlation methods to driveability analysis

This research described in this thesis aimed to produce a tool for simplifying and speeding the calibration of vehicle powertrains. However driveability analysis is applicable to a number of areas including the following (List & Schoeggl, 1998; Dorey & Holmes, 1999; Dorey et al., 2001):

- Fast in-vehicle driveability analysis (both during calibration and for testing, characterising and possibly copying competitors' vehicles' driveability behaviour)
- Automated test-rig powertrain driveability analysis
- Optimisation of engine calibration for driveability (in-vehicle or on a test-rig)

Performing driveability analysis on a powertrain or engine on a test rig would allow the powertrain's or engine's calibration to be optimised early in the development process before an actual test vehicle is available. This would save re-design costs by optimising the calibration early in the design process. Applying driveability analysis later in the calibration process could allow a vehicle's driveability to be assessed while test-driving. This process could be used to analyse a competitor's vehicle to determine its driveability or simply to evaluate a finished product without needing to use many test drivers.

Although all of these areas overlap in that they require robust and fast analysis of driveability data, each has specific requirements in terms of data input and output, data acquisition and the particular objective driveability data that may be available. These areas give an idea of the possible future directions that the project may take. The availability of the Torotrak Ford Mondeo with its programmable engine and CVT controller may also afford the possibility of testing the results of the analysis using an actual vehicle. A next step in this process would be the development of code that effectively works in reverse by determining the values of objective metrics that are required to produce given subjective driveability rating.

The analysis of large amounts of data requires that it be automated as much as possible, so that the process can be performed quickly, reliably, and accurately. To this end, the current project has focused on automating both the processing of raw data files (from vehicle data acquisition for example), and the analysis and correlation of the data that is recorded in these files together with subjective assessments so that the user is simply presented with the list of correlation results.

6.2 Overview and selection of a correlation method

Although it is relatively easy to spot linear trends between two variables by simply plotting the data in a 2D scatter plot and looking for a trend, it is more difficult to determine exactly what form this relationship takes if it is curvilinear. When the effects of more than two independent variables are also considered, it becomes very challenging if not impossible to determine the system equation without resorting to some form of multivariate analysis.

There are a large number of multivariate approaches that can be applied to analysing the correlations between subjective and objective metrics. These include a variety of iterative methods such as genetic algorithms (Goldberg, 1989) and neural networks (Aleksander & Morton, 1995), as well as non-iterative methods such as regression. Regression methods (Ezekiel & Fox, 1959) use statistical techniques such as least squares to establish a system equation whose results can then be rated for accuracy using other statistical measures such as correlation coefficients.

Both methods have advantages and disadvantages. Iterative methods, by their nature, require time and inclusive data sets to produce a solution. In the case of neural networks, large amounts of training data and time are required so that the internal structure of the net can be established. However neural networks can simulate very complicated equations due to their internal flexibility (Aleksander & Morton, 1995). Regression techniques require less

training time and data, however they are not as flexible as neural networks, and require external input in the form of selecting the appropriate type of regression equation. This relative simplicity also means that once a regression equation has been produced, it is easier to determine the effects that the different inputs have on the output (Statsoft Inc., 2005). It should be noted that neural networks, unlike regression techniques, do not produce simple equations, and are generally used as a 'black-box' into which data are fed, and results extracted. The simplicity of regression equations will allow a calibration engineer to see more clearly which calibration aspects affect powertrain performance ratings and to what extent. This will also allow informed decisions to be made on what trade-offs can be made for emissions and economy and their effect on driveability.

Although neural networks remain a more flexible technique for simulating complete vehicle driveability, assuming the availability of a comprehensive data set, the use of statistical regression equations may prove useful in assessing specific areas of driveability such as longitudinal driveability. This is in part because of the ease with which a regression equation's structure and the relative importance of its metrics may be determined and also because of the faster training time. It should be noted that both List and Schoeggl (1998) and Dorey et al. (1999, 2000) included many aspects in their driveability analysis including engine start and warm-up behaviour, the effect of gear changes and the application of accessory loads. For the statistical approach being investigated in this thesis, the input metrics were simplified to concentrate solely on the variables affecting longitudinal driveability. The statistical regression approach does not require an iterative training period and will return a deterministic result each time it is executed. This is a significant advantage when compared with neural networks. In addition, the structure and relative importance of the metrics in the regression equations will be more easily understandable than those produced by a comparable neural network.

6.2.1 Spline methods

Splines are piecewise polynomial functions (Ahlberg, 1967). This means that a curve can be fitted to a set of points and the result is made up of a number of sections each of which is described by a different polynomial equation.

Although spline techniques were considered for use in this project, it was decided to concentrate on a regression approach as it has the ability to produce equations that are more intuitive. The adoption of a sectioning technique similar to the spline technique may be a useful extension of the current research. This might allow a number of multivariate correlation equations to be fitted to different parts of a curve. The number of curve sections

would need to be kept relatively low otherwise the simplicity of the regression approach would be overwhelmed by the sheer number of equations, however by splitting the data into smaller sections with similar, simpler behaviour, it may be possible to generate a set of less complex equations.

This would have the advantages of correlation equations, namely simple, understandable equations that can be analysed easily, combined with the ability of the sectioning technique to represent regions of a curve with differing behaviour using simple equations.

6.3 Application of regression

6.3.1 Types of least squares regression technique

There are a number of least-squares derived fitting techniques available in the literature some of which offer resistance to outliers, but often at the cost of iterative and hence slow calculations. The techniques that were considered are outlined here.

6.3.1.1 Least Squares (LS) regression

Least squares is a mathematical procedure for finding the curve which best fits a set of data points. The basic least squares method works by minimising the sum of the squares of the error between each point and the curve (the 'residuals'). In practise, this distance is measured vertically rather than perpendicularly from the line (or surface, hyper-plane, etc.) to the point.

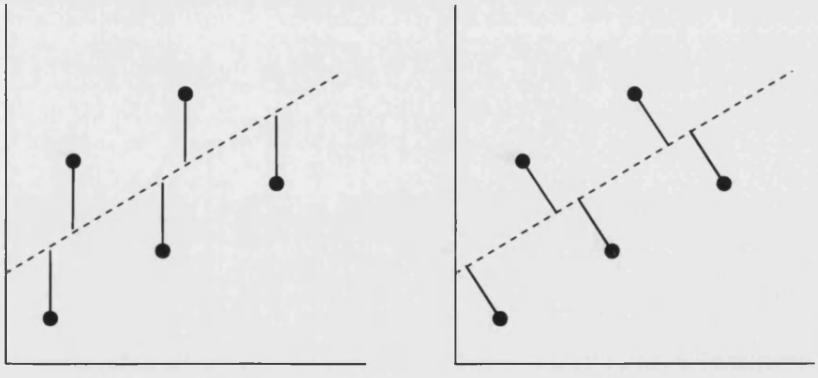

Figure 6-1 – Offset directions

This produces a fitting function that predicts the Y value for a given X, and makes the form of the fitting parameters far simpler than would be obtained using a fit based on the perpendicular distance.

Supposing a simple curvilinear equation is to be used to represent the relationship between a single independent variable, X and the dependent variable, Y. The value, Y', calculated using this equation can be written as:

$$Y' = a + bX + cX^2$$ **Equation 6-1**

which is equivalent to:

$$Y = a + bX + cX^2 + e$$ **Equation 6-2**

The coefficients a, b and c must be determined so that the sum of the squared errors, e, between the calculated values of Y' and the actual values of Y is minimised.

$$\sum_{i=1}^{n} e_i^2 = \sum_{i=1}^{n} (Y_i - Y_i')^2$$ **Equation 6-3**

$$\sum_{i=1}^{n} e_i^2 = \sum_{i=1}^{n} (Y_i - (a + bX_i + cX_i^2))^2$$ **Equation 6-4**

The total error can now be defined as:

$$E = \sum_{i=1}^{n} e_i^2$$ **Equation 6-5**

The following simultaneous equations can be constructed by setting the partial differential of the total error, E, with respect to each coefficient, equal to zero:

The goal is to reduce the error to a minimum, therefore using calculus this means solving with the differential of the equation equal to zero. As there are multiple parameters to be found, a number of differential equations must be solved. Equation 6-4 can be expanded:

$$E = \sum_{i=1}^{n} (c^2 X_i^4 + 2bcX_i^3 + (2ac + b^2)X_i^2 + 2abX_i - 2cX_i^2 Y_i - 2bX_i Y_i + a^2 - 2aY_i + Y_i^2)$$ **Equation 6-6**

Now solving for the differential of the error with respect to each of the parameters and setting them equal to 0:

$$\frac{\partial E}{\partial a} = \sum\left(-Y_i + a + bX_i + cX_i^2\right) = 0 \qquad \textbf{Equation 6-7}$$

$$\frac{\partial E}{\partial b} = \sum\left(-X_iY_i + aX_i + bX_i^2 + cX_i^3\right) = 0 \qquad \textbf{Equation 6-8}$$

$$\frac{\partial E}{\partial c} = \sum\left(-X_i^2Y_i + aX_i^2 + bX_i^3 + cX_i^4\right) = 0 \qquad \textbf{Equation 6-9}$$

These equations can be re-arranged

$$\Sigma Y = n \cdot a + \Sigma(X)b + \Sigma\left(X^2\right)c \qquad \textbf{Equation 6-10}$$

$$\Sigma YX = (\Sigma X)a + \left(\Sigma X^2\right)b + \left(\Sigma X^3\right)c \qquad \textbf{Equation 6-11}$$

$$\Sigma YX^2 = \left(\Sigma X^2\right)a + \left(\Sigma X^3\right)b + \left(\Sigma X^4\right)c \qquad \textbf{Equation 6-12}$$

These can then be solved using a Singular Value Decomposition (SVD) technique (Nash, 1979) provided by the *MATLAB* software (*pinv* method), to produce the coefficients of the best-fit equation.

This technique can be extended to include additional powers of the independent variable (X), and extra independent variables (more X-type variables). The technique can also be applied, by substitution, to allow non-linear terms to be included in the equation. For example, a similar method is used to fit the following equation with a log term:

$$Y = a + b \cdot log(X) \qquad \textbf{Equation 6-13}$$

The following simple substitution can be used:

$$Z = Log(X) \qquad \textbf{Equation 6-14}$$

to turn Equation 6-13 into a more familiar form:

$$\hat{Y} = a + b \cdot Z \qquad \textbf{Equation 6-15}$$

This can be solved using the technique explained above.

This technique lends itself to computational use, as the resulting simultaneous equations can be solved quickly by computational SVD techniques. It should be noted that the equations produced using this technique are liable to be skewed by outlying data points. Therefore, a number of more robust techniques are currently being investigated as replacements. These techniques are outlined in the following sections.

6.3.1.2 Least Median of Squares (LMS) regression

The LMS technique minimises the median of the squared errors of the data points (Rousseeuw & Leroy, 1987). This technique requires that a random subset of the data is iteratively chosen and evaluated to determine the regression equation. A value of 75% is often chosen as the percentage of the data set to use for the subset, theoretically allowing for and ignoring up to 25% of bad (perhaps outlying or incorrectly recorded/calibrated) data in the complete set. The number of subsets that must be chosen can be calculated to give a high (99% for example) probability of one of the data sets containing only good data. This chosen subset is that which has the lowest median of squared errors. This technique is iterative and can therefore unfortunately take a long period of time to run.

6.3.1.3 Least Trimmed Squares (LTS) regression

The LTS is operates in a similar way to the LMS algorithm, but in this case it is the sum of the squared error which is being minimised rather than the median of the squared error (Rousseeuw & Leroy, 1987).

6.3.1.4 Least Weighted Squares (LWS) regression

The LWS technique is very similar to the standard LS technique with the simple addition of a weighting to each data point (Rousseeuw & Leroy, 1987). This changes Equation 6-16 to the following:

$$\sum_{i=1}^{n} e_i^2 = \sum_{i=1}^{n} w_i (Y_i - (a + bX_i + cX_i^2))^2 \qquad \textbf{Equation 6-16}$$

The weighting value w_i is a number between zero and one. This value is then given a value that becomes smaller as the coordinate points become outliers.

The technique used in this research is provided by the MATLAB programming environment. The MATLAB bi-square weighting technique (MATLAB function *robustfit* with *bisquare* weight function) uses an iteratively re-weighted least squares algorithm. It follows the following procedure (DuMouchel & O'Brien, 1989):

1. Fit the model by weighted least squares (initial weights are all equal, w=1).
2. Computer the adjusted residuals and standardise them. The adjusted residuals are given by the equation:

   $$r_{adj} = \frac{r_i}{\sqrt{1-h_i}}$$

   where r_i is the least squares residual (error between calculated and original values) and h_i are leverages (one divided by the square of the error between the predicted and actual values for each point) that adjust the residuals by weighting high-leverage (outlying) data points to reduce their effect.
   The standardised adjusted residuals are then given by:

   $$u = \frac{r_{adj}}{K \times s}$$

   where K is a tuning parameter and s is the robust variance given by the mean absolute deviation of the residuals divided by 0.6745.
3. The bisquare weights are then given by:

   $$w_i = \begin{cases} \left(1-u_i^2\right)^2 & |u_i| < 1 \\ 0 & |u_i| \geq 1 \end{cases}$$

4. This process continues until the fit converges.

6.3.2 Statistical considerations

Possibilities for minimising the variance of the data used in this project, namely by collecting and analysing more data, were constrained due to the limited resources of the University in terms of time and materials. These constraints resulted in only a limited number of tests being performed during this project.

The research presented in this thesis used two statistical methods: F-tests and regression. There are certain statistical requirements that must be met to ensure that the use of these techniques produces accurate results. The justification for the use of these techniques is explained below.

6.3.2.1 F-tests

F-tests were used in this research to determine whether terms should be added to the correlation equation as is explained in section 6.4.2.2.4.1. F-tests were also used to determine whether the resulting equations were statistically significant as explained in section 6.4.2.2.4.2. The use of F-tests requires a normal distribution of data, however Hays states that with a sufficiently large number of data points (>30), the test is valid for use with non-normally distributed data (Hays, 1998, p.335). Therefore the use of the F-test was justified in this research, no matter what the distribution of the data, as the data sets and subsets in question generally contained a minimum of 90 data points.

6.3.2.2 Regression

Assuming a general model of the form that was used in this research:

$$y_{ij} = \mu_Y + \beta_{Y.X}(x_j - \mu_X) + e_{ij}$$ **Equation 6-17**

where y_{ij} is a dependent variable data point, μ_Y is the true population mean value for the dependent variable, $\beta_{Y.X}$ is an array of coefficients for the regression equation, x_j is an array of independent variable data points, μ_X is the true population mean value for the independent variables and e_{ij} is an error.

The application of regression on a set of data using such a regression equation requires that within each population j, the distribution of y_{ij} values must be normal (Hays, 1988, p.571).

It should be noted that no assumption is made about the distribution of the *x* (independent) variables (Hays, 1988, p.571). Therefore we assume the true distribution of *x* is represented in the sample of *x*. This means that the inferences made in a regression are conditional upon the distribution of *x* as obtained from the sample. This means that no distributional requirements are made of the objective data that were used, other than that any data used in future with a given regression equation have the same distribution. This assumption was valid for this research.

6.3.2.2.1 Determination of normality for y_{ij} values

The following histograms show the distribution of data for the six subjective metrics:

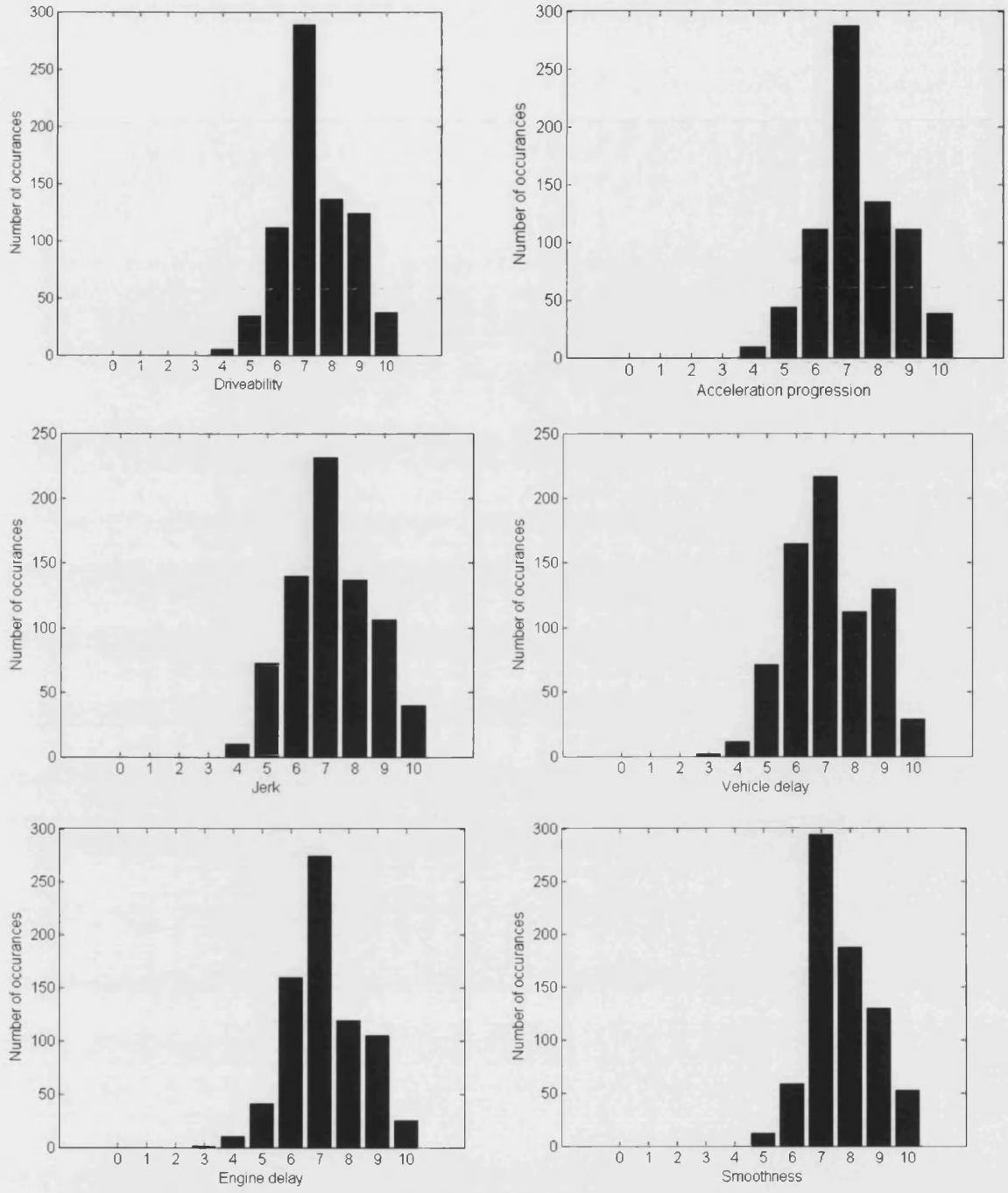

The following tables shows the results of a set of Kolmogorov-Smirnov tests (Chakravarti et al., 1967). These are hypothesis tests of whether the subjective metric data are members of a given distribution. A number of distributions were used in the tests and the tests were performed with an alpha level of $\alpha=0.05$ (95% confidence).

Table 6-1 – Probability values for Smoothness metric

Distribution	p-value
Chi-squared (4 deg. of freedom)	0
Gamma	1.549E-10
Normal	1.548E-13
Poisson	7.106E-79
Weibull	4.091E-21

Table 6-2 – Probability values for Engine delay metric

Distribution	p-value
Chi-squared (4 deg. of freedom)	0
Gamma	0
Normal	7.988E-13
Poisson	2.518E-79
Weibull	2.038E-16

Table 6-3 – Probability values for Vehicle delay metric

Distribution	p-value
Chi-squared (4 deg. of freedom)	2.964E-305
Gamma	0
Normal	1.300E-11
Poisson	9.245E-61
Weibull	1.535E-15

Table 6-4 – Probability values for Jerk metric

Distribution	p-value
Chi-squared (4 deg. of freedom)	3.911E-316
Gamma	2.089E-08
Normal	5.723E-08
Poisson	6.668E-59
Weibull	7.241E-11

Table 6-5 – Probability values for Acceleration progression metric

Distribution	p-value
Chi-squared (4 deg. of freedom)	0.000E+00
Gamma	7.814E-07
Normal	7.650E-08
Poisson	3.820E-68
Weibull	1.922E-11

Table 6-6 – Probability values for Driveability metric

Distribution	p-value
Chi-squared (4 deg. of freedom)	0.000E+00
Gamma	0
Normal	1.410E-13
Poisson	3.353E-72
Weibull	5.528E-16

It can be seen that all of the probability values are very small, indicating that the confidence of fitting any distribution to these data was not high. In fact none of the distributions or subjective metric combinations passed the Kolmogorov-Smirnov test due to these low p-values. It can also be seen that of these probability values, those for the normal distribution are amongst the highest, meaning that although the data are not a statistically significant fit, their being distributed normally is one of the most likely explanations considering the tests that have been performed and the data that are available. Therefore the normal distribution was chosen as the basis of the subjective metric data for use in this research. It is acknowledged that the low significance of the normal distribution of this data may cause statistical inaccuracies, however this in unavoidable with the data available in this research.

6.4 Correlation technique comparison and selection

The research began by fitting equations containing single objective metrics to a single subjective rating. The set of equations that were used were chosen as they were considered

to represent the majority of trends that might be shown by typical physical data (Ezekiel & Fox, 1959). This research is explained in Section 6.4.1 and was reported by Pickering et al. (2002). The goal of the project, to perform driveability analysis using multivariate methods, was then considered and the various techniques considered and employed to perform such analysis are presented in Section 6.4.2.

6.4.1 Simple (single variable equation) regression

Wicke drew tentative conclusions about the effects of acceleration, jerk and delay-time on a vehicle's driveability rating by looking for trends in simple mean value plots. For this project a more quantitative approach was required, and therefore a correlation code was initially developed to produce single objective variable linear and curvilinear correlations which could be rated both by producing graphs for visual inspection, and also by calculating the degree of correlation statistically.

This first analysis code fitted the experimental objective and subjective data to one another using a simple least squares technique. For each combination of the subjective and objective metrics, the data were fitted using seven different algebraic forms, which were recommended for statistical analysis (Ezekiel & Fox, 1959). It was considered that these curves would approximate the majority of possible trends in the data. The form of these equations is shown in Table 6-7 below and in graphical form in Figure 6-2 to Figure 6-8.

Table 6-7 - Regression equations

Equation Type	General Form
Linear	$Y = a + bX$
Parabolic	$Y = a + bX + cX^2$
Cubic	$Y = a + bX + cX^2 + dX^3$
Log (1)	$Log(Y) = a + bX$
Log (2)	$Log(Y) = a + b\ Log(X)$
Log (3)	$Y = a + b\ Log(X)$
Hyperbolic	$Y = 1/(a + bX)$

Figure 6-2 to Figure 6-8, on the next page, show the form of these equations.

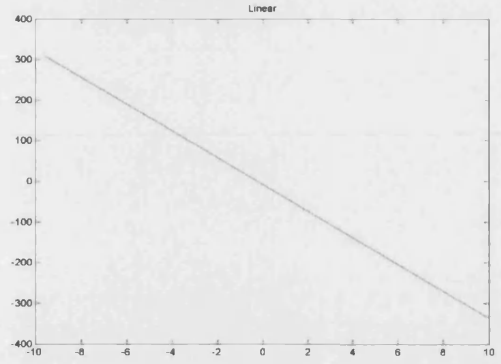

Figure 6-2 - Linear curve

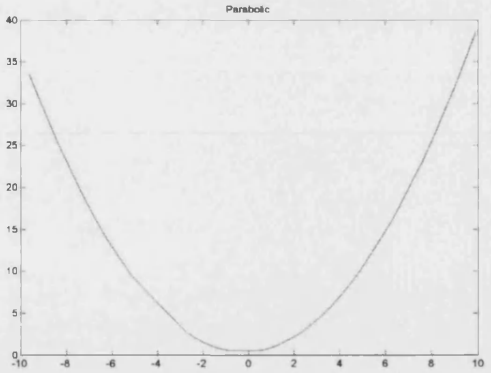

Figure 6-3 - Parabolic curve

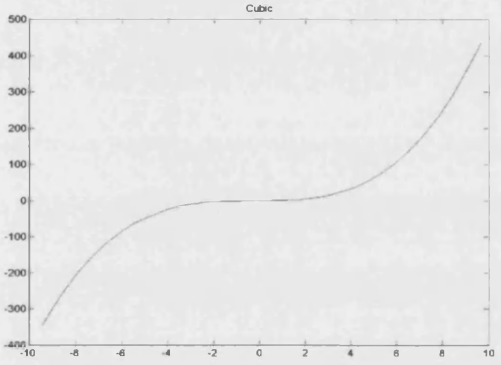

Figure 6-4 - Cubic curve

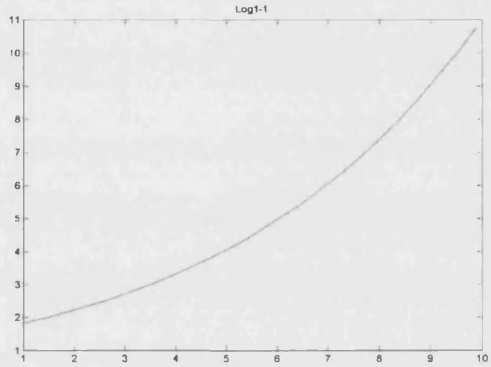

Figure 6-5 - Log curve (1)

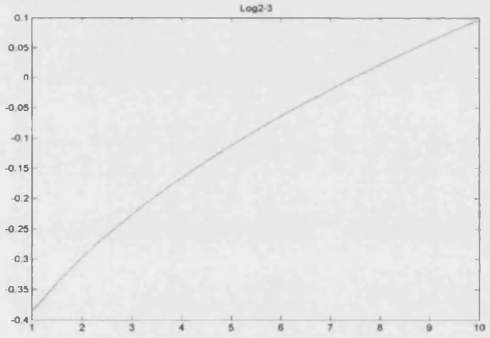

Figure 6-6 - Log curve (2)

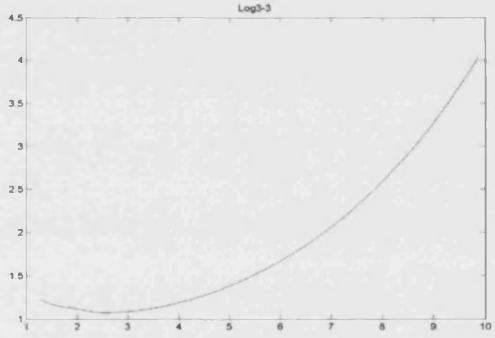

Figure 6-7 - Log curve (3)

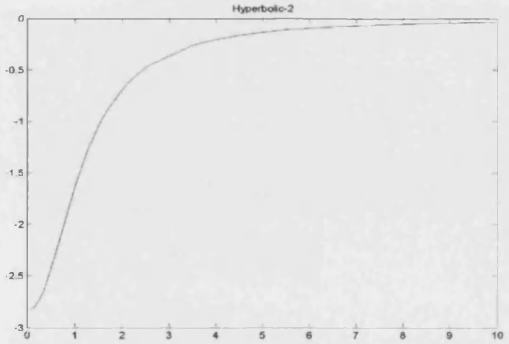

Figure 6-8 - Hyperbolic curve

The results of the single variable correlations applied to driveability data are shown in Section 7.5.

6.4.2 Multivariate regression

After applying the single variable code to the available data, it was seen that the coefficients of determination were generally low (R^2<0.25) indicating a lack of fit. It was seen from the data and fit lines that there was a large amount of scatter which pointed to the conclusion that each subjective metric was being affected by more than one objective metric. This was always assumed to be the case, however the low coefficients of determination showed that a simple, single variable approach would not be able to produce the necessary predictive accuracy. Therefore it was decided that a multivariate technique would have to be developed.

It was decided that two least-squares regression techniques would be tried: conventional least-squares (LS) and Least Weighted Squares (LWS) fitting, which would be more robust and resistant to the effects of outliers.

The method chosen for the generation of the correlations provides both a relatively simple implementation in code, as well as separating each term in the correlation equation so that its importance and effect can be determined independently of the other terms in the equation. An additional benefit to the calibration engineer, is that the individual terms can be represented graphically, providing another method to determine the effect of different objective metrics in relation to one another and the subjective ratings which they will provoke.

There are a number of methods that could be used to implement a multivariate version of the simple regression that has already been outlined. Care must be taken when choosing a method to ensure that it can fully represent the data (that the resultant fit is not constrained by the method used to attain it), but also that it is relatively simple to interpret and very importantly, possible to implement as a computer program which will run at a reasonable speed.

The first possibility considered was that of simply extending the equations listed in Table 6-7 so that extra power terms could be added. Although this method is reasonably simple to implement as a computer program, and produces equations that are simple to interpret, it suffers from the fact that the number of families of curves, and therefore behaviours of the resultant curves, is constrained by the initial choices. It was decided that a more flexible

approach should be taken to allow curves that did not conform to these families to be fitted. One such technique is that illustrated by Dolby (1963), whereby a large variety of curve types can be represented by Equation 6-18.

$$Y = a + b(c + x)^p$$ **Equation 6-18**

An equation of this form, using set *c* and *p* parameters can represent a vast range of curves from polynomials and hyperbolic to logarithmic and exponential equations.

Although this construct escapes the problem of representation of various curve types, a non-linear fitting process must be used. Non-linear fitting methods are iterative and therefore can take significant lengths of time to solve and can also suffer from convergence problems (Mathworks Inc., 2002). This method of representing various curve types also does not easily lend itself to multivariate use.

Therefore it was decided to use a linear style equation whose terms can contain non-linear operators. This method allows the computer program to handle the addition and removal of terms very simply, while still being able to produce non-linear behaviour. This scheme was implemented as a linear equation as shown in Equation 6-19 where each individual term can contain any single variable/metric with a combination of power and log operators operating upon it.

$$Y = a + b.(term_1) + c.(term_2) + \ldots$$ **Equation 6-19**

The major advantage of this method is that a single, simple solution to the linear least squares problem can be used to calculate the fit, and this can be applied to any combination of different terms by pre-calculating the value of each term. This makes the method relatively simple to implement in computer code.

It was decided to limit this method to allow each equation term to contain a constant multiplied by single variable term which could consist of a logarithm or the plain variable raised to an integer power between -3 and +3 or a positive or negative square or cube root (i.e. a power of ±⅓ or ±½). Although more complex schemes could have been implemented, for example allowing multiple variables to exist within a term, and then allow a further log/exponential/power or combination therefore operation to be performed on the whole, it was decided that this method was too complex and cumbersome, and that the fitting process would take far too long due to the number of possible combinations which would have to be

tried to find the best fit. Appendix II illustrates that the techniques adopted produced good approximations (R^2>0.90) to a large number of representative curves (Ezekiel & Fox, 1959).

The operators that can be applied to an objective variable were initially based on an extension of those present in the single variable correlation equations, which are shown in Table 6-7. This meant that an objective variable, X, could have any power from -5 to 5 (excluding a power of 0) applied to it or any root from -5th to the 5th. These power limits were chosen as it is generally assumed when testing regression equations that low order polynomials (with an order of 5 or lower) will fit any given set of data (Hoel, 1968). In addition to these 'power' operations, the exponent or logarithm of the variable X could be taken. The logarithm/exponentiation operation was performed after the power had been applied to the variable. This approach was taken, despite the fact that only ln(X) terms can be included (as $\ln(X^n) = n.\ln(X)$) as it was found that powers of the logarithms were not added to the correlation equations (e.g. $(\ln(X))^2$) while exponents containing powers were added (e.g. $e^{\sqrt{X}}$).

Further testing showed that exponential terms were problematic as they often produced fits that tended to very large magnitudes resulting in a significant number of failures when applying the correlation equations to different data sets (this was caused by failures of the least squares fitting due to its parameters tending towards infinity).

Although polynomials of degree five are considered to be sufficient to fit the majority of data (Hoel, 1968), it was found that the higher powers and roots were also largely superfluous as they appeared infrequently in the correlation equations. The use of these extra powers and roots also served to increase the time required to generate the correlation equations and they were therefore removed. Therefore the powers were limited to ±3 and ±3rd power roots. Appendix IV presents an analysis of the difference the removal of these different operators makes to the correlation equations.

The removal of logarithm and root operators as well as negative polynomial powers was tested as these operations can require that data points are lost. Data must be removed if it is zero or negative before applying a log or root operation and zero values produce infinite values when raised to a negative power. This requirement for positive data is not a problem when fitting a correlation equation as the scaling and offsetting (see Section 6.5.1) which is carried out before the least squares process can ensure positive values, however when applying a correlation equation to a new set of data, the original offsetting and scaling will sometimes produce negative values and these data points must then be removed.

Although it was found that correlation equations could be produced for all subsets, it was also found that overall the fits were not as good. It should also be noted that it is not generally advisable to extrapolate beyond the bounds of the data used to produce a correlation equation and this is effectively what is happening when the negative (and the majority of zero) values are present in an equation. Therefore, these logarithm, root and negative polynomial power operations were retained.

In its current form, the fitting method cannot produce compound equations of the form of the hyperbolic equation from Table 6-7:

$$Y = \frac{a}{b + cX}$$ **Equation 6-20**

Although the equation could be reduced to the following:

$$Y = \frac{a}{term_1}$$ **Equation 6-21**

where term1 contains two separate terms: a variable (X) multiplied by a constant (c) and a separate constant (b) (the constant, a, can be considered as a multiplier to the entire term, if the term is assumed to have a power of -1 i.e. $Y = a.\ term_1^{-1}$). Although equations containing terms of this type (i.e. compound terms) can be solved relatively simply using ordinary least squares methods, as the equations become more complex (see Equation 6-22) these methods no longer work, and the implementation of the process as an extensible computer program becomes difficult.

$$Y = \frac{a}{b + cX} + \frac{d}{e + fX}$$ **Equation 6-22**

The regression method used during this work cannot represent such equations in their original form. Therefore, it was necessary to check whether a different form of equation could be accurately fitted to data of this form to ensure, should such data occur, it could still be represented. Therefore, a number of sets of data representing a set of standard curves (Ezekiel and Fox, 1959) were produced, and the fitting code was applied to these data to see how well it reproduced the original.

It was found that the current fitting method produced good fits for almost the of the test curves. The only exceptions were those curves that showed a very steep gradient followed

or preceded by a constant value region. This behaviour was exhibited by some of the logarithmic test curves shown in Appendix II. The full set of curve fitting tests is shown in Appendix II.

6.4.2.1 The addition and use of interaction terms

One feature that the author initially tested was that of interaction terms (Eriksson et al., 2000). This is where two objective variables are multiplied together to produce more complex behaviour in the correlation equation.

A form of interaction of terms was originally added to the correlation generation code. In this code, individual terms such as those explained above are multiplied together and then tested in the correlation equation in much the same as has already been explained. However it was found that this method produced little useful effect due to the large amount of scatter in the data. This means that many interaction terms may be added but that they all have very low partial correlations and are simply fitting to the scatter in the data. In addition, the fitting method became very slow as each combination of the variables had to be tested one by one for entry to the equation. For a single variable to be added from a set of n variables with p possible powers, n*p tests must be carried out to determine the partial correlation coefficients; for a single interaction term to be added from the same set of n variables and p powers, $(n*p)^2$ tests must be carried out. Therefore interaction terms with no powers were tested, however these also suffered from low partial correlation coefficients.

The combination of the amount of scatter producing many additional terms with low partial correlations as well as the extreme increase in the time required to test the interaction terms meant that this approach was not adopted.

6.4.2.2 Selection of the 'best' multivariate regression equation

As not every available independent variable will have an effect on the dependent variable, some method of deciding which variables should be present in the regression equation must be used.

There are a number of methods that can be used to achieve this (Draper & Smith, 1981). For single variable equations, the available independent variables are normally regressed one by one, in no particular order, on the dependent variable. Each independent variable

can then be ranked according to how well the resultant equation fitted. This is often achieved by comparing the coefficient of determination values (e.g. R^2 value).

With a multivariate equation, the same technique is often employed to determine the first variable to try in the equation and the order in which subsequent variables will be added/tested.

6.4.2.2.1 All possible regressions

This procedure involves creating a set of regression equations that corresponds to every possible combination of the independent variables. This technique is simple to implement, however as the number of available variables increases the number of computations that need to be run increases. Assuming that there are r independent variables, the total number of equations that need to be generated and tested is 2^r. In the current research, two sets of variables were investigated, a full set containing 23 independent variables, and a set that related to jerk and acceleration based metrics containing eight independent variables. These would require 8,388,608 and 256 equations to be fitted respectively. The former number is rather large and, although optimised methods have been proposed (for example by Schatzoff et al., 1968) and Furnival and Wilson (1974), a more time-economical method would be preferred considering the large number of potential metrics.

6.4.2.2.2 "Best subset" regression

In this technique (Draper & Smith, 1981), a subset size is determined in advance, normally by performing a step-wise regression and determining how many variables are present in the eventual regression equation (Neter et al., 1985). The technique then attempts to find the best subset containing this number of variables to produce the best fit.

It should also be noted that this technique requires a significant amount of time to run as it must first produce a step-wise regression equation and must then test the various subsets that it has selected. The selections which are tested are generated at random rather than each possibility being tested, and the 'best' set is chosen by determining statistically how many subsets need to be tested to have a high enough chance of selecting the best one. Optimised methods to perform this selection have been proposed by, for example, Hocking and Leslie (1967).

6.4.2.2.3 Backward elimination procedure

In this technique (Draper & Smith, 1981), a regression is initially calculated for an equation containing all of the available metrics and then the metrics are removed one by one until and optimum solution has been found. The following steps are taken after the equation containing all of the metrics has been produced:

1. A partial f-test is performed on each variable as if it were the last to enter the equation;
2. The lowest partial F-test value is then compared with a pre-selected threshold value (see Section 6.4.2.2.4.1);
3. If the F-test value is less than the threshold value, the term to which it corresponds is removed and the regression is calculated for the new equation.
4. If no F-test value is found to be less than the threshold value, the equation is assumed to be the optimum and the process is stopped.

6.4.2.2.4 Step-wise regression procedure

This technique is similar to the backward elimination procedure except that in this case the variables are added to the equation one-at-a-time, and tested for their significance once they have been added.

The first step of this process is to decide upon the initial variable to enter the equation. Each independent variable is fitted to the dependant variable in turn. The most correlated variable is selected and added to the equation as the first term. If the equation is not significant at this point the process is stopped and the equation is assumed to be of the form Y = average(Y). Otherwise, the process proceeds as follows:

1. Partial correlation coefficients are calculated for all of the variables not in the equation at this point (the partial correlation coefficient is like a normal regression coefficient with the effect of the other variables in the equation removed so that it provides a true reflection of the correlation of the variable in question with the dependent variable). The variable with the highest partial correlation coefficient is added to the equation.
2. The equation is tested for significance. If it is found to be non-significant, the last variable to enter the equation is removed and the process is stopped and the last equation is used as the final result.
3. A partial F-test is then calculated for each term in the equation. If a term falls below the threshold value (see Section 6.4.2.2.4.1) it is removed from the equation (if at this

point the procedure stops as the last term to enter the equation was rejected, there a small chance that later variables will be significant, however this is an infrequent occurrence and therefore the process is stopped at this point).

4. The process returns to step 1 and continues.

6.4.2.2.4.1 Partial F test

The partial F test measures the effect of the addition of a term on the correlation equation assuming all of the other terms are already present. This is effectively the same as quantifying the effect that the additional term would have on the equation if it were added last.

When a regression model is being created, this technique can be used to assess the value of adding a new term to a current equation. By the same reasoning, the F test can be applied to terms that are already in the equation, effectively seeing whether the terms that are present still provide a statistical contribution so as to determine whether any should be removed.

This test is required because as new terms are added to a regression model, the statistical effect of the previously added terms on the response variable will change. This technique of applying a partial F-test as terms are added to an equation is known as a sequential F-test. In the F-test, the F value for the term in question is calculated and then compared with a threshold value known as the F-statistic.

A partial F statistic with 1 and v degrees of freedom tests the hypothesis

$H_0 : \beta_j = 0$ versus $H_a : \beta_j \neq 0$ **Equation 6-23**

Where β_j is the coefficient of the term in question, 1 is the degrees of freedom on the single coefficient being tested and v is the number of degrees of freedom of the correlation equation. In the current research, v is equal to $(n - k - 1)$ in which n is the number of observations and k is the number of coefficients in the correlation equation.

Therefore, if the F value of the term exceeds the F-statistic this shows that the coefficient should be non-zero and therefore included in the equation and conversely if it is less than the F-statistic, this shows that the coefficient should be zero and therefore not included in the equation.

The threshold F value is identical to the square of the t statistic with v degrees of freedom (Draper & Smith, 1981) and can therefore be obtained from a t-distribution. This value is compared against the calculated F value for the term in question. The F value is calculated as follows:

$$F = \frac{\left(\frac{R_{inc}^2 - R_{excl}^2}{1}\right)}{\left(\frac{1-R_{inc}^2}{n-k-1}\right)}$$

Equation 6-24

Where R^2_{inc} is the coefficient of determination of the equation with the term included and R^2_{excl} is the coefficient of determination of the equation with it excluded; n is the number of observations and k is the number of parameters in the correlation equation.

If the calculated F value is greater than the F threshold then the term is considered to add to the equation in a statistical sense. In this project, a confidence level of 95% was used to calculate the F threshold.

6.4.2.2.4.2 Equation F-tests

The equation F-test is carried out to determine whether an entire equation is statistically significant. It tests for the hypothesis that $b_1=b_2=...=b_n=0$, where b_x is a parameter in the equation. This is therefore a test for the case that the entire regression is not significant (i.e. none of the coefficients in the equation is non-zero):

$H_0 : C\beta = 0$ versus $H_a : C\beta \neq 0$

Equation 6-25

The $F_{threshold}$ value is obtained from the F-distribution using k and n-k-1 degrees of freedom, where n is the number of observations and k is the number of parameters. The F-distribution is identical to the square of the well-known t-distribution.

The F-value for the equation is calculated as:

$$F = \frac{\left(\frac{R^2}{k}\right)}{\left(\frac{1-R^2}{n-k-1}\right)}$$

Equation 6-26

where R^2 is the coefficient of determination, n is the number of observations and k is the number of parameters.

If $F > F_{threshold}$ then the equation is considered to be significant and the process continues. In this project, a confidence level of 95% was used to calculate the F threshold value.

6.4.3 Comparison of LS and LWS regression techniques

It was originally planned to compare the abilities of the least squares (LS) and least weighted squares (LWS) techniques, to ascertain which would be the better for use in driveability analysis. However, as the research progressed, it was found that equations fitted with one or the other of the techniques produced significantly better correlations when applied to certain datasets. The fact that a LWS equation produces better correlations is most probably due to its ability to ignore scatter and outliers. However, the fact that a LS equation is better than the LWS equation in some cases indicates that it is this scatter that is producing some significance.

The conclusion is that for this project, with relatively limited data sets, it is worth using both techniques as they provide information about the degree of scatter, however, if applied in practice to larger data sets, LWS would be the more useful technique as it can ignore the small numbers of outliers which would be expected while taking into account the important trends in the data which should be better represented by greater volumes of data.

6.4.4 Effect of the choice of metrics

As was stated in Section 5.3.1, the choice of metrics used in this project was decided by a process of testing and then deciding, based on statistical and physical significance, whether they should be used or removed. The addition or use of metrics can make a large difference to the usefulness of the resulting correlation equations.

One set of metrics was found to occur in many of the correlation equations with relatively high partial correlations. This set of metrics consisted of:

- *aAverageSpeed* - the average vehicle speed over the course of the test
- *aAveragePedalPosition* - the average pedal position over the course of the test
- *aAverageEngineSpeed* - the average engine speed over the course of the test

Although these variables were often found in the correlation equations, their physical meaning is not useful for either prediction or modelling of powertrain performance. At first glance it might appear that a correlation which has anything to do with vehicle speed, pedal position or engine speed would be a useful finding, this is not the case as these variables are averages.

As these metrics are all averages, a range of different manoeuvres could return identical data. If these metrics were to be used, other data would also have to be present to qualify the test. In the case of aAverageSpeed, metrics such as initial speed, acceleration and deceleration rates and maximum speed would be required in addition to the average speed to characterise the test in a useful manner. It was therefore decided that as these other metrics were already present, the 'average' metrics were effectively redundant despite an apparent correlation.

Table 6-8 shows the differences between the correlation equations which were fitted to the entire data set using conventional least squares and the full set of metrics. The left-hand column used the full set of metrics as employed in the rest of this research while the right-hand column used these but with the addition of the three 'average' metrics: aAverageSpeed, aAveragePedalPosition and aAverageEngineSpeed.

It should be noted that when the 3 'average' metrics were present at the time the correlations were generated, they were added into the correlation equations; however if the equations were generated without these metrics, and subsequently the resultant equation was tested against these metrics to see whether their effect was sufficiently statistically significant that they should be added, it was found that they were not significant at a 95% confidence level using a partial F-test as described in 6.4.2.2.4.1.

A table containing the full set of results is shown in Appendix III.

Table 6-8 - Differences between correlation equations with the addition of extra terms

	Full metric set-LS	
	without aAverage metrics	**with aAverage metrics**
smoothness	aAverageAccelToMaxSpeed^2 aDeltaEngSpd2MaxSpeed R^2 = 0.428	aMaxEngSpeed^(1/2) aAverageSpeed^-1 aDesiredPedalPosition^(1/2) aEngSpdAtMaxVSpeed^(1/-2) R^2 = 0.438
eng_delay	IDENTICAL R^2 = 0.300	IDENTICAL R^2 = 0.300
vehicle_delay	aMaximumQuirk^(1/-3) R^2 = 0.399	aAveragePedalPosition^2 R^2 = 0.392
init_accel	AccelDelayTime^3 R^2 = 0.407	aAverageAccelToMaxSpeed^(1/-2) aInitialSpeed^-2 aAverageEngSpeed^3 aMaxEngSpeed^2 R^2 = 0.403
accel_prog	aEngSpdAtMaxVSpeed^(1/2) R^2 = 0.291	aAveragePedalPosition^2 aEngSpdAtMaxVSpeed^3 aEngSpdAtMaxVSpeed R^2 = 0.317
performance	aMaximumJerk^(1/-2) LN(aEngSpdAtMaxVSpeed^2) aInitialSpeed^-1 aMaximumQuirk^-2 R^2 = 0.336	aDeltaEngSpd2MaxSpeed^2 aAverageEngSpeed^3 aEngSpdAtMaxVSpeed^(1/2) aInitialSpeed^-1 LN(aMaximumJerk^-1) aDeltaEngSpd2MaxSpeed^3 R^2 = 0.362

It can be seen that the addition of these extra metrics influenced the correlation equation fitting code, as the equations are different in all but one case. The effect in terms of the quality of the correlation equations, as measured by their R^2-values, was not particularly large, though there was a general trend that indicates that the fits were better with the inclusion of these 'average' metrics. One thing that should be noted is that in each case where the inclusion of these 'average' metrics increased the R^2-value, the number of terms in the equation also increased. Although the increase in R^2 was not due to the extra terms, as all of the R^2 values in this project were adjusted for sample size and the number of equation coefficients, increasing the number of coefficients when the increase in R^2 is minimal makes the analysis more complex for no real gain.

Despite the slight increase in the R^2 value with the addition of these metrics, it is considered by the author that the equations which were generated without them are more useful as they contain no metrics whose values could apply equally well to a range of manoeuvres.

6.5 *Data pre-processing*

There are a number of issues that need to be addressed before a least squares regression can be accomplished effectively. These relate to the values and ranges of the variables to be regressed. There are two main issues:

- The existence of ill-conditioned numbers – these are numbers that are so large or small that the operations performed by the least squares fitting will produce useless results.
- The existence of outlying data points – these are points that lie far from the rest of the data and due to their location can have an unduly large effect on the fit of the curve.

The approaches taken to overcome these two issues are explained in the next sections.

6.5.1 Normalising and scaling input data

If numbers are ill-conditioned then the results of certain mathematical operations (such as those required to solve the least squares problem and obtain a best-fit equation) can produce incorrect answers. There are a number of ways in which ill-conditioned numbers can affect the answer of a calculation.

One of these is round-off error. This is the error caused by the rounding that has to be applied to floating-point numbers so that they can be stored in the computer's memory in a finite form. Irrational numbers and fractional numbers with infinite decimal expansions cannot be stored exactly (at least not without using specialised software which handles numbers in symbolic form which is often prohibitively slow). This means that any calculations which use these numbers involve some level of error.

Cancellation error and loss of significance occur when two nearly equal numbers are subtracted, producing a result which is much smaller than either of the original numbers and with very little significance. The same effect is seen when two numbers whose magnitudes are very different are added or subtracted. The result is a loss of precision because the result has too many significant digits to be stored.

To ensure that the Gaussian elimination method which is used to calculate the least squares solution (see Section 6.3.1.1) is able to perform correctly the input data need to be of around the same order of magnitude, if the scale of data in the matrices is significantly different (i.e.

ill-conditioned data), the returned parameters will contain errors, often to such an extent that the resultant least-squares result will be useless or misleading.

There is a possible difficulty with applying a single normalisation and scaling to any data which will be analysed with a given correlation equation. If a set of data with different magnitudes for its objective and/or subjective metrics is to be analysed later using the same equation, these data will be scaled and treated the same as the original data which have a lesser range/magnitude (and vice versa). This will lead to the fit line being offset from the data so that even if the same trends occur, the correlation will be poor. This can be seen in Figure 6-9, which shows a correlation equation that was fitted using all of the vehicle data except for the BMW, plotted against the BMW data. It can be seen that there is a definite offset, and if the data points could be moved downwards (by changing their normalisation and scaling), they would improve the fit of the correlation equation. In fact, it is possible to see that the data do appear to roughly follow the trend shown by the fit lines.

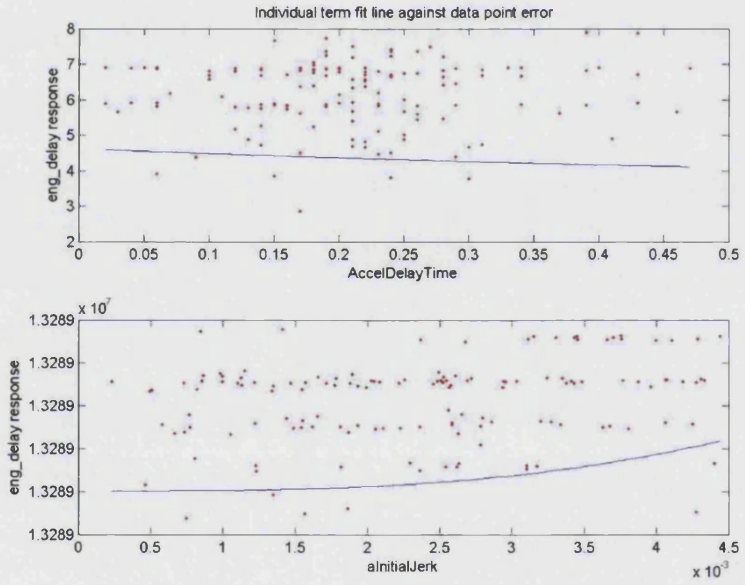

Figure 6-9 – Engine delay response

The approach of using the original normalisation and scaling is taken in this project and is valid, as one should not extrapolate beyond the bounds of the 'training' data. Assuming sufficient data (and data with a sufficient range of values) were used this problem will not manifest itself. In the example shown in Figure 6-9 it would appear that the range of the non-BMW data and BMW data differ sufficiently to make the normalisation and scaling parameters erroneous.

It should be noted that re-normalising and re-scaling could obviously not be performed for single data points, therefore any re-normalisation and re-scaling approach would be limited to offline (or at least slightly delayed) usage, however if a new data set appeared to contain different magnitude data it may be useful to perform re-normalised to see whether these data follow similar trends.

It should be noted that part of the normalisation and scaling process is performed to avoid any of the data points with which the equation is being generated from exceeding the allowable bounds of the equation type. For example if the correlation equation contains logarithms or fractional powers, the scaling ensures that none of these data will be less than or equal to 0. Ideally the scaling and offsetting is performed so that any new data will always be within the allowable bounds of the equation terms (>0 generally), however it is possible, if small data sets or data subsets are being used, that new data will have a different range, which may result in zero or negative numbers after the scaling. These illegal zero or negative values are automatically detected for any terms which contain logarithm or fractional powers and the data are removed to avoid imaginary answers. It should be noted that a 'removal limit' is enforced in the code so that no more than 40% of the entire data set can be removed through a combination of such value illegal detections as well as outlier removals.

If more data are removed than allowed by the removal limit, then the correlation is returned as zero. This means that the variable that was being tested to enter the equation will be rejected without affecting the equation. The use of a 'removal limit' avoids a problem which was seen whereby almost all of the data points from a particularly scattered metric would be removed due to their values or outlier status, resulting in a perfect or almost perfect correlation which would end the equation generation process but produce an equation which was almost useless when it came to be used.

6.5.2 Outlier removal

The removal of outliers or leverage points is very important in the generation of correlations, where it can both skew the fit and cause the standard errors of the regression coefficients to be much smaller than if they were excluded. This leads to an artificial inflation of the apparent 'goodness of fit' (the coefficient of determination) of an equation. Section 6.6.3.2 contains an analysis of these effects. The removal of outliers, especially those which lie a long distance from the sample mean, is the only way to overcome these problems and therefore special attention has been paid to their removal in this project.

The subjective variables are subjected to a strict test: if the value lies outside the range from 0 to 10, then the data for that particular test are ignored as it is not possible for such a value to be recorded in a test and it is therefore assumed that the data are either corrupt, or an input mistake has been made. Whichever is the case, there is no way to retrieve the correct data.

The objective variables all have their values checked for outliers. First of all an outlier test is performed on the data (this is explained in the next section, 6.5.2.1). Then the values are checked to ensure than none fall outside their individual allowable values. The following tests are performed. If any are failed, the value of the variable is set to the special value *NaN* (Not a Number), which ensures that it will not be used in the rest of the procedure.

Some metrics can immediately be marked as faulty if they have certain values. These are values which are not physically possible and which are generated if the metric generation code was unable, for whatever reason, to produce the metric correctly. These metrics are *aChangeInSpeed*, *aAccelGradient*, *aInitialJerk*, *aMaximumJerk* and *aAverageJerk*. These metrics are marked as faulty if their values fall below 0 kph or g/s respectively.

Other metrics are merely adjusted to ensure that their values remain within a valid range as shown in Table 6-9. It should be noted that this technique may be prone to error should there be large numbers of poorly calibrated data points in the dataset. However these poorly calibrated tests should have been detected and disallowed during the metric generation process and initial stages of outlier detection procedure.

Table 6-9 - Objective metric outlier substitutions

Variable	Minimum value	Assigned value if less an minimum	Maximum value	Assigned value if more than maximum
aInitialSpeed	0 kph	0 kph	100 kph	100 kph
aMaxSpeed	0 kph	NaN	200 kph	200 kph
aInitialPedalPosn	0 %	0 %	100 %	100 %
aMaxPedalPosition	0 %	NaN	100 %	100 %
aAveragePedalPosition	0 %	NaN	100 %	100 %
aDesiredPedalPosition	0 %	NaN	100 %	100 %
aMaxAccel	0 g	NaN	10 g	NaN
AccelDelayTime	0 s	NaN	10 s	NaN
aMaxEngSpeed	0 rpm	NaN	7500 rpm	NaN
aAverageEngSpeed	0 rpm	NaN	7500 rpm	NaN

It should also be noted that the number of outlying data points in a given test is limited to a certain percentage of the total number. For this research this has been 40%. This means 60% of the original number of data points must pass both the outlier and data validity tests, as well as any data removals which are necessary due to the presence of logarithms or roots in the correlation equation. This threshold value is necessary as otherwise it is possible that almost all of the data points in a given dataset might be removed and then the correlation equation may not be representing the true trends of the dataset.

6.5.2.1 Grubbs' outlier test

Although the automatic rejection of outliers is not a recommended approach in regression analysis (Draper & Smith, 1981), in the case of this project it is required to avoid skewing any regressions through the inclusion of erroneously calculated metrics. Although every precaution is taken to try to avoid this situation, it must still be checked and catered for should it occur. There have been many theories and equations proposed for the categorisation of outlying data points, the most important of which are summarised by Anscombe (1960).

In the absence of any contra-indications, the relatively simple Grubbs' outlier test (Grubbs, 1969; NIST/SEMATECH handbook) was chosen as it is a well tested and well known outlier test that produced good results in the test cases which were analysed manually. The Grubbs' test detects data points that do not follow the expected normal distribution of data for a given probability value. Alternative names for the Grubbs' test are the maximum normalised residual test and the extreme studentised deviate. Grubbs' test is defined for the hypothesis H_0: no outliers in the dataset and H_a: there is at least one outlier in the dataset. The Grubbs' test statistic is defined as

$$G = \frac{\max\left|Y_i' - \bar{Y}\right|}{std}$$ **Equation 6-27**

where $\bar{Y}$ is the sample mean, Y_i is the *ith* observation from a data set and *std* the sample standard deviation.

For the two sided test (that is testing that both the minimum and the maximum Y values are not outliers), the hypothesis of no outliers is rejected if:

$$G > \frac{(N-1)}{\sqrt{N}} \sqrt{\frac{t^2_{(\alpha/(2N),N-2)}}{N-2+t^2_{(\alpha/(2N),N-2)}}}$$ **Equation 6-28**

where N is the number of data points, and $t^2_{(\alpha/(2N),N-2)}$ is the critical value of the t-distribution with (N-2)/2 degrees of freedom and a significance value of α/(2N).

Once an outlier has been identified, it is excluded from the data set and the test is repeated until no more outliers are found. Points marked as outliers are not used in the generation and testing of the correlations.

6.5.3 Principal Component Analysis (PCA)

In some situations, when the dimension of the input data are large, but the components of the data are highly correlated (and therefore redundant) it is advisable to run a principal component analysis on the data (Tatsuoka, 1971). This technique acts to reduce the number of dimensions of the input data by selecting only the main components of all of the inputs. This means that a problem can be simplified by replacing a groups of variables with a single new variables. This technique has three effects: it orthogonalises the components of the input variables (so that they are uncorrelated with one other); it orders the resulting orthogonal components (principal components) so that those with the largest variation come first; and it eliminates those components that contribute the least to the variation in the data set.

The method proceeds as follows (Jolliffe, 1986):

1. The mean value of each set of data points (for a given observation) is subtracted from those points.
2. A covariance matrix is formed from the data calculated in step 2.
3. Eigen vectors and values are calculated from the covariance matrix.
4. The eigen vectors and values are re-arranged in order of decreasing eigen value. The eigen values represent the 'energy' of the source data.
5. A threshold 'cumulative energy' value is set and eigen values are chosen above (or within) this value to represent the new axes of the dataset.
6. The data are projected onto the new axes (represented by the chosen eigen values/vectors).

This technique produces a number of new axes (the principal components). The first axis is that which produces the greatest variance in all of the data. When each observation is

projected on this axis, the combination of the values form a new variable. The second (and so on) principal components then for additional axes in space, each perpendicular to the others. Projecting the original observations onto these axes generates the new variables.

The variance of each variable is the maximum among all possible choices for each axis (assuming that each axis is orthogonal to all others, and that the first axis produces the maximum variance for all of the data). The full set of principal components created by this method is as large as the original set of variables, however it is often found that the sum of the variances of a reduced set of these principal components accounts for nearly all of the variance of the original data and therefore the number of dimensions of the data can be reduced while still accounting for the majority of the variance.

It should be noted that PCA was not used in this work for two reasons. Firstly it was found that the improvement in the results using the principal components was not significantly better than using the unmodified variables. Secondly, the goal of this work is to produce equations that can clearly and easily show the relations between the different subjective and objective metrics. The use of PCA would make it significantly more difficult for a calibration engineer to interpret the resultant correlation equations.

6.6 Rating the fit

The following are a number of methods which can be used to rate the quality of the fit of a correlation equation.

6.6.1 Residual mean square

For models where the number of possible variables, r, is large (>10 for example) and the number of data points is also large (5r to 10r) the analysis of the residual mean square error can be used to determine how many parameters (with associated variables) to add to a model (Draper & Smith, 1981). A graph of the residual mean square error plotted against the number of parameters tends to decrease and stabilise around about the value of the square of the standard deviation, σ^2, of the population from which the samples are drawn. Adding more parameters to a model once this level has been attained is pointless as little more of the variance can be explained. This stabilisation is relatively easy to detect.

Although the number of metrics available in this project is sufficient to make this technique applicable, the relatively small number of samples makes it less desirable, as does the very

large number of calculations that would be required to determine the optimum number of equation parameters due to the number of metrics. For example, the first data point plotted on the residual mean square graph, which is the average of the squared residual error for all regressions with one coefficient, would require 630 combinations regressions to be performed before the results were averaged (35 metrics x 6 powers x 3 equation types). The second point would then require 396,270 regressions before the averaging, and so on. This detracts from one of the principal advantages of using multivariate correlations, that the data processing and regression is a fast process and this therefore makes the use of the residual mean square technique less attractive.

6.6.2 Mallows C_p statistic

An alternative measure of the goodness of fit is the Mallows C_p statistic is defined as (Draper & Smith, 1981):

$$C_p = \frac{RSS_p}{s^2 - (n - 2p)}$$ **Equation 6-29**

Where RSS_p is the residual sum of squares for a model containing p parameters, p is the number of parameters in a model (including the constant term) and s^2 is the residual mean square error from the largest equation which was tried containing all of the objective metrics, and is assumed to be a reliable estimate of the error variance σ^2.

The Mallows C_p statistic can be used in a similar way to the coefficient of determination (Gorman and Toman, 1966), which is introduced in the next section, and is in fact similar to the adjusted R^2 statistic that was used in this research (Kennard, 1971).

6.6.3 Pearson's correlation coefficient and the coefficient of determination

The coefficient of determination, R^2, was chosen as the measure of how well a correlation equation predicts data points due to the relative simplicity of its calculation and its ease of understanding and comparison. The index itself is a number between zero and one, where one indicates that the regression equation accounts for all of the variance in the recorded data (dependent variable) and zero indicates that it accounts for none of the variance. The coefficient of determination is calculated using the following equation (Ezekiel & Fox, 1959):

$$R^2 = \left(\frac{s_{y'}}{s_y} \right)^2$$ **Equation 6-30**

Where $S_{y'}$ is the standard deviation of the calculated data points, and S_y is the standard deviation of the actual data points.

This may be more easily interpreted when considered in terms of the error associated with the regression itself and the residuals (or leftover error):

$$R^2 = \frac{SS_{regression}}{SS_{regression} + SS_{residual}} \qquad \textbf{Equation 6-31}$$

where:

$$SS_{residual} = \sum (X - X')^2 \qquad \textbf{Equation 6-32}$$

$$SS_{regression} = \sum (X' - \bar{X})^2 \qquad \textbf{Equation 6-33}$$

Therefore:

$$R^2 = \frac{\sum (X' - \bar{X})^2}{\sum (X' - \bar{X})^2 + \sum (X - X')^2} \qquad \textbf{Equation 6-34}$$

Although the meaning of the coefficient of determination is defined – it represents the percentage of variance in the dependent variable that is accounted for by the regression equation, the interpretation of this number in qualitative terms, and therefore the determination of limits for the use or non-use of equations is open to interpretation.

This interpretation depends on the application to which the correlation will be put. When the regression equation is to be used for prediction purposes, for example the prediction of driveability from test-rig data, high limits (>0.80) may be favoured as otherwise the predictions are of limited accuracy and therefore of limited use. When the regression equation is to be used to investigate trends between the dependent and independent variable, for example in the case of a calibration engineer being interested to find trends in the variables that may influence driveability, then lower limits (>0.50) may be used, as these correlations will still contain useful information, even though external factors may still be influencing the results.

The latter approach is that taken in this research, because the influence of external factors cannot be excluded in this initial research. Therefore the following approximate scale has

been used to evaluate the coefficients of determination. This scale was suggested by Cohen (1988) for use in psychological research:

Table 6-10 - Interpretation of coefficient of determination value

Degree of Correlation	Coefficient of determination value
Small	0.10 – 0.29
Medium	0.30 – 0.49
Large	0.50 – 1.00

6.6.3.1 Degrees of freedom adjustment for coefficients of determination

Before being used, the coefficients of determination are adjusted to take account for the number of observations and the number of coefficients in the correlation equation as both of these factors has an effect of the result. This change is required as small sample sizes and large numbers of equation coefficients/parameters tend to overestimate the amount of variance in the dependent variable that is accounted for by the independent variables. This adjustment is therefore based on adjusting the standard deviations and therefore the estimate of variance in the universe from which the samples are drawn.

The calculated R^2-value is adjusted using the following equation (Draper & Smith, 1981; Ezekiel & Fox, 1959):

$$R^2_{adjusted} = 1 - \left(1 - R^2\right)\frac{n-1}{n-p} \qquad \textbf{Equation 6-35}$$

where $R^2_{adjusted}$ is the adjusted coefficient of determination, R^2 is the original coefficient of determination, n is the number of observations and p is the number of parameters in the correlation equation.

6.6.3.2 Limiting the response of the correlation equation

Outlying data points can cause a number of problems both in the generation of the correlation equations and in their application to prediction. The effect that these points have on the generation of correlations is discussed in Section 6.5.2. The effect of these points on the application of correlation equations is discussed below.

The problem of outliers becomes apparent when a correlation equation, due to its constituent terms, produces predictions which contain significant errors. The difference

between these predicted points and the actual data points is then significantly greater than the mean error of the other predicted points. Therefore it is necessary to limit the range over which the terms of the correlation equation can range to ensure that they cannot produce outliers which artificially inflate the correlation coefficient of the term and consequently entire equation.

If the response (which we will call 'y') variable's range is not limited, the R^2-value can be artificially inflated – this occurs because:

$$R^2 = \frac{SS_{regression}}{SS_{regression} + SS_{residual}}$$ **Equation 6-36**

where:

$$SS_{residual} = \sum (X - X')^2$$ **Equation 6-37**

$$SS_{regression} = \sum (X' - \bar{X})^2$$ **Equation 6-38**

This means that $SS_{regression}$ can become large if there is a single Y' point (predicted response variable) which is significantly larger than the others (significantly larger than the mean of Y, the actual response variable). It should be noted that the same effect might also be seen when the correlation equations are fitted, however the raw data are processed to remove outliers, thereby avoiding this problem.

Therefore the fitted variable, Y', is limited to a range of 0-10 (these are the same limits as are imposed on the original subjective metrics). This ensures that as little as possible artificial inflation of the R^2-value of a given equation occurs. This can, however, produce some irregularities where a curve might be moving to exceed the 0-10 boundaries and then is suddenly limited and becomes completely flat with a value of 10 or 0 (see Figure 6-10); this is, however, seen infrequently.

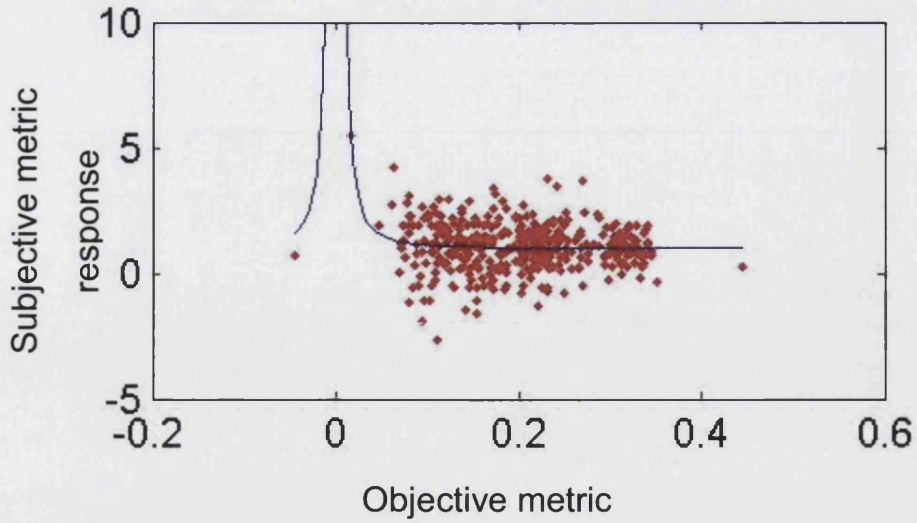

Figure 6-10 - Subjective metric response limit

The current method has been found to reduce the addition of metric terms solely due to outlying data points and the results of the correlations do not usually contain any terms that affect the overall correlation equations' results. However should such terms occur more often, it might be desirable to investigate algebraic methods of limiting the terms' responses to ensure that the correlation equations contain trends that are a simple and realistic as possible.

It was decided that the use of such terms would significantly increase the complexity of the correlation code and they were therefore excluded in favour of the limit method explained in section 6.6.3.2. There are a variety of methods by which the output value of a given term (Atkinson, 1969) or entire correlation equation (Mantel, 1969) can be limited to a certain range. Although prediction outliers have not caused significant problems, the implementation of an algebraic equation limit method may be useful.

6.6.4 Partial correlation coefficient

The partial correlation coefficient measures the importance of a single term in a regression equation after taking account of the effect of the other terms in the equation. This measure is calculated by comparing the regression coefficient for the entire equation with and without the term in question, thereby giving an indication of how much the term itself contributes. The following equation is used to calculate the partial correlation coefficient (Ezekiel & Fox, 1959):

$$r^2_{partial} = \frac{\left(1 - R^2_{excluding}\right) - \left(1 - R^2_{including}\right)}{\left(1 - R^2_{excluding}\right)}$$ **Equation 6-39**

where $R^2_{excluding}$ is the coefficient of determination of the equation excluding the term in question and $R^2_{including}$ is the coefficient of determination with the term included.

6.7 *Visualisation methods*

The results of this research consist of multivariate equations, and visualising these data is difficult if not impossible once the number of data dimensions rises beyond two or three. Therefore, techniques are required that allow the data to be represented in a useful fashion so the effect of single variables and their interactions can be seen.

6.7.1 Sammon Plots

Sammon mapping (Sammon, 1969) is a method of mapping a multi-dimensional dataset into a lower number of dimensions. It is impossible to visualise 10 dimensional data, but by using Sammon mapping, these data can be mapped into a more useful number of dimensions. This means that the multidimensional data can be represented in a more easily interpreted two or three-dimensional Sammon plot.

The algorithm used to achieve the Sammon mapping is iterative and attempts to keep the Euclidean distances between all of the points in the higher and all of the points in the lower dimensional spaces identical. The algorithm proceeds as follows (Sammon, 1969):

1. Interpoint distances are calculated for every point in the higher dimensional space.
2. All of the points from the higher dimensional space are initially generated at random locations in the lower dimensional space.
3. The mapping error, E, which is the difference between the interpoint distances in the higher and lower dimensional projections, is calculated using the following equation:

$$E = \frac{1}{\sum_{i<j}\left[d^*_{ij}\right]} \sum_{i<j} \frac{\left[d^*_{ij} - d_{ij}\right]}{d^*_{ij}}$$

where d^*_{ij} is the interpoint distance between point *i* and point *j* in the higher dimensional space, and d_{ij} is the interpoint distance between point *i* and point *j* in the lower dimensional space.

4. An iterative steepest descent procedure is used to find the minimum error, E. At this point, the points are as close to having identical Euclidean distances in both the higher and lower dimensional spaces as possible.
5. If the error, E, is sufficiently small, the procedure ends.

Figure 6-11 shows a 3-dimensional data plot of the *aInitialJerk* and *aMaxAccel* objective metrics against the *smoothness* subjective metric; although it is possible to visualise such a plot, it is difficult when the plot cannot be viewed from different angles or rotated. Obviously any greater number of dimensions could not be easy shown in pictorial form.

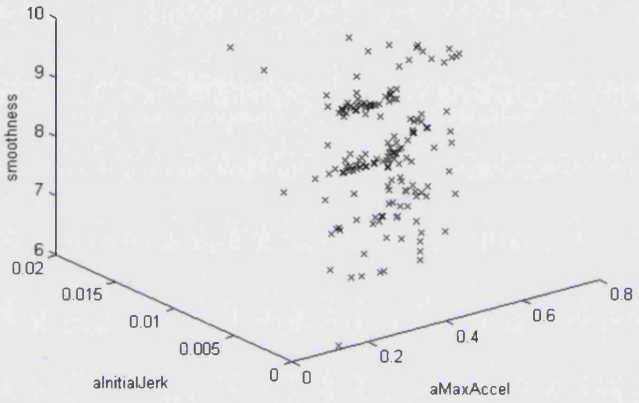

Figure 6-11 - 3D data representation

Figure 6-12 shows the same data reduced to two dimensions. It can be seen that there are a number of groups of data, which may indicate that the different vehicles exhibit different behaviour affecting their *smoothness* ratings.

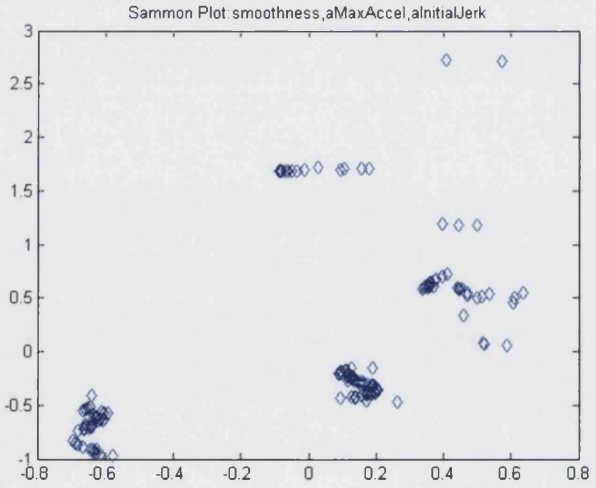

Figure 6-12 - 2D (Sammon plot) data representation

The method is not constrained by the number of dimensions of the input data set, and can reduce any multidimensional data to a lower dimensional data space. The SOM Toolbox v2 (Alhoniemi et al., 1999) was used in MATLAB to produce the Sammon plots shown in this thesis.

6.7.2 Multivariate plotting technique

As was explained in Section 6.7.1, it is very difficult to visualise the effects of individual terms of metrics in an equation that contains more than three independent terms. The Sammon plot technique is useful in that it can reduce the number of dimensions of a set of data points, however it still cannot represent the trends exhibited by the data points in each of these dimensions. Therefore the author developed a plot which shows the trends for each term or metric (as the equation may contain a combination of terms containing the same metric and it is more useful to see the trend displayed by the overall combination) in a given equation.

This means that the following equation (Equation 6-40) can be plotted against its error with a set of data points as seen in Figure 6-13 below. Here the blue line shows the contribution to the overall equation provided by the metric in question (the same can be done for each term) and the red points show the total error between the line and the overall fit.

Equation 6-40

Subjective rating	Equation	Coefficient of determination
vehicle_delay	-3298.411107 +436.402789* aMaximumJerk^(1/-2) -436.837309* aMaximumJerk^(1/-3) -0.357524* aMaxAccel^-1 -1.302969* aMaximumJerk^3 +0.123737* aAverageAccelToMaxSpeed^-3 -0.289839* aAverageAccelToMaxSpeed^3 +0.155508* aInitialJerk^2	0.539

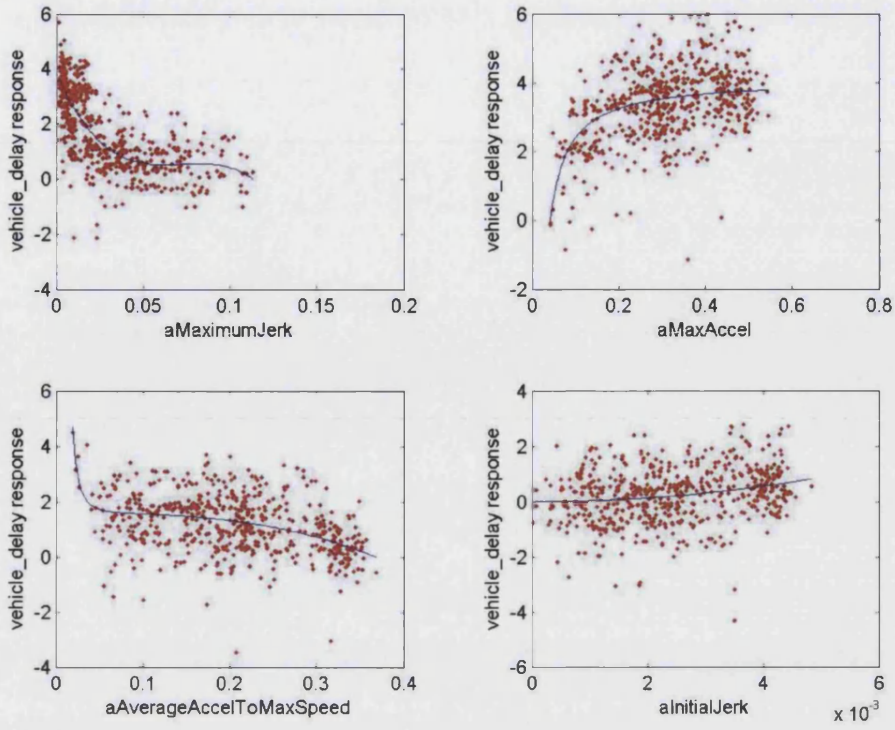

Figure 6-13 - Example multivariate plot

These plots are produced in the following way:

First, the error between the actual and fitted data points is calculated. The range of the independent data in each term is then calculated and the equation response for each individual term is calculated over the range of the data that it contains.

By adding together these responses for each term, plus the constant term from the equation, the overall predicted values for the equation can be produced, however the goal here is to keep the terms split (or to combine them only with other terms which contain the same metric) so that their responses can be seen.

Therefore each term or metric's response is plotted after adjusting the values (by subtracting the smallest value of the response) to ensure that the scale remains reasonably small. The error points are then plotted by calculating the response of the term for the recorded data points and adding the overall error to this. Therefore, the graphs show the response of each term/metric along with the total error for the entire equation.

7 Results of the correlation analysis

7.1 Vehicle analysis

It was found that there were some inaccuracies in the pedal positions and pre-manoeuvre vehicle speed data collected during the testing. Therefore it was decided that an analysis of the accuracy of the data collected from each vehicle should be performed to determine whether these inaccuracies are a generic problem associated with the testing methodology, which should be addressed for future research, or if they are specific to certain vehicles and their particular setup.

7.1.1 Speed accuracy

Figure 7-1 shows the mean speed demand error (the mean error in the value attained by the test drivers when compared with the speed which was supposed to be achieved for a given test), plotted for each vehicle. Both maximum/minimum and standard deviation bars are shown on the figure.

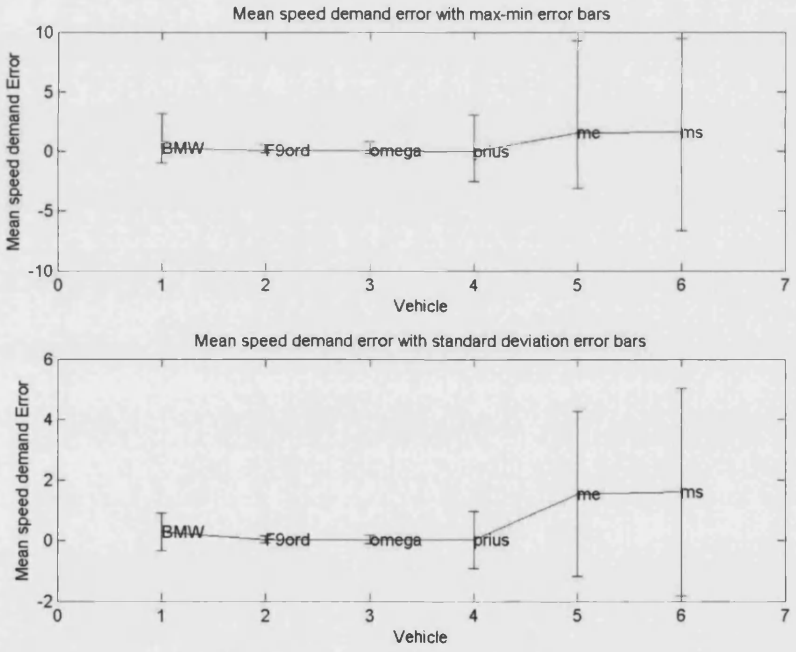

Figure 7-1 - Speed error by vehicle

It can be seen from Figure 7-1 that the speed accuracy during the testing of the AT Mondeo (economy and sports mode) was lower than for the other test vehicles as indicated by the standard deviation and maximum/minimum value lines. This is because the precision of the initial vehicle speeds was not a major factor for the new experimental tests performed by the

author because the goal of the research was to apply multivariate correlations, which would account for differences in speed, to the data. The Prius data, which were also collected during the current research, have a smaller standard deviation as this testing took place early in the study while the testing scheme used during Wicke's project was being followed and tested. It may be noted that the speed accuracy for the BMW is less (standard deviation is greater) than that for the Omega and CVT Mondeo, which were part of the same test group, however it would appear that suggest that this is simply the result of random differences in the testing. This hypothesis is supported by the following figures that the error between the demand speed and the actual speed data is close to normally distributed (considering the small sample sizes) as would be expected if there were no systematic vehicle-related cause of the variation.

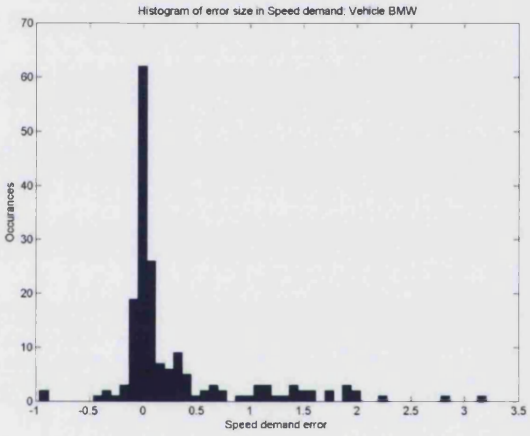

Figure 7-2 – BMW speed error histogram

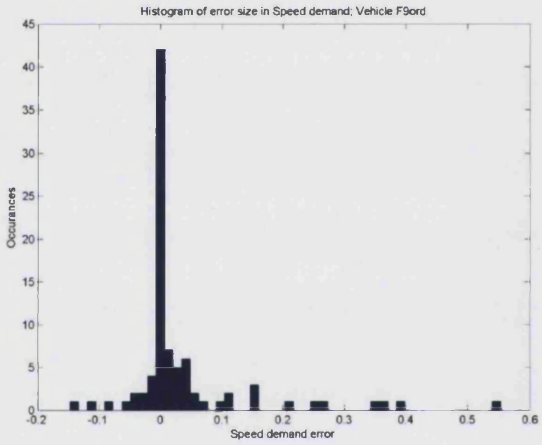

Figure 7-3 - Torotrak Ford Mondeo speed error histogram

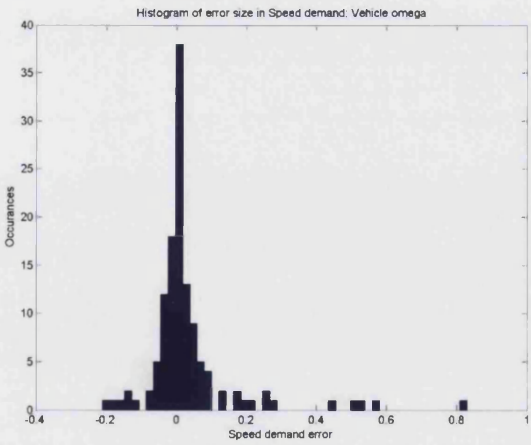

Figure 7-4 - Omega speed error histogram

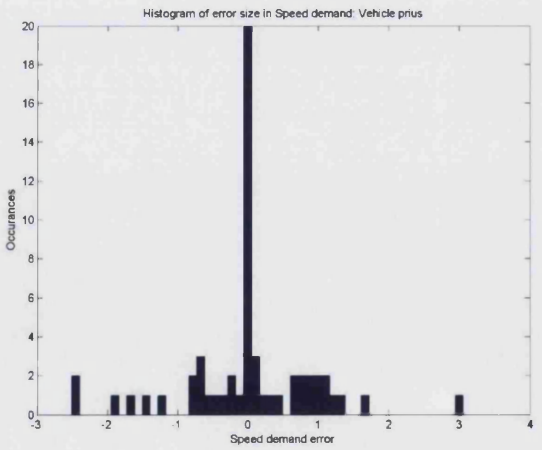

Figure 7-5 - Prius speed error histogram

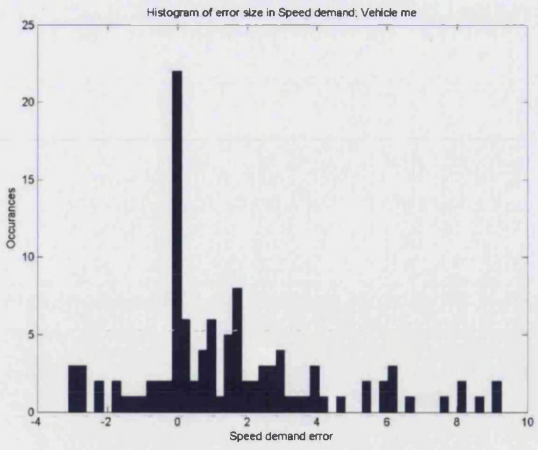

Figure 7-6 – AT Ford Mondeo (economy mode) speed error histogram

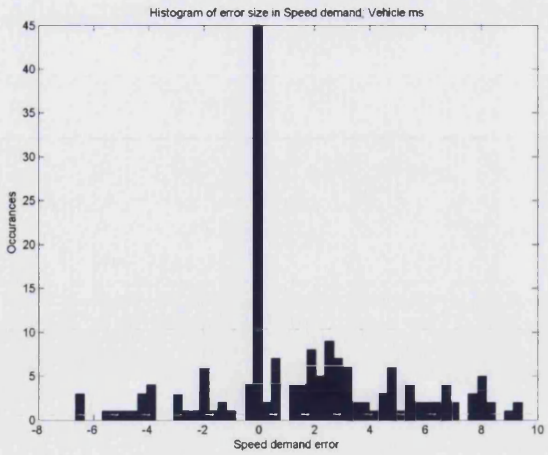

Figure 7-7 - AT Ford Mondeo (sports mode) speed error histogram

7.1.2 Pedal position accuracy

Figure 7-8 shows the mean pedal position error (the mean error in the value attained by the test drivers when compared with the pedal position which was supposed to be achieved for a given test), plotted for each vehicle. Both maximum/minimum and standard deviation bars are shown on the figure.

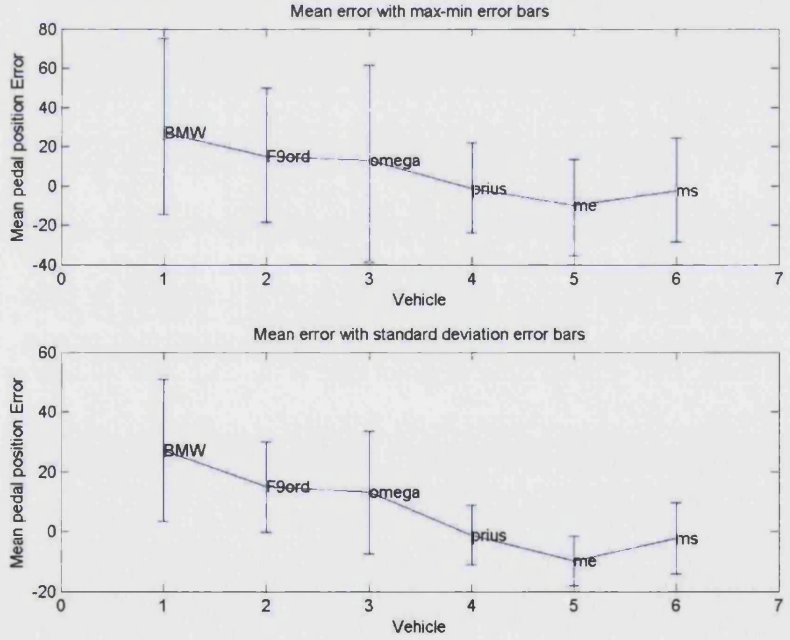

Figure 7-8 - Pedal position error by vehicle

It can be seen that the Prius and AT Mondeo (both economy and sports modes) have relatively small pedal position errors, both in terms of the mean error and the

maximum/minimum and standard deviations, compared with those of the BMW, CVT Mondeo and Omega. This is most likely due to the use of a visual pedal position indicator for the testing of these vehicles during the current project.

7.2 *Driver analysis*

It was found that there were some inaccuracies in the pedal positions and pre-manoeuvre vehicle speeds that each driver produced during their testing. Therefore it was decided that an analysis of each driver's accuracy should be performed to determine whether these inaccuracies are a generic problem associated with the testing methodology, which should be addressed, or if they are specific to certain drivers, in which case either these drivers should be offered more familiarisation time and/or visual/aural indications of the correct vehicle speeds and pedal positions, or they should be excluded from the testing to avoid producing inaccurate data.

7.2.1 Speed accuracy

Figure 7-9 shows the mean speed demand error (the mean error in the value attained by the test drivers when compared with the speed which was supposed to be achieved for a given test), plotted for each pedal demand position. In the top graph, the error bars show the maximum and minimum errors while in the bottom graph, the error bars show the standard deviation of the errors about the mean.

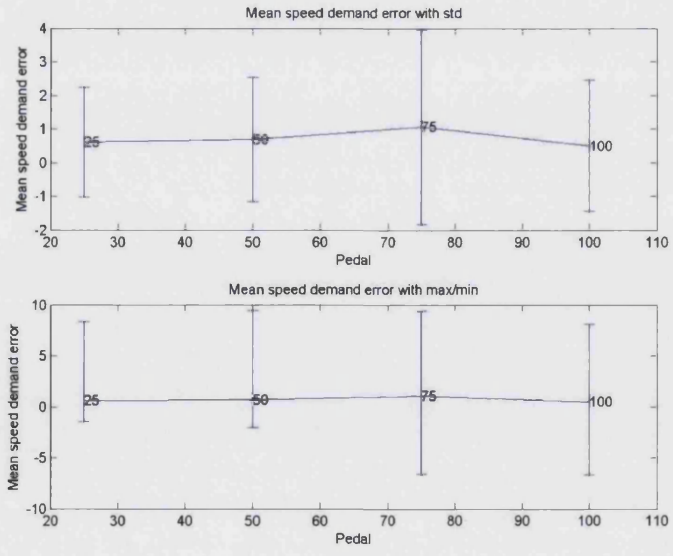

Figure 7-9 - Mean speed error by pedal demand position

There appears to be no link between the vehicle initial speed error and the initial pedal position as would be expected, however it should be noted that 75% pedal tests show a slightly greater standard deviation. While the 75% and 100% tests have an approximately symmetrical maximum/minimum spread, the 25% and 50% tests show a larger range in the positive direction.

This may be caused by the drivers having difficulties judging the position of the smaller pedal inputs. It was seen that drivers generally did apply a larger accelerator pedal position than was specified in the test descriptions. For the larger pedal positions, it is easier to estimate how far the pedal has moved.

Figure 7-10 shows the mean speed demand error (the mean error in the value attained by the test drivers when compared with the speed which was supposed to be achieved for a given test), plotted for demanded vehicle speed. In the top graph, the error bars show the standard deviation of the errors about the mean, while in the bottom graph, the error bars show the maximum and minimum errors.

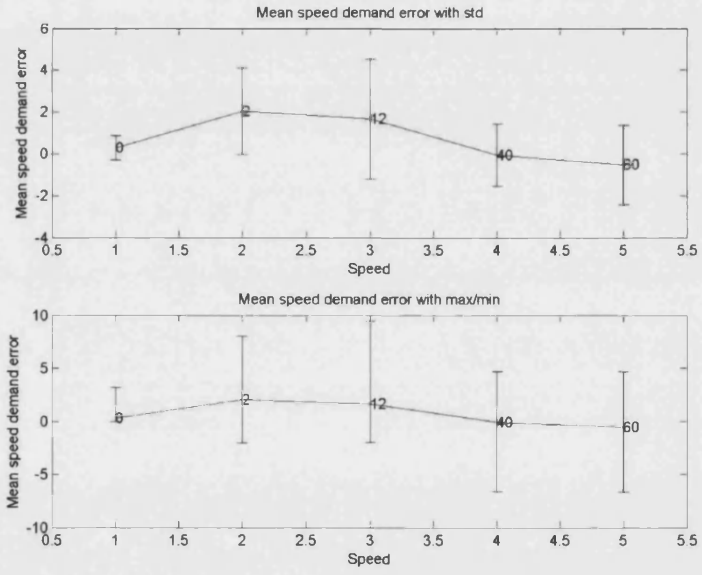

Figure 7-10 - Mean speed demand error by speed

It can be seen that the 12kph tests have the largest (standard deviation) error with the 2kph tests following close behind, this may be due to the combined difficulties of judging the vehicle speed at such low speed and maintaining a steady speed with a very small pedal depression (small movements in the pedal position are more likely at small pedal positions

as it is more difficult to judge the pedal position and this will produce a relatively large vehicle speed change due to the vehicle's low speed).

It should be noted that while testing the AT Mondeo vehicle (Me/Ms), the 2kph initial speed was attained by running the vehicle in gear (with Drive selected on the AT) with no application of the accelerator pedal. It is understood that the same process was used during Wicke's testing. At such low speeds, any small changes in the gradient of the test road could result in either a higher speed than required (when running on a slight downward gradient), or the vehicle not moving at all (on an upward gradient). In the case of the vehicle not moving, some application of the accelerator pedal was required, however this was also problematic as it was almost impossible to judge the required pedal movement precisely enough to control the vehicle at such a low speed (in part due to the effect of the torque converter). This meant that the vehicle was then prone to speed up more than was wanted affecting the accuracy with which the 2kph speed could be maintained.

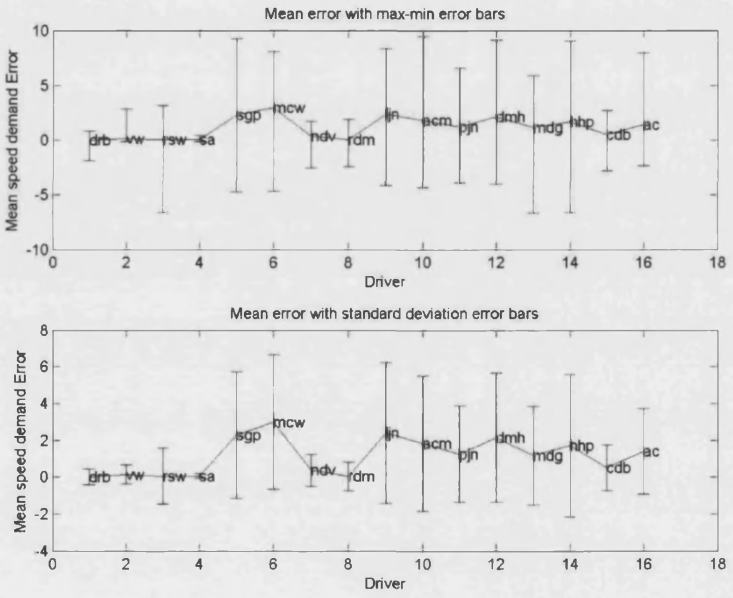

Figure 7-11 - Mean speed error by driver

Figure 7-11 shows the mean speed demand error (the mean error in the value attained by the test drivers when compared with the speed which was supposed to be achieved for a given test), plotted for each driver. In the top graph, the error bars show the maximum and minimum errors while in the bottom graph, the error bars show the standard deviation of the errors about the mean.

Table 7-1 shows which vehicles the drivers shown in Figure 7-11 drove as part of the test programme.

Table 7-1 - Drivers' vehicle test history

Driver	Vehicles tested
drb	BMW, CVT Mondeo, Omega, Prius
vw	BMW, CVT Mondeo, Omega
rsw	BMW, CVT Mondeo, AT Mondeo (e/s modes) , Omega, Prius
sa	BMW, CVT Mondeo
sgp	AT Mondeo (e/s modes) , Prius
mcw	AT Mondeo (e/s modes), Prius
ndv	BMW, Prius
rdm	BMW, Omega, Prius
cjb	BMW, AT Mondeo (e/s modes) , Omega
ljn	AT Mondeo (e/s modes)
acm	AT Mondeo (e/s modes)
pjn	AT Mondeo (e/s modes)
dmh	AT Mondeo (e/s modes)
mdg	AT Mondeo (e/s modes)
hhp	AT Mondeo (e/s modes)
cdb	AT Mondeo (e/s modes)
ac	BMW, CVT Mondeo, AT Mondeo (e/s modes)

It can be seen that the drivers who took part in the current project show larger speed accuracy errors than those in Wicke's tests. This is most likely because during the current project it was decided that achieving an exact start speed was not required (though the same general speeds were used to achieve a range of values) as the multivariate technique should be able to operate on data with a range of speeds rather than requiring an exact match.

7.2.2 Pedal position accuracy

Figure 7-12 shows the mean pedal position error (the mean error in the value attained by the test drivers when compared with the pedal position which was supposed to be achieved for a given test), plotted for each driver. Both maximum/minimum and standard deviation bars are shown on the figure.

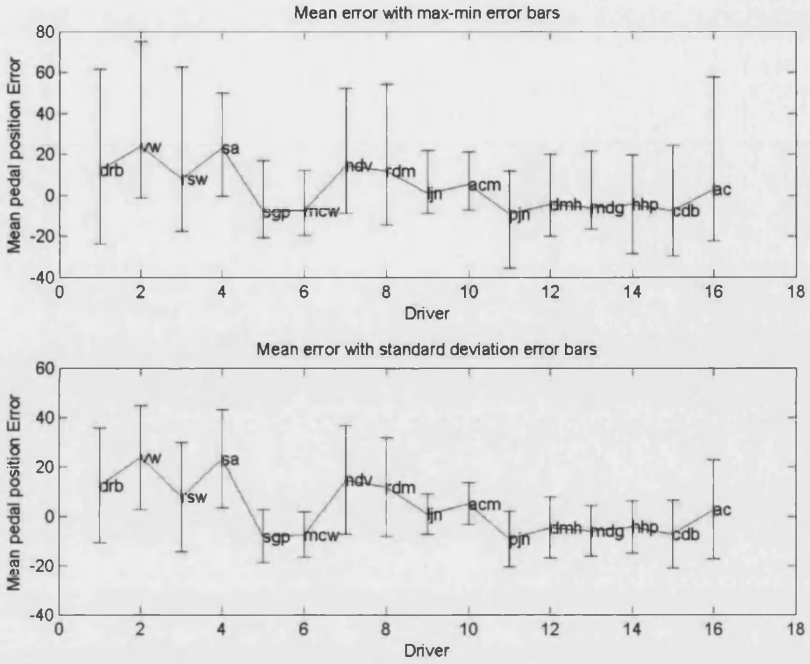

Figure 7-12 - Pedal position error by driver

There appear to be two groups of drivers, those with relatively large standard deviations in their pedal position, and those with smaller standard deviations.

These two groups match with the drivers who took part in the testing for Wicke's project and those who took part in the testing for the current project. The drivers who took part in the current project are the group with the smaller standard deviations. This difference could be attributed to a number of factors, however the most reasonable and obvious is the fact that in the current testing the drivers were aided by a pedal position display on the dashboard and Wicke's drivers did not have this facility. It was also decided in the current project that the drivers should be allowed to familiarise themselves with the pedal positions by driving the vehicle just before the tests were carried out. In the author's opinion, both of these factors produced significantly less error in the pedal position than was achieved during Wicke's testing.

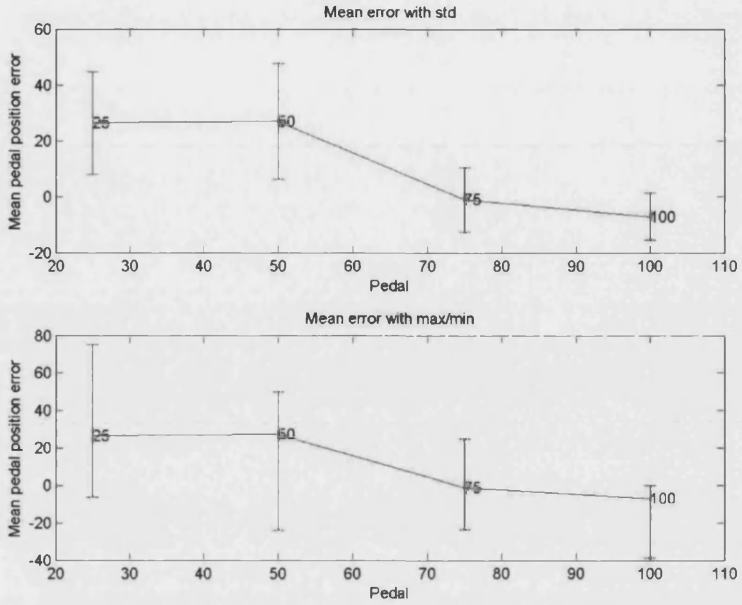

Figure 7-13 - Pedal position error by pedal position

Figure 7-13 shows the mean pedal position error (the mean error in the value attained by the test drivers when compared with the pedal position which was supposed to be achieved for a given test), plotted for each test pedal position. Both maximum/minimum and standard deviation bars are shown on the figure.

The 25% and 50% pedal positions shows the largest errors, followed by 75% and 100%. The fact that 100% pedal position shows the smallest error is expected as it is the only position that has a physical limit (and the drivers should therefore have no problem with this); the fact that there is an error is due to the drivers not pushing hard enough on the pedal, and therefore achieving less than the full movement. The larger error seen in the two smaller pedal positions is caused by the drivers finding it difficult to judge their foot and leg movement over the smaller distance changes required for these pedal movements.

7.3 Correlations between the subjective metrics

The following tables show the correlations between the different subjective metrics:

Table 7-2 - Single subjective variable LS inter-correlations

Correlation Equation	Coefficient of determination (R^2)
smoothness = 2.968713+0.725806* performance^2	0.526
eng_delay = 0.900349+0.872711* vehicle_delay	0.762
vehicle_delay = 0.260984+0.872711* eng_delay	0.762
init_accel = 0.893026+0.848357* performance	0.719
accel_prog = 1.147352+0.837484* performance	0.701
performance = 0.441786+0.848357* init_accel	0.719

Table 7-3 - Single subjective variable LWS inter-correlations

Correlation Equation	Coefficient of determination (R^2)
smoothness = 1.513545+0.772165* performance	0.554
eng_delay = -3.112877+0.922017* vehicle_delay^(1/2)	0.774
vehicle_delay = -4.570953+0.981655* eng_delay^(1/2)	0.776
init_accel = 0.874413+0.851722* performance	0.721
accel_prog = -2.997347+0.917193* LN(performance^2)	0.707
performance = 0.123986+0.877997* accel_prog	0.719

It can be seen that the coefficients of determination for each metric are relatively high and that the values match very closely for the least squares and least weighted squares fitting methods. It can also be seen that the correlated metrics match in all but one case, even if the exact terms differ slightly is some cases.

The diagram below shows the links between the subjective metrics.

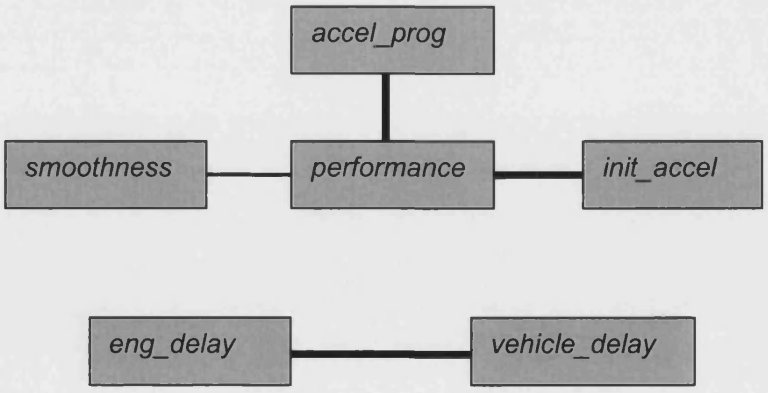

Figure 7-14 - Subjective metric links

It can be seen that *eng_delay* and *vehicle_delay* are only correlated with one another; this is not surprising as the two would be expected to be similar. Whether this is due to the actual physical events being similar or to the test drivers' having difficulties differentiation between the two subjective metrics is unknown.

The *performance* metric is linked to the remaining metrics. The link to the *smoothness* metric is drawn as a thinner line to illustrate the fact that it is *performance* only appears in the equation predicting *smoothness* and not vice versa. For *init_accel* and *accel_prog*, both contain *performance* in their correlations, and the *performance* equation contains either one or the other in the LS and LWS fit equations. This indicates that these metrics all heavily influence one another's scores. As the *performance* metric is evaluating the overall driveability, it can be concluded that the overall driveability (*performance*) is heavily influenced by the *smoothness*, *init_accel* and *accel_prog* metrics, rather than vice versa.

The relationships between the *performance* metric and the *accel_prog, init_accel* and *smoothness* metrics indicate that there is either a cognitive link in the way these metrics are considered by the test drivers, or that the objective factors which affect these subjective metrics are themselves linked and therefore vary with one another. In fact, as the *performance* metric is summarising the entire driveability experience, both of these facts is true. This is the expected and desired behaviour.

It is interesting to see the two subjective delay metrics are correlated with one another, rather than with any of the other subjective metrics (*performance* in particular). This may indicate one of two things: that the values of these metrics (and therefore the objective events which are rated by these subjective metrics) do not have as strong an effect on the overall driveability (*performance*) rating as the others; or that these two subjective metrics are very difficult to discriminate between for the drivers.

It is presumed that the latter conclusion is in fact true, as some of the test drivers noted that they had difficulties differentiating between the two subjective metrics. It may be possible to overcome this problem by giving the drivers more familiarisation with the events and factors in question, otherwise the questionnaire should to be re-designed to remove this duplication.

7.4 Correlations between the objective metrics

Although the use of objective metrics which have correlations with one another should result in the least correlated metrics being removed from the eventual correlation equations, it is

sensible to remove as many additional objective metrics as possible for the following reasons:

- Additional objective metrics mean that the correlation equations take longer to produce;
- If some metrics are highly correlated, there is a possibility that the least correlated of the number may be added to the correlation equation due to chance values of the other constituent terms in the correlation equation. This will mean that an extra variable is present in the eventual equations making the analysis more difficult. This effect can be seen in Section 6.4.4.

The single variable correlations between the objective variables are shown in the following tables. Only those variables for which statistically significant correlations could be found are shown in the tables below.

Table 7-4 – Single objective metric inter-correlation (LS)

Equation	R^2
aInitialSpeed = -0.462552+0.972193* aDesiredStartSpeed^(1/2)	0.036
aDesiredStartSpeed = -0.049407+0.988903* aInitialSpeed	0.037
aRateOfChangeOfPedalPosition = 885.283106-0.192263* aMaxSpeed^2	0.036
aMaxAccel = -2.063966+0.875372* aAverageAccelToMaxSpeed	0.767
aAverageAccelToMaxAccel = 0.674303+0.919275* aAverageAccelToMaxSpeed	0.843
aAverageAccelToMaxSpeed = 56.694790-0.921499* aAverageAccelToMaxAccel^(1/-3)	0.845
AccelDelayTime = 6.450407+0.330542* aDesiredStartSpeed^3	0.108
aAccelGradient = 4326.919677+0.781979* aAverageAccelToMaxSpeed^2	0.612
aInitialJerk = 850.001333+0.832476* aMaxAccel	0.692
aMaximumJerk = 161.787763-0.916563* aMaximumQuirk^(1/-2)	0.839
aInitialQuirk = 0.000265+1.867509* aMaximumJerk^3	0.367
aMaximumQuirk = 15.783651+0.915341* aMaximumJerk	0.835
aAverageQuirk = 0.000265+2.768520* aMaxEngSpeed^-2	0.466
aDeltaEngSpd2MaxSpeed = -51.469132+0.650292* aAverageAccelToMaxSpeed^3	0.423
aDeltaEngSpd2MaxAccel = 7.078370-0.580878* aDeltaEngSpd2MaxSpeed^(1/-3)	0.075

Table 7-5 - Single objective metric inter-correlation (LWS)

Equation	R^2
aInitialSpeed = 0.001955+1.023157* aDesiredStartSpeed	0.038
aDesiredStartSpeed = -0.602200+0.959781* aInitialSpeed^(1/2)	0.037
aMaxAccel = -3.483804+0.970175* aAverageAccelToMaxSpeed	0.794
aAverageAccelToMaxAccel = -0.243205+0.986943* aAverageAccelToMaxSpeed	0.856
aAverageAccelToMaxSpeed = 44.666634-0.938263* aAverageAccelToMaxAccel^(1/-2)	0.848
AccelDelayTime = 6.335011+1.353029* aDeltaEngSpd2MaxAccel^-3	0.379
aAccelGradient = 4338.247852+0.864525* aAverageAccelToMaxSpeed	0.645
aInitialJerk = 849.205347+0.919163* aMaxAccel	0.721
aMaximumJerk = 158.868919-0.893675* aMaximumQuirk^(1/-2)	0.828
aInitialQuirk = 12747.951338+0.198840* aMaxEngSpeed^(1/-2)	0.029
aMaximumQuirk = 13.911013+0.955245* aMaximumJerk	0.845
aAverageQuirk = 28891.552820+0.259253* aMaxEngSpeed^(1/-2)	0.052
aDeltaEngSpd2MaxSpeed = -18.495906+0.688284* aAverageAccelToMaxSpeed^2	0.448
aDeltaEngSpd2MaxAccel = -1.227763+0.577425* LN(aDeltaEngSpd2MaxSpeed)	0.079

There is little difference in the metrics contained in the LS and LWS equations for each objective metric and the coefficients of determination for each objective metric equation show very small differences.

It can be seen that there are some high correlations between acceleration related variables, and of particular interest is the correlation between *aMaximumJerk* and *aMaximumQuirk*. It was decided that the quirk related metrics would be removed for the final correlations (in Section 8) as they were so highly correlated with the jerk metrics, and because the jerk metrics are a more useful physical aspect of vehicle behaviour.

7.5 Simple equation, single variable regressions

The single variable equation technique was the first stage of the analysis carried out during this project. It is explained in Section 6.4.1. The following tables show the most highly correlated results of the single variable equation correlations for each subjective metric. Full tables of the fits for each equation type can be found in Appendix V.

Table 7-6 – Full metric set LS fitting

Subjective rating	Objective metric	Equation type	R^2
smoothness	aEngSpdAtMaxVSpeed	Cubic	0.203
eng_delay	aEngSpdAtMaxVSpeed	Cubic	0.125
vehicle_delay	aMaximumQuirk	Cubic	0.224
init_accel	aMaximumQuirk	Cubic	0.241
accel_prog	aEngSpdAtMaxVSpeed	Cubic	0.133
performance	aMaximumJerk	Parabolic	0.207

Table 7-7 – Full metric set LWS fitting

Subjective rating	Objective metric	Equation type	R^2
smoothness	aMaximumJerk	Cubic	0.243
eng_delay	aAverageJerk	Parabolic	0.166
vehicle_delay	aMaximumQuirk	Cubic	0.270
init_accel	aAverageJerk	Parabolic	0.264
accel_prog	aMaximumQuirk	Cubic	0.156
performance	aMaximumQuirk	Cubic	0.234

It can be seen that for each subjective metric, the most highly correlated equation types are the cubic and parabolic equations. It should also be noted that the jerk and quirk related metrics as well as *aEngSpdAtMaxVSpeed* metric are the most highly correlated. The jerk and quirk metrics are unsurprising, as these are expected to have an effect agreeing with Wicke et al.'s findings (2000), however the appearance of the *aEngSpdAtMaxVSpeed* metric is not easily explained.

For the LWS fits shown in the following tables, the jerk related metrics are the most highly correlated with parabolic and cubic equations producing the highest correlations.

Table 7-8 – Acceleration and jerk metric subset LS fitting

Subjective rating	Objective metric	Equation type	R^2
smoothness	aMaximumJerk	Cubic	0.194
eng_delay	aMaximumJerk	Cubic	0.095
vehicle_delay	aMaximumJerk	Parabolic	0.207
init_accel	aMaximumJerk	Parabolic	0.207
accel_prog	aMaximumJerk	Parabolic	0.110
performance	aMaximumJerk	Parabolic	0.207

Table 7-9 – Acceleration and jerk metric subset LWS fitting

Subjective rating	Objective metric	Equation type	R^2
smoothness	aMaximumJerk	Cubic	0.243
eng_delay	aAverageJerk	Parabolic	0.166
vehicle_delay	aMaximumJerk	Parabolic	0.243
init_accel	aAverageJerk	Parabolic	0.264
accel_prog	aMaximumJerk	Parabolic	0.144
performance	aMaximumJerk	Parabolic	0.233

It can be seen from the results of both fitting methods, that the most highly correlated equation types are the cubic or parabolic equations. This may indicate a real trend in the data, or it may indicate that there is simply a large amount of scatter in the data, which means that the cubic and parabolic equations' larger number of degrees of freedom makes them more flexible and therefore allows them to produce the smallest errors between the actual and fitted data points. It can be seen that few of the correlations exceed a coefficient of determination value of 0.25 which is probably not sufficient for use in driveability prediction; therefore, a coefficient of determination value of 0.25 is the minimum target that must be exceeded using multivariate correlation techniques to make sure that an improvement is seen.

7.6 Single variable correlations – single variable with various modifiers

The following results show the correlation between single objective metrics with a variety of modifiers (such as the log function and various power functions) and the subjective ratings. It is combinations of such terms that the multivariate correlation equations use.

Table 7-10 – Full objective metric set, LS fit, single variable fit

Subjective variable	Equation	Coefficient of determination R^2
smoothness	6.566592-0.433187* aMaxEngSpeed^(1/2)	0.187
eng_delay	6.552319-0.329012* aEngSpdAtMaxVSpeed^(1/2)	0.107
vehicle_delay	-48.591774+0.427017* aMaximumQuirk^(1/-2)	0.181
init_accel	-51.505626+0.451826* aMaximumQuirk^(1/-2)	0.203
accel_prog	6.550329-0.331331* aEngSpdAtMaxVSpeed^(1/2)	0.108
performance	-36.559380+0.434380* aMaximumJerk^(1/-2)	0.187

Table 7-11 – Full objective metric set, LWS fit, single variable fit

Subjective variable	Equation	Coefficient of determination, R^2
smoothness	-42.704062 +1.720256* aEngSpdAtMaxVSpeed^(1/-3)	0.206
eng_delay	-86.819784 +3.355890* aEngSpdAtMaxVSpeed^(1/-2)	0.144
vehicle_delay	4.077674+0.508575* aMaximumQuirk^-1	0.212
init_accel	-39.289739+0.466458* aMaximumJerk^(1/-2)	0.213
accel_prog	6.767971-0.366971* aAverageEngSpeed^(1/3)	0.130
performance	-38.561474+0.455955* aMaximumJerk^(1/-2)	0.203

The selection of all of the metrics selected by the single variable technique agrees with the results of the 'various equation' fitting techniques in Section 7.5.

Table 7-12 – Acceleration and jerk objective metrics, LS fitting, single variable fit

Subjective variable	Equation	Coefficient of determination, R^2
smoothness	-33.271269+0.404953* aMaximumJerk^(1/-2)	0.162
eng_delay	-21.433471+0.277908* aMaximumJerk^(1/-2)	0.076
vehicle_delay	-35.492305+0.424296* aMaximumJerk^(1/-2)	0.179
init_accel	-37.519853+0.447366* aMaximumJerk^(1/-2)	0.199
accel_prog	-24.970505+0.315330* aMaximumJerk^(1/-2)	0.098
performance	-36.559380+0.434380* aMaximumJerk^(1/-2)	0.187

Table 7-13 – Acceleration and jerk objective metrics, LWS fit, single variable fit

Subjective variable	Equation	Coefficient of determination, R^2
smoothness	-35.955259+0.433917* aMaximumJerk^(1/-2)	0.182
eng_delay	-24.908217+0.315416* aMaximumJerk^(1/-2)	0.095
vehicle_delay	-38.745199+0.459358* aMaximumJerk^(1/-2)	0.203
init_accel	-39.289739+0.466458* aMaximumJerk^(1/-2)	0.213
accel_prog	-28.159530+0.349815* aMaximumJerk^(1/-2)	0.118
performance	-38.561474+0.455955* aMaximumJerk^(1/-2)	0.203

All of these metrics are correlated with *aMaximumJerk^(1/-2)*. This agrees with the results shown in Section 7.5 and although the correlations themselves are not very strong. This confirms Wicke et al.'s (2000) findings that jerk is an important factor in vehicle driveability.

7.7 *Coefficient of determination calculation failures*

It should be noted that the correlation technique employed in this research is not perfect and it cannot be applied to every set of data and a result produced. There are a number of reasons why the coefficient of determination (R^2) value of a given correlation equation and data set combination will be impossible to calculate and therefore be equal to zero (or 'Not a Number' (NaN)). These reasons are listed below:

- As the R^2-values are adjusted to account for the number of terms in the correlation equations as well as the number of data points used in the calculation, if there are too few data points this can result in the adjustment producing a negative correlation. In this case, the R^2-value is set to zero. This can result from poor scalings of the data when log or root terms are involved. As negative values are not allowed for these particular operations they are automatically removed, however, depending on the scaling, this can result in the majority of the data set being removed from the correlation (see Section 6.5.1).
- If there is no data, the R^2-value will be set to zero.
- The standard deviation of the subjective data predicted by the correlation equation is zero. This is caused by no statistically valid fits being produced for the subjective data (this is performed using an Equation F-test as explained in section 6.4.2.2.4.2). When this happens, the best fit is assumed to be the mean of the data, which means that any predictions from this 'equation' will produce constant-value data with a standard deviation of zero. Mathematically, the failure occurs because when the standard deviation is used to calculate the coefficient of determination, this produces a 'divide by zero' error due to its value.

8 Application of correlations

The correlation generation and metric generation code developed during the research described in this thesis is generic and is not limited to use for the analysis of longitudinal driveability data. These techniques could be applied to other aspects of vehicle driveability, or other processes in which there is a requirement to transform large volumes of time-dependent data into the more concise form of metrics and then find correlations between dependent and independent factors.

This section begins by outlining possible applications of multivariate driveability rating prediction equations in the field of vehicle calibration and driveability. An example of the process of generating a correlation equation is then presented. This shows the steps that are taken in processing the raw time series data to generating metrics and then the generation of the correlation equation and its use in prediction.

The main part of this Section shows the analysis of the driveability data collected during this and Wicke's projects. Correlation equations are generated from a variety of data subsets and the quality of the fits and the metrics included in the correlation equations are analysed. Overall vehicle driveability ratings (smoothness, engine and vehicle delay times, initial jerk, acceleration progression and overall driveability) are first analysed. This is followed by an analysis of gearshift ratings and metrics. The final part of this Section looks at evaluating driver types or styles using the objective and subjective data that were collected.

8.1 Different approaches to using driveability correlations

There are a variety of aspects of the vehicle design, calibration and testing phases to which the prediction of vehicle driveability can be applied.

8.1.1 Vehicle benchmarking and synthesis of brand identity

Vehicle benchmarking is performed to assess the various driveability characteristics of a vehicle and to determine its character (Dorey et al., 2001). This character will influence the type of driver to whom the vehicle will appeal. Vehicle benchmarking may be carried out as part of the process of brand synthesis, the process whereby groups of vehicles from a manufacturer are given similar characteristics to ensure a consistent experience across the range of vehicles produced by the brand. This type of synthesis would be the type of process that Ford would apply to their standard, ST and RS vehicles, giving each set of

vehicles a different combination of various driveability aspects to reflect their sporty aspirations.

8.1.2 Automated calibration

The process of calibration for emissions and economy is becoming increasingly automated (Schoeggl et al. 2002; McNicol et al. 2004) and the addition of driveability aspects to this process will result in time and cost savings by allowing calibration for driveability to be performed simultaneously. This means that the trade-offs between driveability behaviour and emissions and economy constraints can be decided on explicitly at the simulation/test-bed stage rather than once the powertrain is fitted to a test vehicle. Allowing driveability to be addressed so much earlier in the design and testing process means that any re-designs will occur earlier and will therefore incur less cost in terms of wasted and additional development time. This automated approach will also cut down on the need for calibration engineers to perform repetitive basic calibration tasks, instead presenting them with a powertrain that requires less time and work to fine tune into a finished product. An added benefit of this process is that the calibration is repeatable and could be applied to an entire range of vehicles allowing manufacturer-specific driveability characteristics to be established and applied easily.

Another possibility is that a number of different calibrations could be developed for a given powertrain to suit different vehicle and driver types (e.g. sporty or normal, or small car/large car calibrations which would require different calibrations due to the difference in the vehicle masses) – this would allow manufacturers to develop a single powertrain aimed at different vehicles/drivers which would reduce cost and complexity.

8.1.3 Automated vehicle driveability rating

Manufacturers will be able to characterise and benchmark the driveability performance of a wide range of vehicles to allow a calibration engineer to copy and improve on a vehicle that has been assessed as exhibiting particularly good driveability. As mentioned above, this would allow a manufacturer to produce consistent driveability across their entire range (or subsets thereof), or to model the characteristics of an existing vehicle which demonstrates desirable driveability.

8.2 *Example correlation equation generation and application*

Figure 8-1 shows the overall process that is used when applying the correlation generation process to a physical system such as vehicle driveability. This process is illustrated in this section.

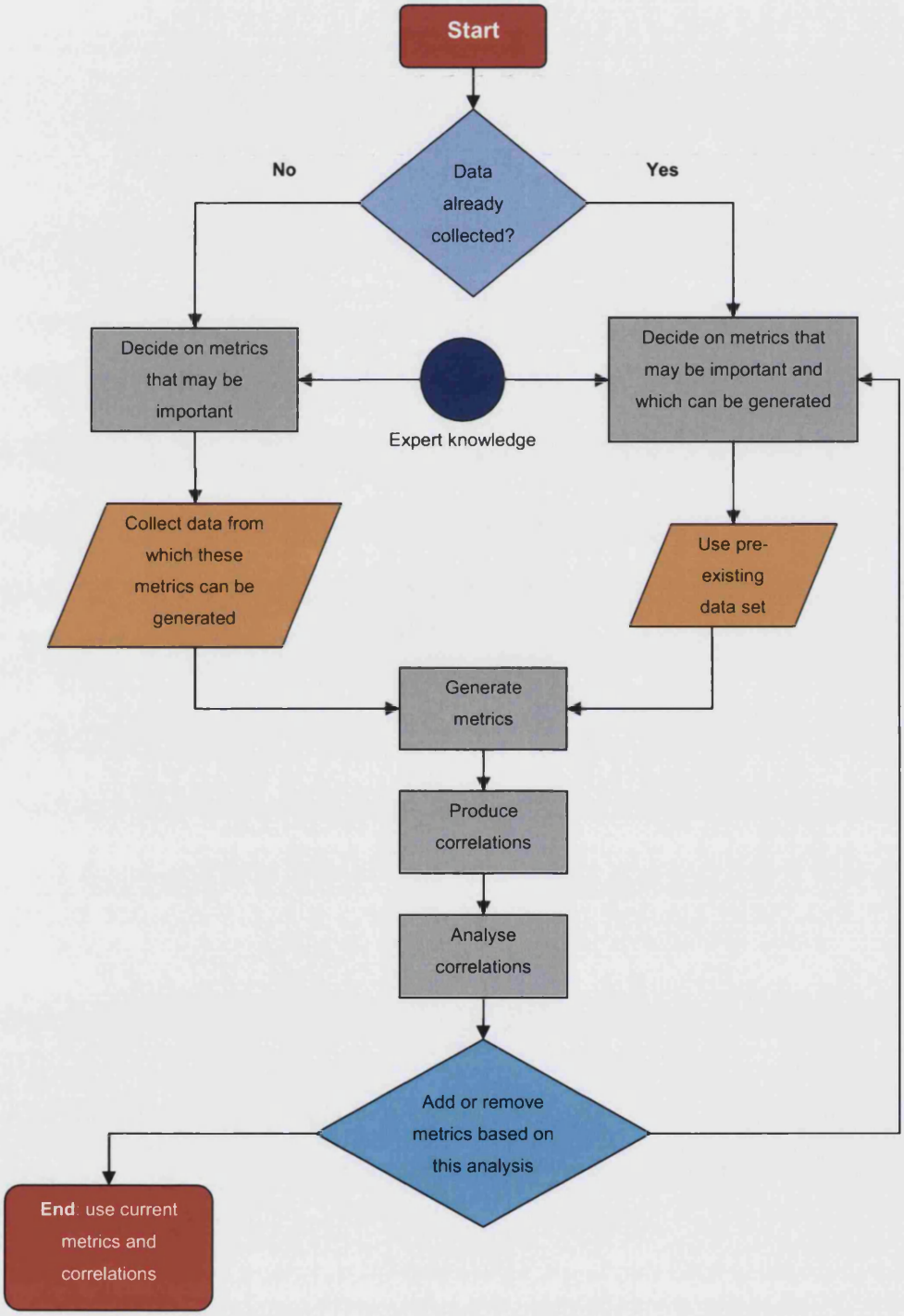

Figure 8-1 – Metric and correlation equation generation process

The following sections show examples of the process of metric generation, followed by the generation of a correlation equation and then its application to predict subjective ratings.

8.2.1 Time series data

The process starts with the time series data collected from a test vehicle. Figure 8-2 shows a set of data collected from the AT Mondeo (sports mode) using a 0kph initial speed and a pedal demand of 100%.

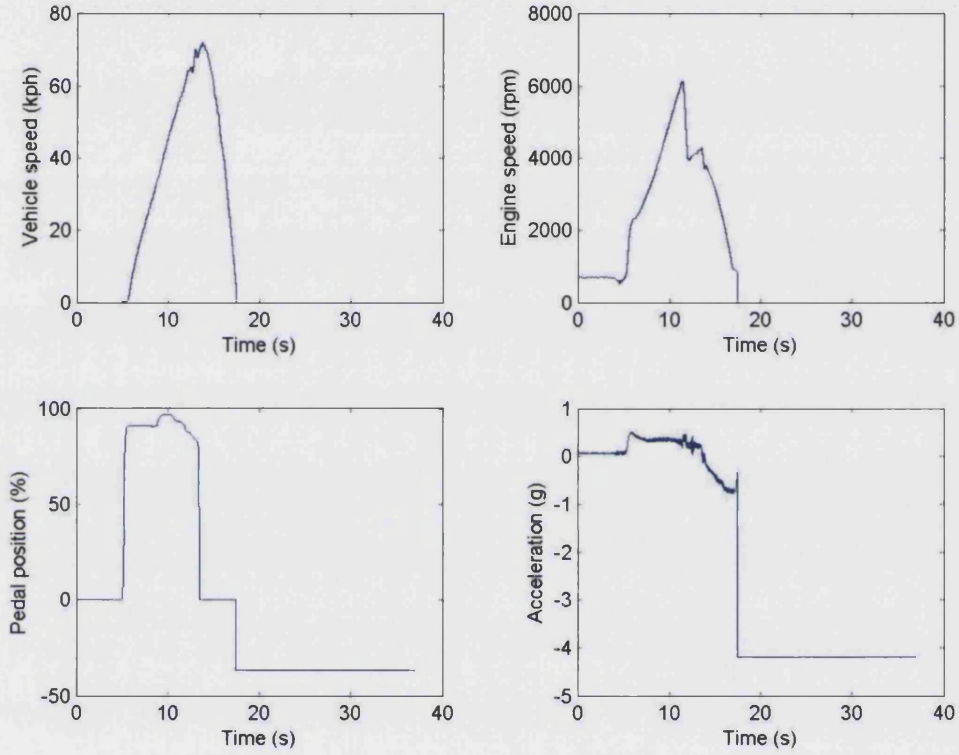

Figure 8-2 – Time series data

It can be seen that the initial speed was 0kph as per the test specification, though the pedal input is slightly less than was required by the test. It can also be seen that the driver realised that there was more pedal travel halfway through the test and depressed the pedal further. A gearshift is clearly visible in the engine speed data and is reflected by a number of spikes in the vehicle speed and acceleration data.

8.2.2 Metric extraction

The next stage is to analyse these time series data and produce a small number of metrics that can be analysed.

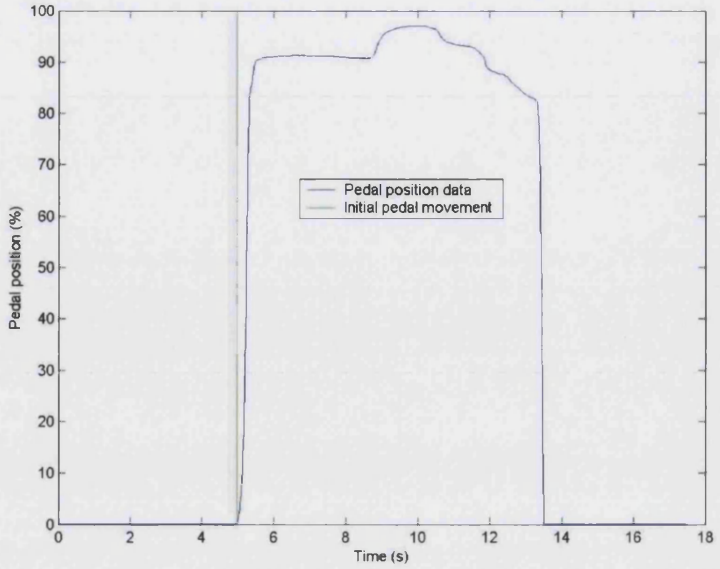

Figure 8-3 - Pedal position data

Figure 8-3 shows the pedal position data. The first step of the metric extraction is to determine when the pedal was first moved. For this 0kph initial speed test, this is relatively easy however for higher initial speeds the small changes in pedal position produced as the driver tries to keep a constant speed make the process more difficult (see Section 5.3.4.1).

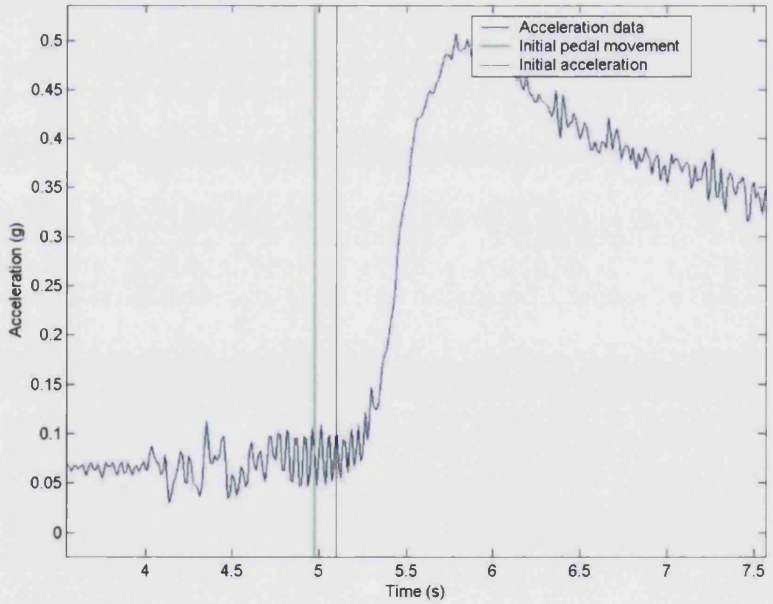

Figure 8-4 – Acceleration data

The next step is to determine when the vehicle started accelerating in response to the pedal input and subsequent engine torque increase (see Section 5.3.4.1). Figure 8-4 shows the point of pedal movement followed shortly afterwards by the start of vehicle acceleration. The time between these two events is known as the delay time (metric name: *AccelDelayTime*)

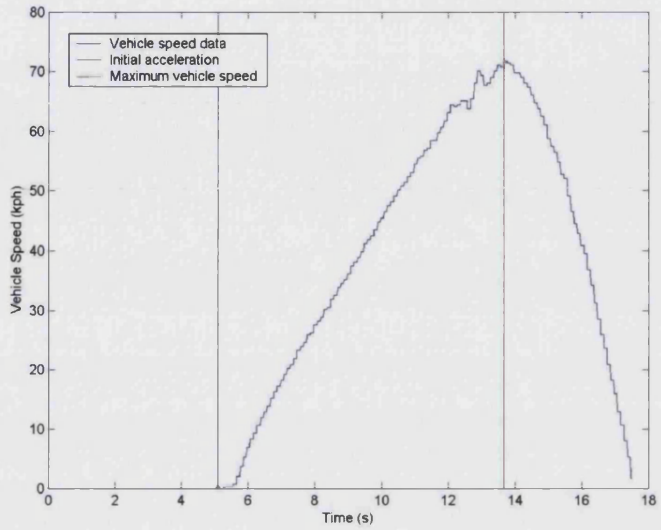

Figure 8-5 - Vehicle speed data

The next step is to determine the maximum vehicle speed (*aMaxSpeed*). This point signifies the end of the vehicle acceleration and is used as a limit in which the maximum acceleration is detected. Figure 8-5 shows the point at which acceleration starts and the point of maximum vehicle speed.

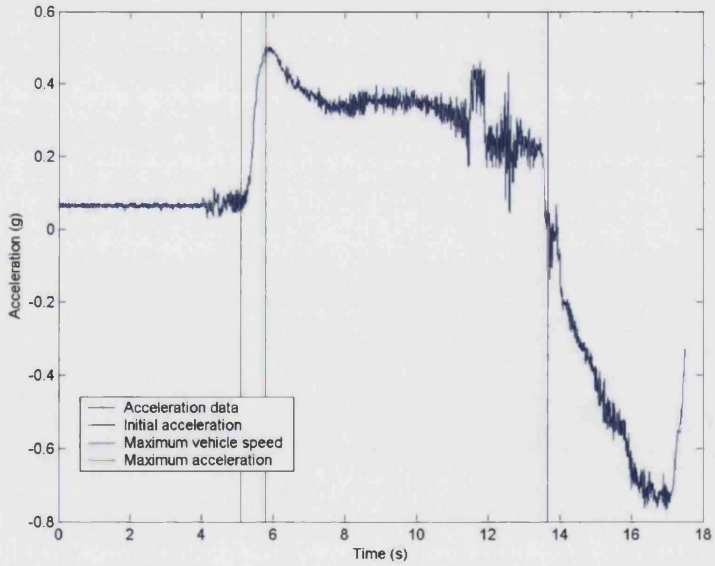

Figure 8-6 - Acceleration data

Figure 8-6 shows the two boundaries produced by the initial acceleration and the maximum speed. The maximum acceleration (*aMaxAccel*) is detected between these points and is shown on the graph. It can be seen that the acceleration rises rapidly to a peak and then tails off to a relatively constant level. The peak is caused by the torque multiplying effect of the torque converter fitted to this vehicle, the acceleration then decays as the speed builds. There are also a number of oscillations between 11 and 14 seconds that are caused by a gearshift.

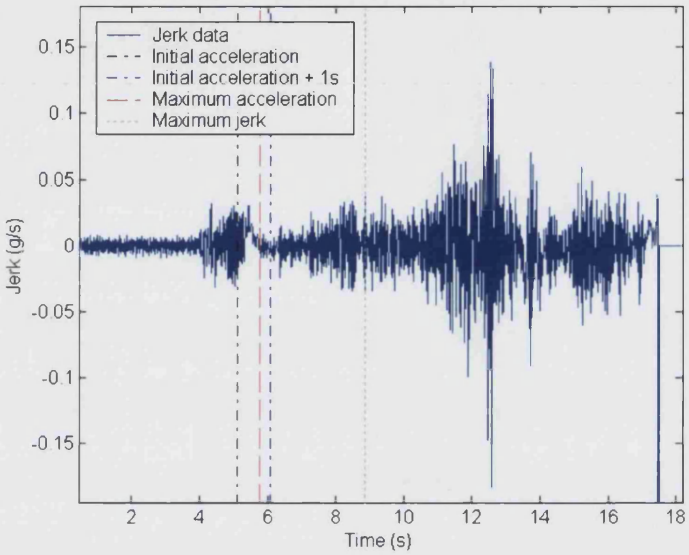

Figure 8-7 - Jerk data

Figure 8-7 shows the differential of the acceleration, the jerk. The initial acceleration and maximum acceleration points are shown and between these, the maximum jerk (*aMaximumJerk*) is detected. The mean acceleration gradient during the second after the initial acceleration is detected is recorded as a metric (*aInitialJerk*). Figure 8-7 shows both the initial acceleration detection time and one second boundary after this time.

The following metrics were produced from these data:

Table 8-1 - Calculated metrics

Metric	Value
aMaximumJerk	0.030395
aMaxAccel	0.507265
aAverageAccelToMaxSpeed	3.238918e-001
aInitialJerk	0.004826

8.2.3 Correlation generation

The following data show the sequence in which metrics are added to a correlation equation. The correlation equation is being fitted using a LWS fitting process, using the acceleration and jerk metrics and AT vehicle data as described in Section 9.1.2.

The first step of the process is to perform correlations for the subjective metrics with each objective metric (raised to powers in the range ±3, roots in the range ±3rd power, and with logarithmic transformations. See section 6.4.2.) This is the process as is shown in Section 7.6. The initial objective metric is chosen as that which is most highly correlated with the subjective metric.

Objective Metric	R
aMaximumJerk^(1/-2)	0.630176

The *aMaximumJerk^(1/-2)* term is chosen and it has a correlation coefficient of 0.630176.

At this point, and after each subsequent addition, the overall statistical significance of the correlation is tested, and if it fails, the last variable is removed and the process is stopped. In this case, the equation passes and further terms are tested to be added.

Each additional objective metric is now tested in the equation to determine which has the highest partial correlation coefficient (see Section 6.6.4). This comparison is performed by calculating an F value (see Section 6.4.2.2.4.1), the values of which are shown in the tables below. To ensure that a metric is still significant, each metric in the equation is compared with an F-threshold to determine whether it should be removed from the equation, those metrics that are less than the threshold are removed from the equation. This process is required, as the metrics that have been added may have replaced the existing metrics' effects.

The following tables show the terms that are present in the equation. The bottom-most terms shown in italics are those that have just been added. The tables also show the F values for each term that is compared with the F threshold value in the table. The R_{inc} and R_{exc} values are produced as part of the F-value calculation and show the correlation coefficients of the equation with and without the term in question.

Iteration 1			
Objective Metric	**F**	$\mathbf{R_{inc}}$	$\mathbf{R_{exc}}$
aMaximumJerk^(1/-2)	91.985531	0.694061	0.629510
aMaximumJerk^(1/-3)	*91.081510*	*0.694061*	*0.630176*
F threshold	3.858148		
R	0.694061		

Iteration 2			
Objective Metric	**F**	$\mathbf{R_{inc}}$	$\mathbf{R_{exc}}$
aMaximumJerk^(1/-2)	119.084562	0.708338	0.628664
aMaximumJerk^(1/-3)	118.285594	0.708338	0.629232
aMaxAccel^-1	*22.383822*	*0.708338*	*0.694061*
F threshold	3.858148		
R	0.708338		

Iteration 3			
Objective Metric	**F**	$\mathbf{R_{inc}}$	$\mathbf{R_{exc}}$
aMaximumJerk^(1/-2)	42.113104	0.719165	0.693275
aMaximumJerk^(1/-3)	41.889279	0.719165	0.693415
aMaxAccel^-1	38.229033	0.719165	0.695703
aMaximumJerk^3	*17.798227*	*0.719165*	*0.708338*
F threshold	3.858148		
R	0.719165		

Iteration 3			
Objective Metric	**F**	$\mathbf{R_{inc}}$	$\mathbf{R_{exc}}$
aMaximumJerk^(1/-2)	49.314989	0.724347	0.694582
aMaximumJerk^(1/-3)	49.077108	0.724347	0.694728
aMaxAccel^-1	47.640398	0.724347	0.695613
aMaximumJerk^3	22.245395	0.724347	0.711075
aAverageAccelToMaxSpeed^-3	*8.734245*	*0.724347*	*0.719165*
F threshold	3.858148		
R	0.724347		

Iteration 4			
Objective Metric	**F**	R_{inc}	R_{exc}
aMaximumJerk^(1/-2)	38.540566	0.730846	0.708327
aMaximumJerk^(1/-3)	38.360601	0.730846	0.708433
aMaxAccel^-1	58.814479	0.730846	0.696188
aMaximumJerk^3	19.944664	0.730846	0.719280
aAverageAccelToMaxSpeed^-3	12.978945	0.730846	0.723341
aAverageAccelToMaxSpeed^3	*11.246114*	*0.730846*	*0.724347*
F threshold	3.858148		
R	0.730846		

Iteration 5			
Objective Metric	**F**	R_{inc}	R_{exc}
aMaximumJerk^(1/-2)	36.045470	0.734220	0.713467
aMaximumJerk^(1/-3)	35.848105	0.734220	0.713582
aMaxAccel^-1	33.213574	0.734220	0.715119
aMaximumJerk^3	19.504157	0.734220	0.723064
aAverageAccelToMaxSpeed^-3	8.465178	0.734220	0.729399
aAverageAccelToMaxSpeed^3	15.857401	0.734220	0.725163
aInitialJerk^2	*5.930267*	*0.734220*	*0.730846*
F threshold	3.858148		
R	0.734220		

A final term is then tested to see whether it should be added to the equation:

Iteration 6			
Objective Metric	**F**	R_{inc}	R_{exc}
aMaximumJerk^(1/-2)	400.660949	0.735985	0.712680
aMaximumJerk^(1/-3)	40.513956	0.735985	0.712766
aMaxAccel^-1	15.440626	0.735985	0.727223
aMaximumJerk^3	22.944784	0.735985	0.722927
aAverageAccelToMaxSpeed^-3	5.646503	0.735985	0.732793
aAverageAccelToMaxSpeed^3	8.391470	0.735985	0.731236
aInitialJerk^2	4.055180	0.735985	0.733694
aAverageAccelToMaxSpeed^2	*3.126211*	*0.735985*	*0.734220*
F threshold	3.858148		
R	0.735985		

However in this case the term fails the partial F-test and it is therefore rejected. As this was the last term to enter the correlation equation, the regression process now ends and the last equation is assumed to be the optimum correlation equation. This equation is show below:

Subjective rating	Correlation equation	Coefficient of determination
vehicle_delay	-3298.411107 +436.402789* aMaximumJerk^(1/-2) -436.837309* aMaximumJerk^(1/-3) -0.357524* aMaxAccel^-1 -1.302969* aMaximumJerk^3 +0.123737* aAverageAccelToMaxSpeed^-3 -0.289839* aAverageAccelToMaxSpeed^3 +0.155508* aInitialJerk^2	0.539

The responses of the metrics in the correlation equation are shown in Figure 8-8 below.

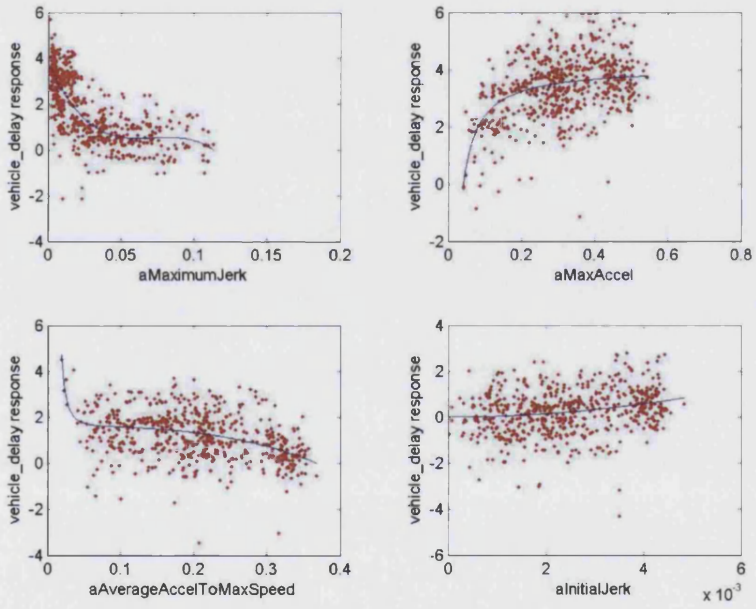

Figure 8-8 - Response for each metric

8.2.4 Prediction of subjective driveability using this correlation equation

Applying this correlation equation to the metrics on which it was created gives a coefficient of determination of R^2= 0.539.

Applying the correlation equation to the metrics that were calculated in Section 8.2.2 gives the following prediction of subjective driveability for this manoeuvre:

Vehicle_delay rating = 7.0 (on a scale from 0-10).

This can be compared with the actual value returned by the test driver who performed the manoeuvre. Note that this value has been manipulated using the transform presented in section 4.2.1.1 and so is no longer an integer value:
Vehicle_delay rating = 6.7 (on a scale from 0-10).

The actual and predicted data points are shown in Figure 8-9 below with the metric data point that was calculated earlier indicated by an arrow.

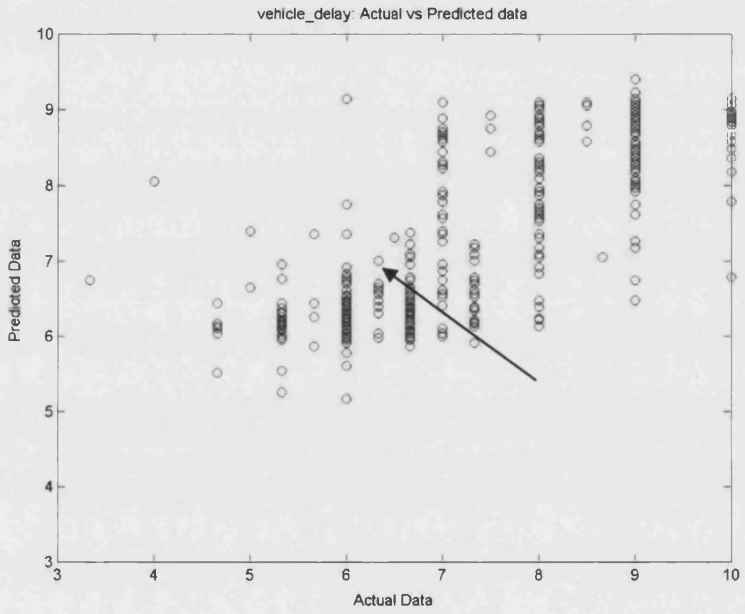

Figure 8-9 – Comparison of fitted and actual predictions for *vehicle_delay* rating

9 Driveability analysis

This section uses the techniques developed in section 8 to identify correlations between subjective and objective metrics describing the characteristics of six test vehicles and comments on the physical causes of the driveability trends represented by these correlations.

The data sets used during the course of the research contain driveability data collected from a variety of vehicles and drivers. The vehicle powertrains range from an experimental CVT/IVT, through a dual-power petrol-electric, to a variety of AT equipped vehicles with differing numbers of gears and engine sizes. This is by no means a uniform group of vehicles, and their driveability characteristics are expected to differ; the question is whether the data which have been collected are sufficient (in both quantity and volume) to enable the accurate prediction of any given vehicle's driveability.

The drivers also differ to an unknown degree. Few of them have extensive testing experience, and from the driver questionnaire, it can be seen that they differ in their driving styles and demands (see Table 3-12). The question is again whether the data which were collected are sufficient to reproduce these drivers' ratings, with a supplementary question as to whether the drivers' ratings can be used to determine groupings amongst them based on their driving style and demands.

There are therefore a number of ways in which the driveability data can be handled to perform the analysis. One must consider that some of the drivers/vehicles/manoeuvres may produce poor data that will skew any correlations produced for the rest of the data, therefore the analysis was carried out in a number of stages, both to avoid such problems and to determine how generic the data is.

9.1 Create equation and test data from same group of vehicles

Ideally, a broad range of data would be available with which to produce the correlation equations. These equations should then be able to predict the driveability ratings for any of the vehicles, whose data were used to produce the correlation equations, as well as similar vehicles. Therefore the entire data set was initially used to determine whether this was possible using the data that were available.

If this approach works, it will prove that the correlation equations are generic for a range of vehicles, drivers and manoeuvres. If it fails, it may indicate that there are insufficient data available to produce correlation equations that are sufficiently accurate to represent the full range of behaviours, or it may indicate differences between the ways the vehicles/manoeuvres are rated, which cannot be described by a single correlation equation.

9.1.1 Train using all vehicles

The first dataset to be tested consisted of all of the data. The results of these correlations should indicate how well the correlation equations are able to predict the range of behaviours from different vehicles and drivers over a variety of manoeuvres.

Four different types of correlations were fitted to the entire set of data. These used either the least squares (LS) or least weighted squares (LWS) fitting technique applied to either the full set of objective metrics (full set) or just the acceleration and jerk related metrics (acceleration and jerk subset). The metrics in these sets are listed and explained in Section 5.4.

The tables below summarise the results by presenting the overall correlations for each metric set and fitting method for the three manoeuvre types considered in this research. The values from each table are compared and the highest value is highlighted in green. The full results for each correlation equation are listed in Appendix X.

Table 9-1 - Full metric set LS fitting

Data subset	accel_prog	eng_delay	init_accel	performance	smoothness	vehicle_delay
Launch Feel	0	0	0	0	0	0
Performance Feel	0.250	0.125	0.324	0.297	0.070	0.225
Traffic Crawl	0.188	0.202	0.094	0.152	0	0.139

Table 9-2 - Full metric set LWS fitting

Data subset	accel_prog	eng_delay	init_accel	performance	smoothness	vehicle_delay
Launch Feel	0	0	0	0	0	0
Performance Feel	0.343	0	0.376	0.372	0.323	0.192881
Traffic Crawl	0.229	0	0.164	0.206	0.316	0.159

Table 9-3 - Acceleration and jerk metrics, LS fitting

Data subset	accel_prog	eng_delay	init_accel	performance	smoothness	vehicle_delay
Launch Feel	0.052	0.211	0.169	0.082	0.154	0.077
Performance Feel	0.152	0.114	0.178	0.270	0.293	0.294
Traffic Crawl	0.094	0.056	0.074	0.118	0.252	0.186

Table 9-4 - Acceleration and jerk metrics, LWS fitting

Data subset	accel_prog	eng_delay	init_accel	performance	smoothness	vehicle_delay
Launch Feel	0.147	0.159	0.256	0.100	0.321	0.247
Performance Feel	0.318	0.097	0.221	0.331	0.099	0.319
Traffic Crawl	0.112	0.001	0.126	0.275	0.386	0.175

It can be seen that the two full metric set equations produce no correlations for the *Launch Feel* manoeuvres. This is most likely caused by a lack of correlations for the 0kph data set caused by poor data.

In general, the acceleration and jerk subset LWS fit equation produces the best correlations for the *Launch Feel* manoeuvres, the full metric set, LWS fit produces the best correlations for the *Performance Feel* manoeuvres. The best results for the *Traffic Crawl* manoeuvres are scattered amongst the equations with all of the equations producing similar results.

If all of the metrics are grouped together, the full metric set, LWS fit equations are found to produce the best average followed very closely by the acceleration and jerk subset, LWS fit equations. When the metrics are analysed one by one, these two equations again produce the best fits for each metric. This is interesting to see as it indicates that the data are noisy and therefore require the LWS fit, which is able to reduce the effect of outliers, to produce optimum correlations. It should also be noted that the fits produced using the full metric set and the acceleration and jerk subset are close together.

It can be seen that the coefficients of determination for each of the metric set and fitting type combinations are similar, with an acceleration and jerk equation the best by a small margin. The similarity between the full metric and acceleration and jerk metric subsets indicates that it is likely the acceleration and jerk metrics provide the majority of the generic correlation effect. Looking at the metrics which make up the 'full set' equations in Table 9-5 and Table 9-6 below, it can be seen that at least one of the acceleration and jerk subset metrics appears in each equations (these metrics are highlighted in bold font), and there is a very high occurrence of quirk related metrics. Although these were not included in the acceleration and jerk subset as its goal was to test the findings of Wicke et al. (2000) with regard to acceleration and jerk metrics, these quirk metrics have a direct relation to the jerk metrics as was seen in Table 7-4 and Table 7-5.

Table 9-5 - Least squares fit equation metrics

Subjective metric	Objective metrics
smoothness	aMaximumQuirk, aDesiredStartSpeed, aAverageQuirk, aInitialPedalPosn, **aAverageAccelToMaxSpeed**, aDeltaEngSpd2MaxSpeed
eng_delay	aEngSpdAtMaxVSpeed, aMaximumQuirk, aDeltaEngSpd2MaxSpeed, **aMaxAccel**, aDesiredStartSpeed, **aAverageAccelToMaxAccel**, aInitialSpeed, aEngSpdAtMaxVSpeed
vehicle_delay	aMaximumQuirk, aMaximumQuirk, aDesiredStartSpeed, **aMaxAccel**, aDesiredPedalPosition, aMaxPedalPosition
init_accel	aDesiredStartSpeed, aMaximumQuirk, aEngSpdAtMaxVSpeed, aDeltaEngSpd2MaxSpeed, aChangeInSpeed, **AccelDelayTime**, aMaxSpeed
accel_prog	aEngSpdAtMaxVSpeed, aMaximumQuirk, aDeltaEngSpd2MaxSpeed, aMaxPedalPosition, aDesiredStartSpeed, **aAverageAccelToMaxSpeed**, aInitialSpeed
performance	**aMaximumJerk**, aDesiredStartSpeed, aEngSpdAtMaxVSpeed, aMaximumQuirk, **aMaxAccel**, aInitialSpeed

Table 9-6 - Least weighted squares fit equation metrics

Subjective metric	Objective metrics
smoothness	aEngSpdAtMaxVSpeed, **aMaximumJerk**, aDesiredStartSpeed, aMaxPedalPosition, **aMaxAccel**, aDeltaEngSpd2MaxSpeed, aEngSpdAtMaxVSpeed
eng_delay	aEngSpdAtMaxVSpeed, aMaximumQuirk, **aAverageJerk**, aInitialSpeed, aDeltaEngSpd2MaxSpeed, **aAverageAccelToMaxAccel**, aInitialPedalPosn, aMaxPedalPosition, **aMaxAccel**
vehicle_delay	aMaximumQuirk, aDesiredStartSpeed, **aMaxAccel**, aDeltaEngSpd2MaxSpeed, aDesiredPedalPosition, aDeltaEngSpd2MaxAccel, aMaxSpeed
init_accel	**aMaximumJerk**, aEngSpdAtMaxVSpeed, aDesiredStartSpeed, **aMaxAccel**, aInitialSpeed, **AccelDelayTime**, aMaximumQuirk
accel_prog	aEngSpdAtMaxVSpeed, aDesiredStartSpeed, aMaximumQuirk, **aInitialJerk**, aDeltaEngSpd2MaxSpeed, aEngSpdAtMaxVSpeed, aMaximumQuirk
performance	**aMaximumJerk**, aMaximumQuirk, **aMaxAccel**, aDesiredStartSpeed, aDeltaEngSpd2MaxSpeed, aEngSpdAtMaxVSpeed, aInitialSpeed, aDeltaEngSpd2MaxAccel

The fact that the equation that produced the highest correlations only contains acceleration and jerk metrics, and that these metrics and those derived from them are also prevalent in all of the other equations should be stressed. This finding confirms Wicke et al.'s (2000) preliminary research which found that jerk and delay-time were important influences on the subjective evaluation of vehicle driveability.

This indicates that the acceleration-based metrics produced by a vehicle are the most important of those tested here to predict driveability. In fact, the majority of the objective metrics used in this research are acceleration or jerk based, with the exception of the engine speed and pedal position derived metrics. This does not necessarily indicate that these factors are the only ones which are important, just that they are the most important amongst the metrics that have been used.

Table 9-7 below lists the correlations (R^2) between the acceleration and jerk metric subset fitted using LWS and the data subsets.

Table 9-7 - Acceleration and jerk metrics, LWS fitting

Data subset	accel_prog	eng_delay	init_accel	performance	smoothness	vehicle_delay
All data	0.329	0.268	0.235	0.315	0.306	0.323
25% pedal	0	0	0	0	0.196	0
50% pedal	0	0	0	0.080	0	0
75% pedal	0.141	0.085	0.084	0.212	0.079	0.106
100% pedal	0.262	0.138	0.251	0.219	0.084	0.189
0 kph	0.244	0.230	0.310	0.135	0.338	0.291
2 kph	0.060	0.033	0.014	0.230	0.048	0.338
12 kph	0.125	0.028	0.113	0.203	0.141	0.073
40 kph	0.292	0.349	0.335	0.402	0.489	0.388
60 kph	0.126	0	0.050	0.193	0.294	0.305
Launch Feel	0.147	0.159	0.256	0.100	0.321	0.247
Performance Feel	0.318	0.097	0.221	0.331	0.099	0.319
Traffic Crawl	0.112	0.001	0.126	0.275	0.386	0.175
BMW	0	0	0	0	0	0
Me	0.284	0.100	0.255	0.114	0.024	0.097
Ms	0.220	0.085	0.252	0.261	0.006	0.354
Omega	0.138	0.179	0.250	0.275	0.335	0.056
PRIUS	0	0.007	0	0	0	0
CVT Mondeo	0	0	0	0	0	0

Overall, the acceleration and jerk subset equations fitted using LWS fitting produced correlation equations that fit the data to a reasonable extent. However, these correlations are not generally large enough to be useful as anything other than a guide. Table 9-8, below, shows the correlations for the specific manoeuvre subsets taken from Table 9-7. The manoeuvre subsets are used as they should provide a method by which the data can be condensed without losing information that is specific to certain driving conditions.

Table 9-8 - Manoeuvre subset correlations

Data subset	accel_prog	eng_delay	init_accel	performance	smoothness	vehicle_delay
Launch Feel	0.147	0.159	0.256	0.100	0.321	0.247
Performance Feel	0.318	0.097	0.221	0.331	0.099	0.319
Traffic Crawl	0.112	0.001	0.126	0.275	0.386	0.175

Although there are some differences in the trends shown for each metric, it is difficult to pick out any definite trends. The majority of the metrics show the best correlation for the *performance feel* manoeuvre and the worst for *traffic crawl* with *launch feel* in between. Although the *traffic crawl* manoeuvre dataset contains more data points than either of the other metrics (which both contain the same number of points as shown in Table 4-4 which contains descriptions of the manoeuvre datasets), it may be that the mix of speeds does not produce any uniform trends. It is also possible that the different vehicles in the full data set produce different driveability trends and therefore their combination makes the prediction less accurate.

It can be seen from the results that the 25% and 50% pedal position subsets produce worse correlations than the 75% and 100% subsets. This indicates that the 75% and 100% subsets most probably contain data whose trends the overall correlation equation follows. This may be due to these data points having more effect when the correlation equation was fitted due to their greater number (for the higher speed tests no 25% and 50% tests are performed as described in Section 4.1). Or, alternatively, it may indicate that there is less of a trend and more random scatter in the 25% and 50% data points.

9.1.1.1 Low/zero correlations for CVT Mondeo and Prius

It should be noted that there are either no correlations or low correlations for the CVT Mondeo, Prius and BMW vehicle subsets.

In fact, it can be seen in Appendix X that the full metric set equations do produce fits for the BMW data, therefore the lack of correlations for the acceleration and jerk equations may be due to the particular choice of metrics in the correlation equation rather than to fundamental differences between the vehicles. The CVT Mondeo and Prius, however, still have low or zero correlations and are constant across all of the correlation equation combinations.

This may be caused by the subjective data collected from these vehicles containing a wide range of ratings as the different driveability behaviour exhibited by their CVTs was not to the liking of all of the test drivers. The difference between the correlations with the individual

vehicle subsets indicates the fact that the vehicles have some different traits. Despite this, the correlations for the different speeds and manoeuvre types show that these equations are reasonably generic across the test types which indicates that the differences between these vehicles and the average is not that large. The CVT Mondeo and Prius datasets are compared to the behaviour of correlation equations produced from AT vehicles in Section 9.1.2.1.

9.1.2 AT vehicle data correlations – full metric set

It has been seen from the results of Section 9.1.1 that although correlations are produced for the majority of vehicles by the acceleration and jerk subset LWS fitted equation, the correlations for the BMW, CVT Mondeo and Prius vehicle subsets were very poor or non-existent. It can be seen in Appendix X that the full metric set equations do in fact produce fits for the BMW data. It is not known why this difference exists, however it likely be a anomaly of the fitting process and choice of metrics, especially considering the low values of these correlations, rather than an indication that the BMW is significantly different from the other vehicles when compared using the acceleration and jerk metric subset.

Therefore, it was decided to produce correlation equations excluding the data from the Prius and CVT Mondeo vehicles for which either no or very poor correlations were produced for any of the metric set and fitting method combinations. The remaining vehicles all use ATs while neither of the excluded vehicles uses an AT, which may explain the apparent difference in these vehicles' results. Using only the AT-equipped vehicles will produce a set of data that should exhibit the greatest similarities in its behaviour, ideally excluding any extraneous differences produced by the transmission type.

All of the metric and fitting method combinations using just the AT vehicles were found to be significantly better than those created using all of the vehicle data. The full metric set LWS fit equation was found to be the best on average. The full results can be found in Appendix X.

Table 9-9 – Full metric set, LWS fit, correlations

Subset	accel_prog	eng_delay	init_accel	performance	smoothness	vehicle_delay
All data	0.569	0.533	0.542	0.584	0.585	0.624
25%	0.207	0.475	0.332	0.279	0.404	0.413
50%	0.331	0.446	0.354	0.397	0.391	0.383
75%	0.021	0	0.027	0.040	0	0
100%	0.531	0.359	0.507	0.497	0.348	0.490
0	0	0	0	0	0	0
2	0	0	0.110	0.048	0	0.059
12	0.567	0.399	0.476	0.578	0.462	0.513
40	0.516	0.572	0.258	0.573	0.057	0.554
60	0.460	0.373	0.327	0.486	0.450	0.527
Launch feel	0	0	0	0	0	0
Performance feel	0.382	0.401	0.399	0.413	0.342	0.457
Traffic crawl	0.372	0.518	0.428	0.442	0.473	0.487
BMW	0.162	0	0.120	0.168	0.156	0.252
AT Mondeo (economy mode)	0	0	0.058	0.058	0	0
AT Mondeo (sports mode)	0.165	0.116	0.165	0.187	0.078	0.326
Omega	0	0.342	0.213	0.082	0.061	0.178

It can be seen that no fits were produced for the *Launch Feel* or *0kph* initial speed subsets. This is caused by the presence of the *aDesiredStartSpeed* metric raised to a negative power in each of the correlation equations. To avoid this type of problem it may be necessary to add an offset to any variable that can have a value of 0. Alternatively, it would be possible to remove any logarithm, root and negative power terms from the correlation equation generation process, although this has been seen to produce a smaller range of possible curve shapes, it may be sufficient for the data in question.

Table 9-10 shows the full metric set LWS correlation equations for each subjective metric.

Table 9-10 - Correlation equations

Equation	Coefficient of determination
smoothness = 1859.901030+57.222327* aMaximumJerk^(1/-2) -57.029004* aMaximumJerk^(1/-3) -0.066817* aDesiredStartSpeed^-1 -0.245797* LN(aEngSpdAtMaxVSpeed^-1) +0.308191* aDeltaEngSpd2MaxSpeed +0.226141* aInitialSpeed^-3 +0.078260* aRateOfChangeOfPedalPosition^(1/-2) -0.297009* aMaxAccel^3 +0.185367* aMaxPedalPosition^3 +0.215314* aMaximumJerk^-1 -0.583897* aEngSpdAtMaxVSpeed^(1/3) -0.116341* aChangeInSpeed^(1/-3)	0.585
eng_delay = 23472.389246+537.301132* aMaximumJerk^(1/-2) -538.052023* aMaximumJerk^(1/-3) -0.179600* aChangeInSpeed^-2 -0.153806* aDesiredStartSpeed^-3 +0.165540* aDeltaEngSpd2MaxSpeed^2 +0.179450* aMaxSpeed^-3 -0.154383* AccelDelayTime^-3 +0.420031* aAverageAccelToMaxSpeed^-3 -0.433461* aMaxAccel^-1 -1.643149* aMaximumJerk^3 +0.348325* aEngSpdAtMaxVSpeed^(1/-3)	0.533
vehicle_delay = 24384.426942+551.079547* aMaximumJerk^(1/-2) -551.763734*	0.624

aMaximumJerk^(1/-3) -0.204031* aDesiredStartSpeed^-3 -0.573761* aMaxAccel^-1 -0.212863* LN(aDesiredPedalPosition) +0.183472* aDeltaEngSpd2MaxSpeed^2 -1.716598* aMaximumJerk^3 +0.491402* aMaxAccel^-3 +0.106910* aMaxSpeed^-3 -0.104086* LN(aDeltaEngSpd2MaxAccel^3) -0.303466* aAverageAccelToMaxAccel^-2 +1.356811* aDeltaEngSpd2MaxAccel^-2	
init_accel = -631.252133+39.600162* aMaximumJerk^(1/-2) +39.663731* aMaximumJerk -1.222803* aMaxAccel^-1 -0.201601* aDesiredStartSpeed^-1 +0.875688* aMaxAccel^-2 -0.188010* AccelDelayTime^-2 -0.266033* LN(aEngSpdAtMaxVSpeed^2) -0.972017* aMaximumJerk^3 +0.136140* aInitialSpeed^-2	0.542
accel_prog = 2899.381927+3.386954* aMaximumJerk^(1/-2) +4.813424* aMaximumJerk^2 -1.048221* aMaxAccel^-1 +0.723607* aMaxAccel^-2 -2.202510* aMaximumJerk^3 -0.187889* aDesiredStartSpeed^-1 +0.195919* aDeltaEngSpd2MaxSpeed^2 -0.203139* aEngSpdAtMaxVSpeed^(1/3) +0.587511* aRateOfChangeOfPedalPosition^-2 -0.041150* aAccelGradient^-1 +11.513688* aDeltaEngSpd2MaxAccel^-3 +0.158601* aMaxSpeed^-3	0.569
performance = 25997.164846+553.141313* aMaximumJerk^(1/-2) -553.682580* aMaximumJerk^(1/-3) -0.727833* aMaxAccel^-1 +0.379557* aMaxAccel^-3 -1.592442* aMaximumJerk^3 -0.101840* aDesiredStartSpeed^-1 +0.220487* aDesiredPedalPosition^(1/-2) -0.126836* LN(aDeltaEngSpd2MaxAccel) -0.152226* aAccelGradient^(1/-2)	0.584

9.1.2.1 Comparison with the CVT Mondeo and Prius data

Correlation equations were also fitted to the combined data from the CVT Mondeo and Prius since fitting to either dataset alone results in very poor correlations due to the combination of scatter and small datasets (see Section 9.2).

The following tables show the results for those subjective ratings for which correlation equations were created. The acceleration and jerk LWS results have been omitted as no correlations were found.

Table 9-11 - Full metric set, LS fitting

Subjective rating	Correlation equation	Coefficient of determination
smoothness	6.656300-0.558506* aDeltaEngSpd2MaxSpeed^3 -0.739715* aMaxEngSpeed^(1/3) +0.777615* aEngSpdAtMaxVSpeed	0.256

Table 9-12 - Full metric set, LWS fitting

Subjective rating	Correlation equation	Coefficient of determination
smoothness	-7.213444-0.781568* aDeltaEngSpd2MaxSpeed^3 +0.507677* aDeltaEngSpd2MaxSpeed +0.921913* aMaxEngSpeed^(1/-2)	0.202
eng_delay	-0.276932-16.103951* aInitialQuirk^-3 +0.430749* aMaxPedalPosition^(1/-3) +0.208151* aMaxSpeed^(1/3)	0.216
init_accel	87240643.255572-0.619312* aInitialJerk^-3 -0.237156* aInitialQuirk^2	0.192
accel_prog	2.097050-1.185096* aInitialJerk^-3 +0.206262* aDesiredStartSpeed^-1	0.187
performance	98814388.478845-0.793900* aMaxEngSpeed^(1/-2) -0.293626* aDeltaEngSpd2MaxSpeed^3 -0.247182* aInitialQuirk^2 -	0.294

	0.558763* aInitialPedalPosn^-3	

Table 9-13 – Acceleration and jerk metric subset, LWS fitting

Subjective rating	Correlation equation	Coefficient of determination
init_accel	4.353651-0.615610* aInitialJerk^-3	0.159
accel_prog	3.595478-0.569708* aInitialJerk^-3	0.118

Although these correlations are not very high, they do shown some similarities with the equations produced using only the AT vehicles.

The acceleration and jerk subset LWS fit produces correlations for the *init_accel* and *accel_prog* subjective ratings containing the *aInitialJerk* metric. The *aInitialJerk* metric also appears in the full metric equations. These results are similar to those for the AT vehicle equations. A mix of engine speed related metrics are found in the *smoothness* equations and this is similar to the metrics found in the AT vehicle equations.

Overall the metrics look similar to those in the AT vehicle equations, however the equations produced when fitted to all of the vehicles' data produced no fits for these vehicles.

Table 9-14, below, shows the correlations produced when the CVT Mondeo and Prius data are tested using the best acceleration and jerk metric based AT vehicle correlation equation (the best equation, based on all of the metrics, produced no correlations for any of the subjective metrics for either the Prius or CVT Mondeo data sets).

Table 9-14 – AT vehicle only, acceleration and jerk subset, LWS fit

Directory	accel_prog	eng_delay	init_accel	performance	smoothness	vehicle_delay
PRIUS	0.092	0.032	0	0.075	0.196	0.247
CVT Mondeo	0	0	0	0	0	0

It can be seen that the Prius produces correlations, some of which are average. The CVT Mondeo still produces no correlations.

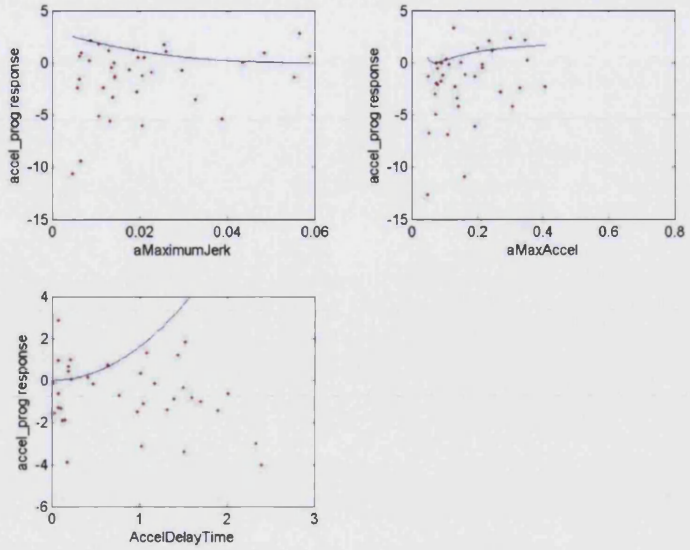

Figure 9-1- *accel_prog* response. Prius data. AT vehicles equation

Figure 9-1, above, shows the response for each term of the *accel_prog* prediction equation produced using AT vehicle data when applied to the Prius data. It appears that although the *aMaximumJerk* and *aMaxAccel* fit lines appear to be in approximately the correct location, the values for *AccelDelayTime* are very large (and therefore erroneous). All of the data also contains a very high level of scatter and these issues as well as the small number of data points explains why the fits against the Prius data produce very low or zero correlations.

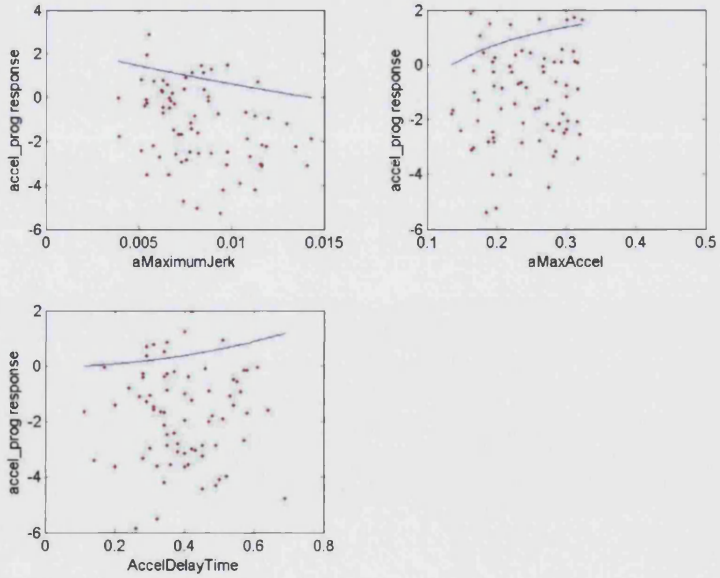

Figure 9-2 - *accel_prog* response. CVT Mondeo data. AT vehicles equation

Figure 9-2, above, shows the response for each term of the *accel_prog* prediction equation produced using AT vehicle data when applied to the CVT Mondeo data. It can be seen that all of the fit lines lie at the edges of the data. These data points also show large amounts of scatter with no clear trends and, in addition, there are only a small number of data points. All of these factors will lead to very low or zero correlations. Looking at the values of the data it can be seen that the maximum jerk and acceleration levels are rather low when compared with the results for the AT vehicles (see Figure A13-18). This may be caused by the lack of a torque converter fitted to the CVT Mondeo.

9.1.2.2 Influence of acceleration and jerk metrics

As was seen in the results of Section 9.1.1 there are a number of similar terms in each correlation equation and the coefficients of determination for each of the metric set and fitting type combinations are similar. However the full metric set equations proved to produce the highest correlations. This in the values of the coefficients of determination is most likely due to the occurrence of acceleration and jerk subset metrics in the 'full metric set' equations. Table 9-15, below, show the metrics in the 'full metric set' LWS equation which was found to produce the best correlations. The metrics highlighted in bold font are those that are members of the acceleration and jerk subset.

Table 9-15 - Least weighted squares fit equation metrics

Subjective metric	Objective metrics
smoothness	**aMaximumJerk**, aDesiredStartSpeed, aEngSpdAtMaxVSpeed, aDeltaEngSpd2MaxSpeed, aInitialSpeed, aRateOfChangeOfPedalPosition, **aMaxAccel**, aMaxPedalPosition, **aMaximumJerk**, aEngSpdAtMaxVSpeed, aChangeInSpeed
eng_delay	**aMaximumJerk**, aChangeInSpeed, aDesiredStartSpeed, aDeltaEngSpd2MaxSpeed, aMaxSpeed, **AccelDelayTime**, aAverageAccelToMaxSpeed, **aMaxAccel**, aEngSpdAtMaxVSpeed
vehicle_delay	**aMaximumJerk**, aDesiredStartSpeed, **aMaxAccel**, aDesiredPedalPosition, aDeltaEngSpd2MaxSpeed, aMaxSpeed, aDeltaEngSpd2MaxAccel, **aAverageAccelToMaxAccel**
init_accel	**aMaximumJerk**, **aMaxAccel**, aDesiredStartSpeed, **AccelDelayTime**, aEngSpdAtMaxVSpeed, aInitialSpeed
accel_prog	**aMaximumJerk**, **aMaxAccel**, aDesiredStartSpeed, aDeltaEngSpd2MaxSpeed, aEngSpdAtMaxVSpeed, aRateOfChangeOfPedalPosition, **aAccelGradient**, aDeltaEngSpd2MaxAccel, aMaxSpeed
performance	**aMaximumJerk**, **aMaxAccel**, aDesiredStartSpeed, aDesiredPedalPosition, aDeltaEngSpd2MaxAccel, **aAccelGradient**

It can be seen that there are a large number of acceleration and jerk-related metrics in these equations which confirms the findings of List and Schoeggl (1998), Dorey and Holmes (1999), Wicke et al. (2000) and Pickering et al. (2002) that acceleration based metrics are

the most influential on vehicle driveability ratings. An analysis of the correlation equations found when using the acceleration and jerk metric subset was carried out and is shown in Appendix XIII. The correlations using these acceleration and jerk metrics were found to be less accurate (in terms of the coefficient of determination when comparing the actual and predicted subjective metrics) than the correlations produced using the full metric set. It was, however, found that the trends of the acceleration and jerk metrics in the acceleration and jerk metric correlation equations were very similar to those that were present in the full metric set equations.

The correlation equations, produced using the full set of metrics, for each of the subjective metrics are analysed in the following sections.

9.1.2.3 The acceleration progression correlation equation

This section analyses the *acceleration progression* (metric name: *accel_prog*) correlation equation. Figure A13-17 below shows predicted vs. actual ratings for the *accel_prog* rating. A perfect fit would show all of the data points lying on a line stretching diagonally across the graph from the lower left-hand corner to the upper right-hand corner. The coefficient of determination for this dataset is R^2= 0.569.

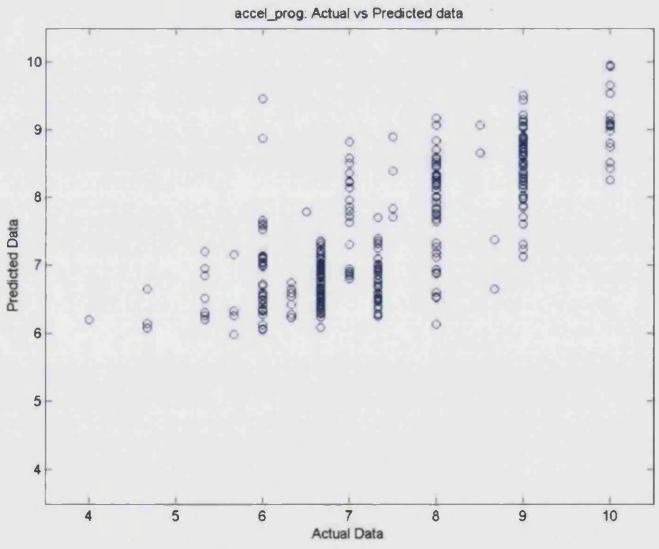

Figure 9-3 – Plot of predicted and recorded *accel_prog* ratings

A histogram showing the predicted and actual subjective metrics is shown in Figure 9-4 and the standard deviations and means of the two sets of data are shown in Table 9-16, below.

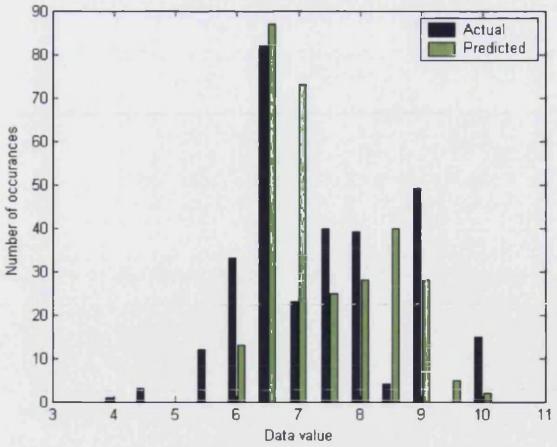

Figure 9-4 – Actual and predicted subjective metric histogram

Table 9-16 – Statistical measures

Actual		Predicted	
Standard deviation	**Mean**	**Standard deviation**	**Mean**
1.216	7.368	0.954	7.398

It can be seen that the distribution of the two data sets appears to be close, this is reflected in the combination of the coefficient of determination value and the similar means and standard deviations of the datasets. In fact the standard deviation of the predicted subjective metrics is lower than that of the actual data showing that the technique does not add scatter to the predicted results.

This procedure has been repeated for all of the subjective metrics and is shown in Figure 9-5 and Figure 9-6, below. These figures compare the means and standard deviations of the actual and predicted datasets for all of the subjective metrics. The diagonal line indicates the point at which the actual and predicted values are identical.

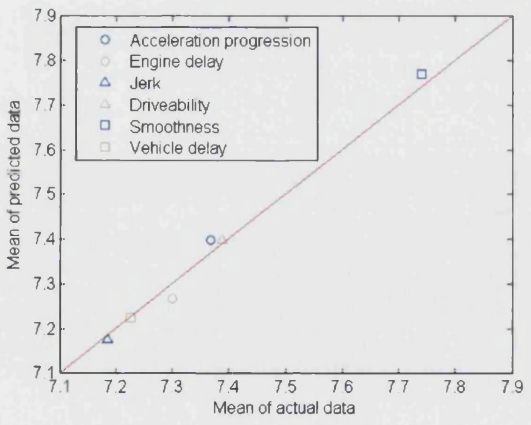

Figure 9-5 - Comparison of means for actual and predicted datasets

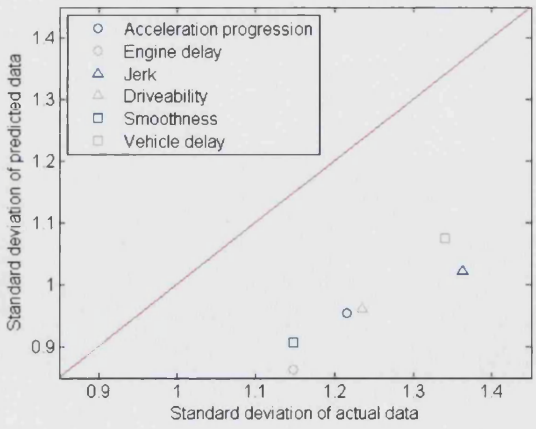

Figure 9-6 - Comparison of standard deviations for actual and predicted datasets

It can be clearly seen that the means all lie on or close the line, indicating that they are similar between the actual and predicted metrics. The standard deviations all lie beneath the line, indicating that the predicted metrics have smaller standard deviations.

Figure 9-7, below, shows the behaviour of the individual metrics in this correlation equation.

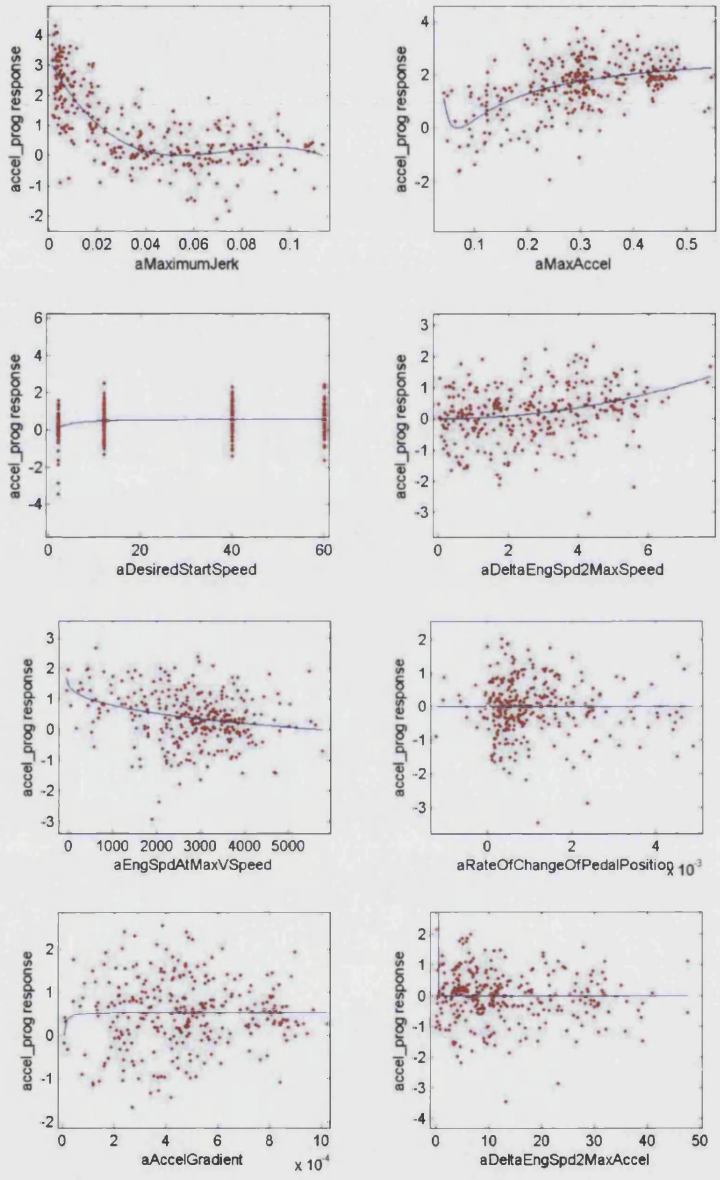

Figure 9-7 - Response for each metric in *accel_prog* prediction equation

It can be seen that an increase in *aMaximumJerk* shows a general downward trend for the *accel_prog* response with a plateau and slight increase as the level reaches a threshold

value of 0.04 g/s. This negative trend for *aMaximumJerk* is shared by all of the subjective rating prediction equations. This shared trend is analysed further in Section 9.1.2.8.1.

The *aMaxAccel* metric shows a clear positive correlation with *accel_prog* with the exception of an initial downward trend. This initial downward movement is very short and appears to be an artefact of the particular curve fitted to these data and can therefore be safely ignored.

The *aDesiredStartSpeed* metric shows a slight positive correlation. It appears that the higher speed tests (40 and 60kph) have an identical positive response, which reduces as the initial vehicle speed is reduced. This effect is relatively small but may reflect the fact that at low speeds there may be torque converter and drive line wind-up effects, which will influence the acceleration that the driver feels.

The *aDeltaEngSpd2MaxSpeed* metric shows a positive correlation, however it should be noted that there is a significant amount of scatter in the data. This metric may be related to the value of the acceleration in the test (a larger average engine speed gradient would be associated with a greater acceleration) or it may be a causal effect whereby the drivers prefer the tests in which the engine speed is changing more rapidly. As the *aMaxAccel* metric is also included in the equation, the latter conclusion seems to be more likely.

The *aEngSpdAtMaxVSpeed* shows that the drivers rated the vehicle more highly the lower its engine speed was at the point where they stopped accelerating (maximum vehicle speed). This rating is understandable in some ways, as it would indicate to the driver that the vehicle has performance in reserve (in terms of higher engine speed and therefore higher power), however this may not be an accurate picture as gearshifts may have occurred.

The *aRateOfChangeOfPedalPosition* metric shows no real correlation. Its inclusion appears to be an artefact of the rating process produced by the shape of the curve. This is analysed further in Section 9.1.2.8.1. Similarly, *aAccelGradient* and *aDeltaEngSpdToMaxAccel* show no real correlation. The explanation for their inclusion is the same as for *aRateOfChangeOfPedalPosition*.

9.1.2.4 The engine delay correlation equation

This section analyses the *engine delay* correlation equation. Figure A13-20 below shows predicted vs. actual ratings for the *eng_delay* rating. The coefficient of determination for this dataset is R^2= 0.533. A plot showing the actual and predicted subjective metric data can be

found in Appendix XII. Comparisons of the means and standard deviations of these data can be found in Figure 9-5 and Figure 9-6. Figure 9-8, below, shows the behaviour of the individual metrics in this correlation equation.

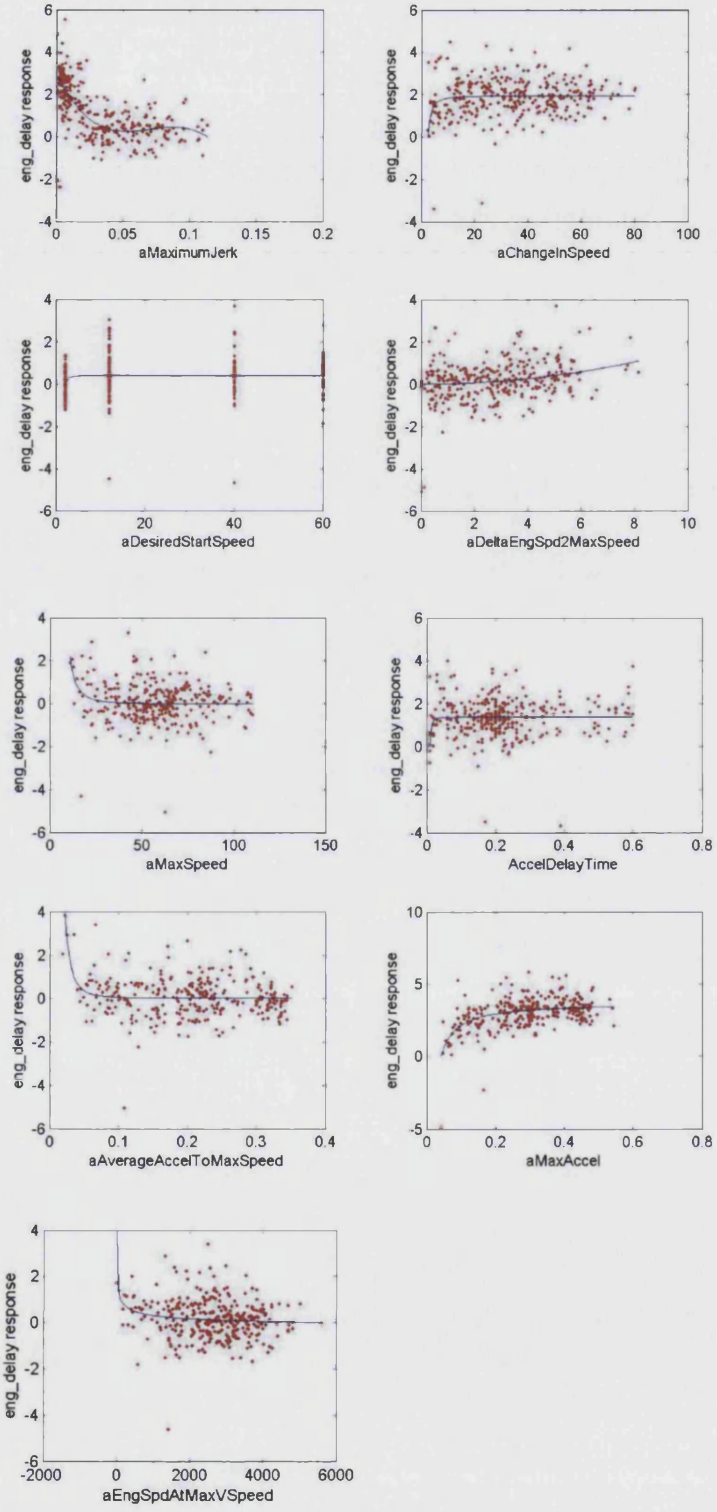

Figure 9-8 - Response for each metric in *eng_delay* prediction equation

It can be seen that an increase in *aMaximumJerk* shows a general downward trend for the *eng_delay* response with a plateau and slight increase as the level reaches a threshold value of 0.04 g/s. This negative trend for *aMaximumJerk* is shared by all of the subjective rating prediction equations and is analysed further in Section 9.1.2.8.1.

The *aMaxSpeed*, *AccelDelayTime*, *aAverageAccelToMaxSpeed* and *aChangeInSpeed* metrics show very little trend and their overall effects are small. Their inclusion appears to be an artefact of the fitting process and is analysed further in Section 9.1.2.8.1.

The *aDesiredStartSpeed* metric shows a constant positive response for the 12kph and higher initial vehicle speeds and a slightly lower response for the 2kph initial speed tests. This may be indicative of the torque converter and driveline wind-up that occurs at low speed and increases the apparent delay in acceleration.

The *aDeltaEngSpd2MaxSpeed* metric shows a positive trend, which indicates that drivers preferred a vehicle whose engine speed, changed rapidly over the accelerative phase. This may be a secondary effect as a rapid change in engine speed would be associated with a rapid change in vehicle acceleration.

The *aMaxAccel* metric shows a clear positive correlation with *eng_delay* indicating that the drivers liked a high maximum acceleration.

Although the *aEngSpdAtMaxVSpeed* metric appears to show a slight negative trend, the data are so scattered that it is difficult to be sure. If this metric is considered to be valid, it appears to show a similar trend to that shown in the *accel_prog* equation.

9.1.2.5 The initial jerk correlation equation

This section analyses the *initial jerk* correlation equation. Figure A13-23 below shows predicted vs. actual ratings for the *init_accel* rating. The coefficient of determination for this dataset is R^2= 0.542. A plot showing the actual and predicted subjective metric data can be found in Appendix XII. Comparisons of the means and standard deviations of these data can be found in Figure 9-5 and Figure 9-6.

Figure 9-9, below, shows the behaviour of the individual metrics in this correlation equation.

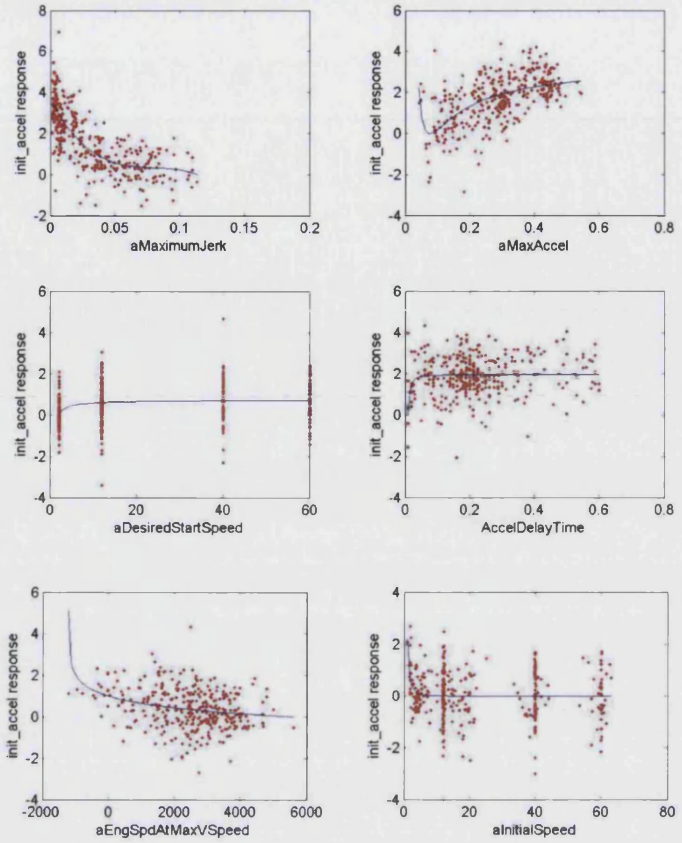

Figure 9-9 - Response for each metric in *init_accel* prediction equation

It can be seen that an increase in *aMaximumJerk* shows a downward trend for the *init_accel* response with a change in gradient as it reaches a value of 0.04 g/s. This overall negative trend for *aMaximumJerk* is shared by all of the subjective rating prediction equations and is analysed further in Section 9.1.2.8.1.

The *aMaxAccel* metric shows a clear positive correlation with *init_accel* with the exception of an initial downward trend. This initial downward movement is very short and appears to be an artefact of the particular curve fitted to these data and can therefore be safely ignored.

The *aDesiredStartSpeed* metric shows a positive trend that is only significant for the lowest vehicle initial speeds (2kph). As was the case in the *accel_prog* equation, this may be due to torque converter and driveline wind-up.

The *AccelDelayTime* and *aInitialSpeed* metrics show very little effect overall. Their inclusion appears to be an artefact of the fitting process. This is analysed further in Section 9.1.2.8.1.

The *aEngSpdAtMaxVSpeed* metric shows a slight negative trend, which is similar to that seen in the *accel_prog* and *eng_delay* equations.

9.1.2.6 The overall driveability correlation equation

This section analyses the *overall driveability* correlation equation. Figure A13-25 below shows predicted vs. actual ratings for the *performance* rating. The coefficient of determination for this dataset is R^2= 0.584. A plot showing the actual and predicted subjective metric data can be found in Appendix XII. Comparisons of the means and standard deviations of these data can be found in Figure 9-5 and Figure 9-6.

Figure 9-10, below, shows the behaviour of the individual metrics in this correlation equation.

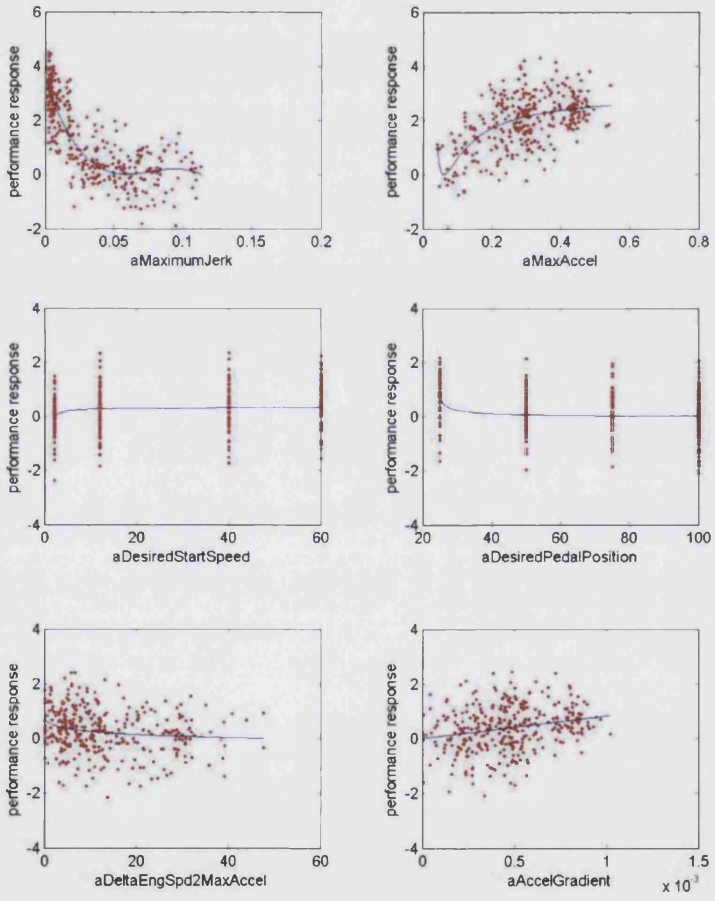

Figure 9-10 - Response for each metric in *performance* prediction equation

It can be seen that an increase in *aMaximumJerk* shows a general downward trend for the *performance* response with a plateau and slight increase as the level reaches a threshold

value of 0.04 g/s. This negative trend for *aMaximumJerk* is shared by all of the subjective rating prediction equations and is analysed further in Section 9.1.2.8.1.

The *aMaxAccel* metric shows a clear positive correlation with *performance* with the exception of an initial downward trend. This initial downward movement is very short and appears to be an artefact of the particular curve fitted to these data and can therefore be ignored.

The *aDesiredStartSpeed* metric shows a slight positive trend whose main effect is seen at the lower initial vehicle speeds. This may reflect the additional delays that occur at low speeds due to torque converter and driveline wind-up.

The *aDesiredPedalPosition* metric shows an overall negative trend meaning that smaller pedal positions produce better ratings. In fact, the effect is rather small and the majority of the effect is seen for the 25% pedal position. It can be seen that the ranges of the ratings at each pedal position are approximately equal and this may simply be experimental variance. A physical explanation for the difference would have to take account of the fact that the 25% pedal position tests often had higher pedal positions as this small movement is difficult to judge (see Section 7.1.2), this may mean that the drivers experience greater performance than they had expected based on the pedal position which they thought they were using.

The *aDeltaEngSpd2MaxAccel* metric shows a slight negative trend, this indicates that the test drivers liked the rate of change of engine speed to be low up until the point of maximum acceleration. This is strange as other subjective metrics showed a positive correlation for the rate of change of engine speed and the rating. High rates of change of engine speed would be expected in low gears and at low to medium engine speeds. Therefore this may be indicating that the drivers prefer a progressive acceleration rather than one which peaks early in the engine speed range.

The *aAccelGradient* metric shows a clear positive trend. This indicates that the vehicle rating is improved by a higher mean acceleration over the duration of the accelerative phase.

9.1.2.7 The smoothness correlation equation

This section analyses the *smoothness* correlation equation. Figure A13-27 below shows predicted vs. actual ratings for the *smoothness* rating. The coefficient of determination for this dataset is R^2= 0.585. A plot showing the actual and predicted subjective metric data can

be found in Appendix XII. Comparisons of the means and standard deviations of these data can be found in Figure 9-5 and Figure 9-6.

Figure 9-11, below, shows the behaviour of the individual metrics in this correlation equation.

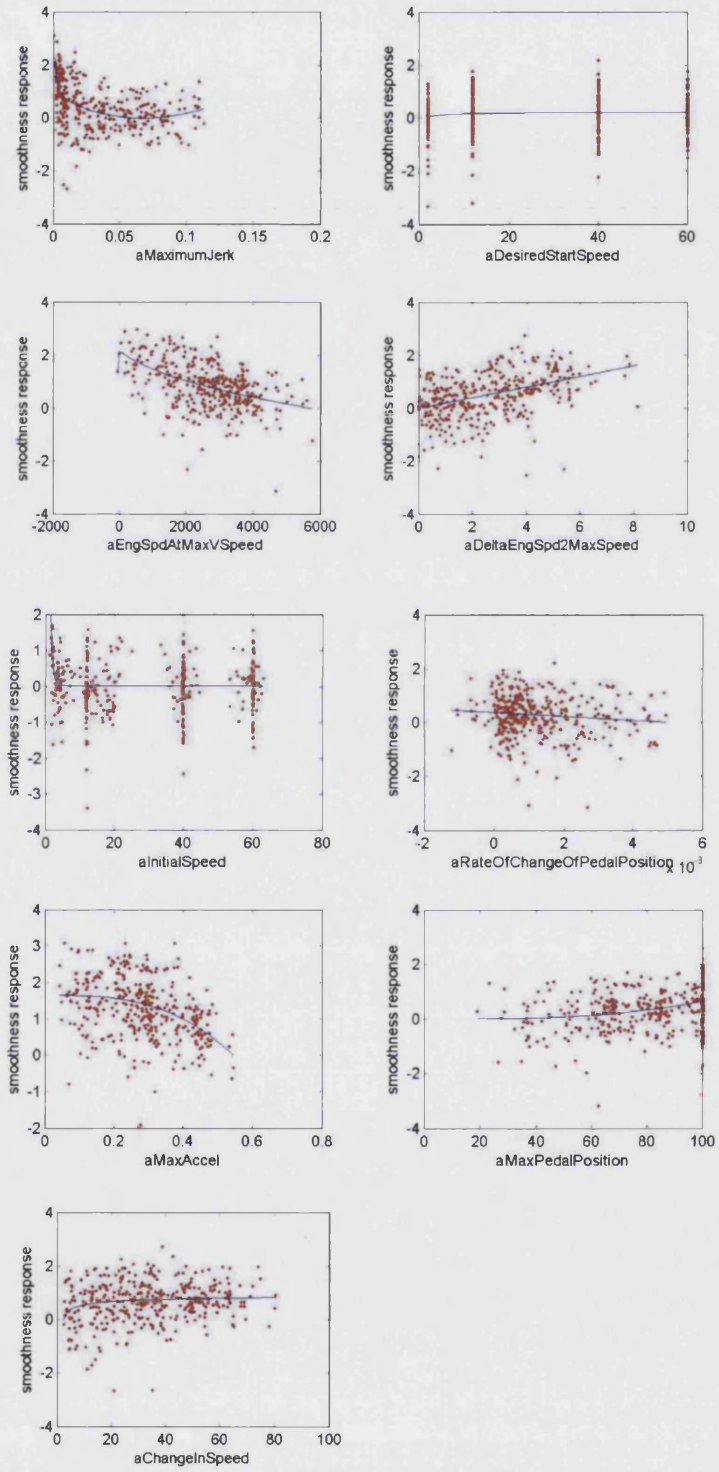

Figure 9-11 - Response for each metric in *smoothness* prediction equation

The *aMaximumJerk* metric shows a negative trend, which levels off and then starts increasing slightly, however the negative aspect of this metric is markedly reduced from that of the other metrics that have been considered thus far. This may indicate that the *smoothness* rating has a far lower threshold for maximum jerk than the other subjective ratings, which produces the very steep negative gradient at low values of *aMaximumJerk.*

The *aDesiredStartSpeed* metric shows a slight positive trend; however this may simply be due to experimental variance as the results show a significant range. A physical explanation might be that at low speeds the acceleration will tend to be significantly stronger than at higher speeds. This would tend to reduce *smoothness.*

The *aEngSpdAtMaxVSpeed* metric shows a clear negative trend (there is an initial, very short, upward trend which is a fitting artefact). This indicates that tests that had lower maximum engine speeds produced better *smoothness* ratings. The presence of gear-shift events makes determining the physical reason for this trend difficult. Higher maximum vehicle speeds would indicate the possibility that a gearshift event may have taken place, however if the maximum vehicle speed occurs just after a gear shift a lower engine speed would be detected. However a threshold value could be established as in general the gearboxes will not change up during a tip-in event unless the engine speed reaches some relatively high value, therefore the theory that gearshifts reduce the smoothness rating should hold true.

The *aDeltaEngSpd2MaxSpeed* metric shows a clear positive correlation. This means that those tests that had a high rate of change of engine speed produced higher *smoothness* ratings. This may be due to the drivers' changing their expectations due to their pedal demand.

The *aInitialSpeed* metric shows very little trend and its overall effect is very small. Its inclusion appears to be an artefact of the fitting process. This is analysed further in Section 9.1.2.8.1.

The *aRateOfChangeOfPedalPosition* metric shows a slight negative trend, however this is small when compared with the overall scatter. Nevertheless, a physical explanation for this correlation may be that more rapid applications of the accelerator pedal result in more jerky acceleration, which has been seen to have a negative effect on all of the ratings.

The *aMaxAccel* metric shows a negative trend, which would be expected as a high maximum acceleration, will tend to result in more jerky acceleration and gearshifts.

The *aMaxPedalPosition* metric shows a slight positive trend which may be showing that the driver takes account of the pedal position and therefore the expected level of the acceleration when deciding what they expect in terms of vehicle smoothness.

The *aChangeInSpeed* metric shows a slight positive trend, however this is not very large when compared with the scatter in the data. This may be related to driver expectations. A large change in speed over the course of the test implies a large pedal position input and therefore this may be reflecting the slight trend seen for the *aMaxPedalPosition* metric.

9.1.2.8 The vehicle delay correlation equation

This section analyses the *vehicle delay* correlation equation. Figure A13-29 below shows predicted vs. actual ratings for the *vehicle_delay* rating. The coefficient of determination for this dataset is R^2= 0.624. A plot showing the actual and predicted subjective metric data can be found in Appendix XII. Comparisons of the means and standard deviations of these data can be found in Figure 9-5 and Figure 9-6.

Figure 9-12, below, shows the behaviour of the individual metrics in this correlation equation.

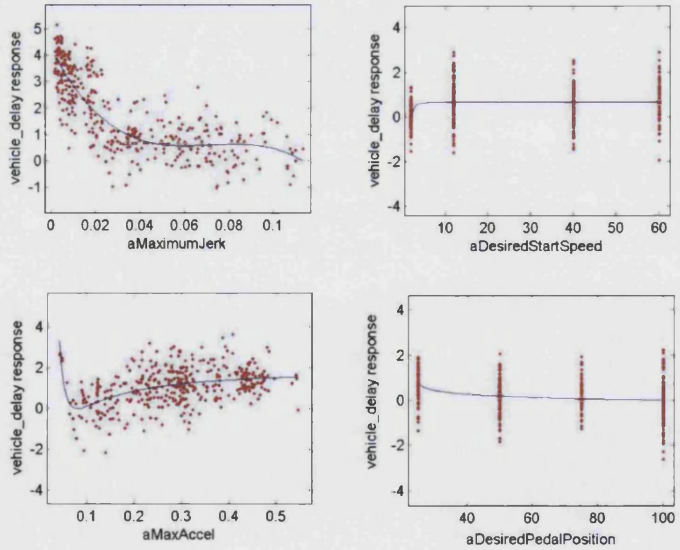

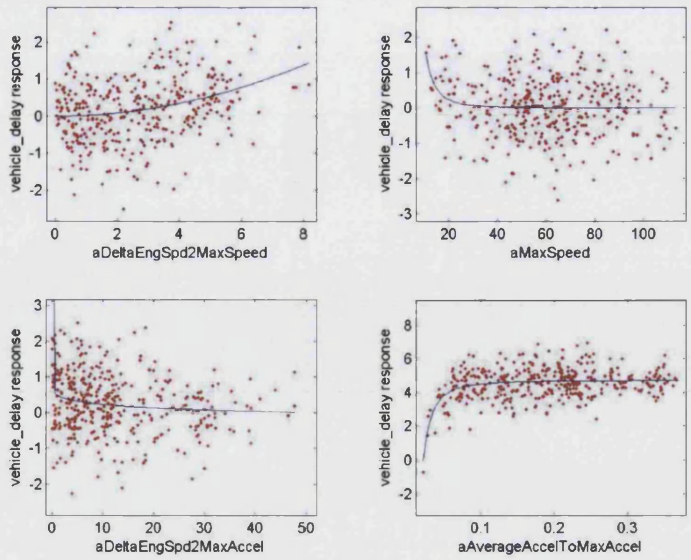

Figure 9-12 - Response for each metric in *vehicle_delay* prediction equation

It can be seen that an increase in *aMaximumJerk* shows a general downward trend for the *vehicle_delay* response with a plateau as the level reaches a threshold value of 0.04 g/s. This negative trend for *aMaximumJerk* is shared by all of the subjective rating prediction equations and is analysed further in Section 9.1.2.8.1.

The *aDesiredStartSpeed* metric indicates that the 2kph tests produced lower *vehicle_delay* ratings. This effect may be produced by torque converter and driveline wind-up.

The *aMaxAccel* metric shows a positive correlation with *vehicle_delay* with the exception of an initial downward trend. This initial downward movement is short and appears to be an artefact of the particular curve fitted to these data and can therefore be safely ignored.

The *aDesiredPedalPosition* metric shows a negative correlation. This may be caused because a kick-down gearshift will tend to occurs with large pedal demands and this will introduce an interruption on the acceleration.

Despite the large degree of scatter, the *aDeltaEngSpd2MaxSpeed* metric appears to show a positive correlation. This implies that tests which had a higher pedal position produced better ratings – this makes sense as acceleration also shows a positive correlation and the higher acceleration should reduce any driveline delays. It may also be that the increased acceleration overshadows any delay effects that occur earlier in the test.

The *aMaxSpeed* metric shows almost no effect. Its inclusion appears to be an artefact of the fitting process. This is analysed further in Section 9.1.2.8.1.

The *aDeltaEngSpd2MaxAccel* metric shows a slight negative correlation however there is a large amount of scatter and therefore this trend may not be valid. If this does represent a true correlation then it is unexpected. The *aDeltaEngSpd2MaxSpeed* metric shows a trend that moves in the opposite sense.

The *aAverageAccelToMaxAccel* metric shows an initial large positive correlation which then decreases to a far smaller positive correlation. The initial trend may be an artefact caused by the distribution of the data, however there appears to be a definite trend for these data points. Therefore this may be an actual trend, in which case it may indicate that there is a threshold average acceleration value below which (<0.075g) the *vehicle_delay* rating is far worse than it is above it.

9.1.2.8.1 The addition of terms that produce little effect on the response

It has been noted that a number of terms that remain constant for the majority of their range have been added to the correlation equations. These terms always have a non-constant section, which often has a very large gradient. When such terms are evaluated, they are able to produce an artificially high coefficient of determination due to the non-horizontal portion of the curve. This portion of the curve produces a number of predicted data points that are far removed from the mean value of the data.

As the error between the fitted data point and the mean becomes large (and therefore ΣY' becomes significantly larger than ΣY), the value of the coefficient of determination tends towards a value of 1/2, even if it would otherwise show no correlation. The reason for this is as follows:

$$R^2 = \frac{SS_{Reg}}{SS_{Tot}} \qquad \textbf{Equation 9-1}$$

$$R^2 = \frac{SS_{Reg}}{SS_{Reg} + SS_{Res}} \qquad \textbf{Equation 9-2}$$

$$R^2 = \frac{\sum (Y' - \bar{Y})^2}{\sum (Y' - \bar{Y})^2 + \sum (Y - Y')^2} \qquad \textbf{Equation 9-3}$$

If ΣY'>>ΣY, this reduces to:

$$R^2 = \frac{nY'^2}{nY'^2 + nY'^2}$$ **Equation 9-4**

$$R^2 = \frac{nY'^2}{2nY'^2}$$ **Equation 9-5**

Therefore

$$R^2 = \frac{1}{2}$$ **Equation 9-6**

This effect is not confined to cases where the entire fitted data set consists of outliers, it affects any cases where ΣY'>> ΣY and conversely where ΣY'<< ΣY and this can be found where an outlying data point produces a sufficiently large error to affect the summation process.

This artificial inflation of the coefficient of determination will not have a large effect as the range of the fitted points are limited to a range from 0 to 10 to stop just such an issue (see Section 6.6.3.2). This may result in a given term which has a small standard deviation (almost all of the data lie at or around a single subjective rating number) having a small boost in its effective coefficient of determination which may mean that the term in question will be tried in the overall correlation equation earlier than would otherwise happen (the terms are added in order of their single variable correlation with the subjective rating).

Therefore, the effect that these terms have on the total coefficient of determination and their own partial correlation coefficients is limited. However some of these terms still remain in the final correlation equations, indicating that the interaction of these terms, which produce some outlying values, with the other terms in the equation produces interactions and an overall effect that adds to the predictive power of the correlation equation.

Unfortunately, such interactions will almost certainly be chance interactions and ideally, such terms would be removed automatically, perhaps by looking at the shape or ranges of the fitted equation. Another option is to remove negative polynomial powers as the majority of the terms that produce these outlying terms use such powers. It should, however, be noted that there are other terms present in the equations with negative polynomial powers which do produce significant responses. The last option is to let the operator look at the individual terms and decide which should be included.

9.1.2.8.2 Jerk and acceleration metric behaviour

It can be seen that for all of the equations an increase in *aMaximumJerk* shows a downward trend for the *accel_prog* response with a plateau and slight increase as the level reaches an *aMaximumJerk* value of 0.05 g/s. Figure 9-13 shows an example of this.

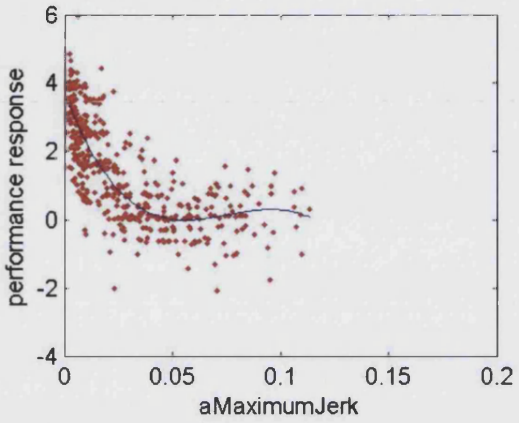

Figure 9-13 – *performance* response for *aMaximumJerk* metric

This metric is measuring the maximum jerk in the period between the start of the vehicle test and the point at which maximum acceleration is reached. It is thought that this response represents the effect of bad driveline jerk, which is known to be undesirable.

Acceleration trends

Wicke states in his thesis that he was unable to find any correlations between the subjective driveability rating and the maximum acceleration during a test. This is, however, one of trends that are shown in the current correlation equations.

Wicke related the subjective driveability ratings for tests performed with single vehicles to the initial vehicle acceleration (the mean acceleration from the start of acceleration in a test until a significant lessening of the acceleration gradient). He also showed similar trends by plotting the mean values for multiple vehicles' data.

In fact, the *aMaxAccel* response agrees very well with Wicke's findings (2001) and although this metric does not measure an identical quantity (it measures the maximum acceleration during the accelerative portion of the test), the two are directly related.

A direct comparison would be to use the *aAverageAccelToMaxAccel* metric. In fact, this metric was available to the correlation equation fitting code, but was not selected. This indicates that the maximum acceleration has a greater effect (though the effect may not be significantly greater).

The aMaxAccel metric is in fact highly correlated with the *aAverageAccelToMaxAccel* metric as can be seen from Table 7-5 and Figure 9-14, below.

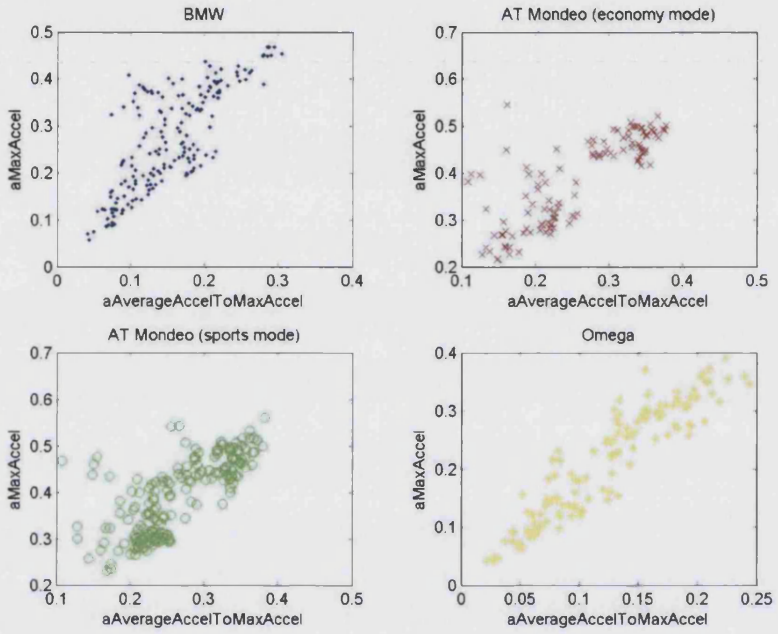

Figure 9-14 – Plots of *aMaxAccel* against *aAverageAccelToMaxAccel* metric for each vehicle

Therefore, Wicke's single-vehicle and mean-value multiple vehicle correlations have been confirmed for raw multiple vehicle data and the multivariate technique has clarified a relationship with was not readily found using single variable techniques.

Jerk trends

Wicke's findings (2001) show a positive correlation between the driveability evaluation and vehicle jerk. Although this correlation is in the opposite sense to that found in this research, he was calculating a different type of jerk metric and therefore the two are not in disagreement. This is because there tend to be a large number of high frequency oscillations in the jerk data meaning that the maximum value may occur at any point during the test period. Wicke calculated the average jerk over the initial phase of the acceleration. The acceleration is broken down into an initial period, the end of which can be identified by a reduction in acceleration and engine speed acceleration. This is a task far more easily

accomplished by a human than by a computer program so therefore this metric was not calculated due to the variability of the data making the automatic calculation rather difficult.

A different metric was included in an attempt to emulate this measurement in a more automation-friendly manner. The *aAccelGradient* metric measures the average gradient of the vehicle acceleration over the first 4 seconds of the test. Figure 9-15, below, shows the mean driveability rating plotted against the mean acceleration gradient for the vehicles tested in this research.

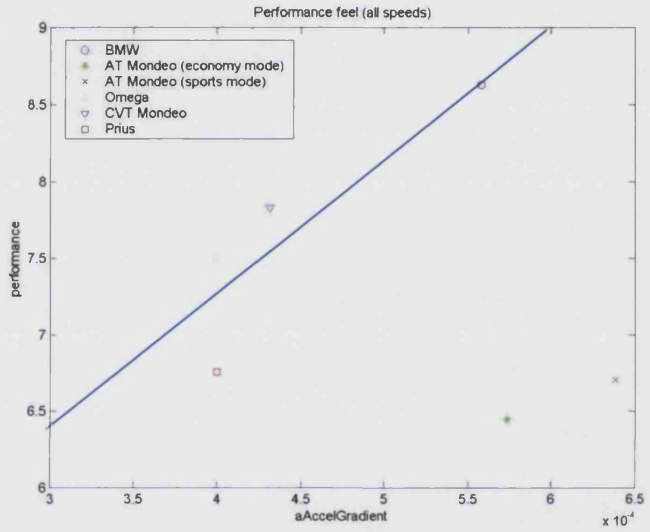

Figure 9-15 – Mean *performance* rating for each vehicle

Excluding the data from the AT Mondeo vehicle, these points show a reasonably linear trend (indicated by the blue line), which is the same as that highlighted by Wicke et al. (2000) and Wicke (2001). The outlying AT Mondeo data points are most probably due to the poor gearshift.

In fact the maximum vehicle acceleration tends to be related to the average jerk, assuming that the test vehicles have similar acceleration performance (which is the case for the vehicles which were evaluated in this project and in Wicke's), and this is most probably why the *aAccelGradient* metric was not automatically chosen to be included in the correlation equations. Therefore the *aMaxAccel* metric response also approximates Wicke's average jerk response.

In the current correlation equations, it can be seen that there is a negative trend for *aMaxJerk* followed by a plateau or slight increase.

Figure 9-16 below shows the values of *aMaximumJerk* plotted against those of *aMaxAccel* for the AT vehicle dataset.

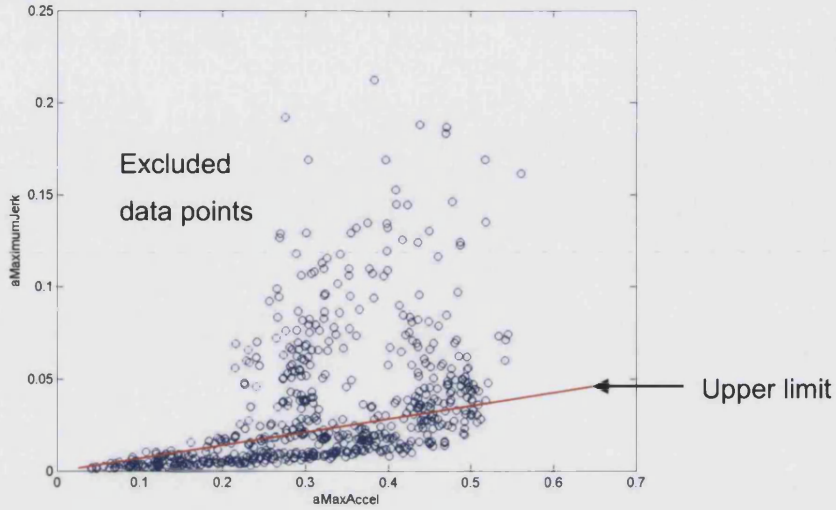

Figure 9-16 - aMaximumJerk against aMaxAccel for AT vehicle dataset

It can be seen that there is a clearly defined linear relationship between the variables, which produces a lower limit to the data. If the data are marked to show which vehicle they came from, as is shown in Figure 9-17 below, it can be seen that it is the data from the AT Mondeo (both economy and sports modes) which produces the scattered results, while the data from the BMW and Omega remain within the linear boundaries explained above.

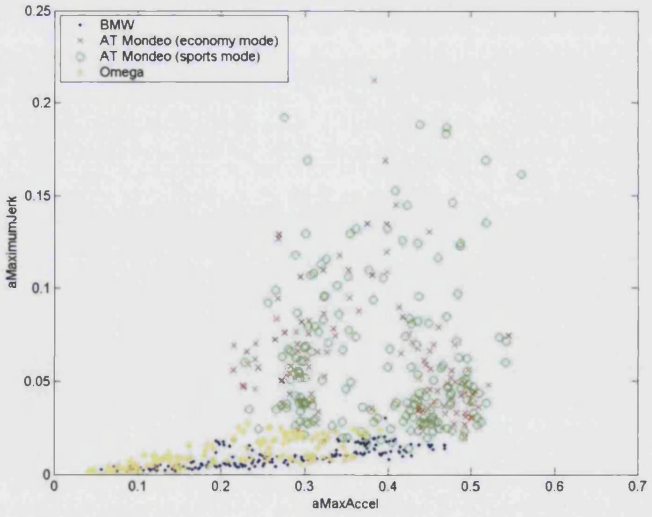

Figure 9-17 - aMaximumJerk against aMaxAccel for AT vehicle dataset (split by vehicle)

This difference might be attributed to the fact that the AT Mondeo's gearbox produced poor gearshifts with large values of jerk corresponding to those seen in Figure 9-17 above.

It should also be noted that the threshold value of *aMaximumJerk=0.05g/s* which indicated the change in the response of the metric from a downward trend to a plateau or slight upward trend in Figure 9-13 corresponds approximately with the limit of the upper bound of the non-AT Mondeo data seen in Figure 9-17. Therefore the scattered data points with values of greater than *aMaximumJerk=0.05* could be excluded as they are not measuring the same data as for the other vehicles. It can be seen that the remainder of the data lie in an approximately triangular region. Above values of *aMaxAccel*=0.2, the *aMaximumJerk* values are caused by the AT Mondeo vehicle and it can be seen that these data did not have any significant effect on the correlation equation (due to this portion of the curve being approximately flat).

Figure 9-18, below, shows a plot of the maximum jerk against the time at which it occurs.

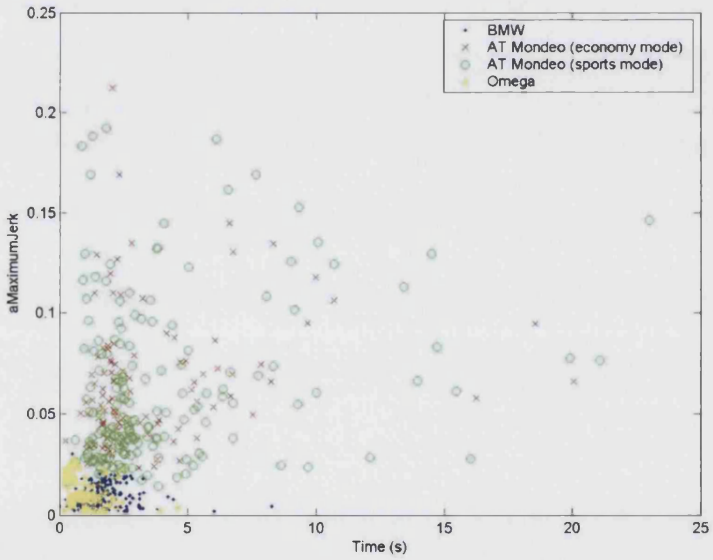

Figure 9-18- Maximum Jerk plotted against time

It can be seen that the majority of the maximum jerk points fall within the first 4 seconds after the acceleration has been detected which places them early in the accelerative phase (all of the data points are from the accelerative phase of the manoeuvre by definition), however a large number of the AT Mondeo (both economy and sports mode) points occur at later times. By definition, the maximum jerk point must occur between the start of acceleration

and the maximum acceleration point. The maximum acceleration point must occur between the start of acceleration and the point at which maximum vehicle speed was reached (as this is the end of acceleration).

Therefore, it can be seen that values of jerk greater than approximately 0.05g/s, which tend to be caused by the AT Mondeo, do not have an effect on the subjective rating. It is likely that if the AT Mondeo data were not included, there would be no plateau and therefore the negative trend would continue for higher jerk values. The most likely explanation for the AT Mondeo's high jerk values not having an effect is that they occur late in the test during gearshift events.

9.1.2.8.3 Acceleration delay metric

One unexpected finding is that the *AccelDelayTime* metric, although present in many of the correlation equations, has very little effect on the predicted ratings. Figure 9-19 shows a plot of the *AccelDelayTime* metric plotted against the *performance* rating (the *performance* rating was chosen as it has been showed to have a link to the majority of the other non-delay metrics). It should be noted that a single variable plot like this would not be able to produce as good a correlation as a multivariate plot, which can take account of many different factors, however major trends should be visible.

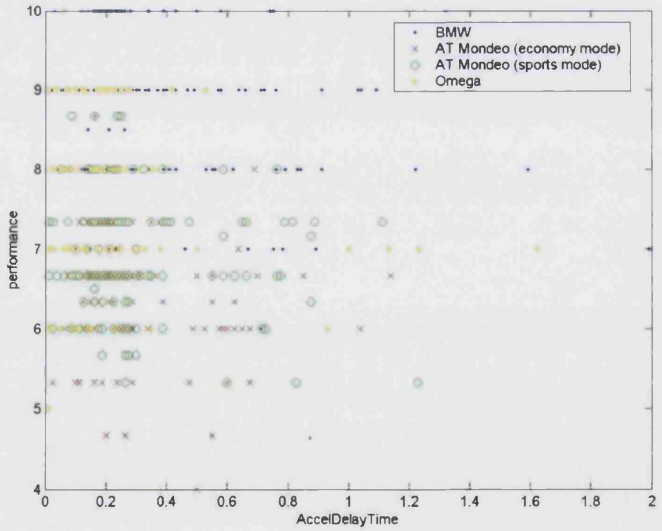

Figure 9-19 – *performance* rating plotted against *AccelDelayTime* for each vehicle

No easily discernable trends can be seen, nor can any consistent trend be seen when these data are plotted for the individual vehicles as shown in Figure 9-20.

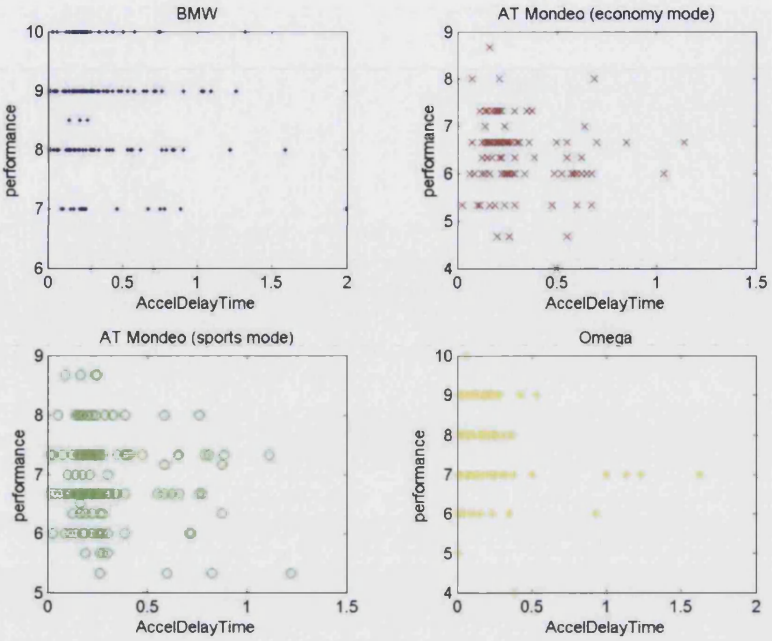

Figure 9-20 – Subplots of *performance* rating against *AccelDelayTime* for each vehicle

This may indicate a number of things:

- There is a lower threshold for the acceptability of delay time and that the majority of the tests that were performed fall within this threshold and are therefore acceptable to the test-drivers.
- There is a lower threshold for human perception of delay time and the majority of the tests that were performed fall within this threshold and are therefore imperceptible to the test-drivers.
- There is a problem with the calculation of the *AccelDelayTime* metric – the metric is too sensitive and that when a human determines the delay time, they allow the acceleration to rise to a certain level before recording the delay time
- There is a problem with the calculation of the *AccelDelayTime* metric – the exact pedal position and acceleration start positions have not been measured correctly due to the noise in the data from both of these channels.

Testing has shown that the calculation of the pedal and acceleration start positions appears to be correct, therefore there must either be a lower threshold for the delay time, or a different calculation for the acceleration delay time metric should be used that takes into account the level of acceleration that the driver can actually detect.

9.2 *Single vehicle correlations*

The previous tests have shown that although good correlations can be obtained by producing a correlation using all of the available data, or large subsections of it, the best possible correlations should be produced by generating correlation equations using the data for a single vehicle and then applying that equation to the subsets of data for that vehicle.

The application of these single-vehicle correlations would be just as valuable as that of generic equations and by looking at the equations for different vehicles, it would be possible to characterise different vehicle types. This characterisation data could subsequently be used for vehicle simulation or as a method of copying another vehicle's character.

The coefficients of determination for the equations fitted to the vehicle data are shown in the tables below. In all of these tables, an empty cell indicates that no equation could be fitted to the dataset in question and a missing row indicates that none of the correlation equations could be produced for the missing metric and fit combination.

Table 9-17 - BMW Auto-correlation coefficients of determination

Equation type	Coefficient of determination					
	smoothness	eng_delay	vehicle delay	init accel	accel prog	performance
Full metric set, LS				0.117		
Full metric set, LWS			0.358	0.251	0.216	
Accel and jerk subset, LS				0.085		
Accel and jerk subset, LWS			0.269	0.251	0.210	

Table 9-18 – AT Mondeo (economy mode) Auto-correlation coefficients of determination

Equation type	Coefficient of determination					
	smoothness	eng_delay	vehicle delay	init accel	accel prog	performance
Full metric set, LS				0.221	0.159	0.287
Full metric set, LWS			0.235	0.413	0.315	0.460
Accel and jerk subset, LS					0.136	0.186
Accel and jerk subset, LWS				0.317	0.315	0.348

Table 9-19 – AT Mondeo (sports mode) Auto-correlation coefficients of determination

Equation type	Coefficient of determination					
	smoothness	eng_delay	vehicle delay	init accel	accel prog	performance
Full metric set, LS			0.208		0.166	
Full metric set, LWS		0.181	0.352	0.181		
Accel and jerk subset, LS					0.085	
Accel and jerk subset, LWS		0.122				

Table 9-20 – CVT Mondeo Auto-correlation coefficients of determination

Equation type	Coefficient of determination					
	smoothness	eng_delay	vehicle delay	init accel	accel prog	performance
Full metric set, LWS	0.398	0.334	0.342			

Table 9-21 – Omega Auto-correlation coefficients of determination

Equation type	Coefficient of determination					
	smoothness	eng_delay	vehicle delay	init accel	accel prog	performance
Full metric set, LS	0.315		0.123			0.164
Full metric set, LWS	0.272	0.111	0.300		0.195	0.173
Accel and jerk subset, LS	0.114					

Table 9-22 – Prius Auto-correlation coefficients of determination

Equation type	Coefficient of determination					
	smoothness	eng_delay	vehicle delay	init accel	accel prog	performance
Full metric set, LWS					0.323	0.331
Accel and jerk subset, LWS					0.323	0.331

It can be seen that there are a large number of datasets/equation type combinations for which no fit was possible. This indicates that these data sets contain a large amount of scatter when compared to the number of available data points. This also indicates that those equations that were fitted may not actually be representing real vehicle trends but rather are

fitted to the scatter in the data. Nevertheless, correlations were carried out using the functions for the different vehicles applied to subsets of their data. Full tables of these results can be found in Appendix X.

9.2.1 Summary

It can be seen that the generation of any useful correlation equations is difficult for the individual vehicle data sets. There is both a large variation in which subjective metrics produce correlations, as well as the strength of these correlations. Although this might be presumed to illustrate a lack of any firm trends in the data for the vehicles, it is more likely that this is the result of a large amount of scatter present in the data combined with the relatively small number of data points for each vehicle; this means that the correlation generation process is either unable to find a statistically significant solution, or the correlation is not particularly strong.

The results range from around 0.08 to 0.40, with the majority falling in the 0.16-0.40 band: These results show a small to medium correlation (see section 6.6.3) and although no conclusions can be drawn from such varied results, it can be seen that the LWS correlation equations were more likely to result in fits. This is expected as the LWS method is designed to be more robust to outliers than normal LS and therefore to be more able to produce results from noisy data.

9.2.2 Comparison of different vehicles' correlations

It was hoped that to compare the different vehicles' driveability characteristics it would be possible to create correlation equations from each vehicle's data and then apply these correlation equations to each of the other vehicles' data. The data and correlation functions from vehicles that possess similar driveability characteristics should show strong correlations with one another.

Unfortunately the small number of correlation equations which could be produced from the individual vehicles' data as well as the low correlations obtained from those correlation equations which were produced make this a pointless exercise. It is still thought that if more data were available, this technique would provide a useful way of comparing the vehicle behaviours with one another.

9.3 *Gear shift analysis*

It was decided that due to the non-ideal behaviour of the AT Mondeo test vehicle's gearbox, it would be interesting to investigate gearshift rating as an addition to the standard driveability ratings. Küçükay (1995) evaluated the various factors that affect the subjective impression of an AT gearshift. He highlighted a number of metrics as being important:

- Magnitude of vehicle acceleration
- Noise inside the vehicle
- Vehicle responsiveness (in terms of both delay time and acceleration)
- Frequency of gear changes

He highlighted the vehicle acceleration during the shift as being the most important of these. Therefore, it was decided to collect subjective gearshift rating data for the AT Mondeo vehicle (economy and sports mode), which would be correlated with the existing acceleration, jerk and delay-time metrics amongst others.

9.3.1 Ratings and metrics

Descriptions of the subjective and objective metrics used in this process can be found in Chapters 4.2.1 and 5.4 respectively: The subjective metrics were different for gear up-shift and down-shift events, although other than the addition of the *upshift_timing* metric to the up-shift events, the two sets of metrics were identical, just rating the same event occurring in different directions.

For gear downshift events the following ratings were collected:

- *kickdown_smooth*
- *gearbox_response*

For gear up-shift events the following ratings were evaluated:

- *upshift_smooth*
- *upshift_timing*
- *gearbox_response*

9.3.2 Down-shift events

Table 9-23 – Least squares fits

Metric name	Equation	Coefficient of determination
gearbox_response	600.457053 +0.568106* aMaxSpeed^(1/-3) +0.361651* aInitialPedalPosn^3 -0.009632* aInitialPedalPosn^-3 -0.263681* LN(aAccelGradient^-3) +0.741863* DownshiftAccelDiff1^3 -0.605725* DownshiftAccelDiff2^3	*0.634*
kickdown_smooth	*No equation*	*0*

Table 9-24 – LWS fits

Metric name	Equation	Coefficient of determination
gearbox_response	*No equation*	*0*
kickdown_smooth	8.529597 -0.617855* aInitialQuirk^-3	*0.170*

No correlation is produced for the *kickdown_smoothness* rating using the least squares fitting process although the LWS fit did produce a relatively poor correlation, this indicates that the data are noisy and relatively un-correlated as indicated by the coefficient of determination value of 0.17. Although the correlation is not very strong, it should perhaps be noted that the objective metric with which *kickdown_smoothness* is correlated is again an acceleration related metric, in this case the second differential of acceleration.

The *gearbox_response* metric, conversely, has produced a correlation using least squares fitting, but not with LWS fitting. This difference is caused by the different fitting methods producing different coefficients of determination during the fitting process; in this case the initial variable to enter the LWS equation failed the significance test (see Section 6.4.2.2.4 for an explanation of the correlation equation generation method) while a different variable with a higher correlation was first to enter the least-squares equation.

Figure 9-21, below, shows the partial correlation coefficients for the terms in the least-squares *gearbox_response* equation.

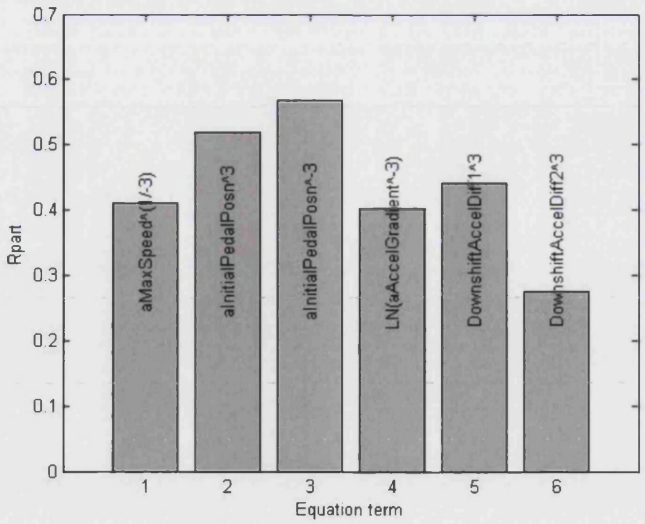

Figure 9-21 – Partial correlation coefficients for *gearbox_response* metric (least squares fit)

It can be seen that the *aInitialPedalPosn* metric is the most highly correlated of the metrics. Figure 9-22 shows that the *aInitialPedalPosn* data are all quite low – it is assumed that this occurs as the transmission only 'kicks down', selecting a lower gear, for large changes in the pedal position.

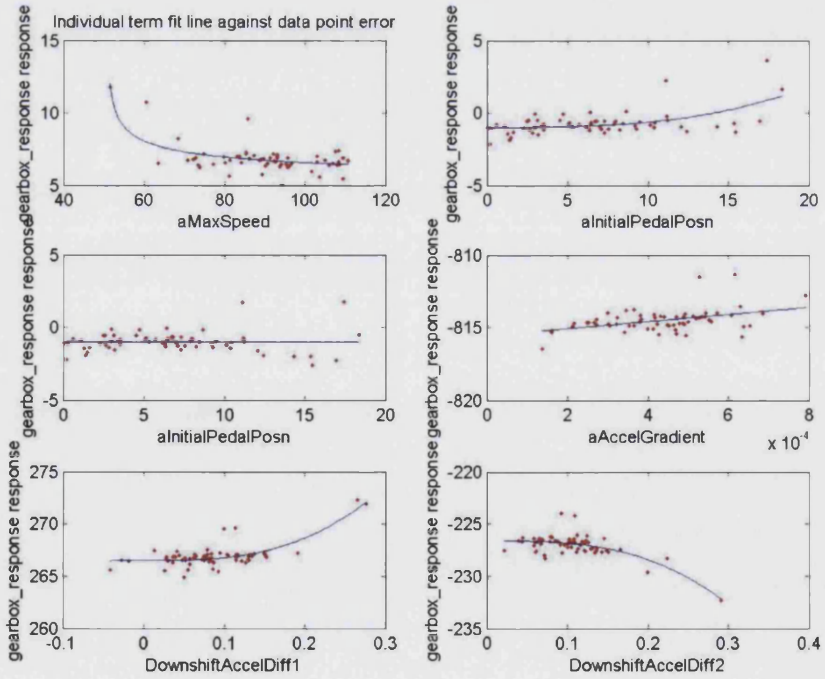

Figure 9-22 – Individual term fits for *gearbox_response* metric (least squares fit)

This positive correlation between the *gearbox_response* rating and the *aInitialPedalPosn* metric may be caused by the fact that the initial pedal position is higher for faster initial vehicle speeds, this in turn means that the vehicle will most likely have selected a higher gear before the 'kick down', during the steady-state period. This means that the gear change may well produce a more significant acceleration difference by moving more gears (e.g. moving from 4th to 2nd gear rather than from 2nd to 1st gear).

The trends shown by the *DownshiftAccelDiff1* and *DownshiftAccelDiff2* metrics are interesting in that they show opposite trends even though they both measure almost the same aspect of the gearshift. *DownshiftAccelDiff1* is the acceleration difference across the gearshift (acceleration measured at the exact start and end points of the gearshift) while *DownshiftAccelDiff2* is again the acceleration difference across the gearshift but with the acceleration averaged for 1/20th of a second at the beginning and the end of the gearshift. It is possible that these metrics should not show different trends. It can be seen that the majority of the data follow similar flat trends with only the last points producing the upward and downward trends. It is therefore possible that these points are outliers. It is also possible that the averaging that takes place in the calculation of the *DownshiftAccelDiff2* metric means that it captures a different aspect of the gearshift (it may be that the *DownshiftAccelDiff1* metric is capturing the acceleration difference while the gearshift manoeuvre is taking place). With the small sample size it is difficult to draw any conclusions.

9.3.3 Up-shift events

Table 9-25 – Least squares fits

Metric name	Equation	Coefficient of determination
gearbox_response	0.456590 +0.373233* aInitialPedalPosn^-3 +0.614695* aMaximumQuirk^-3	*0.464*
upshift_smooth	*No equation*	*0*
upshift_timing	*No equation*	*0*

Table 9-26 – LWS fits

Metric name	Equation	Coefficient of determination
gearbox_response	0.638574 + 0.122305* LN(aDesiredPedalPosition^2) + 0.229843* AccelDelayTime^-3	*0.044*
upshift_smooth	*No equation*	*0*
upshift_timing	2.211293 +0.663239* UpshiftPostAccelAvg^-1	*0.098*

Figure 9-23, below, shows the partial correlation coefficients of the least squares fit equation for *gearbox_response*. It can be seen that both variables are very similar in value (and therefore importance to the equation).

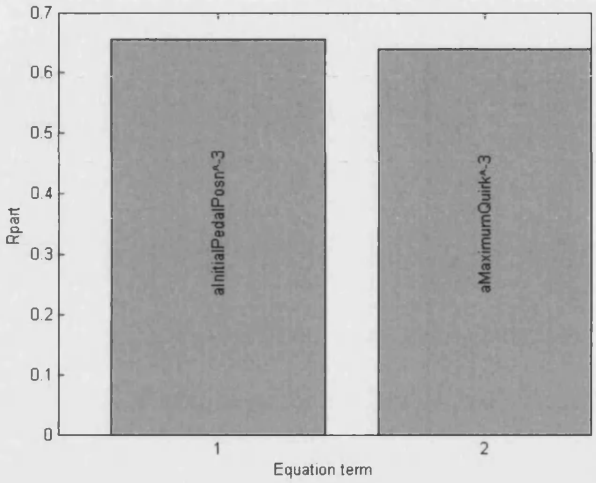

Figure 9-23 – Partial correlation coefficients for *gearbox_response* metric (least squares fit)

The coefficients of determination of the equation with and without each term are shown in Table 9-27, below (note that for the excluded terms, the coefficients of the correlation equation were re-calculated to obtain the best fit). It can be seen that the removal of a single term makes a significant difference to the overall correlation.

Table 9-27 - gearbox_response rating equation term significance (least squares fit)

Term	R^2 value with term included	R^2 value with term excluded
aInitialPedalPosn^-3	*0.464*	*0.085*
aMaximumQuirk^-3	*0.464*	*0.241*

It should also be noted that although the coefficient of determination of the LWS fit equation for *gearbox_response* is not very good, it does still contain similar acceleration and pedal position metrics.

9.3.4 Summary

It can be seen that despite the significant amount of scatter, which has been seen throughout this project, and the small number of observations, it is predominantly

acceleration base metrics that appear in the correlation equations. Of particular interest are the *DownshiftAccelDiff1, DownshiftAccelDiff2* and *UpshiftPostAccelAvg* metrics as these are all specifically related to the gearshift acceleration highlighted by Küçükay (1995).

It would be interesting to focus specifically on gearshift events and develop metrics to describe gearshift spontaneity and frequency, which were other metrics identified by Küçükay.

10 Discussion

This section presents a reflective commentary on aspects of the research in order to assist any researcher attempting to implement the results or continue with this avenue of development.

10.1 Experimental driveability investigations

The experimental driveability investigations of this thesis can be divided into two stages.

Stage 1 started with analysis of driveability data inherited from a previous research project by Wicke (2001). Though four different vehicles were tested during this project, it was found that the data collected from one of these vehicles was too incomplete to be used. While this data analysis was underway, and only two months after the start of this research, an opportunity arose to perform driveability testing of a Toyota Prius vehicle. The methods and equipment used for the testing of this vehicle were the same as had been used by Wicke due to the timing of this testing.

In Stage 2, the combined driveability data collected from the Prius testing and that performed by Wicke were analysed and metric and correlation methods were developed. Using the experienced gained in Stage 1, a new data acquisition system was developed to overcome the shortcomings of the original and the testing methodology was altered to incorporate new subjective ratings and a new rating method that is easier to understand for test drivers who are not highly trained. At the same time, single variable correlation methods and then multivariate methods were used to analyse the existing data. Driveability testing was then performed using the new equipment and methodology on an AT Mondeo vehicle and the data from this testing was added to that already used.

10.2 Testing methodology

The adoption of a symmetrical 'adequacy' rating scale for the testing of the AT Mondeo made the process of formulating ratings easier for the test drivers. The extreme lower range of the rating scale was not generally used by the test drivers, however the extreme upper range was. This may reflect the fact that the majority of the vehicles being tested were production standard and all of similar performance, which was deemed more that adequate by the test drivers. This tends to cluster the ratings for the vehicles and this reduced range for the driveability variables means that natural driver variation had a relatively larger effect.

There was in fact a moderate to large degree of scatter in the data for the fitted equations, which is indicated by the values of the coefficients of determination. It is probable that the scatter in the subjective data was caused by a combination of real driver variation and random driver inaccuracy caused by a lack of testing experience/aptitude, which results in the inability of drivers to rate accurately and consistently. Despite the drivers all being male and engineering staff and students, their driving experience and requirements differed considerably, which will have added to the amount of scatter in the ratings.

The testing carried out in this project and in Wicke's used an absolute rating of a vehicle's driveability. This absolute approach is problematic for drivers with different levels of experience as they will naturally be performing the 'absolute' rating within the scale of their own experiences. This approach is in fact preferable in some testing scenarios, for example when rating customer satisfaction with a vehicle, as the only important factor is customer satisfaction, which is naturally based on each drivers' experience. However, it should be noted that such testing would most likely be carried out on a demographic to whom a given vehicle would appeal and these drivers would tend to have similar driving expectations. For driveability testing a more uniform set of test drivers (in terms of driving experience) would be expected to produce less scatter in the rating data and this is therefore preferable. The use of a number of groups of test-drivers, each with different levels of experience, is beneficial to determine customer demands and how closely a given vehicle meets these demands. However, each group would need to be relatively uniform (or there would need to be a large number of drivers so that each driving style has sufficient representation) to reduce the degree of scatter.

The use of a comparison test vehicle (or calibration in the case of vehicles or test-rigs with variable calibration) and a comparative/relative testing scheme would remove much of the effect of driver experience from the scatter that has been seen in the data collected and used during this project. This is, however, a more time consuming process and expensive process due to the requirement for the two vehicles. An alternative is to give all of the test drivers a similar range of experience of different vehicles. This approach is valid for facilities or groups who perform testing regularly (e.g. driveability calibration engineers and test-drivers), but is too expensive and time consuming in the context of a PhD project. One method that may be applicable in the low budget context of a PhD project is to test a range of vehicles that have more extreme driveability traits (i.e. there are some vehicles with very good driveability traits and others with very poor). This would effectively serve to broaden the test-drivers' experience of a range of vehicles without requiring extensive pre-test training. Another option to reduce the degree of scatter is to reduce the number of drivers,

have each driver perform more tests; the use of a combination of small numbers of highly trained test drivers is the approach taken when OEMs carry out commercial driveability calibration testing. If this concept of uniformity is taken to the extreme, only one expert test driver would be used. In this case, the correlations developed would capture the preferences of the expert and could be used as a tool to assess further vehicles against a common standard without requiring the expert to be present. Such an approach could be used to reinforce brand identity by ensuring that all new calibrations conformed to a common driveability specification.

When using non-expert drivers, the amount of time allowed for the drivers to familiarise themselves with a test vehicle is problematic, too little time may result in unfamiliarity and consequently poor vehicle speed and pedal position control, whereas too much time in the vehicle may cloud the drivers' opinions as they become used to the vehicle and any possible shortcomings. How generic this trend is, and how people's perception levels vary are unknown and therefore further research is needed to establish the optimum level of vehicle exposure for non-trained test drivers.

During the current research some test drivers commented that they had difficulty concentrating on all of the driveability aspects that occur over the course of an average 12 second test. This generally occurred as the drivers were focusing on some particular aspects to the detriment of the others. It may therefore be advisable to provide drivers with more testing experience (preferably in a vehicle that is not to be tested, so that they do not become too familiar nor pre-judge the test vehicle(s)) to help them become familiar with the testing process, and the difficulties of judging the various driveability aspects accurately. This training would fall into two categories – training the drivers on what particular aspects of driveability they are looking for, perhaps by allowing them to drive vehicles with very good and very poor driveability characteristics, and also training them to concentrate on all of the aspects of driveability rather than becoming too focused on any one and therefore ignoring or forgetting the others.

It can be seen from the correlations between the subjective ratings and the occurrence of similar metrics in the subjective-objective correlation equations that these subjective metrics are all closely linked. This may indicate a real link between the underlying driveability aspects or it may indicate that the drivers were subjectively swayed and chose an overall score depending on how they rated the overall driveability before then making small adjustments for any significant characteristics affecting specific aspects of the subjective driveability. The degree to which the second conclusion is correct could be tested using a

vehicle or test-rig with variable-calibration by adjusting single driveability aspects (such as delay times or degree of jerk) to see how much a good overall driveability feel can overcome individual shortcomings in the vehicle and its calibration. It is also possible that the drivers were to some extent not able to detect the differences between different tests, this would tend to lead to the ratings for all of the questions being similar in value. Testing for the limits of human perception of driveability aspects such as accelerations, jerk and delay times would be beneficial when deciding what kinds of tests to perform and also when prioritising the optimisation of different aspects of a vehicle's driveability calibration.

One major factor that could not be accounted for in this project was that of non-longitudinal driveability differences between the vehicles. It is unknown how much of an effect such differences have in the drivers' possible pre-judgement of a vehicle. Such effects could be removed by performing testing using a single vehicle or rig that has adjustable powertrain calibration. Adjustable calibration could also allow more precise changes to be made between tests (e.g. allowing initial jerk to be increased without necessarily increasing later acceleration). These aspects would be even easier to implement on a sliding test-rig rather than a vehicle, which would require significant modelling work to predict the exact calibration changes required to enable a given objective driveability change, though the unfamiliar/unrealistic environment of such a test-rig may also have an effect on the drivers' ratings.

The occurrence of gearshift events during the testing is troublesome as these will affect the overall driveability rating. Gearshift calibration is in some ways a separate process and the occurrence of these events (and the subjective/objective differences between the gearshifts for the different vehicles) confuses the process of rating the longitudinal driveability aspects that are produced by the engine and drivetrain (including the gearbox itself, but not the gearshift events). It was seen from the testing that the modified AT Mondeo vehicle (in both sports and economy mode) scored lower driveability ratings than the other test vehicles. This may be related to its poor gearshift, resulting from a mismatch of components. In this project the ratings for gear-shifts and driveability were rated from the same test and the driveability rating was for the entire test, and included any gearshifts. The process of rating the gearshift and driveability aspects using a single test was carried out because of the limited time available for the testing and also because this was the approach taken by Wicke. It would be best to have the drivers rate solely the in-gear aspects and then the gearshift events in separate tests to ensure that they concentrate fully on each aspect.

It should be noted that the tip-in manoeuvres that were performed in this research do not provide a complete representation of a vehicle's driveability. There are a large number of other aspects of longitudinal driveability, including tip-outs, coast-downs, engine behaviour (e.g. flare) and a variety of tip-in and out speeds that could be used. The use and analysis of only a small part of the vehicles' driving ranges was necessitated by the available time and to allow compatibility with the data inherited from Wicke's project.

10.3 Implementation of new data acquisition system

The new data acquisition system that was developed as part of this research performs well, allowing a large number of data channels to be recorded and easily monitored. The ability to add extra acquisition and control cards will make this system very useful for future in-vehicle testing.

Converting the PC that is used to control the system to operate using 12V DC from the vehicle's power supply, rather than requiring an inverter, would make the system simpler, more portable and more robust. The availability of small and lightweight LCD screens and small keyboards with integrated trackballs also means that the laptop could be removed from the system and the PC used directly by way of monitor, keyboard and mouse extension cables. This would again reduce the bulk and complexity of the system.

10.4 Metric development

The metrics used in this research were developed from those described in the driveability and gear-shift testing literature. It was often found that the literature was not precise in its description of a metric (e.g. maximum acceleration – over what period?) and therefore a range of metric definitions were used to generate the majority of the acceleration and jerk based metrics.

The metric generation code required the development of automated methods for the analysis of the time-based test data. This included the detection of faulty data, the re-calibration of poorly calibrated data, the re-generation of missing data and the automatic detection of acceleration and pedal movement start positions from noisy time-based data.

The automation of the metric generation techniques has worked very well, allowing the entire process from raw data files to metrics and then to their evaluations, to be performed

without any operator input required. The system has also shown few errors considering the variety of the input data, both in terms of manoeuvres and any data corruption, which must be automatically detected and then corrected or rejected.

10.5 Correlation method development

The correlation generation code that was developed during this research has shown that it produces robust multivariate correlation equations. The metrics seen in the correlation equations agree with the findings seen in the driveability literature. For example, the negative correlation between maximum jerk and driveability rating is seen, as is the positive correlation between maximum acceleration and driveability rating. It has been shown that the use of a robust fitting method such as the LWS technique used in this project generally produces significantly better correlations when fitted to data sets. This is due to the degree of scatter in the project data and the LWS fitting method's robustness to outliers.

The production of some outlying predictions has resulted in certain terms being added to a correlation equation that are in fact not truly significant and this is caused by the definition used to calculate the regression coefficient. There are two possibilities to overcome this problem: One is to use an adjusted regression coefficient that trims some of the data points and should therefore remove the effect of single (or small numbers of) outliers; the other is to alter the measure used to rate the fit of the equation and the terms contained within it.

A relatively unsophisticated method of limiting the range of the equation outputs has been implemented to reduce the number of outlying predictions. It is possible to implement mathematical constraints to the overall predictions and this method may be preferable to that currently employed if for no other reason than to eliminate any possible discontinuities where the predictions exceed the 0 or 10 limits. It should be noted that none of the correlation equations generated in this project showed such discontinuities, which indicates that the limiting method is effective if not mathematically elegant.

10.6 Driveability analysis

A variety of datasets were used to generate correlation equations, and these correlation equations were then applied to subsets of the initial data and to excluded data. It was found that the correlation equations generated using only the data from the AT vehicles produced better correlations with its subsets than the equations generated using all of the vehicle data.

The correlation equations generated using the AT vehicle data were generally good, however it was found that tests with a 0 kph initial speed were excluded from the analysis by the inclusion in each of the correlation equations of a term representing the initial vehicle speed raised to a negative power. To overcome such problems, any data that can have a valid value of zero will need to be adjusted in the same way as term data are pre-processed if they contain a logarithmic or root operator.

The choice of the AT vehicle only dataset was indicated by the fact that when the correlation equations were fitted to the full dataset, the non-AT vehicles' subsets produced either no or very low correlations. This indicated that these vehicles' behaviour did not follow the trend of the overall dataset. Correlation equations were fitted to the data from the Prius and CVT Mondeo vehicles and the terms in the equations fitted using the acceleration and jerk metrics were found to have some similarities to those found in the equations fitted to the AT vehicle subset. It was found that, when the AT vehicle correlation equations were applied to the Prius and CVT Mondeo data, the Prius data produced some average correlations but that the CVT Mondeo produced none. It was seen that there was significant scatter in both the Prius and CVT Mondeo data, but that the degree of scatter in the CVT Mondeo data was so great as to make the correlations zero. The large scatter of the CVT Mondeo may be attributed to its developmental CVT transmission, which was less well developed, in a driveability sense, than the transmissions of the other test vehicles. Both the CVT Mondeo and Prius also had unusual (when compared to AT vehicles with which many drivers were familiar) driveability characteristics, the CVT Mondeo due to its CVT and the Prius due to the combination of its silent electric motor assist and CVT.

Correlation equations were also generated for the data from individual vehicles, though these correlations were found to be generally poor. The single vehicle datasets either produced an average correlation (c.50%) or no correlation. It was also found that there were no clear trends for the metrics that appeared in each vehicle's correlation equations. It can be seen from the correlations between the correlation equations that were produced from the AT vehicle data subset and the individual vehicle data subsets, that the trends for each vehicle are generally similar. Therefore the low correlations for the individual vehicle equations are attributed to the large degree of scatter in the data combined with the relatively small datasets.

The AT vehicle correlation equations were then analysed. It was seen in the correlation equations for all of the subjective rating equations that there was a negative correlation between the subjective metric and maximum jerk. This is the same trend that other authors

have found. Although Wicke found a positive correlation with jerk, his measurement of jerk was different from that which appears in the correlation equations generated during this project. Wicke's jerk metric was the mean rate of change of acceleration over the initial stages of the test (judged to be approximately the first 4 seconds or so) and is therefore more closely related to the absolute magnitude of the acceleration. Though an equivalent metric to that used by Wicke was included in this research, it did not appear in any of the correlation equations. It was found that this equivalent measure of jerk is closely correlated with the maximum acceleration metric, which this research found to have a consistent positive correlation with all of the subjective driveability ratings. This trend for maximum acceleration also corresponds with the findings reported in the literature.

The *AccelDelayTime* metric, which measures the delay time between the start of accelerator pedal movement and the start of vehicle acceleration, has not shown the expected correlation with driveability as is shown in the literature. This may indicate a number of causes. The first is that there may be a lower threshold for the acceptability or human perception of delay time and that the majority of the tests that were performed fall within this threshold and are therefore either acceptable or imperceptible to the test-drivers. Alternatively this may indicate a problem with the calculation of the *AccelDelayTime* metric. This problem may either be that the metric is too sensitive and that when a human determines the delay time, they allow the acceleration to rise to a certain level before recording the delay time. Lastly, it may indicate that exact pedal position and acceleration start positions have not been measured correctly due to the noise in the data from both of these channels. Testing has shown that the calculation of the pedal and acceleration start positions appears to be correct, therefore there may be a lower threshold for the perception of delay time and/or acceleration. This would mean that the acceleration delay time metric would need to be calculated differently taking into account the minimum levels of delay time and acceleration that drivers are able to detect (e.g. Kingma, 2005; Berglund, 1991).

10.7 Further research

This research has covered a large range of areas and shown that completely automated metric generation and driveability correlation is possible, however it has also shown where some improvements or extensions could be made to the techniques that were used. This section discusses possibilities for the application of automated driveability prediction techniques.

10.7.1 Additional metrics

Although this research developed and tested a range of objective metrics, there are always additional metrics that might be tested. This is especially true when looking at particular areas of driveability such as specific engine or gearbox driveability aspects.

The literature shows acceleration overshoot and oscillations as being important metrics in the evaluation of certain aspects of driveability, however these metrics were not included in the current research due to the difficulty of automating their generation. It was found that the overshoot and oscillations were often not visible when the data were viewed – this may be caused by the testing process because the acceleration overshoot and oscillations will be very difficult to detect with the changing acceleration that might be produced by the test-drivers' inability to keep a steady pedal position. The addition of such metrics may be useful, but may require that the testing scheme be changed to allow their addition.

10.7.2 Real-time calibration alteration

The use of a vehicle (or test-rig) with adjustable powertrain calibration (or longitudinal behaviour) would make it easier to study the effects of individual objective criteria and to establish their effects on driveability one at a time. This would eliminate any other factors that might influence drivers (such as marque, comfort, suspension, expectations, noise, etc.) as well as enabling the removal of typical interaction effects (such as higher maximum engine speed with a larger throttle input).

10.7.3 Linking vehicle and engine test data

Testing a vehicle with a fully instrumented engine would enable direct comparison of driveability data with that collected from a powertrain test-rig. This would allow two possibilities:

- Driveability testing to be carried out in the vehicle, then the results of this testing used in the test-cell powertrain calibration, then applied to the vehicle to see what effect it has.
- Driveability testing carried out on a number of vehicles; then this data used for test cell powertrain calibration which is subsequently applied to the actual powertrain and evaluated for its effect on vehicle driveability.

10.7.4 Determining the importance of different driveability aspects

Driveability can be broken down into different aspects, and each should be considered separately (for example engine idling, engine start-up overshoot, engine speed decay rate, tip-in/out performance, etc.) and this will be facilitated using an automated system, which can predict ratings for each of these aspects. The recombination of the different driveability aspects into an overall driveability rating for a vehicle will require each aspect to be weighted. Such weightings are not often mentioned in the literature on driveability testing, but they are a necessary part of the goal of optimising driveability on a test-rig. Determining these weightings will allow the vehicle calibration (and research) to be focused on those factors that are deemed important by the drivers (through their weightings) for whom a given vehicle is being designed.

10.7.5 Instrumentation improvements

One of the major issues that was encountered in both this project and Wicke's was the ability to instrument a vehicle quickly and without causing damage; this is particularly true for engine speed measurement, which is often difficult to setup (see Section 3.2.3). A possibility to overcome the majority of these problems is to acquire vehicle data by interfacing with the vehicle's data and/or engine buses. Although vehicles have previously used data buses, they have generally used proprietary protocols and connections, however with the wide-spread adoption of the OBD port, this should provide a quick and easy way to perform testing without needing to fit a vehicle with many intrusive and time consuming instrumentation devices.

11 Conclusions

This thesis presents research investigating the application of multivariate correlation techniques to vehicle driveability. The aims were to develop a method of analysing objective time-based data and subjective ratings that were recorded during transient tests on a number of vehicles, with the goal of being able to use the objective data to predict the subjective ratings that a driver would give any of the manoeuvres performed during these tests. Such a capability has many uses in addition to the primary application of in-vehicle engine and powertrain calibration, such as competitor benchmarking and rig-based transient calibration.

The research involved the development of an experimental methodology for vehicle testing, the development of an in-vehicle data acquisition system, the development of a data pre-processing and metric generation system and the development of a correlation code to determine the links between the subjective and objective metrics.

The experimental methodology was developed from that established in previous research carried out at the University. Data were collected using the new methodology and data acquisition system and were combined with data collected in the previous research. These data were then used in the development of metrics and the development of a multivariate analysis technique.

Development of data acquisition system

The new data acquisition system that was developed as part of this research allows a large number of data channels (up to 256) to be recorded and easily monitored. The ability to add extra acquisition and control cards with little or no setup time makes this system very flexible which should be useful for future driveability testing. The main advantages of this system are that there are a large variety of data acquisition cards available and that the system is able to handle large numbers of channels at high frequencies. In addition, the system is not significantly more expensive than other comparable offerings, with an approximate cost of £6,000.

Testing methodology

The procedure developed for driveability testing began with a period of familiarisation in which the driver was able to drive the vehicle and obtain feedback on their pedal position accuracy and speed control. Following this, a set of 16 tip-in tests were performed, which were combinations of five steady-state initial vehicle speeds: (0, 2, 12, 40 and 60 kph) and

four final pedal position demands: (25, 50, 75 and 100%), which were applied after the steady state initial vehicle speed had been attained. Data were recorded for approximately 12 seconds over the duration of the test, starting just before the pedal input. This enabled both steady state and transient data to be recorded to ensure that the starts of the transient events were detected successfully resulting in approximately 48Kb of data per second during the testing. Although storing this amount of data was not a problem, its analysis was made easier by producing metrics, which condense the essential characteristics of the time-series data making their later analysis easier and faster.

Principal metrics

It can be seen from both the correlations between the subjective ratings and the occurrence of similar metrics in the subjective-objective correlation equations that the subjective metrics used in this research are closely linked. In particular the subjective *engine delay* and *vehicle delay* metrics, which were originally recorded for use with CVT vehicles, show little or no difference for AT equipped vehicles.

It should also be noted that the subjective *performance* (overall driveability), *init_accel* (jerk) and *accel_prog* (acceleration progression) subjective metrics were highly correlated with one another. This indicates a link between the underlying driveability aspects that are used to rate these metrics and shows that the *performance* (driveability) subjective metric is more highly dependent on the subjective *init_accel* (jerk) and *accel_prog* (acceleration progression) ratings than on the either of the delay ratings (engine and vehicle delays) that were also recorded.

The correlation equations produced using the AT vehicle data were analysed and it was seen that for each subjective metric there was a negative correlation with the objective maximum jerk metric. This is the same trend as a number of other authors have found and shows that jerk is an undesirable driveability trait. Wicke, in his work, found a positive correlation with jerk, though his method of measuring jerk was different from that used during this project. Wicke's jerk metric was the mean rate of change of acceleration over the initial stages of the test (judged to be approximately the first 4 seconds or so) and is therefore more closely related to the absolute magnitude of the acceleration as measured in this research. Although an equivalent metric to that used by Wicke was included in this research, it was not found to be present in any of the correlation equations. It was found that this equivalent of Wicke's measure of jerk was closely correlated with the maximum acceleration metric, which this research found to have a consistent positive correlation with all of the subjective driveability ratings. As the objective maximum acceleration metric was

present in the correlation equations, the jerk related metric was no longer producing a significant effect due to its correlation with the maximum acceleration metric and was therefore not included itself. This trend for maximum acceleration also corresponds with the findings reported in the literature.

The *AccelDelayTime* metric, which measures the delay time between the start of accelerator pedal movement and the start of vehicle acceleration, has not shown the expected correlation with driveability as is shown in the literature. This may indicate a number of things. The first is that there may be a lower threshold for the acceptability or human perception of delay time and that the majority of the tests that were performed fall within this threshold and are therefore either acceptable or imperceptible to the test-drivers. Alternatively this may indicate a problem with the calculation of the *AccelDelayTime* metric – this problem may either be that the metric is too sensitive and that when a human determines the delay time, they allow the acceleration to rise to a higher level before recording the delay time, or lastly it may indicate that exact pedal position and acceleration start positions have not been measured correctly due to the noise in the data from both of these channels. Testing has shown that the calculation of the pedal and acceleration start positions appears to be correct, therefore further work should be carried out to investigate drivers' detection thresholds for delay time and longitudinal acceleration (Kingma, 2005; Berglund, 1991) and the calculation of the acceleration delay time metric altered accordingly.

Predictive Ability of the Correlations

The correlation code developed during this work has shown good (R^2>0.50) predictive abilities and is able to accurately reproduce the mean and standard deviation for sets of test data recorded from test drivers over a range of tests. It is therefore concluded that the objective metrics presented and the correlations found between them and subjective metrics elicited from test drivers form the basis of a suitable tool for the prediction of aspects of subjective vehicle driveability.

A variety of datasets were used to generate correlation equations, and these correlation equations were then applied to subsets of the initial data and to excluded data. It was found that the correlation equations generated using only the data from the AT vehicles produced better correlations with its subsets than the equations generated using all of the vehicle data. This is as expected due to the closer similarity between the behaviour of the AT vehicles when compared with the other vehicles in the dataset which were equipped with CVTs.

It has been shown that the use of a robust fitting method such as the LWS technique used in this project generally produces significantly better correlations than a non-robust technique such as simple least squares when used to produce correlations between subjective and objective driveability data.

Achievements

The tools developed to process the data as part of an automated, robust process are both novel and reusable. The metric generation code developed as part of this research required the development of automated methods for the analysis of the time-based test data. This included the detection of faulty data, the re-calibration of poorly calibrated data, the re-generation of missing data and the automatic detection of acceleration and pedal movement start positions from noisy time-based data.

The automation of these methods has worked successfully with 89% of tests needing no manual attention following the automated processing. Of the 11% of tests requiring manual intervention, 64% proved irrecoverable due to problems with the data and were rejected. The automation of the metric generation techniques has also worked well, allowing the entire process from raw data files to metrics and then to their evaluations, to be performed without any operator input being required.

12 References

Ahlberg, J., Nilson, E., Walsh, J. (1967). *The Theory of Splines and Their Applications.* New York. Academic Press Inc.

Ajovalasit, M. and Giacomin, J. (2005). Human subjective response to steering wheel vibration caused by diesel engine idle, Proceedings of the IMechE, Part D - Journal of Automobile Engineering, Vol 219, No. 4, pp. 499-510.

Akehurst, S. (2001). *An investigation into the loss mechanisms associated with a pushing metal V-belt Continuously Variable Transmission.* PhD Thesis, University of Bath.

Akehurst, S., Brace, C.J., Vaughan, N.D., Milner, P., Hosoi, Y. (2001). *Performance Investigations of a Novel Rolling Traction CVT.* SAE paper no. 2001-01-0874.

Aleksander, I., Morton, H. (1995). *An introduction to neural computing.* 2nd ed. International Thompson Computer Press. London.

Alhoniemi, E., Himberg, J., Parviainen, J., Vesanto, J. (1999). *SOM Toolbox 2.0 [online].* 1999

Anscombe, F. J. (1960). *Rejection of Outliers.* Technometrics Vol. 2, No. 2. 1960. pp. 123-147.

Arfken, G., Weber, H. (2001). The Method of Steepest Descents. In: *Mathematical methods for physicists.* 5th ed. Harcourt Academic Press. San Diego.

Atkinson, A. C. (1969). *Constrained Maximisation and the Design of Experiments..* Technometrics Vol. 11, No. 3. 1969. pp. 616-618.

Autocar, (2002). News: Porsche 911 Facelift. *Autocar.* pp. 18-19. 6th November 2002.

Baker, D., Girling, T., Kennedy, G, Pates, D, Porter, B. (2006). *Driveability Validation using MAHLE Powertrain's IDAA Toolset.* Accepted for publication, IMechE conference Integrated Powertrain and Driveline Systems (IPDS) 2006, London, October 2006.

Balfour, G., Dupraz, P., Ramsbottom, M., Scotson, P. (2000). *Diesel Fuel Injection Control for Optimum Driveability.* SAE paper no. 2000-01-0265.

Balich, G.W., Aschenbach, C.R. (2004). *Study of the 4 Stroke Gasoline Internal Combustion Engine.* Department of Aerospace and Mechanical Engineering. University of Notre Dame. Notre Dame, IN, USA.

Berglund, L.G. (1991). *Societal and environmental aspects of tall buildings.* ASHRAE Transactions , pt 1, pp. 819-823. 1991.

Bergman, W. (1973). *Measurement and subjective evaluation of vehicle handling.* SAE paper no. 730492.

Box, G. E. P. and Cox, D. R. (1964), *An Analysis of Transformations*, Journal of the Royal Statistical Society, pp. 211-243, discussion pp. 244-252. 1964.

Brace, C.J., Deacon, M., Vaughan, N.D., Horrocks, R.W., Burrows, C.R. (1999). *An operating point optimizer for the design and calibration of an integrated diesel/continuously variable transmission powertrain.* Proc Instn Mech Engrs, Vol 213, Part D, pp.215-226.

Brace, C.J., Deacon, M., Vaughan, N.D., Horrocks, R.W., Burrows, C.R. (1999). *The Compromise in Reducing Exhaust Emissions and Fuel Consumption from a Diesel CVT Powertrain Over Typical Usage Cycles.* International Congress of Continuously Variable Transmissions (CVT'99), Eindhoven, The Netherlands, September 1999.

Brace, C.J., Deacon, M., Vaughan, N.D., Horrocks, R.W., Burrows C.R. (1999). *Impact of Alternative Controller Strategies on Exhaust Emissions from an Integrated Diesel/ CVT Powertrain*, Proceedings of The Institution of Mechanical Engineers Journal of Automobile Engineering (Part D) Vol 13, March 1999, pg 95-107, ISSN: 0954-4070, 1999.

Chakravarti, I. M., Laha, R. G., and Roy, J. (1967). *Handbook of Methods of Applied Statistics, Volume I.* John Wiley and Sons Inc., New York. pp. 392-394.

Chen, D.C., Whitehead, J.P., Crolla, D.A., Alstead, C.J. (1997). *Collecting subjective vehicle handling data.* MIRA. C524/103/97.

Cohen, J. (1988). *Statistical power analysis for the behavioral sciences* (2nd ed.) Hillsdale, NJ: Lawrence Erlbaum Associates.

CP Engineering. (2000). *CADET V12 Software.* CP Data Sheet, CP Engineering Systems Ltd.

CP Engineering. (2001). *CP128 Control and Monitoring I/O System.* CP Data Sheet, CP Engineering Systems Ltd.

Crolla, D.A., Chen, D.C., Whitehead, J.P., Alstead, C.J. (1998). *Vehicle Handling Assessment Using a Combined Subjective-Objective Approach.* SAE paper no. 980226.

Crolla, D.A., King, R.P., Ash, H.A.S. (2000). *Subjective and Objective Assessment Of Vehicle Handling Performance.* Seoul 2000 FISITA World Automotive Congress. F2000G346.

Deacon, M. (1996). *The Control of a Passenger Car Diesel Engine and CVT.* PhD Thesis, University of Bath.

Dolby, J.L. (1963). *A Quick Method for Choosing a Transformation.* Technometrics Vol. 5, No. 3. 1963. pp. 317-325.

Dorey, R.E., Holmes, C.B. (1999). *Vehicle Driveability – Its Characterisation and Measurement.* SAE paper no. 1999-01-0949.

Dorey, R.E., Martin, E.J. (2000). *Vehicle Driveability The Development of an Objective Methodology.* SAE paper no. 2000-01-1326.

Dorey, R.E., McLaggan, J.D., Harris J.M.S., Clarke D.P., Gondre B.A.C. (2001). *Transient Calibration on the Testbed for Emissions and Driveability.* SAE paper no. 2001-01-0215.

Draper, N. R., Smith, H. (1981). *Applied Regression Analysis.* 2nd Ed. John Wiley & Sons, Inc. New York.

DuMouchel, W., O'Brien, F. (1989). *Integrating a Robust Option into a Multiple Regression Computing Environment.* Computing Science and Statistics: Proceedings of the 21st Symposium on the Interface. American Statistical Association, Alexandria, VA, pp. 297-301, 1989.

Dunne, W.J. (2005). *Transient Calibration of Passenger Car Engines.* MPhil/ PhD Transfer Report, University of Bath, 2005.

Eriksson, L., Johansson, E., Kettaneh-Wold, N., Wikström, C., Wold, S. (2000). *Design of Experiments – Principles and Applications.* Umetrics AB, Umeå, Sweden.

Ezekiel, M., Fox, K.A. (1959). *Methods of Correlation and Regression Analysis – Linear and curvilinear,* 3rd Ed., John Wiley & Sons, Inc. New York.

Farrer, D.G. (1993). *An Objective Measurement Technique for the Quantification of On-Centre Handling Quality.* SAE paper, 930827, 1993.

Field, M., Burke, M. (2005). *Powertrain Control of the Torotrak Infinitely Variable Transmission.* SAE paper no. 2005-01-1461.

Fisher, R.A. (1963). *Statistical Methods for Research Workers.* 13th Ed., Oliver and Boyd, Edinburgh.

Friedenberg, L. (1995). *Psychological Testing: Design, Analysis and Use.* Allyn and Bacon, Boston.

Furnival, G.M., Wilson Jr., R.W. (1974). *Regression by Leaps and Bounds.* Technometrics Vol. 16, No. 4. 1974. pp. 499-511.

Giacomin, J., Bretin, S. (1997), *Measurement of the comfort of automobile clutch pedal actuation*, ATA 4th International Conference on Comfort in the Automobile Industry, Bologna, Italy, October 2-3

Giacomin, J., Mackenzie, T.J.P. (2001), *Human sensitivity to gearshift loads*, International Journal of Industrial Ergonomics, Vol. 27, pp. 187-195.

Giacomin, J. (2005), *Perception Enhancement for Steer-by-Wire Systems*, ATA Ingegneria dell'Autoveicolo, Vol. 58, No. 8/9, Sept./Oct.

Goldberg, D. (1989). *Genetic Algorithms in Search, Optimization and Machine Learning.* Addison-Wesley. Reading, Massachusetts.

Goppelt, G. (2000). *Stufenloses Automatikgetriebe Multitronic von Audi.* ATZ Automobiltechnische Zeitschrift 102 (2000) 2, pp. 110-111, (in German).

Gorman, J.W., Toman, R.J. (1966). *Selection of Variables for Fitting Equations to Data.* Technometrics Vol. 8, No. 1. 1966. pp. 27-51.

Grubbs, F.E. (1969). *Procedures for Detecting Outlying Observations in Samples.* (1969). Technometrics, Vol. 11, No. 1.

Hays, W.L. (1988). *Statistics.* 4th ed. Holt, Rinehart and Winston, New York.

Hellman, K.H., Peralta, M.R., Piotrowski, G.K. (1998). *Evaluation of a Toyota Prius Hybrid System (THS).* US Environmental Protection Agency, August 1998, EPA 420-R-98-006.

Hendriks, E. (1993). *Qualitative and Quantitative Influence of a Fully Electronically Controlled CVT on Fuel Economy and Vehicle Performance.* SAE paper no. 930668

Heywood, J. (1988). *Internal Combustion Engine Fundamentals.* New York. McGraw-Hill Book Company. pp. 184-186.

Hocking, R.R., Leslie, R.N. (1967). *Selection of the Best Subset in Regression Analysis.* Technometrics Vol. 9, No. 4. 1968. pp. 531-540.

Hoel, P.G. (1968). *On Testing for the Degree of a Polynomial.* Technometrics Vol. 10, No. 4. 1968. pp. 757-767.

Hockschwarzer, H., Kriegler, W., Schon, M. (1992). *Fully Automatic Determination and Optimization of Engine Control Characteristics.* SAE paper no. 920255.

Ingham, R. (2005). Photograph [online]. Available from: http://ukga.com/content/view.cfm?contentId=2176 [Accessed 1st August 2005]

Jansz, N.M., Delasalle, S.A., Jansz, M.A., Willey, J., Light, D.A. (1999). *Development of Driveability for the Ford Focus; A systems approach using CAE.* STA99c214, AEEC 99, 1999.

J.D. Power (2005). *J.D. Power and Associates 2005 Automotive Performance, Execution and Layout (APEAL) Study.* J.D. Power and Associates. Westlake Village, California.

Jolliffe, I. (1986). *Principal Component Analysis.* Springer-Verlag New York Inc. New York.

Karlsson, J., Jacobsson, B. (2000). *Optimal Control of an Automotive Powertrain System for Increased Driveability.* Proceedings of AVEC 2000.

Kämmer, A.,Liebl, J., Krug, C., Munk, F., Reuss, H.-C. (2003). *Real-Time Engine Models.* SAE paper no. 2003-01-1050.

Kendall, M.G. (1949). *The Advanced Theory of Statistics*, Vol I, 1949.

Kennard, R.W. (1971). *A note on C_p statistics*, Technometrics, 13, 1971, pp. 899-900

Kimberley, W. (1999). A multi-step forward. *Automotive Engineer.* November 1999.

Kingma, H. (2005). Thresholds for perception of direction of linear acceleration as a possible evaluation of the otolith function [online]. *BMC Ear, Nose and Throat Disorders* 2005. Available from: http://www.biomedcentral.com/1472-6815/5/5 [Accessed: August 2005]

Kirkpatrick, S., Gelatt, C., Vecchi, M. (1983). *Optimization by Simulated Annealing.* Science, Number 4598, 13th May 1983.

Kluger, M.A., Fussner, D.R. (1997). *An Overview of Current CVT Mechanisms, Forces and Efficiencies.* SAE paper no. 970688.

Kriegler, W. (1997). *IC Engines and CVT's in Passenger Cars: A System Integration Approach.* Advanced Vehicle Transmissions and Powertrain Management Conference, London, 1997.

Küçükay, F. (1995). *Electronic Control of Automatic Transmissions in BMW Cars.* Autotech 95, C498/30/205.

List H., Schoeggl P. (1998). *Objective Evaluation of Vehicle Driveability.* SAE paper no. 980204.

Lumsden, G., Browett, C., Taylor, J., Kennedy, G. (2004). *Mapping Complex Engines.* SAE paper no. 2004-01-0038.

Mantel, N. (1969). *Restricted Least Squares Regression and Convex Quadratic Programming.* Technometrics Vol. 11, No. 4. 1969. pp. 763-773.

Mathworks Inc., The (2002). *MATLAB (version 6.5).* Documentation [online] available from: http://www.mathworks.com/products/matlab/, [Accessed August 2005].

McNicol, A., Figueroa-Rosas, H., Brace, C.J., Ward, M.C., Watson, P., Ceen, R.V. (2004). *Cold Start Emissions Optimisation Using an Expert Knowledge Based Calibration Methodology.* SAE paper no. 2004-01-0139.

Mo, C.Y., Beaumount, A.J., Powell, N.N. (1996). *Active Control of Driveability.* SAE paper no. 960046

Morita, S. (1993). *Optimization Control for Combustion Parameters of Gasoline Engines using Neural Networks – In the Case of On-Line Control.* JSAE Review Vol. 14, No. 3, pp. 4-9. July 1993.

Multimap [online], (2005). Available from: http://multimap.com/map/photo.cgi?client=public&X=380500&Y=171000&gride=&gridn=&scale=10000&coordsys=gb&db=&lang=&mapsize=big [Accessed 1st August 2005]

Nash, J. (1979). *Compact numerical methods for computers : linear algebra and function minimisation*. Adam Hilger. Bristol.

Neter, J., Wasserman, W., & Kutner, M. H. (1985). *Applied linear statistical models: Regression, analysis of variance, and experimental designs.* Homewood, IL: Irwin.

NIST/SEMATECH e-Handbook of Statistical Methods [online]. Available from: http://www.itl.nist.gov/div898/handbook/eda/section3/eda35h.htm [Accessed 12st June 2005]

Ohashi, A., Sato, Y., Kajikawa, K., Sakuma, S., Urano, J., Yamaguchi, M., Shibahara, A. (2005). Development *of High-efficiency CVT for Luxury Compact Vehicle*. SAE paper no. 2005-01-1019.

Patel, D., Ely, J., Overson, M. (2005). *CVT Drive Research Study*. SAE paper no. 2005-01-1459.

Pfalzgraf, B., Fitzen, M., Siebler, J., Erdmann, H-D. (2001). *First ULEV Turbo Gasoline Engine – The Audi 1.8l 125 kW 5-Valve Turbo*. SAE Paper no. 2001-01-1350.

Pick, D., Wang, D-Y., Wang, D., Proctor, R., Patel, D. (2005). *Dead Pedal and the Perception of Performance of a Continuously Variable Transmission*. SAE paper no. 2005-01-1596.

Pickering, S.G., Brace, C.J., Vaughan, N.D. (2002). *The application of multivariate correlation techniques to driveability analysis*. IMechE Conference; Statistics and Analytical Methods in Automotive Engineering. C606/015/2002 pp. 135-148. SAE paper no. 2002-04-0085.

Quadrant Scientific (1989). *Cam Doctor software*. Louisville, CO, U.S.A.

Reid, L.D., Nahon, M. (1988). *Response of Airline Pilots to Variations in Flight Simulator Motion Algorithms*, AIAA Journal of Aircraft, Vol. 25, No.7, pp. 639-646, 1988.

Ricardo Consulting Engineers Ltd. (1995). *Ricardo Engine Management Prototyping System Version 4.0 User's Guide*. Report DP 95/1933.

Ross-Martin, T.J., Pendlebury, K.J. (1997). *Experience in the rapid prototyping of new control systems*. SAE paper no. 8-50-5-289.

Rousseeuw, P. J., Leroy A.M. (1987). *Robust Regression and Outlier Detection*. New York: John Wiley and Sons, Inc.

Sammon, J.W. (1969). *A nonlinear Mapping for Data Structure Analysis*. IEEE trans. On Computers, Vol. C-18, No. 5, pp. 401-409. May 1969.

Sasaki, S. (1998). *Toyota's Newly Developed Hybrid Powertrain*. Proceedings of 1998 International Symposium on Power Semiconductor Devices & ICs. Kyoto, Japan.

Sawamura, K., Saito, Y., Kuroda, S., Katoh, A. (1998). *Development of an integrated powertrain control system with an electronically controlled throttle*. JSAE Review 19 (1998), pp. 39-48.

Schatzoff, M., Tsao, R., Fienberg, S. (1968). *Efficient Calculation of All Possible regressions*. Technometrics Vol. 10, No. 4. 1968. pp. 769-779.

Schöggl, P., Ramschak, E. (2000). 'Adaptive Driveability' – Improvement of driving pleasure and individualisation of platform vehicles. Motor und Umwelt 2000, 7-8th September 2000, Graz.

Schoeggl, P., Ramschak, E., Bogner, E. (2001). On-board Optimization of Driveability Character Depending on Driver Style by Using Closed Loop Approach. SAE paper no. 2001-01-0556.

Schwab, L.F. (1994). *Development of a Shift Quality Metric for an Automatic Transmission*, SAE paper no. 941009, 1994.

Shimizu, K., Waki, H., Saito, T., Sawayama, M., Nishiyama, H., Kuroda, S., Oohori, T. (2006). *Development of a New-Generation CVT with Medium Torque Capacity for Front-Drive Cars*. SAE paper no. 2006-01-1306.

StatSoft, Inc. (2006). *Electronic Statistics Textbook* [online]. Tulsa, OK: StatSoft. Available from: http://www.statsoft.com/textbook/stathome.html. [Accessed August 2005].

Steiner, G. (2005). *In-Vehicle Combustion Measurement for Emission, Performance and Driveability Improvement*. SAE paper no. 2005-01-1048.

Takada, Y., Morita S., Takiyama T. (1996). *Investigation of Accelerator Pedal Sensitivity by DBW.* Proc. of IASTED MSO'96, 1996.

Takiyama, T., Morita S. (1996). *Analysis of Improvement of Fuel Consumption by Engine-CVT Consolidated Control.* AVEC '96 International Symposium on Advanced Vehicle Control, pp.1159-1167.

Tatsuoka, M. (1971). *Multivariate Analysis: Techniques for Educational and Psychoiogical Research.* John Wiley & Sons, Inc. New York.

Thompson, A.C., Lipman J.M. (1992). *The Lotus CVT and Evolution of the Smart Transmission Concept.* SAE paper no. 922106.

Torgerson, W. (1958). *Theory and Methods of Scaling.* John Wiley and Sons, Inc. New York.

Trotter, H. F. (1959). *An Elementary Proof of the Central Limit Theorem.* Arch. Math. **10**, 226-234.

USAF School of Aerospace Medicine. *Flight Surgeon's Guide, Section 4, EFFECTS OF ACCELERATION [online],* Available from: http://www.brooks.af.mil/web/af/files/fsguide/html/00_index.html, [Accessed August 2005].

Weir, D.H., DiMarco, R.J. (1978). *Correlation and evaluation of driver/vehicle directional handling data.* SAE paper no. 780010.

Whitehead, J. P., Crolla, D. A. Chen, D. C., Alstead, C. J. (1998). *Vehicle handling assessment using a combined subjective-objective approach.* SAE International Congress and Exposition, Detroit, Michigan, USA, SAE Paper No. 980226, 1998.

Wicke, V., Brace, C.J., Deacon, M., Vaughan, N.D. (1999). *Preliminary Results from Driveability Investigations of Vehicles with Continuously Variable Transmissions.* CVT'99 - International Congress on Continuously Variable Power Transmission September 16-17, 1999, Eindhoven University of Technology.

Wicke, V., Brace, C.J., Vaughan, N.D. (2000). The Potential for Simulation of Driveability of CVT Vehicles. SAE paper no. 2000-01-0830.

Wicke, V. (2001). Integration and Control aspects of CVT vehicles. Ph.D. Thesis, University of Bath. 2001.

13 Bibliography

Agresti, A. (1984). *Analysis of Ordinal Categorical Data.* John Wiley & Sons, Inc. New York.

Aiken, L.R. (1979). *Psychological Testing and Assessment.* 3rd ed. Allyn and Bacon. Boston.

Anastasi, A. (1961). *Psychological Testing.* 2nd ed. The Macmillan Company. New York.

Cleveland, W.S. (1985). *Visualizing Data.* Hobart Press, Summit, New Jersey.

Cleveland, W.S. (1993). *The Elements of Graphing Data.* Wadswoth Advanced Books and Software, Monterey, California.

Draper, N. R., Smith, H. (1981). *Applied Regression Analysis.* 2nd Ed. John Wiley & Sons, Inc. New York.

Edwards, A.L. (1984). *An Introduction to Linear Regression and Correlation.* 2nd ed. New York: W.H.Freeman and Company.

Ezekiel, M., Fox, K.A. (1959). *Methods of Correlation and Regression Analysis – Linear and curvilinear,* 3rd Ed., John Wiley & Sons, Inc. New York.

Fisher, R.A. (1963). *Statistical Methods for Research Workers.* 13th ed., Oliver and Boyd, Edinburgh.

Friedenberg, L. (1995). *Psychological Testing: Design, Analysis and Use.* Allyn and Bacon, Boston.

Hays, W.L. (1988). *Statistics.* 4th ed. Holt, Rinehart and Winston, New York.

Heisler, H. (1995). Advanced Engine Technology. Arnold, London.

Heisler, H. (1999). Vehicle and Engine Technology. 2nd ed. Butterworth Heinemann, Oxford.

Heywood, J. (1988). *Internal Combustion Engine Fundamentals*. New York. McGraw-Hill Book Company.

Jolliffe, I.T. (1986). *Principal Component Analysis*. New York: Springer-Verlag.

Lange, H.F.H. (1967). *Correlation Techniques – Foundations and Applications of Correlation Analysis in Modern Communications, Measurement and Control*. London: Iliffe Books Ltd.

Loewenthal, K.M. (2001). *An introduction to psychological tests and scales*. 2nd ed. Psychology Press Ltd., Hove.

Marriott, F.H.C. (1974). *The Interpretation of Multiple Observations*. London: Academic Press.

Rousseeuw, P. J., Leroy A.M. (1987). *Robust Regression and Outlier Detection*. New York: John Wiley and Sons, Inc.

StatSoft, Inc. (2006). *Electronic Statistics Textbook* [online]. Tulsa, OK: StatSoft. Available from: http://www.statsoft.com/textbook/stathome.html. [Accessed August 2005].

Stone, R. (1999). *Introduction to Internal Combustion Engines*. 3rd ed. Macmillan Press.

Tacq, J. (1997) *Multivariate Analysis Techniques in Social Science Research*. Sage Publications, London.

Tatsuoka, M.M. (1971). *Multivariate Analysis: Techniques for Educational and Psychological Research*. John Wiley & Sons, Inc. New York.

Torgerson, W. (1958). *Theory and Methods of Scaling*. John Wiley and Soncs, Inc. New York.

Wiseman, S. (1966). *Statistical Guides in Educational Research No. 1: Correlation Methods*. Manchester: Manchester University Press.

Appendix I - Toyota Prius test data

Detailed Prius subjective results

Smoothness

Smoothness is fairly constant across all speeds and pedal positions. However the smoothness is slightly higher for 12 km/h and slightly lower for 60 km/h tests. 25% and 50% pedal positions tests were also smoother than those at 75% and 100%. This is typical behaviour for a city car, which has been optimised for low accelerations at low speeds.

Delay

The delay time at 12 km/h was rated as being good, while the delays at 40 and 60 km/h were rated as poor. 50% and 75% pedal position tests were also rated as being good, while 100% was rated as being poor. This behaviour is also to be expected from a city car which requires small to medium pedal movements and low to medium speeds.

Initial acceleration/jerk

Initial acceleration was best at 12 and 40 km/h, and was fairly constant for 50%, 75% and 100% pedal positions, although 50% and 75% were slightly better. 25% pedal position was rated as being worse than all of the others. This behaviour also reflects the Prius' status as a city car. The poor performance with 25% pedal position may be to reduce jerk whilst driving in traffic.

Progression of acceleration

40 km/h was better than average, while 0 and 60 km/h were below average. 75% pedal position tests were above average, while 25% tests were below average. Reasonable acceleration progression at the mid range speeds is good for a city car, while the poor 25% performance may again be to reduce jerkiness in traffic.

Driveability

The highest averages were for 12 and 40 km/h tests, and for tests with 50% and 75% pedal positions. As mentioned above, the best performance is tuned for the mid-range speeds, and mid-range pedal movements.

Drivers' comments

- Drivers commented on a noticeable delay when applying 100% throttle no matter what the initial speed. Almost all of the drivers preferred 75% throttle at all speeds for its subjectively superior acceleration and smaller delays.
- Tests performed at 40 km/h and 60 km/h received the best comments from the test drivers.
- All of the drivers noted the smooth acceleration and many commented that the Prius was pleasant to drive, but not very exciting.
- Some drivers also noted that the accelerator pedal felt soggy and unresponsive in the first half of its travel (e.g. during 25% -50% pedal position tests)
- Many drivers voiced a concern that the vehicle leaves you feeling that you do not know exactly what performance you will receive for a given pedal movement and vehicle speed.

Tables A1-1 and A1-2 show the top five rankings between individual subjective and objective variables for various groupings of tests. These rankings were performed using the initial correlation code, which is explained in Section 6.4.1:

Table A1-1 - Correlation results for all tests

Ranking	Subjective Parameter	Objective Parameter
1	Acceleration Progression	Initial Jerk
2	Driveability	Initial Pedal Position
3	Initial Acceleration	Desired Pedal Position
4	Initial Acceleration	Max Acceleration
5	Acceleration Progression	Acceleration Gradient

Table A1-2 - results for 0 km/h starting speed tests

Ranking	Subjective Parameter	Objective Parameter
1	Smoothness	Initial Jerk
2	Engine delay	Max Speed
3	Initial acceleration	Acceleration Gradient
4	Acceleration progression	Average Jerk
5	Smoothness	Max Engine Speed

Some of the results shown above are fairly self-explanatory, for example the fact that various subjective ratings of acceleration are related to objective measurements of acceleration or rate of change of acceleration. However, the fact that driveability is

correlated with initial pedal position is more difficult to understand. This particular example shows that the vehicle's driveability was rated quite consistently depending on the initial vehicle speed. The initial vehicle speed is most probably not the reason for this rating (unless looking at a speedometer or seeing the world go by can alter people's rating, which is a possibility); rather there is some type of correlation which is related to the speed which causes this effect. As no other single variable correlation is shown in the table above, it is most likely that there is some type of multivariate correlation which is dependent on the vehicle speed, producing the variation in driveability rating. The same is true for the correlation between desired pedal position (as specified by the test type) and the initial acceleration. The desired pedal position will to some extent reflect the actual pedal position during a test, which will then alter the engine behaviour and power delivery. This is another case in which looking at correlations between objective parameters would be beneficial, especially using multivariate techniques.

Author's comments

The difference in power between the electric motor and IC engine combination and the IC engine alone is marked and it should perhaps be signalled better when then battery charge level is becoming low. This problem was highlighted for the author as he overtook a slow moving vehicle after climbing a hill. The Prius had performed well, climbing the hill at 60mph, but this had drained the battery which the author did not notice. This caused the electric motor to cut out half way through the overtaking manoeuvre, drastically reducing power. Currently, the battery level warning is a small picture of a tortoise in the centre console next to the speedometer, however this symbol is small and can be missed quite easily. The option to use an audible warning or a far larger and more visible battery level indication would be a good idea, especially when the driver might be busy looking at the road rather than concentrating on looking at the centre console.

Not knowing exactly how much power will be available when the accelerator pedal is depressed means that the driver does not have as much confidence in the Prius as one might with other normally powered vehicles. Another unsettling effect of the hybrid system is that a driver might be waiting at a junction to pull out into traffic, but with no engine noise to indicate that the car is running, which adds to the doubts about whether the car will perform at all. However the Prius does provide a large amount of initial torque due to the electric motor.

The Toyota Prius was designed as a city car, especially the Japanese version which was tested in this thesis. Therefore the following points about driving out of town and at relatively high speeds may be slightly unfair to a car which was not designed for this purpose.

The Prius demonstrated a lack of steering feel, which can be attributed to its low rolling-resistance tires and very light steering rack which is set up for easy town driving. The Prius tends to dive under heavy braking. It is not clear whether this could be fixed by altering the anti-dive aspects of the suspension or whether it is an inherent effect of the heavy battery in the back of the car.

The Prius' handling has been set up to under-steer. This is understandable, as with a heavy battery in the back of the car, any over-steer could end up with the car spinning out of control if not corrected early. However this makes it quite unexciting to drive the car and it feels as if more and more steering lock has to be applied to turn in to a corner. This under-steering behaviour is safe, although the author was able to provoke the Prius to over-steer by lifting off the throttle sharply when driving quickly through a wet corner.

Hybrid System Operation

When pulling away from a standstill or when driving under light load, the electric motor drives the front wheels via the gearbox without help from the IC engine. However when the load exceeds about 10kW (at high speeds or high acceleration demands for example), the IC engine is started automatically to assist the electric motor.

During normal driving, power from the IC engine is divided by the planetary gearbox between the wheels and an electric generator. The generator charges the batteries which power the electric motor. Under full-throttle acceleration, the power to the electric motor is supplemented by power from the batteries.

The battery state is regulated to maintain a constant charge. When the charge falls below around 50% (based on the author's experience of testing the Prius rather than any technical information), the electric generator routes power from the IC engine to charge the battery. If necessary the IC engine is started (e.g. when the car is stationary or operating at low speed using the electric motor alone). The IC engine is able to charge the battery without providing any motive power (i.e. when parked) or it can charge and provide motive power at the same time via the planetary gearbox.

The Prius employs 'Regenerative braking' to improve fuel economy by charging the battery using the vehicle's kinetic energy. Regenerative braking takes place when the vehicle is on the overrun (coasting with a closed throttle but no braking) or as it slows down under light braking. As the braking force is increased the standard brakes are also applied. The regenerative braking produces its power by running the electric drive motor in reverse, using an inverter to correct the polarity, rather than by using the generator. The Prius' automatic gear lever has two 'drive' settings, 'D' is the standard setting as found on most automatic gearboxes, while an extra 'B' setting makes the regenerative braking more intrusive and also uses engine braking to slow the vehicle more quickly.

Appendix II – Curve fitting tests

A number of tests were run to determine how well the chosen multivariate curve fitting method was able to fit a selection of standard curves which are known to have a physical representation.

These tests were performed to ensure that the code would be able to fit trends which might be expected to occur. The fitting code's normal limit on the values which can be generated for the dependent variable (normally the subjective metric, in this case Y) which ensure that its value remains between 0 and 10, was removed for this test as the test data were generated randomly and often fall outside this range.

Boltzmann function

$$y = \frac{A_1 - A_2}{1 + e^{\frac{x - x_0}{dx}}} + A_2$$

Fit type	Equation	Coefficient of determination
LWS	Y = 0.148820+1.409561* X -0.484011* X^3	0.996
LS	Y = 0.143890+1.409255* X -0.482166* X^3	0.996

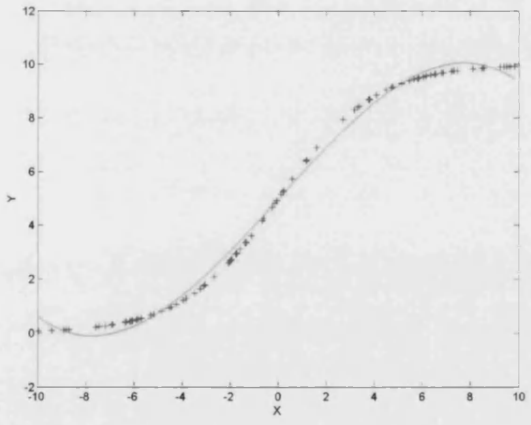

Figure A2-1 - Boltzmann function curve Least squares fit

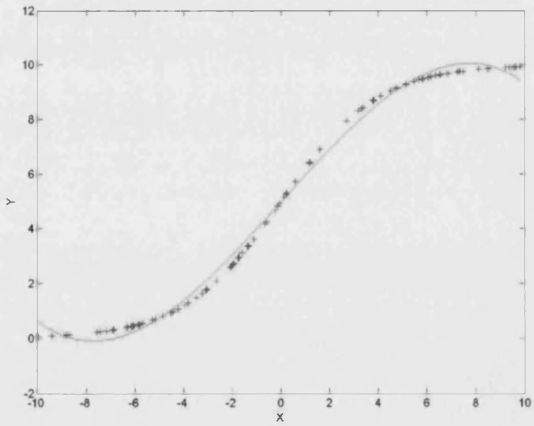

Figure A2-2 - Boltzmann function curve LWS fit

Classic Freundlich

$y = ax^b$

Type 1

Fit type	Equation	Coefficient of determination
LWS	Y = 25.144860+0.845445* X^-1 +8.322575* X^(1/-2) +7.802890* LN(X^-1) -0.016791* X^2 -13.513743* X^(1/-3) -0.209575* X^-3 +2.207320* X^(1/3)	1.000
LS	Y = 2.180334+1.145839* X^-1 +6.129643* X^(1/-2) -0.842569* X^-2 +0.380661* X^-3 -9.983232* X^(1/-3) +9.599932* LN(X^-3) +1.650917* X^(1/3) -0.005579* X^3 +3.741134* LN(X)	1.000

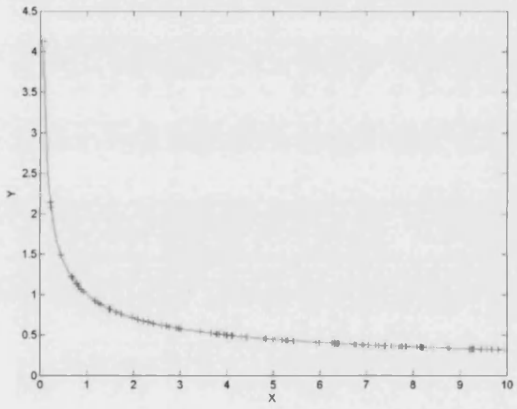

Figure A2-3 – Classic Freundlich Curve (type 1) Least squares fit

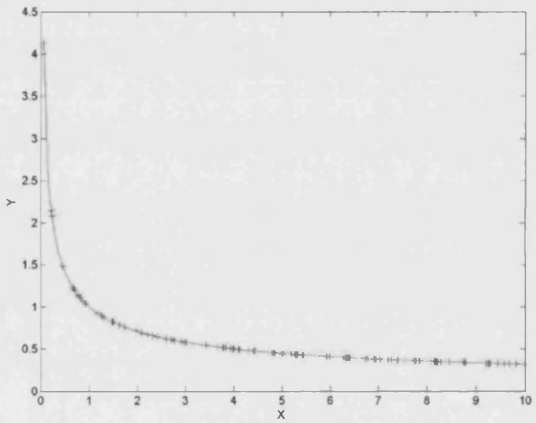

Figure A2-4 - Classic Freundlich Curve (type 1) LWS fit

Type 2

Fit type	Equation	Coefficient of determination
LWS	Y = 17601.604362+27.564567* X^3 -192.286795* X^2 +2515.350621* X -19945.480369* X^(1/2) +26362.360132* X^(1/3) -12797.501024* LN(X) - 6119.059223* X^(1/-3) +2088.899756* X^(1/-2)	1.000
LS	Y = -2932.415787+17.464675* X^3 -84.576334* X^2 +631.136330* X -3128.334167* X^(1/2) +3291.982895* X^(1/3) -790.225342* LN(X) -63.199687* X^(1/-2)	1.000

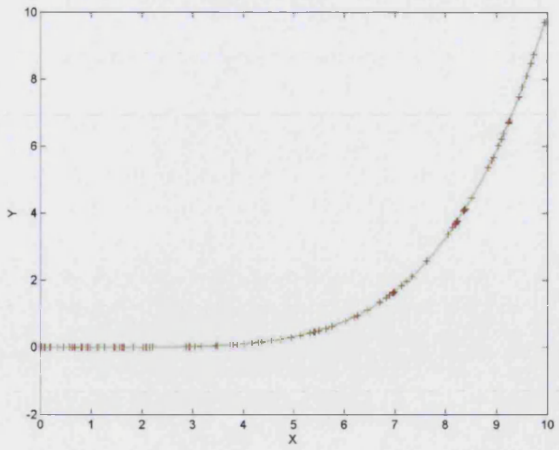

Figure A2-5 - Classic Freundlich Curve (Type 2)
Least squares fit

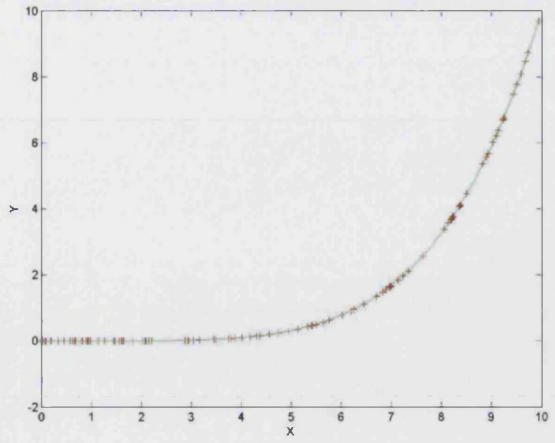

Figure A2-6 - Classic Freundlich Curve (Type 2)
LWS fit

Type 3

Fit type	Equation	Coefficient of determination
LWS	Y = 15.933013-0.988118* LN(X^-2) -0.028895* X^-2	1.000
LS	Y = 14.885226-0.735871* LN(X^-3) +0.052964* X^-2 +0.005917* X^2 -0.016203* X^-3 -0.032455* X - 0.109592* X^-1 +0.239636* X^(1/3) -0.001005* X^3	1.000

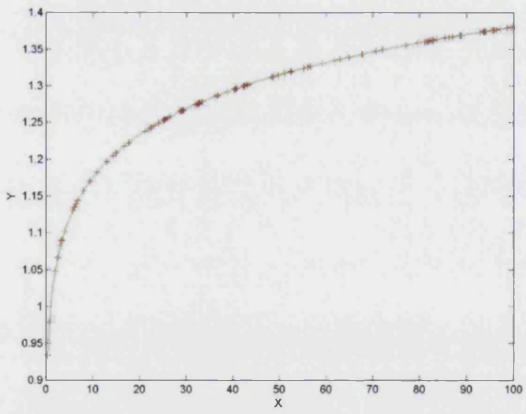

Figure A2-7 - Classic Freundlich Curve (type 3)
Least squares fit

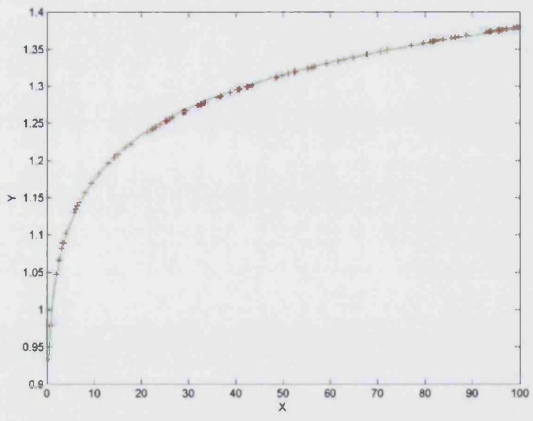

Figure A2-8 - Classic Freundlich Curve (type 3)
LWS fit

Cubic

$$y = a + bx + cx^2 + dx^3$$

Fit type	Equation	Coefficient of determination
LWS	Y = 5.766504-0.787084* X^3 -0.517552* X^2 +0.090662* X	1.000
LS	Y = 5.766505-0.787085* X^3 -0.517552* X^2 +0.090662* X	1.000

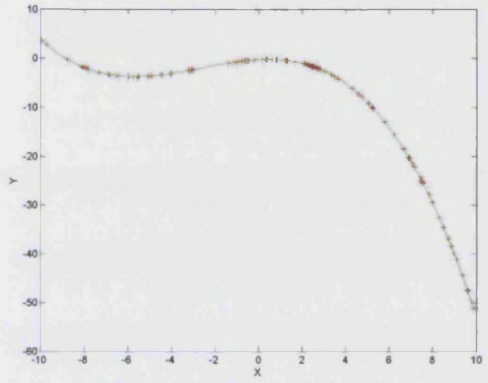

Figure A2-9 - Cubic curve
Least squares fit

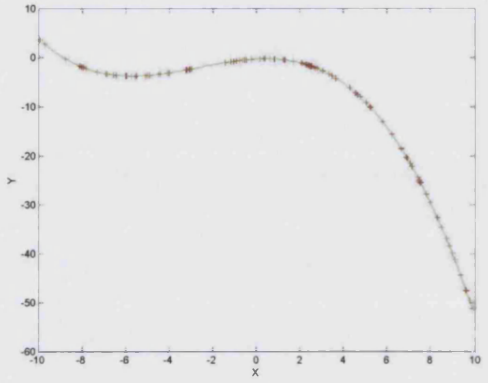

Figure A2-10 - Cubic curve
LWS fit

Exponential Associate

$$y = y_0 + A_1\left(1 - e^{\frac{-x}{t_1}}\right) + A_2\left(1 - e^{\frac{-x}{t_2}}\right) +$$

Fit type	Equation	Coefficient of determination
LWS	Y = 13.507497-1.286008* X^(1/-2) -0.302122* X +0.063346* X^-1 -0.034700* X^-2	1.000
LS	Y = 268.047738+23.624159* X^(1/-2) +2.609330* X -0.388580* X^2 -42.856909* X^(1/-3) -20.502718* LN(X^2)	1.000

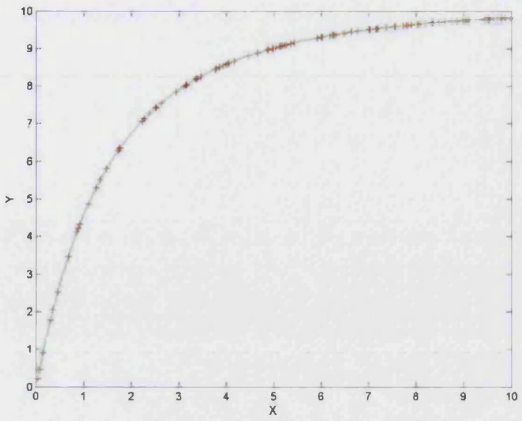

Figure A2-11 - Exponential Associate Least squares fit

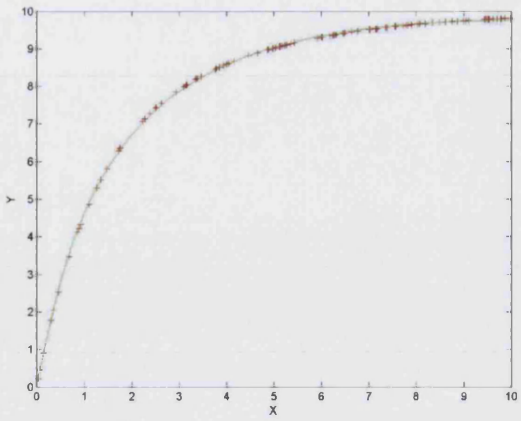

Figure A2-12 - Exponential Associate LWS fit

Exponential Decay with Offset

$$y = y_0 + A_1 e^{\frac{-(x-x_0)}{t_1}} + A_2 e^{\frac{-(x-x_0)}{t_2}} + A_3 e^{\frac{-(x-x_0)}{t_3}}$$

Fit type	Equation	Coefficient of determination
LWS	Y = -13.577430+1.864034* X^(1/-2) +0.885240* X^(1/2) -0.342054* X^-1 -0.088507* X^3 +0.510642* X^-2 -0.266103* X^-3	1.000
LS	Y = -285.006377-53.738911* X^(1/-2) -13.143582* X^(1/2) +0.042383* X^-1 -0.044599* X^-2 +0.018289* X^-3 +0.334492* X^2 +100.205441* X^(1/-3) -58.339310* LN(X^-3)	1.000

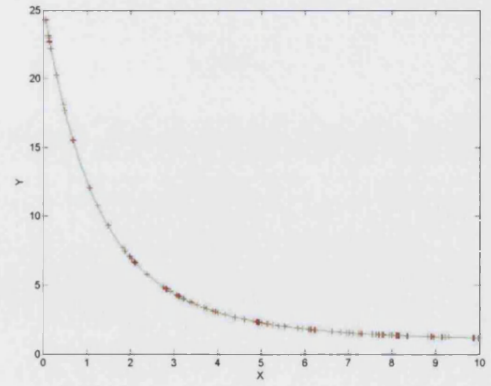

Figure A2-13 - Exponential decay curve with offset (type 3) - LS fit

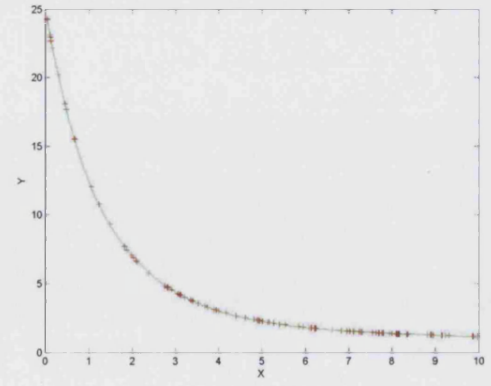

Figure A2-14 - Exponential decay curve with offset (type 3) - LWS fit

Exponential Growth with Offset

$$y = y_0 + A_1 e^{\frac{(x-x_0)}{t_1}} + A_2 e^{\frac{(x-x_0)}{t_2}}$$

Fit type	Equation	Coefficient of determination
LWS	Y = 17391.242971+18.484183* X^3 +1692.491157* X^(1/-2) -142.065436* X^2 +1898.453615* X - 15382.203548* X^(1/2) +20487.804737* X^(1/3) - 10097.199281* LN(X) -4909.841621* X^(1/-3)	1.000
LS	Y = -70.247225+8.372635* X^3 -198.969742* X^(1/-2) -36.719549* X^2 +185.126835* X -340.696037* X^(1/2) -51.446376* X^(1/3) +469.892960* X^(1/-3) - 498.513077* LN(X^-1) +8.684959* LN(X)	1.000

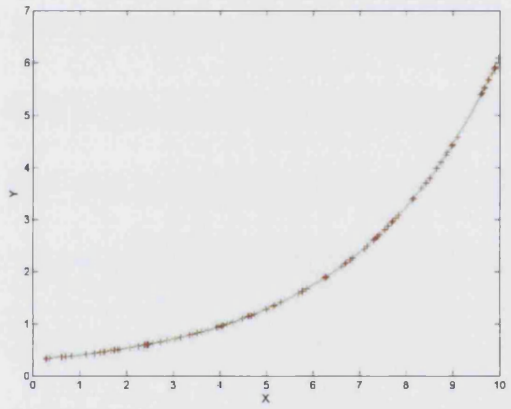

Figure A2-15 - Exponential growth with offset (type 2)
Least squares fit

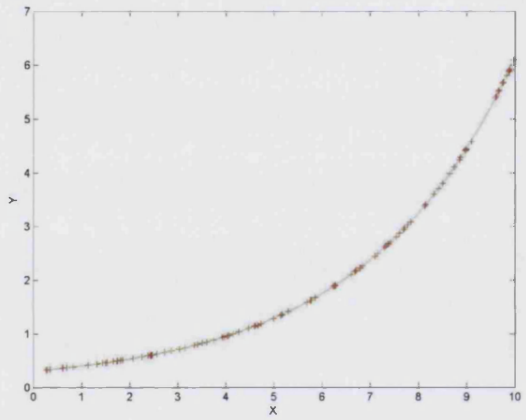

Figure A2-16 - Exponential growth with offset (type 2)
LWS fit

Hyperbolic

$$y = \frac{1}{a + bx}$$

Fit type	Equation	Coefficient of determination
LWS	Y = 17.907301-1.630486* X^(1/-2) +0.652312* LN(X^-3) +0.014722* X^3 +0.002757* X^-3	1.000
LS	Y = 9.860093-3.692261* X^(1/-2) +2.687362* X^(1/-3) +0.143781* X^-1 -0.005721* X^3 +0.017665* X^-3 +0.014519* X^2 -0.072384* X^-2 +0.070796* X^(1/2)	1.000

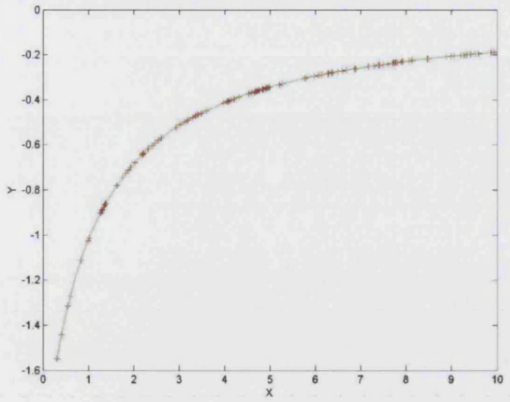

Figure A2-17 - Hyperbolic curve (type 1) Least squares fit

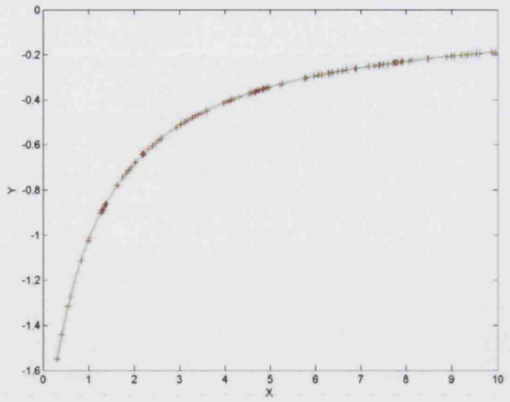

Figure A2-18 - Hyperbolic curve (type 1) LWS fit

$$y = \frac{1}{a + bx + cx^2}$$

Fit type	Equation	Coefficient of determination
LWS	Y = 0.457776+1.820605* X^-1 -0.982344* X^-3	0.953
LS	Y = 542.760284+94.532085* X^(1/-2) -122.391142* X^(1/-3) -6.829166* X^2 +1.955763* X^-2 +0.955109* X^3 -0.821125* X^-3 +41.287483* X -1.939286* X^-1 -65.203405* X^(1/2)	1.000

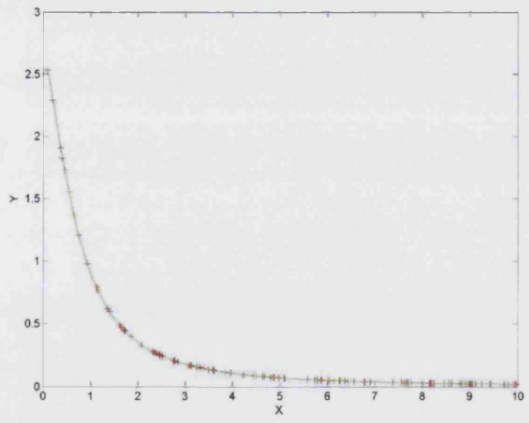

Figure A2-19 - Hyperbolic curve (type 2) Least squares fit

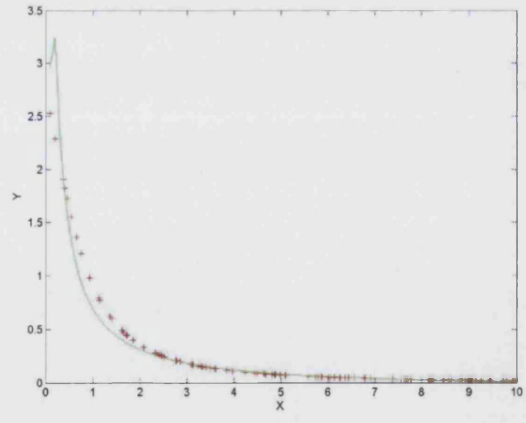

Figure A2-20 - Hyperbolic curve (type 2) LWS fit

$$y = \frac{1}{a + bx + cx^2 + dx^3}$$

Fit type	Equation	Coefficient of determination
LWS	Y = 0.040509+6.520235* X^-1	0.540
LS	Y = 318.197581+60.705771* X^(1/-2) -75.001604* X^(1/-3) -8.258346* X^-3 -1.228921* X^2 +11.436096* X^-2 +15.177822* X -3.697726* X^-1 -29.876602* X^(1/2)	1.000

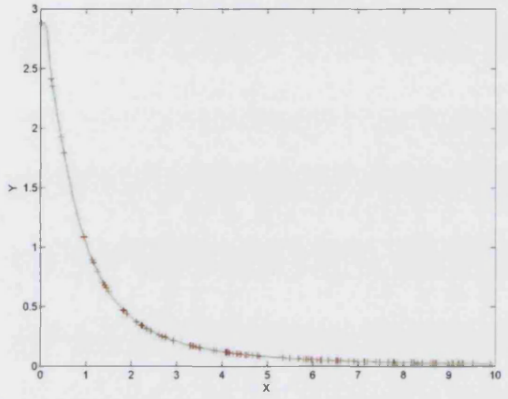

Figure A2-21 - Hyperbolic curve (type 3) Least squares fit

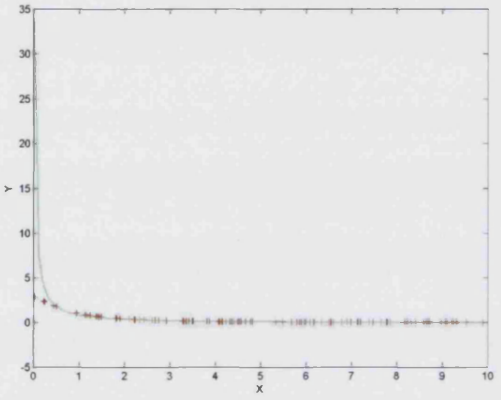

Figure A2-22 - Hyperbolic curve (type 3) LWS fit

Linear

$$y = a + bx$$

Fit type	Equation	Coefficient of determination
LWS	Y = -0.131129+1.000000 * X	1.000
LS	Y = -0.131129+1.000000 * X	1.000

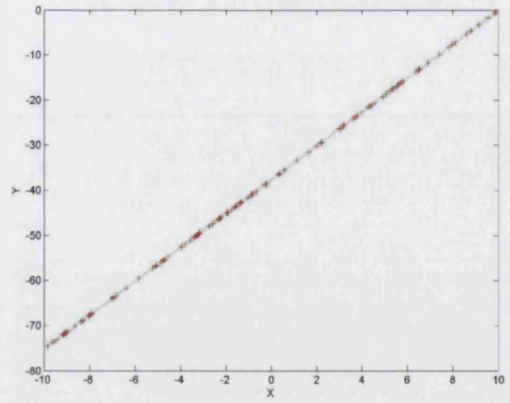

Figure A2-23 - Linear curve
Least squares fit

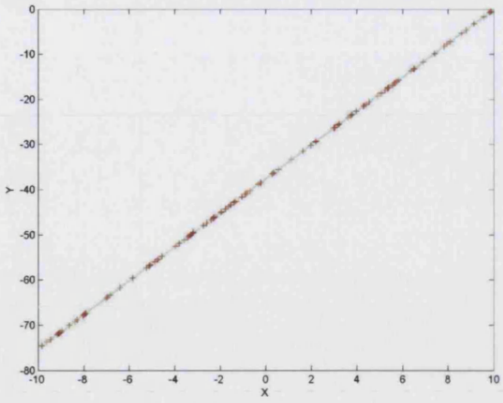

Figure A2-24 - Linear curve
LWS fit

Logarithmic

$$\log(y) = a + bx$$

Fit type	Equation	Coefficient of determination
LWS	Y = -2170.239934-6.062152* X^2 +861.133434* X^(1/3) +79.460485* X +1.057216* X^3 -650.464418* X^(1/2) +388.992645* LN(X^-3) -111.915591* X^(1/-3) +7.120547* X^-1 -0.077402* X^-2	1.000
LS	Y = -12.864008-0.765441* X^2 +10.849571* X^(1/3) +0.511974* X^3 +4.391329* X -12.428970* X^(1/2) -1.546814* LN(X^2)	1.000

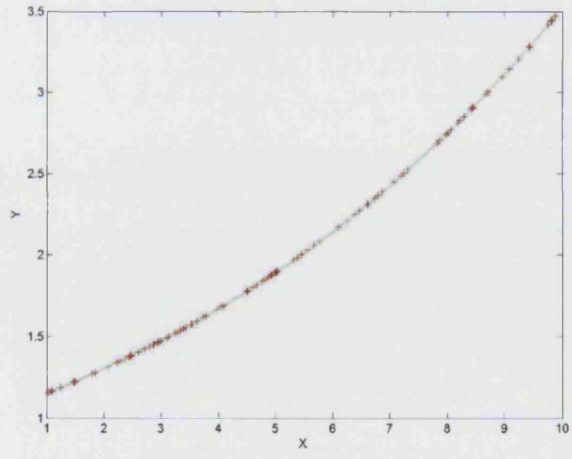

Figure A2-25 - Logarithmic curve (type 1-1)
Least squares fit

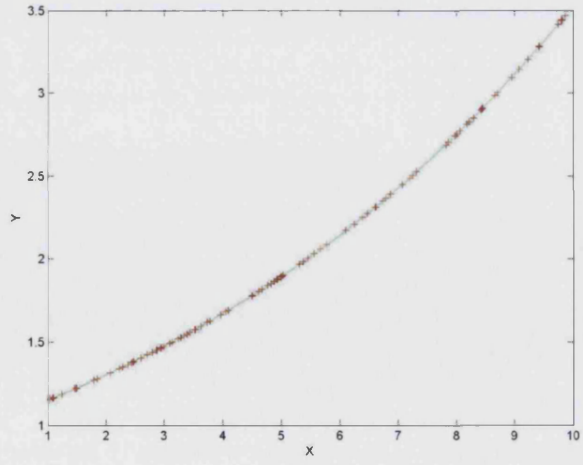

Figure A2-26 - Logarithmic curve (type 1-1)
LWS fit

$$\log(y) = a + bx + cx^2$$

Fit type	Equation	Coefficient of determination
LWS	Y = average(Y)	
LS	Y = -362609.216398+1051.277117* X^3 -6648.798487* X^2 +47362.294832* X -226927.983247* X^(1/2) +231693.392313* X^(1/3) -47563.511829* LN(X^3) -1036.673712* X^-1	0.799

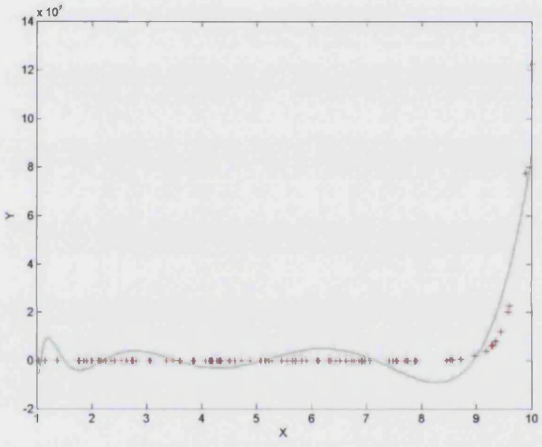

Figure A2-27 - Logarithmic curve (type 1-2) Least squares fit

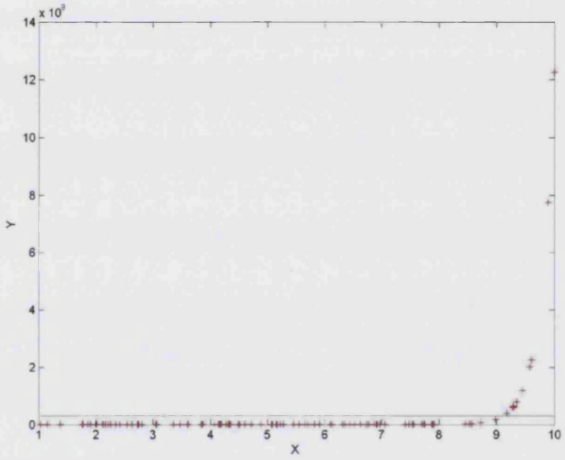

Figure A2-28 - Logarithmic curve (type 1-2) LWS fit

$$\log(y) = a + bx + cx^2 + dx^3$$

Fit type	Equation	Coefficient of determination
LWS	Y = 3.515600+2.100285* LN(X^-3) +0.664976* X^3 -0.744319* X^-2	0.960
LS	Y = 127.483662-21.161912* LN(X^3) -7.977705* X^3 +5.983262* X^-2 +15.342901* X^2 -19.075136* X^-1	0.992

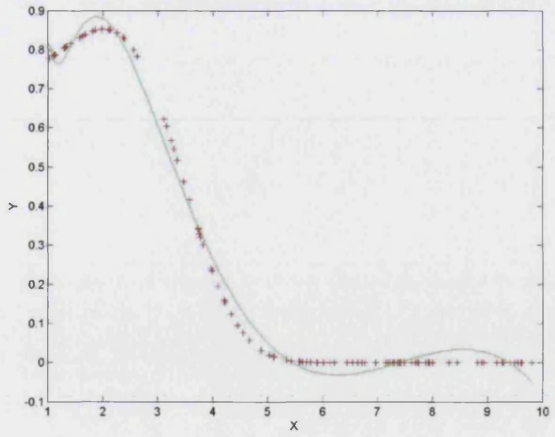

Figure A2-29 - Logarithmic curve (type 1-3) Least squares fit

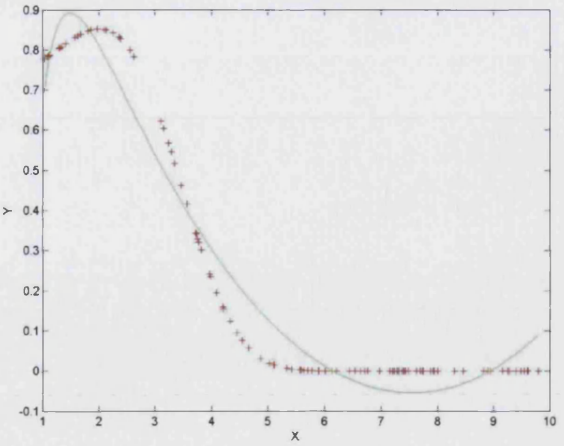

Figure A2-30 - Logarithmic curve (type 1-3) LWS fit

$$\log(y) = a + b\log(x)$$

Fit type	Equation	Coefficient of determination
LWS	Y = 6.520171+1.005923* LN(X^-3) -0.006204* X^-1 - 2.446063e-005 * X^-3	1.000
LS	Y = 6.520172+1.005923* LN(X^-3) -0.006205* X^-1 - 2.417101e-005 * X^-3	1.000

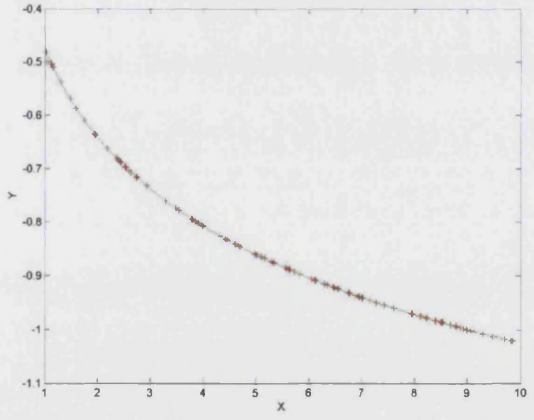

Figure A2-31 - Logarithmic curve (type 2-1) Least squares fit

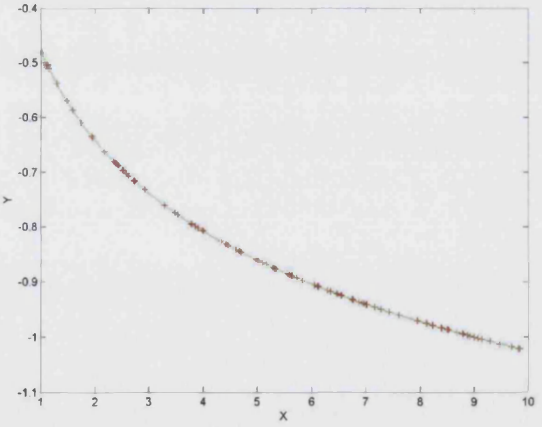

Figure A2-32 - Logarithmic curve (type 2-1) LWS fit

$$\log(y) = a + b\log(x) + c\log(x)^2$$

Fit type	Equation	Coefficient of determination
LWS	Y = 42.263199+0.898369* X^-2 -0.183350* X^-3 - 1.661687* X -2.762329* X^-1 +0.234155* X^2	1.000
LS	Y = 42.384691-0.098329* X^-3 -0.119021* X^3 +0.561686* X^-2 +0.703178* X^2 -2.073844* X^-1 - 2.480835* X -0.904363* LN(X^-3)	1.000

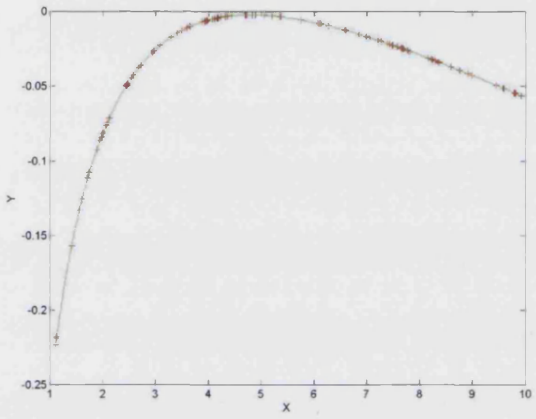

Figure A2-33 - Logarithmic curve (type 2-2) Least squares fit

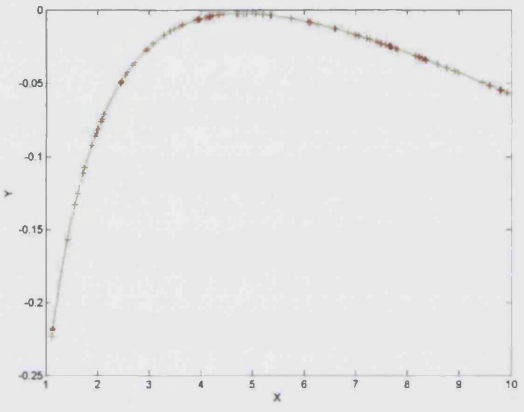

Figure A2-34 - Logarithmic curve (type 2-2) LWS fit

$$\log(y) = a + b\log(x) + c\log(x)^2 + d\log(x)^3$$

Fit type	Equation	Coefficient of determination
LWS	Y = 42.258170-0.225041* X^-1 -14.926701* X^(1/-3) +0.239128* X^2 -0.026268* X^3 +0.018606* X^-3 - 1.835315* X +14.746345* X^(1/-2) -0.161147* X^-2	1.000
LS	Y = 18.725576+4.851665* X^-1 +0.046401* X^3 - 0.792605* X^-2 +0.119984* X^-3 -0.138962* X^2 - 4.058837* X^(1/-2) -0.867493* X	1.000

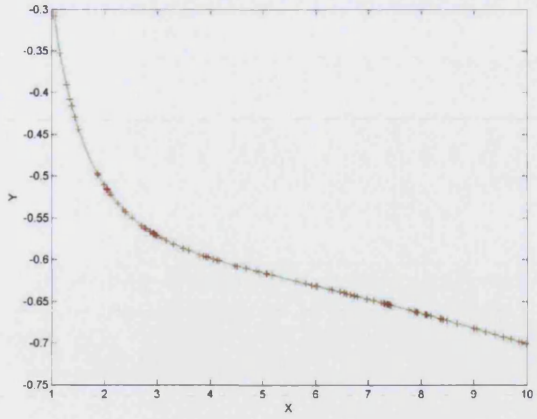

Figure A2-35 - Logarithmic curve (type 2-3)
Least squares fit

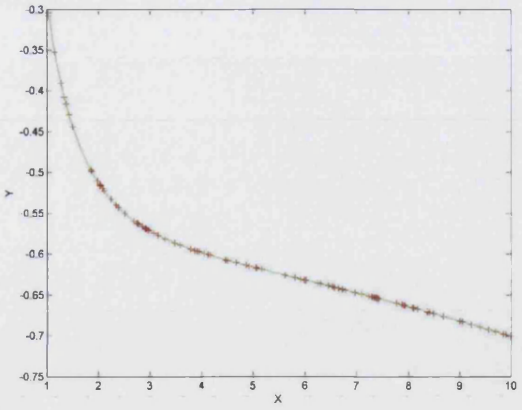

Figure A2-36 - Logarithmic curve (type 2-3)
LWS fit

$$y = a + b\log(x)$$

Fit type	Equation	Coefficient of determination
LWS	Y = 5.552475+1.553989* LN(X^-1) +1.041279* X^(1/3) -0.487823* X^(1/2) +0.000783* X^3 - 0.000285* X^-3	1.000
LS	Y = 7.139403+1.554373* LN(X^-3) +1.042598* X^(1/3) -0.488776* X^(1/2) +0.000800* X^3 - 0.000287* X^-3	1.000

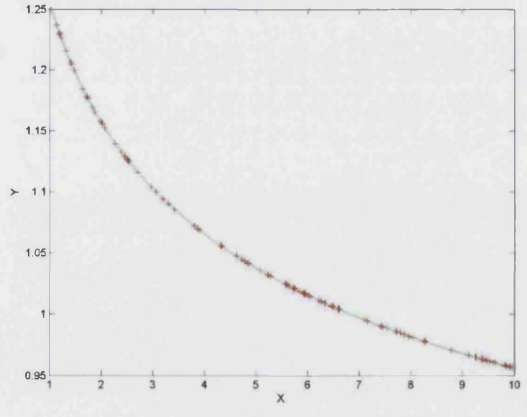

Figure A2-37 - Logarithmic curve (type 3-1)
Least squares fit

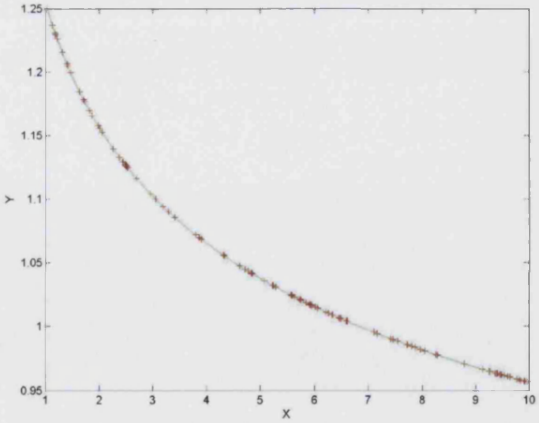

Figure A2-38 - Logarithmic curve (type 3-1)
LWS fit

$$y = a + b\log(x) + c\log(x)^2$$

Fit type	Equation	Coefficient of determination
LWS	Y = -5.077679+1.445972* X^(1/-2) -0.458958* X^3 -0.155862* X^-3 +0.810769* X^2	1.000
LS	Y = -28.868698-1.954540* X^-1 +0.269406* X^-3 -1.105339* X -1.148109* X^-2 -6.816822* LN(X^-3) +0.057620* X^3 +9.533867* X^(1/-2)	1.000

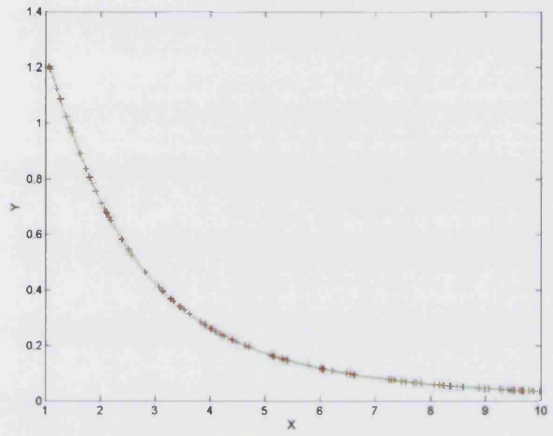

Figure A2-39 - Logarithmic curve (type 3-2) Least squares fit

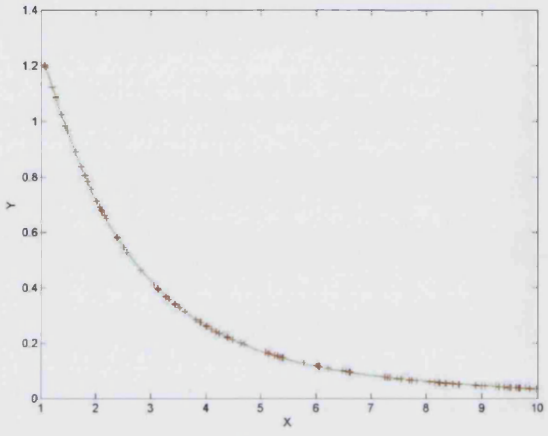

Figure A2-40 - Logarithmic curve (type 3-2) LWS fit

$$y = a + b\log(x) + c\log(x)^2 + d\log(x)^3$$

Fit type	Equation	Coefficient of determination
LWS	Y = 15.167693-1.290995* LN(X^2) -0.213011* X^-3 +0.179499* X^3	1.000
LS	Y = -51.502995+10.277348* LN(X^-1) +0.212304* X^-3 -0.718618* X^2 -0.489125* X^-2 +7.946598* X^(1/3) +0.203366* X^3 -1.666385* X^-1	1.000

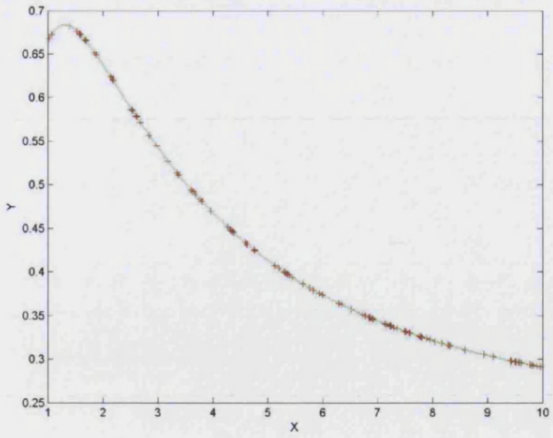

Figure A2-41 - Logarithmic curve (type 3-3) Least squares fit

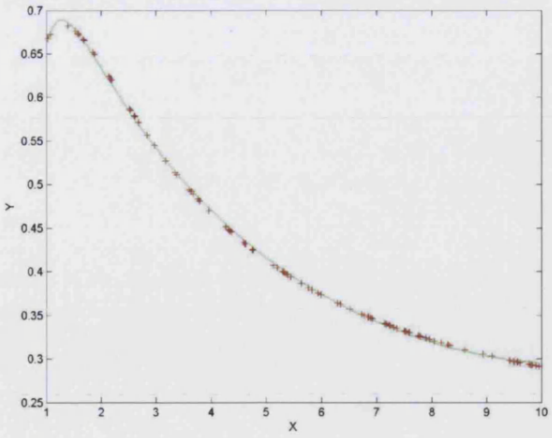

Figure A2-42 - Logarithmic curve (type 3-3) LWS fit

One site competition curve

$$y = \frac{A_1 - A_2}{1 + 10^{(x - \log x_0)}} + A_2$$

Fit type	Equation	Coefficient of determination
LWS	Y = 30.116471+17.132257* X^(1/-2) -16.577495* X^(1/-3) -0.405985* X^2	0.996
LS	Y = -1911.823914+0.260732* X^3 -1.727732* X^-1 -0.756844* X^-3 +1.782379* X^-2 +31.016659* X +133.452473* LN(X^-1) +469.131577* X^(1/3) -368.712067* X^(1/2)	1.000

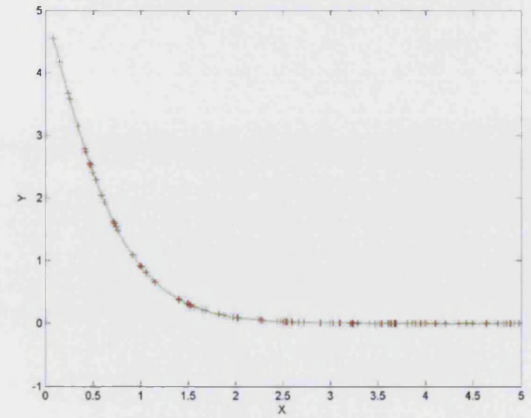

Figure A2-43 - One site competition curve Least squares fit

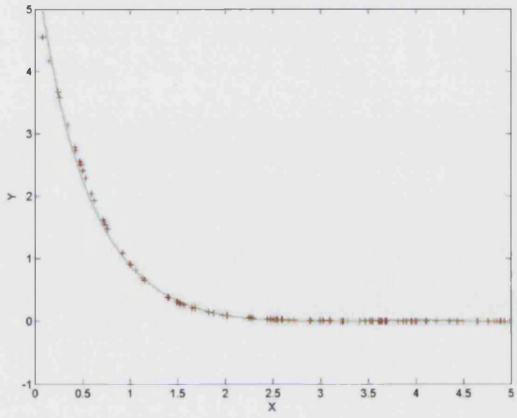

Figure A2-44 - One site competition curve LWS fit

Parabolic

$$y = a + bx + cx^2$$

Fit type	Equation	Coefficient of determination
LWS	Y = 5.393619-0.997172* X^2 -0.452731* X	1.000
LS	Y = 5.393619-0.997172* X^2 -0.452731* X	1.000

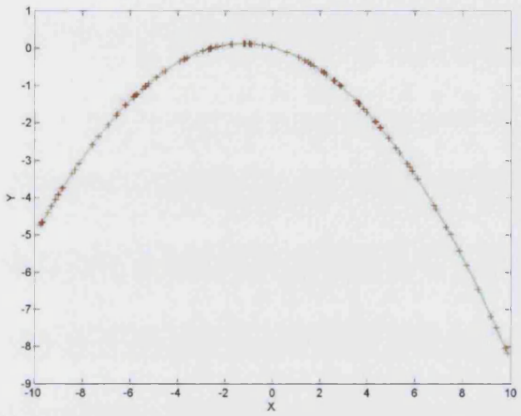

Figure A2-45 - Parabolic curve
Least squares fit

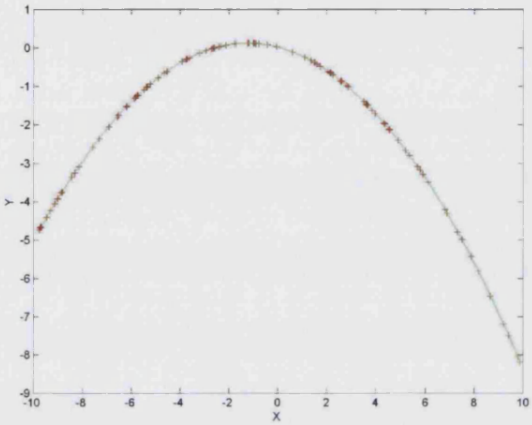

Figure A2-46 - Parabolic curve
LWS fit

Two site competition curve

$$y = \frac{(A_1 - A_2)f}{1+10^{(x-\log x_{0_1})}} + \frac{(A_1 - A_2)(1-f)}{1+10^{(x-\log x_{0_2})}}$$

Fit type	Equation	Coefficient of determination
LWS	Y = -0.796145+1.595664* X^-1 +0.075640* X^2 - 0.741596* X^-3	0.937
LS	Y = -1.832997+4.852014* X^-1 -6.740613* X^-2 +3.156493* X^-3 -0.442509* LN(X^-2)	0.992

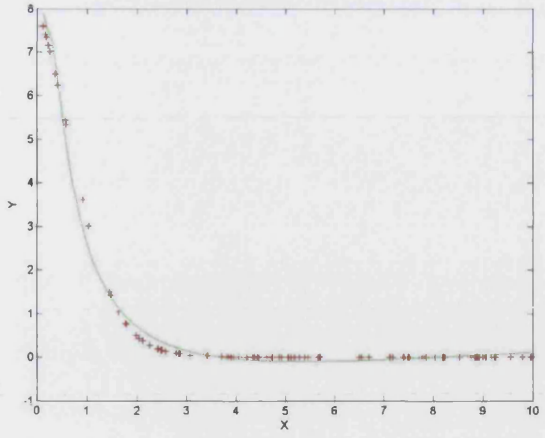

Figure A2-47 – Two site competition curve
Least squares fit

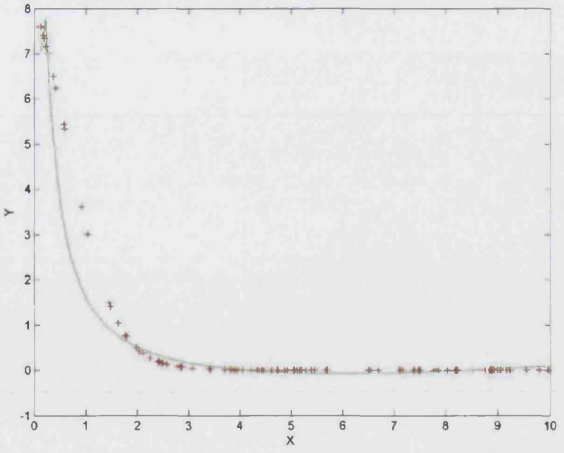

Figure A2-48 - Two site competition curve
LWS fit

Appendix III – Effect of the addition of aAverage objective metrics

Table A3-1 - Comparison between correlation equations with the addition of extra terms

nn_cut_down_set-LS	
without aAverage metrics	**with aAverage metrics**
smoothness = 16.873454 +0.243357* aMaximumQuirk^-1 +0.095750* aDesiredStartSpeed^-1 +0.030330* aAverageQuirk^-2 +0.188106* aInitialPedalPosn^(1/-2) -0.571154* aAverageAccelToMaxSpeed^2 +0.176731* aDeltaEngSpd2MaxSpeed R^2 = 0.428	smoothness = 163.863539 -0.454664* aMaxEngSpeed^(1/2) +0.146823* aMaximumQuirk^-1 +0.197199* aDesiredStartSpeed^-1 +0.011734* aAverageQuirk^-2 -0.414914* **aAverageSpeed**^-1 +0.267363* aInitialPedalPosn^(1/-2) -0.275604* aDesiredPedalPosition^(1/2) -0.327753* aEngSpdAtMaxVSpeed^(1/-2) R^2 = 0.438
eng_delay = 13.604807 -0.539122* aEngSpdAtMaxVSpeed^(1/2) +0.492441* aMaximumQuirk^-1 +0.235625* aDeltaEngSpd2MaxSpeed^3 -0.255957* aMaximumQuirk^-2 -0.135750* aMaxAccel^-1 -0.262308* aDesiredStartSpeed^-3 -0.123743* aAverageAccelToMaxAccel^-2 +0.214476* aInitialSpeed^-1 -0.141459* aEngSpdAtMaxVSpeed^(1/-2) +0.216171* aEngSpdAtMaxVSpeed^3 R^2 = 0.300	eng_delay = 13.604807 -0.539122* aEngSpdAtMaxVSpeed^(1/2) +0.492441* aMaximumQuirk^-1 +0.235625* aDeltaEngSpd2MaxSpeed^3 -0.255957* aMaximumQuirk^-2 -0.135750* aMaxAccel^-1 -0.262308* aDesiredStartSpeed^-3 -0.123743* aAverageAccelToMaxAccel^-2 +0.214476* aInitialSpeed^-1 -0.141459* aEngSpdAtMaxVSpeed^(1/-2) +0.216171* aEngSpdAtMaxVSpeed^3 R^2 = 0.300
vehicle_delay = 5555.884346 +103.091633* aMaximumQuirk^(1/-2) +0.464501* aMaximumQuirk^-1 -0.080760* aDesiredStartSpeed^-3 -0.723686* aMaxAccel^-1 -0.223688* aMaximumQuirk^-2 -0.362171* aDesiredPedalPosition +0.190436* aMaxPedalPosition^3 +0.437285* aMaxAccel^-2 -102.778712* aMaximumQuirk^(1/-3) R^2 = 0.399	vehicle_delay = -12.860624 +0.171281* aMaximumQuirk^(1/-2) +0.539143* aMaximumQuirk^-1 -0.075872* aDesiredStartSpeed^-3 -0.240401* aMaxAccel^-1 -0.258035* aMaximumQuirk^-2 -0.298777* aDesiredPedalPosition +0.300415* aMaxPedalPosition^3 -0.165852* **aAveragePedalPosition**^2 R^2 = 0.392
init_accel = 8864.913919 +170.514560* aMaximumQuirk^(1/-2) -0.146236* aDesiredStartSpeed^-3 -170.075600* aMaximumQuirk^(1/-3) -0.275657* aEngSpdAtMaxVSpeed^(1/3) +0.273874* aDeltaEngSpd2MaxSpeed^2	init_accel = 7838.339269 +147.644884* aMaximumQuirk^(1/-2) -0.176348* aDesiredStartSpeed^-3 -147.151996* aMaximumQuirk^(1/-3) -0.184728* aAverageAccelToMaxSpeed^(1/-2)

-0.264740* aChangeInSpeed^(1/-2) +0.112752* AccelDelayTime^3 +0.190883* aMaxSpeed^(1/-2) R^2 = 0.407	-0.319862* aEngSpdAtMaxVSpeed^(1/3) +0.273185* aDeltaEngSpd2MaxSpeed^2 +0.168328* aInitialSpeed^-2 +0.357019* **aAverageEngSpeed**^3 -0.338887* aMaxEngSpeed^2 -0.130310* aChangeInSpeed^(1/-2) R^2 = 0.403
accel_prog = 8.366749 -0.376147* aEngSpdAtMaxVSpeed^(1/2) +0.242029* aMaximumQuirk^-1 +0.234155* aDeltaEngSpd2MaxSpeed^2 +0.205109* aMaxPedalPosition^3 -0.211103* aDesiredStartSpeed^-3 -0.121936* aAverageAccelToMaxSpeed^-2 +0.214236* aInitialSpeed^-1 R^2 = 0.291	accel_prog = 7.449888 +0.216950* aMaximumQuirk^-1 +0.193251* aDeltaEngSpd2MaxSpeed^2 +0.261827* aMaxPedalPosition^3 -0.161111* aDesiredStartSpeed^-3 -0.141920* **aAveragePedalPosition**^2 -0.115269* aAverageAccelToMaxSpeed^-2 +0.178457* aInitialSpeed^-1 +0.396895* aEngSpdAtMaxVSpeed^3 -0.667681* aEngSpdAtMaxVSpeed R^2 = 0.317
performance = -19.600856 +0.382092* aMaximumJerk^(1/-2) -0.294457* aDesiredStartSpeed^-1 -0.169873* LN(aEngSpdAtMaxVSpeed^2) +0.478490* aMaximumQuirk^-1 -0.376832* aMaxAccel^(1/-2) +0.208163* aInitialSpeed^-1 -0.217147* aMaximumQuirk^-2 R^2 = 0.336	performance = -6.611682 -0.423648* aDesiredStartSpeed^-1 +0.651734* aDeltaEngSpd2MaxSpeed^2 -0.219720* aMaxAccel^(1/-2) +0.236547* **aAverageEngSpeed**^3 +0.199115* aMaximumQuirk^-1 -0.481239* aEngSpdAtMaxVSpeed^(1/2) +0.285981* aInitialSpeed^-1 +0.395477* LN(aMaximumJerk^-1) -0.401465* aDeltaEngSpd2MaxSpeed^3 R^2 = 0.362

Appendix IV – Effect of the removal of exponent terms, ±4th & ±5th powers and ±4th & ±5th roots from the correlation generation

Full metric set, least squares fit	
Standard equation	**With ±4th & ±5th powers, ±4th & ±5th roots**
smoothness = 16.873454 +0.243357 * aMaximumQuirk^-1 +0.095750 * aDesiredStartSpeed^-1 +0.030330 * aAverageQuirk^-2 +0.188106 * aInitialPedalPosn^(1/-2) -0.571154* aAverageAccelToMaxSpeed^2 +0.176731* aDeltaEngSpd2MaxSpeed $R^2 = 0.428$	smoothness = 16.873454 +0.243357* aMaximumQuirk^-1 +0.095750* aDesiredStartSpeed^-1 +0.030330* aAverageQuirk^-2 +0.188106* aInitialPedalPosn^(1/-2) -0.571154* aAverageAccelToMaxSpeed^2 +0.176731* aDeltaEngSpd2MaxSpeed $R^2 = 0.428$
eng_delay = 13.604807 -0.539122* aEngSpdAtMaxVSpeed^(1/2) +0.492441* aMaximumQuirk^-1 +0.235625* aDeltaEngSpd2MaxSpeed^3 -0.255957* aMaximumQuirk^-2 -0.135750* aMaxAccel^-1 -0.262308* aDesiredStartSpeed^-3 -0.123743* aAverageAccelToMaxAccel^-2 +0.214476* aInitialSpeed^-1 -0.141459* aEngSpdAtMaxVSpeed^(1/-2) +0.216171* aEngSpdAtMaxVSpeed^3 $R^2 = 0.300$	eng_delay = 110.695833 -0.665244* aEngSpdAtMaxVSpeed^(1/2) +0.166043* aMaximumQuirk^-1 +0.92841* aDeltaEngSpd2MaxSpeed^3 -0.337325* aDesiredStartSpeed^-5 +0.173702* aEngSpdAtMaxVSpeed^5 -0.20087* aEngSpdAtMaxVSpeed^(1/-4) -0.146747* aAverageAccelToMaxAccel^-2 +0.302959* aInitialSpeed^-1 -0.564151* aDeltaEngSpd2MaxSpeed^5 -0.286322* aAverageAccelToMaxSpeed^5 +0.176274* aInitialJerk +0.162343* aMaxSpeed^2 -0.115593* aDesiredPedalPosition^3 $R^2 = 0.343$
vehicle_delay = 5555.884346 +103.091633* aMaximumQuirk^(1/-2) +0.464501* aMaximumQuirk^-1 -0.080760* aDesiredStartSpeed^-3 -0.723686* aMaxAccel^-1 -0.223688* aMaximumQuirk^-2 -0.362171* aDesiredPedalPosition +0.190436* aMaxPedalPosition^3 +0.437285* aMaxAccel^-2 -102.778712* aMaximumQuirk^(1/-3) $R^2 = 0.399$	vehicle_delay = 7415.102554 +68.765310* aMaximumQuirk^(1/-2) +0.464524* aMaximumQuirk^-1 -0.080895* aDesiredStartSpeed^-5 -0.723283* aMaxAccel^-1 -0.223669* aMaximumQuirk^-2 -0.362188* aDesiredPedalPosition +0.190581* aMaxPedalPosition^3 +0.436988* aMaxAccel^-2 -68.452585* aMaximumQuirk^(1/-4) $R^2 = 0.399$
init_accel = 8864.913919 +170.514560* aMaximumQuirk^(1/-2) -0.146236* aDesiredStartSpeed^-3	init_accel = 11914.834421 +114.454522* aMaximumQuirk^(1/-2) -0.151654* aDesiredStartSpeed^-5

-170.075600* aMaximumQuirk^(1/-3) -0.275657* aEngSpdAtMaxVSpeed^(1/3) +0.273874* aDeltaEngSpd2MaxSpeed^2 -0.264740* aChangeInSpeed^(1/-2) +0.112752* AccelDelayTime^3 +0.190883* aMaxSpeed^(1/-2) R^2 = 0.407	-114.024769* aMaximumQuirk^(1/-4) -0.403606* aEngSpdAtMaxVSpeed^(1/5) +0.289739* aDeltaEngSpd2MaxSpeed^2 -0.266931* aChangeInSpeed^(1/-2) +0.121877* AccelDelayTime^5 +0.188405* aMaxSpeed^(1/-2) -0.147893* aEngSpdAtMaxVSpeed^(1/-5) R^2 = 0.412
accel_prog = 8.366749 -0.376147* aEngSpdAtMaxVSpeed^(1/2) +0.242029* aMaximumQuirk^-1 +0.234155* aDeltaEngSpd2MaxSpeed^2 +0.205109* aMaxPedalPosition^3 -0.211103* aDesiredStartSpeed^-3 -0.121936* aAverageAccelToMaxSpeed^-2 +0.214236* aInitialSpeed^-1 R^2 = 0.291	accel_prog = 18.252285 -1.563790* aEngSpdAtMaxVSpeed^(1/2) +0.224469* aMaximumQuirk^-1 +0.241964* aDeltaEngSpd2MaxSpeed^2 +0.195402* aMaxPedalPosition^5 -0.183295* aDesiredStartSpeed^-5 -0.128970* aAverageAccelToMaxSpeed^-2 +0.185092* aInitialSpeed^-1 +0.216347* aEngSpdAtMaxVSpeed^5 +1.054640* aEngSpdAtMaxVSpeed^(1/3) R^2 = 0.312
performance = -19.600856 +0.382092* aMaximumJerk^(1/-2) -0.294457* aDesiredStartSpeed^-1 -0.169873* LN(aEngSpdAtMaxVSpeed^2) +0.478490* aMaximumQuirk^-1 -0.376832* aMaxAccel^(1/-2) +0.208163* aInitialSpeed^-1 -0.217147* aMaximumQuirk^-2 R^2 = 0.336	performance = -33.203389 -0.357853* aDesiredStartSpeed^-1 -0.407866* aEngSpdAtMaxVSpeed^(1/5) +0.174843* aDeltaEngSpd2MaxSpeed^2 -0.255893* aMaxAccel^(1/-2) +0.205763* aMaximumQuirk^-1 +0.250227* aInitialSpeed^-1 +0.379203* aMaximumJerk^(1/-3) -0.143925* aEngSpdAtMaxVSpeed^(1/-2) +0.144419* aEngSpdAtMaxVSpeed^5 R^2 = 0.354

Appendix V – Single variable equation correlation results

Full metric set,-LS fitting

Subj_Param	Obj_Param	Equation type	R^2
smoothness	aMaxEngSpeed	Straight	0.177
smoothness	**aEngSpdAtMaxVSpeed**	**Cubic**	**0.203**
smoothness	aEngSpdAtMaxVSpeed	Parabolic	0.196
smoothness	aMaxEngSpeed	Log1	0.152
smoothness	aMaxEngSpeed	Log2	0.136
smoothness	aMaximumJerk	Log3	0.162
smoothness	aMaxEngSpeed	Hyperbolic	0.111

Subj_Param	Obj_Param	Equation type	R^2
eng_delay	aEngSpdAtMaxVSpeed	Straight	0.099
eng_delay	**aEngSpdAtMaxVSpeed**	**Cubic**	**0.125**
eng_delay	aEngSpdAtMaxVSpeed	Parabolic	0.119
eng_delay	aEngSpdAtMaxVSpeed	Log1	0.078
eng_delay	aAverageEngSpeed	Log2	0.071
eng_delay	aAverageEngSpeed	Log3	0.086
eng_delay	aEngSpdAtMaxVSpeed	Hyperbolic	0.046

Subj_Param	Obj_Param	Equation type	R^2
vehicle_delay	aMaximumQuirk	Straight	0.179
vehicle_delay	**aMaximumQuirk**	**Cubic**	**0.224**
vehicle_delay	aMaximumQuirk	Parabolic	0.223
vehicle_delay	aMaximumQuirk	Log1	0.147
vehicle_delay	aMaximumQuirk	Log2	0.149
vehicle_delay	aMaximumQuirk	Log3	0.181
vehicle_delay	aMaximumQuirk	Hyperbolic	0.097

Subj_Param	Obj_Param	Equation type	R^2
init_accel	aMaximumQuirk	Straight	0.201
init_accel	**aMaximumQuirk**	**Cubic**	**0.241**
init_accel	aMaximumQuirk	Parabolic	0.241
init_accel	aMaximumQuirk	Log1	0.178
init_accel	aMaximumQuirk	Log2	0.179
init_accel	aMaximumQuirk	Log3	0.203
init_accel	aMaximumJerk	Hyperbolic	0.364

Subj_Param	Obj_Param	Equation type	R^2
accel_prog	aMaximumQuirk	Straight	0.101
accel_prog	**aEngSpdAtMaxVSpeed**	**Cubic**	**0.133**
accel_prog	aEngSpdAtMaxVSpeed	Parabolic	0.127
accel_prog	aEngSpdAtMaxVSpeed	Log1	0.079
accel_prog	aAverageEngSpeed	Log2	0.071
accel_prog	aMaximumQuirk	Log3	0.102
accel_prog	aEngSpdAtMaxVSpeed	Hyperbolic	0.050

Subj_Param	Obj_Param	Equation type	R^2

performance	aMaximumJerk	Straight	0.186
performance	aMaximumJerk	Cubic	0.207
performance	**aMaximumJerk**	**Parabolic**	**0.207**
performance	aMaximumJerk	Log1	0.164
performance	aMaximumJerk	Log2	0.165
performance	aMaximumJerk	Log3	0.187
performance	aMaximumJerk	Hyperbolic	0.127

Full metric set, LWS fitting

Subj_Param	Obj_Param	Equation type	R^2
smoothness	aEngSpdAtMaxVSpeed	Straight	0.201
smoothness	**aMaximumJerk**	**Cubic**	**0.243**
smoothness	aMaximumJerk	Parabolic	0.230
smoothness	aMaxEngSpeed	Log1	0.173
smoothness	aEngSpdAtMaxVSpeed	Log2	0.227
smoothness	aEngSpdAtMaxVSpeed	Log3	0.199
smoothness	aMaxEngSpeed	Hyperbolic	0.125

Subj_Param	Obj_Param	Equation type	R^2
eng_delay	aEngSpdAtMaxVSpeed	Straight	0.120
eng_delay	aEngSpdAtMaxVSpeed	Cubic	0.151
eng_delay	**aAverageJerk**	**Parabolic**	**0.166**
eng_delay	aEngSpdAtMaxVSpeed	Log1	0.094
eng_delay	aEngSpdAtMaxVSpeed	Log2	0.132
eng_delay	aEngSpdAtMaxVSpeed	Log3	0.125
eng_delay	aEngSpdAtMaxVSpeed	Hyperbolic	0.054

Subj_Param	Obj_Param	Equation type	R^2
vehicle_delay	aMaximumJerk	Straight	0.201
vehicle_delay	**aMaximumQuirk**	**Cubic**	**0.270**
vehicle_delay	aMaximumQuirk	Parabolic	0.248
vehicle_delay	aMaximumJerk	Log1	0.182
vehicle_delay	aEngSpdAtMaxVSpeed	Log2	0.203
vehicle_delay	aMaximumJerk	Log3	0.203
vehicle_delay	aMaximumQuirk	Hyperbolic	0.143

Subj_Param	Obj_Param	Equation type	R^2
init_accel	aMaximumJerk	Straight	0.211
init_accel	aMaximumQuirk	Cubic	0.261
init_accel	**aAverageJerk**	**Parabolic**	**0.264**
init_accel	aMaximumJerk	Log1	0.203
init_accel	aMaximumJerk	Log2	0.204
init_accel	aMaximumJerk	Log3	0.212
init_accel	aMaximumJerk	Hyperbolic	0.163

Subj_Param	Obj_Param	Equation type	R^2
accel_prog	aEngSpdAtMaxVSpeed	Straight	0.123
accel_prog	**aMaximumQuirk**	**Cubic**	**0.156**
accel_prog	aAverageEngSpeed	Parabolic	0.144
accel_prog	aMaximumQuirk	Log1	0.098
accel_prog	aEngSpdAtMaxVSpeed	Log2	0.128
accel_prog	aAverageEngSpeed	Log3	0.123
accel_prog	aMaximumQuirk	Hyperbolic	0.064

Subj_Param	Obj_Param	Equation type	R^2
performance	aMaximumJerk	Straight	0.200
performance	**aMaximumQuirk**	**Cubic**	**0.234**
performance	aMaximumJerk	Parabolic	0.233
performance	aMaximumJerk	Log1	0.189
performance	aMaximumJerk	Log2	0.191
performance	aMaximumJerk	Log3	0.202
performance	aMaximumJerk	Hyperbolic	0.157

Acceleration and jerk metric subset,-LS fitting

Subj_Param	Obj_Param	Equation type	R^2
smoothness	aMaximumJerk	Straight	0.160
smoothness	**aMaximumJerk**	**Cubic**	**0.194**
smoothness	aMaximumJerk	Parabolic	0.193
smoothness	aMaximumJerk	Log1	0.129
smoothness	aMaximumJerk	Log2	0.130
smoothness	aMaximumJerk	Log3	0.162
smoothness	aMaximumJerk	Hyperbolic	0.084

Subj_Param	Obj_Param	Equation type	R^2
eng_delay	aMaximumJerk	Straight	0.075
eng_delay	**aMaximumJerk**	**Cubic**	**0.095**
eng_delay	aMaximumJerk	Parabolic	0.094
eng_delay	aMaximumJerk	Log1	0.048
eng_delay	aMaximumJerk	Log2	0.048
eng_delay	aMaximumJerk	Log3	0.076
eng_delay	aAccelGradient	Hyperbolic	0.019

Subj_Param	Obj_Param	Equation type	R^2
vehicle_delay	aMaximumJerk	Straight	0.176
vehicle_delay	aMaximumJerk	Cubic	0.207
vehicle_delay	**aMaximumJerk**	**Parabolic**	**0.207**
vehicle_delay	aMaximumJerk	Log1	0.145
vehicle_delay	aMaximumJerk	Log2	0.146
vehicle_delay	aMaximumJerk	Log3	0.178
vehicle_delay	aMaximumJerk	Hyperbolic	0.095

Subj_Param	Obj_Param	Equation type	R^2
init_accel	aMaximumJerk	Straight	0.197
init_accel	aMaximumJerk	Cubic	0.207
init_accel	**aMaximumJerk**	**Parabolic**	**0.207**
init_accel	aMaximumJerk	Log1	0.177
init_accel	aMaximumJerk	Log2	0.178
init_accel	aMaximumJerk	Log3	0.199
init_accel	aMaximumJerk	Hyperbolic	0.132

Subj_Param	Obj_Param	Equation type	R^2
accel_prog	aMaximumJerk	Straight	0.097
accel_prog	aMaximumJerk	Cubic	0.110
accel_prog	**aMaximumJerk**	**Parabolic**	**0.110**
accel_prog	aMaximumJerk	Log1	0.066
accel_prog	aMaximumJerk	Log2	0.067
accel_prog	aMaximumJerk	Log3	0.098
accel_prog	aMaximumJerk	Hyperbolic	0.030

Subj_Param	Obj_Param	Equation type	R^2
performance	aMaximumJerk	Straight	0.186
performance	aMaximumJerk	Cubic	0.207
performance	**aMaximumJerk**	**Parabolic**	**0.207**
performance	aMaximumJerk	Log1	0.164
performance	aMaximumJerk	Log2	0.165
performance	aMaximumJerk	Log3	0.187
performance	aMaximumJerk	Hyperbolic	0.127

Acceleration and jerk metric subset, LWS fitting

Subj_Param	Obj_Param	Equation type	R^2
smoothness	aMaximumJerk	Straight	0.179
smoothness	**aMaximumJerk**	**Cubic**	**0.243**
smoothness	aMaximumJerk	Parabolic	0.230
smoothness	aMaximumJerk	Log1	0.160
smoothness	aMaximumJerk	Log2	0.162
smoothness	aMaximumJerk	Log3	0.181
smoothness	aMaximumJerk	Hyperbolic	0.122

Subj_Param	Obj_Param	Equation type	R^2
eng_delay	aAverageJerk	Straight	0.099
eng_delay	aAverageJerk	Cubic	0.149
eng_delay	**aAverageJerk**	**Parabolic**	**0.166**
eng_delay	aMaximumJerk	Log1	0.080
eng_delay	aMaximumJerk	Log2	0.081
eng_delay	aAverageJerk	Log3	0.099
eng_delay	aMaximumJerk	Hyperbolic	0.050

Subj_Param	Obj_Param	Equation type	R^2
vehicle_delay	aMaximumJerk	Straight	0.201
vehicle_delay	aMaximumJerk	Cubic	0.243
vehicle_delay	**aMaximumJerk**	**Parabolic**	**0.243**
vehicle_delay	aMaximumJerk	Log1	0.182
vehicle_delay	aMaximumJerk	Log2	0.184
vehicle_delay	aMaximumJerk	Log3	0.203
vehicle_delay	aMaximumJerk	Hyperbolic	0.143

Subj_Param	Obj_Param	Equation type	R^2
init_accel	aMaximumJerk	Straight	0.211
init_accel	aAverageJerk	Cubic	0.230
init_accel	**aAverageJerk**	**Parabolic**	**0.264**
init_accel	aMaximumJerk	Log1	0.203
init_accel	aMaximumJerk	Log2	0.204
init_accel	aMaximumJerk	Log3	0.212
init_accel	aMaximumJerk	Hyperbolic	0.163

Subj_Param	Obj_Param	Equation type	R^2
accel_prog	aMaximumJerk	Straight	0.116
accel_prog	aMaximumJerk	Cubic	0.142
accel_prog	**aMaximumJerk**	**Parabolic**	**0.144**
accel_prog	aMaximumJerk	Log1	0.096
accel_prog	aMaximumJerk	Log2	0.097
accel_prog	aMaximumJerk	Log3	0.117
accel_prog	aMaximumJerk	Hyperbolic	0.060

Subj_Param	Obj_Param	Equation type	R^2
performance	aMaximumJerk	Straight	0.200
performance	aMaximumJerk	Cubic	0.232
performance	**aMaximumJerk**	**Parabolic**	**0.233**
performance	aMaximumJerk	Log1	0.189
performance	aMaximumJerk	Log2	0.191
performance	aMaximumJerk	Log3	0.202
performance	aMaximumJerk	Hyperbolic	0.157

Appendix VI – Correlation equation listings

Correlations generated from all vehicle data

Table A6-2 - Correlation equations from all vehicle data

Full metric set, least squares fitting

Correlation equation	Coefficient of determination, R^2
smoothness = 16.873454+0.243357* aMaximumQuirk^-1 +0.095750* aDesiredStartSpeed^-1 +0.030330* aAverageQuirk^-2 +0.188106* aInitialPedalPosn^(1/-2) -0.571154* aAverageAccelToMaxSpeed^2 +0.176731* aDeltaEngSpd2MaxSpeed	0.428
eng_delay = 13.604807-0.539122* aEngSpdAtMaxVSpeed^(1/2) +0.492441* aMaximumQuirk^-1 +0.235625* aDeltaEngSpd2MaxSpeed^3 -0.255957* aMaximumQuirk^-2 - 0.135750* aMaxAccel^-1 -0.262308* aDesiredStartSpeed^-3 - 0.123743* aAverageAccelToMaxAccel^-2 +0.214476* aInitialSpeed^-1 -0.141459* aEngSpdAtMaxVSpeed^(1/-2) +0.216171* aEngSpdAtMaxVSpeed^3	0.300
vehicle_delay = 5555.884346+103.091633* aMaximumQuirk^(1/-2) +0.464501* aMaximumQuirk^-1 -0.080760* aDesiredStartSpeed^-3 -0.723686* aMaxAccel^-1 -0.223688* aMaximumQuirk^-2 - 0.362171* aDesiredPedalPosition +0.190436* aMaxPedalPosition^3 +0.437285* aMaxAccel^-2 -102.778712* aMaximumQuirk^(1/-3)	0.399
init_accel = 8864.913919+170.514560* aMaximumQuirk^(1/-2) - 0.146236* aDesiredStartSpeed^-3 -170.075600* aMaximumQuirk^(1/-3) -0.275657* aEngSpdAtMaxVSpeed^(1/3) +0.273874* aDeltaEngSpd2MaxSpeed^2 -0.264740* aChangeInSpeed^(1/-2) +0.112752* AccelDelayTime^3 +0.190883* aMaxSpeed^(1/-2)	0.407
accel_prog = 8.366749-0.376147* aEngSpdAtMaxVSpeed^(1/2) +0.242029* aMaximumQuirk^-1 +0.234155* aDeltaEngSpd2MaxSpeed^2 +0.205109* aMaxPedalPosition^3 - 0.211103* aDesiredStartSpeed^-3 -0.121936* aAverageAccelToMaxSpeed^-2 +0.214236* aInitialSpeed^-1	0.291
performance = -19.600856+0.382092* aMaximumJerk^(1/-2) - 0.294457* aDesiredStartSpeed^-1 -0.169873* LN(aEngSpdAtMaxVSpeed^2) +0.478490* aMaximumQuirk^-1 - 0.376832* aMaxAccel^(1/-2) +0.208163* aInitialSpeed^-1 - 0.217147* aMaximumQuirk^-2	0.336

Table A6-3 - Correlation equations from all vehicle data

Full metric set, LWS fitting

Correlation equation	Coefficient of determination, R^2
smoothness = 46.627705+3.157130* aEngSpdAtMaxVSpeed^(1/-3) +0.282659* aMaximumJerk^-1 +0.059563* aDesiredStartSpeed^-1 +0.227722* aMaxPedalPosition^3 -0.345081* aMaxAccel^3	0.401

+0.259773* aDeltaEngSpd2MaxSpeed^2 -4.693334* aEngSpdAtMaxVSpeed^(1/-2)	
eng_delay = -889.966505-2.791493* aEngSpdAtMaxVSpeed^(1/-2) +0.264085* aMaximumQuirk^-1 +0.177542* aAverageJerk^(1/-2) -0.259682* aInitialSpeed^-1 +0.221475* aDeltaEngSpd2MaxSpeed^2 +2.052273* aEngSpdAtMaxVSpeed^(1/-3) -0.138231* aAverageAccelToMaxAccel^-2 +0.430519* aInitialPedalPosn^-1 +0.112920* aMaxPedalPosition^3 -0.301862* aInitialPedalPosn^-2 -0.060006* aMaxAccel^-2	0.372
vehicle_delay = -1279.264316+2.237813* aMaximumQuirk^-1 -4.293080* aMaximumQuirk^-2 -0.184768* aDesiredStartSpeed^-1 -0.268481* aMaxAccel^-1 +3.583961* aMaximumQuirk^-3 +0.189828* aDeltaEngSpd2MaxSpeed^2 -0.241735* aDesiredPedalPosition +0.490103* aDeltaEngSpd2MaxAccel^-1 +0.115251* aMaxSpeed^-3	0.454
init_accel = -371.599201+1.110665* aMaximumJerk^(1/-2) +0.268391* aEngSpdAtMaxVSpeed^(1/-2) -0.272385* aDesiredStartSpeed^-3 -0.457569* aMaxAccel^(1/-2) +0.327629* aInitialSpeed^-3 +0.486936* aMaximumJerk^2 +0.120397* AccelDelayTime^3 +0.371041* aMaximumQuirk^-3	0.403
accel_prog = 8277349.725604+2.603346* aEngSpdAtMaxVSpeed^(1/-2) -0.077394* aDesiredStartSpeed^-3 +153.440934* aMaximumQuirk^(1/-2) -0.322489* aInitialJerk^-1 +1.577470* aDeltaEngSpd2MaxSpeed^-2 -5.756553* aEngSpdAtMaxVSpeed^-3 -153.106464* aMaximumQuirk^(1/-3) +0.298456* aDeltaEngSpd2MaxSpeed^(1/3) +0.307895* aMaximumQuirk^-3	0.356
performance = 55.707605+0.376446* aMaximumJerk^(1/-2) +0.273567* aMaximumQuirk^-1 -0.441869* aMaxAccel^-1 -0.227737* aDesiredStartSpeed^-3 +1.306021* aDeltaEngSpd2MaxSpeed^-2 +5.882823* aEngSpdAtMaxVSpeed^(1/-3) +0.303608* aDeltaEngSpd2MaxSpeed -10.126801* aEngSpdAtMaxVSpeed^(1/-2) +0.263242* aInitialSpeed^-3 +0.162151* aEngSpdAtMaxVSpeed^3 +0.206228* aMaxAccel^-3 -0.099997* aDeltaEngSpd2MaxAccel^(1/3)	0.410

Table A6-4 - Correlation equations from all vehicle data

Acceleration and jerk metric set, least squares square fitting

Correlation equation	Coefficient of determination, R^2
smoothness = -2.584075e-005 +0.597055* aMaximumJerk^-1 +0.259131* aAverageJerk^(1/-2) +0.104146* AccelDelayTime^(1/-2) -0.255914* aMaximumJerk^-3 -0.112298* aAccelGradient^(1/-2) -0.081877* aMaximumJerk^3	0.319
eng_delay = -0.000113-0.101168* aAverageAccelToMaxAccel^-2 +0.247247* aAverageJerk^(1/-2) -0.124216* AccelDelayTime -0.518292* aInitialJerk^(1/-3) +0.412286* aMaximumJerk^-1 -0.377049* aAverageAccelToMaxSpeed^3 -0.140563* aMaximumJerk^-3	0.280
vehicle_delay = 2.490777e-007 +1.162722* aMaximumJerk^(1/-2) +0.747108* aMaximumJerk^2 -0.101395* aMaxAccel^-1 +0.171538* AccelDelayTime^(1/-2) +0.182012* aAverageJerk^(1/-2) -0.000342* aAccelGradient^2	0.343

init_accel = 6.261123e-008 +0.947213* aMaximumJerk^(1/-2) +0.312292* aAverageJerk^(1/-2) -0.348527* aMaxAccel^(1/-2) +0.495893* aMaximumJerk^2 -0.000482* aAccelGradient^2 +0.100952* aMaximumJerk^-2	0.353
accel_prog = -220.995428+0.655118* aMaximumJerk^(1/-2) +0.362433* aMaximumJerk^2 -0.437720* aMaxAccel^(1/-2) +0.219888* aMaximumJerk^-1 -0.201778* aAverageAccelToMaxAccel^3	0.166
performance = -444.940436+1.032522* aMaximumJerk^(1/-2) +0.596771* aMaximumJerk^2 -0.502009* aMaxAccel^(1/-2) +0.130990* LN(aAverageJerk^-1) +0.211125* aMaximumJerk^-1 - 0.305332* aMaxAccel^3 -0.161712* aInitialJerk^(1/-2)	0.328

Table A6-5 - Correlation equations from all vehicle data

Acceleration and jerk metric set, LWS fitting

Correlation equation	Coefficient of determination, R^2
smoothness = -1966992.422902+1.031094* aAverageJerk^(1/-2) +0.692955* aAverageJerk^2 +0.327829* aMaximumJerk^-1 +0.072834* aAccelGradient	0.371
eng_delay = -1123126.790221+0.680820* aAverageJerk^(1/-2) +0.460609* aAverageJerk^2 -0.440709* aInitialJerk^(1/-2) +0.281369* aMaximumJerk^-1 -0.321148* aAverageAccelToMaxSpeed^3 -1.153398* aAverageAccelToMaxAccel^-2 +1.492930* aAverageAccelToMaxAccel^-3 -0.552976* aInitialJerk^-2 +1.234772* aInitialJerk^-3	0.304
vehicle_delay = 7819515.983967+1.753009* aMaximumJerk^(1/-2) +2.509235* aMaximumJerk^2 +2943.627519* aAverageJerk^(1/-2) -0.107831* aAverageAccelToMaxAccel^-2 -0.141469* AccelDelayTime^3 -0.408198* aInitialJerk^(1/-2) -0.309220* aAverageAccelToMaxSpeed^3 -1.175383* aMaximumJerk^3 - 2943.389217* aAverageJerk^(1/-3)	0.438
init_accel = 17633597.044617+0.274603* aMaximumJerk^(1/-2) +6671.261982* aAverageJerk^(1/-2) -0.139662* aInitialJerk^-1 -6670.833313* aAverageJerk^(1/-3) -0.107770* AccelDelayTime^-2 -0.175119* aInitialJerk^(1/-2) +0.108937* aMaximumJerk^-2	0.407
accel_prog = -878292.077836+35.720588* aMaximumJerk^(1/-2) - 0.302982* aInitialJerk^-1 +35.308211* LN(aMaximumJerk^2) - 0.231149* aAverageAccelToMaxSpeed^-2 +0.514250* aAverageJerk^(1/-2) +0.358359* aAverageJerk^2 +0.159729* aAverageAccelToMaxSpeed^2	0.311
performance = 6153.352495+138.291641* aMaximumJerk^(1/-2) - 137.730468* aMaximumJerk^(1/-3) -0.574319* aMaxAccel^-1 +0.246036* aMaxAccel^-3 +0.194896* aMaximumJerk^-1 - 0.125852* aAverageJerk -0.101728* AccelDelayTime^-3	0.388

Correlations generated from AT only vehicle data

Table A6-6 - Correlation equations from AT-only vehicle data

Full metric set, least squares fitting

Correlation equation	Coefficient of determination, R^2
smoothness = -1.800415+54.854408* aMaximumJerk^(1/-2) - 54.617783* aMaximumJerk^(1/-3) -0.077619* aDesiredStartSpeed^-1 -0.334834* aEngSpdAtMaxVSpeed^(1/2) +0.301602* aDeltaEngSpd2MaxSpeed -0.318239* aMaxAccel^2 - 0.260731* aChangeInSpeed^(1/-3) +0.273113* aMaxPedalPosition^2 +0.159195* aDesiredPedalPosition^(1/-2) +0.140580* aMaxSpeed^-3 +0.149281* aMaxAccel^-2	0.570
eng_delay = -1.282772+67.751857* aMaximumJerk^(1/-2) - 67.378617* aMaximumJerk^(1/-3) -0.231785* aDesiredStartSpeed^-3 +0.212963* aDeltaEngSpd2MaxSpeed^2 +0.255147* aMaxSpeed^-2 -0.468114* aEngSpdAtMaxVSpeed^(1/2) - 0.155974* aEngSpdAtMaxVSpeed^(1/-2) +0.113559* aAccelGradient^(1/-3) +0.164236* aMaxPedalPosition^(1/2) +0.176590* aInitialJerk^(1/3) +0.161440* aEngSpdAtMaxVSpeed^3	0.527
vehicle_delay = 0.000139+105.322727* aMaximumJerk^(1/-2) - 104.734480* aMaximumJerk^(1/-3) -0.221174* aDesiredStartSpeed^-3 -0.211128* LN(aDesiredPedalPosition^2) +0.169644* aMaxSpeed^-2 +0.383326* aAccelGradient^(1/3) +0.243342* aMaxPedalPosition -0.450089* LN(aAccelGradient) +0.296750* aInitialJerk -0.106976* aChangeInSpeed^2 - 0.096348* aMaximumJerk^-2	0.650
init_accel = -1575.267209+0.891203* aMaximumJerk^(1/-2) +0.360824* aMaximumJerk^3	0.371
accel_prog = -1941.730580+1.175756* aMaximumJerk^(1/-2) +0.604541* aMaximumJerk^3 -0.107004* aDesiredStartSpeed^-3 - 0.174807* LN(aAccelGradient^-3)	0.437
performance = -418.988478+1.375909* aMaximumJerk^(1/-2) +0.858950* aMaximumJerk^2 -1.177823* aMaxAccel^-1 -0.167625* aDesiredStartSpeed^-2 +0.129039* aDesiredPedalPosition^(1/-2) +0.294814* aMaximumJerk^-1 -0.195565* aDeltaEngSpd2MaxAccel^(1/3) +0.757037* aDeltaEngSpd2MaxSpeed^2 -0.193516* aEngSpdAtMaxVSpeed^(1/3) - 0.103340* AccelDelayTime^-2 -0.485566* aDeltaEngSpd2MaxSpeed^3 +0.394028* aAverageAccelToMaxSpeed^-1 +0.349008* aMaxAccel^-2	0.573

Table A6-7 - Correlation equations from AT-only vehicle data

Full metric set, LWS fitting

Correlation equation	Coefficient of determination, R^2
smoothness = 1859.901030+57.222327* aMaximumJerk^(1/-2) - 57.029004* aMaximumJerk^(1/-3) -0.066817* aDesiredStartSpeed^-1 -0.245797* LN(aEngSpdAtMaxVSpeed^-1) +0.308191* aDeltaEngSpd2MaxSpeed +0.226141* aInitialSpeed^-3 +0.078260* aRateOfChangeOfPedalPosition^(1/-2) -0.297009*	0.585

aMaxAccel^3 +0.185367* aMaxPedalPosition^3 +0.215314* aMaximumJerk^-1 -0.583897* aEngSpdAtMaxVSpeed^(1/3) - 0.116341* aChangeInSpeed^(1/-3)	
eng_delay = 23472.389246+537.301132* aMaximumJerk^(1/-2) - 538.052023* aMaximumJerk^(1/-3) -0.179600* aChangeInSpeed^-2 -0.153806* aDesiredStartSpeed^-3 +0.165540* aDeltaEngSpd2MaxSpeed^2 +0.179450* aMaxSpeed^-3 -0.154383* AccelDelayTime^-3 +0.420031* aAverageAccelToMaxSpeed^-3 - 0.433461* aMaxAccel^-1 -1.643149* aMaximumJerk^3 +0.348325* aEngSpdAtMaxVSpeed^(1/-3)	0.533
vehicle_delay = 24384.426942+551.079547* aMaximumJerk^(1/-2) -551.763734* aMaximumJerk^(1/-3) -0.204031* aDesiredStartSpeed^-3 -0.573761* aMaxAccel^-1 -0.212863* LN(aDesiredPedalPosition) +0.183472* aDeltaEngSpd2MaxSpeed^2 -1.716598* aMaximumJerk^3 +0.491402* aMaxAccel^-3 +0.106910* aMaxSpeed^-3 -0.104086* LN(aDeltaEngSpd2MaxAccel^3) - 0.303466* aAverageAccelToMaxAccel^-2 +1.356811* aDeltaEngSpd2MaxAccel^-2	0.624
init_accel = -631.252133+39.600162* aMaximumJerk^(1/-2) +39.663731* aMaximumJerk -1.222803* aMaxAccel^-1 -0.201601* aDesiredStartSpeed^-1 +0.875688* aMaxAccel^-2 -0.188010* AccelDelayTime^-2 -0.266033* LN(aEngSpdAtMaxVSpeed^2) - 0.972017* aMaximumJerk^3 +0.136140* aInitialSpeed^-2	0.542
accel_prog = 2899.381927+3.386954* aMaximumJerk^(1/-2) +4.813424* aMaximumJerk^2 -1.048221* aMaxAccel^-1 +0.723607* aMaxAccel^-2 -2.202510* aMaximumJerk^3 -0.187889* aDesiredStartSpeed^-1 +0.195919* aDeltaEngSpd2MaxSpeed^2 - 0.203139* aEngSpdAtMaxVSpeed^(1/3) +0.587511* aRateOfChangeOfPedalPosition^-2 -0.041150* aAccelGradient^-1 +11.513688* aDeltaEngSpd2MaxAccel^-3 +0.158601* aMaxSpeed^-3	0.569
performance = 25997.164846+553.141313* aMaximumJerk^(1/-2) - 553.682580* aMaximumJerk^(1/-3) -0.727833* aMaxAccel^-1 +0.379557* aMaxAccel^-3 -1.592442* aMaximumJerk^3 -0.101840* aDesiredStartSpeed^-1 +0.220487* aDesiredPedalPosition^(1/-2) -0.126836* LN(aDeltaEngSpd2MaxAccel) -0.152226* aAccelGradient^(1/-2)	0.584

Table A6-8 - Correlation equations from AT-only vehicle data

Acceleration and jerk metric set, least squares fitting

Correlation equation	Coefficient of determination, R^2
smoothness = 5849.785791+145.760521* aMaximumJerk^(1/-2) - 145.191650* aMaximumJerk^(1/-3) -0.077632* AccelDelayTime^-3	0.421
eng_delay = 4680.449802+120.924665* aMaximumJerk^(1/-2) - 120.402626* aMaximumJerk^(1/-3) -0.485799* aMaxAccel^-1 +0.176101* aAverageAccelToMaxSpeed^-2 -0.134009* aAverageAccelToMaxAccel^3 +0.148312* aMaximumJerk^-1	0.365
vehicle_delay = 5327.191167+137.745862* aMaximumJerk^(1/-2) - 137.064261* aMaximumJerk^(1/-3) -0.778887* aMaxAccel^-1 - 0.230229* aAverageAccelToMaxSpeed^3 +0.669344* aMaxAccel^-2 - 0.187012* aAverageAccelToMaxAccel^-3	0.510
init_accel = -1575.267209+0.891203* aMaximumJerk^(1/-2)	0.371

+0.360824* aMaximumJerk^3	
accel_prog = -3163.936487+1346.568297* aMaximumJerk^(1/-2) - 0.398147* aMaxAccel^-1 +0.247524* aMaxAccel^-3 -639.601168* aMaximumJerk -0.266341* aAverageAccelToMaxAccel -1985.353275* LN(aMaximumJerk^-1) -0.626466* aAverageAccelToMaxSpeed^(1/-2) -0.301980* aAverageAccelToMaxSpeed^3	0.421
performance = -580.748004+1.721606* aMaximumJerk^(1/-2) +1.108995* aMaximumJerk^2 -0.511383* aMaxAccel^-1 +0.212513* aMaxAccel^-3 +0.129688* aMaximumJerk^-1	0.460

Table A6-9 - Correlation equations from AT-only vehicle data

Acceleration and jerk metric set, LWS fitting

Correlation equation	Coefficient of determination, R^2
smoothness = 1574761.207137+12751.535817* aMaximumJerk^(1/-2) -19033.036224* aMaximumJerk^(1/-3) -6282.182285* LN(aMaximumJerk) -0.090406* AccelDelayTime^-3	0.450
eng_delay = 29051.928410+557.903536* aMaximumJerk^(1/-2) - 558.693056* aMaximumJerk^(1/-3) -0.487039* aMaxAccel^-1 - 1.710024* aMaximumJerk^3 +0.179795* aAverageAccelToMaxSpeed^-2	0.394
vehicle_delay = -3298.411107+436.402789* aMaximumJerk^(1/-2) -436.837309* aMaximumJerk^(1/-3) -0.357524* aMaxAccel^-1 - 1.302969* aMaximumJerk^3 +0.123737* aAverageAccelToMaxSpeed^-3 -0.289839* aAverageAccelToMaxSpeed^3 +0.155508* aInitialJerk^2	0.539
init_accel = -527.204817+40.615953* aMaximumJerk^(1/-2) +40.739600* aMaximumJerk -0.698453* aMaxAccel^-1 +0.399683* aMaxAccel^-3 -0.152239* AccelDelayTime^-2 -1.002189* aMaximumJerk^3 -0.160194* aAverageAccelToMaxSpeed^3	0.471
accel_prog = 4947.686925+2.926697* aMaximumJerk^(1/-2) +3.622388* aMaximumJerk^2 -0.872512* aMaxAccel^-1 +0.543683* aMaxAccel^-2 +0.107270* AccelDelayTime^2 -1.475395* aMaximumJerk^3	0.434
performance = 27954.567910+529.835585* aMaximumJerk^(1/-2) - 530.227751* aMaximumJerk^(1/-3) -0.608626* aMaxAccel^-1 +0.306539* aMaxAccel^-3 -1.397983* aMaximumJerk^3 -0.155474* AccelDelayTime^-3	0.514

Appendix VII – Vehicle speed data re-generation

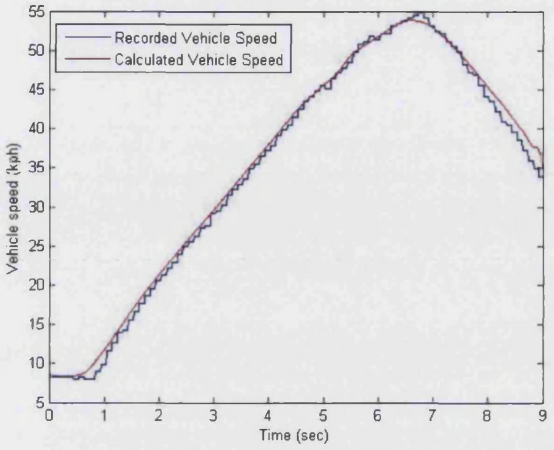

Figure A7-1 - Good accuracy

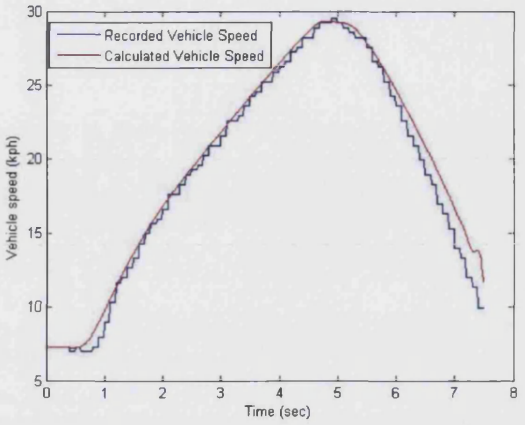

Figure A7-2 - Good accuracy

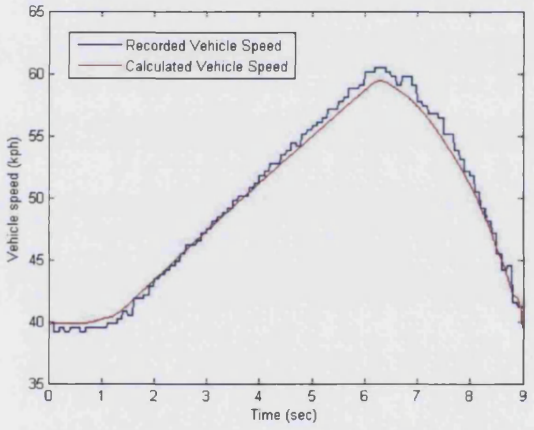

Figure A7-3 - Reasonable accuracy

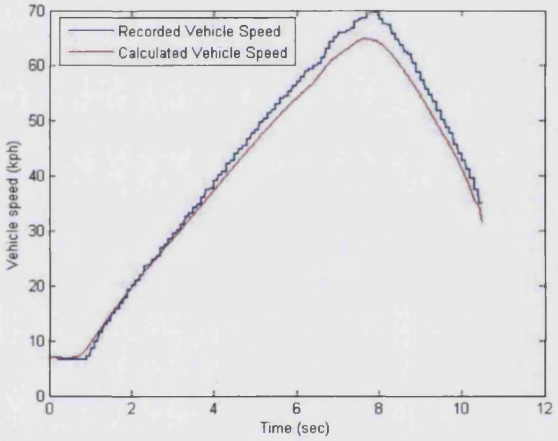

Figure A7-4 - Reasonable accuracy

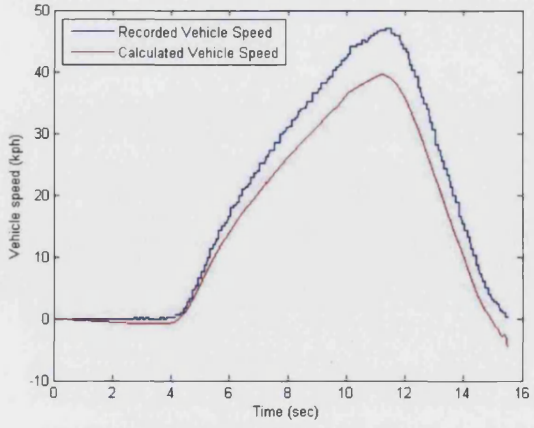

Figure A7-5 - Poor accuracy

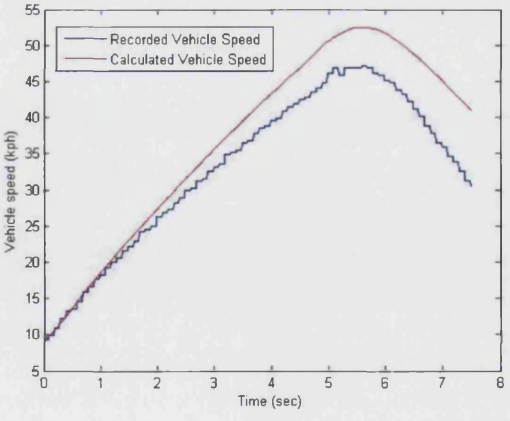

Figure A7-6 - Poor accuracy

Appendix VIII – Driver inter-correlations

The following drivers' correlation equations were tested on one another's data:
drb, vw, rsw, sgp, mcw, rdm, cjb, ac, ljn, acm, pjn, dmh, mdg, hhp, cdb.

The results are shown in the following tables. Any drivers' data which showed no correlations are excluded from the tables to save space.

Full metric set, LS fit

Table A8-10 - Smoothness

		Data														
	Driver	drb	vw	rsw	sgp	mcw	rdm	cjb	ac	ljn	acm	pjn	dmh	mdg	hhp	cdb
function	rsw	0	0	0.702	0.075	0	0	0.272	0.249	0.321	0.172	0	0.046	0.261	0.050	0.265
	mcw	0.241	0	0.317	0	0.674	0.062	0.174	0.370	0	0	0	0	0.102	0	0
	rdm	0	0	0.226	0	0	0.964	0.268	0.017	0.065	0	0.057	0.060	0	0	0
	cjb	0.342	0.214	0.219	0	0.018	0.139	0.336	0.213	0	0	0	0	0	0	0

Table A8-11 – Engine delay

		Data														
	Driver	drb	vw	rsw	sgp	mcw	rdm	cjb	ac	ljn	acm	pjn	dmh	mdg	hhp	cdb
function	mcw	0.088	0.032	0.225	0.190	0.624	0.052	0.072	0.162	0.161	0.150	0.244	0.228	0.191	0.138	0.216
	rdm	0.382	0	0.333	0	0.482	0.088	0.029	0	0	0	0	0	0	0	0
	cjb	0.092	0	0.080	0	0	0	0.582	0.112	0	0.125	0	0	0	0	0.162
	ljn	0	0	0	0	0	0	0.394	0.377	0.814	0	0.036	0	0.137	0.120	0.274
	cdb	0	0	0	0	0	0	0.022	0	0	0	0	0	0	0	0.992

Table A8-12 – Vehicle delay

		Data														
	Driver	drb	vw	rsw	sgp	mcw	rdm	cjb	ac	ljn	acm	pjn	dmh	mdg	hhp	cdb
function	drb	0.945	0	0.264	0	0	0	0	0	0	0	0	0	0	0	0
	sgp	0.187	0	0.324	0.998	0	0.295	0.508	0.269	0.173	0.203	0.195	0.133	0.184	0.311	0
	cjb	0.093	0.005	0.325	0	0	0	0.638	0.208	0.113	0.340	0.018	0.138	0.448	0.158	0.285
	ljn	0	0	0	0	0.449	0	0.460	0.513	0.654	0	0.167	0	0.075	0.112	0.176
	mdg	0.342	0.287	0.372	0.444	0.309	0.458	0.510	0.332	0.384	0.204	0.379	0.311	0.733	0.434	0.345
	cdb	0.009	0.037	0.365	0	0.122	0.078	0.228	0.360	0.155	0.189	0	0	0	0	0.497

Table A8-13 – Init_accel

		Data														
	Driver	drb	vw	rsw	sgp	mcw	rdm	cjb	ac	ljn	acm	pjn	dmh	mdg	hhp	cdb
function	drb	0.307	0	0.011	0	0	0.054	0	0	0	0	0	0	0	0	0
	vw	0.249	0.980	0.089	0	0	0.266	0.179	0	0	0	0	0	0	0	0
	rdm	0.135	0	0.103	0	0	0.857	0.002	0.081	0	0	0	0	0	0.193	0
	cjb	0.030	NaN	0.228	0.200	0	0	0.908	0.449	0.089	0	0.260	0	0.066	0.057	0
	ljn	0.032	0.013	0.189	0.393	0.094	0.050	0.082	0.165	0.428	0.183	0.223	0.263	0.306	0.142	0.209

Table A8-14 – Accel_prog

		Data														
	Driver	drb	vw	rsw	sgp	mcw	rdm	cjb	ac	ljn	acm	pjn	dmh	mdg	hhp	cdb
function	mcw	0.023	0	0.350	0	0.823	0.035	0.148	0.379	0	0	0.035	0.112	0.282	0.129	0.166
	rdm	0.210	0.026	0.078	0	0	0.667	0.097	0	0	0	0	0	0	0	0
	cjb	0	0	0.168	0.286	0	0	0.618	0.048	0.148	0.120	0.029	0.081	0.416	0.228	0.133
	ljn	0.121	0.129	0.365	0.063	0	0.154	0.295	0.366	0.852	0.141	0.310	0.320	0.365	0.332	0.239
	acm	0.398	0.256	0.311	0.394	0.081	0.308	0.503	0.343	0.278	0.513	0.060	0.311	0.497	0.350	0.379
	pjn	0.129	0.065	0.388	0.320	0.213	0.101	0.238	0.244	0.139	0.152	0.468	0.183	0.352	0.389	0.288

Table A8-15 - Performance

		Data														
	Driver	drb	vw	rsw	sgp	mcw	rdm	cjb	ac	ljn	acm	pjn	dmh	mdg	hhp	cdb
function	rdm	0.279	0.042	0.370	0.388	0.413	0.694	0.391	0.410	0.280	0.605	0.352	0.219	0.461	0.448	0.300
	cjb	0	0	0.147	0.002	0.231	0	0.726	0	0.246	0.189	0	0	0.282	0.265	0.247
	ljn	0	0	0	0	0	0	0	0	0.974	0	0.325	0	0.110	0	0.156
	acm	0	0	0	0	0	0	0	0	0	0.906	0	0	0	0	0

Full metric set, LWS fit

Table A8-16 – Smoothness

		Data														
	Driver	drb	vw	rsw	sgp	mcw	rdm	cjb	ac	ljn	acm	pjn	dmh	mdg	hhp	cdb
function	drb	0.368	0	0.340	0	0.401	0	0	0	0	0	0	0	0	0	0
	rsw	0.335	0.033	0.445	0	0.346	0.281	0.433	0	0	0	0	0	0	0	0
	mcw	0.048	0	0.331	0.159	0.656	0.090	0.095	0.151	0.048	0.008	0.164	0.062	0.071	0.018	0.073
	rdm	0	0	0.216	0	0	0.958	0.193	0	0.092	0	0.094	0.100	0	0	0
	cjb	0.083	0	0.480	0	0	0	0.627	0.241	0.076	0	0.080	0	0.024	0	0.444
	acm	0.151	0.131	0.250	0.202	0.152	0	0.187	0.166	0.338	0.417	0.187	0.192	0.151	0.270	0.193
	mdg	0	0	0.104	0.173	0	0	0	0.028	0.120	0	0.112	0	0.618	0.018	0.286
	hhp	0	0	0.083	0	0.036	0	0.004	0.045	0	0.020	0	0	0.066	0.469	0
	cdb	0	0	0	0	0	0	0.183	0	0.407	0	0.004	0	0	0	0.530

Table A8-17 – Engine delay

		Data														
	Driver	drb	vw	rsw	sgp	mcw	rdm	cjb	ac	ljn	acm	pjn	dmh	mdg	hhp	cdb
Function	drb	0.300	0	0	0	0	0.011	0.360	0	0	0	0	0	0	0	0
	sgp	0.326	0.061	0.334	0.487	0.239	0.240	0.312	0.318	0.015	0	0.166	0	0.375	0.153	0.232
	mcw	0.094	0.036	0.233	0.197	0.637	0.057	0.077	0.171	0.168	0.158	0.253	0.237	0.199	0.145	0.227
	ndv	0.305	0.216	0.389	0	0.160	0.269	0.336	0.362	0.242	0.167	0	0	0.147	0.020	0.234
	rdm	0.521	0.011	0.331	0	0.494	0.166	0.039	0	0	0	0	0	0	0	0
	cjb	0.097	0	0.332	0	0	0	0.340	0	0	0	0	0	0.059	0	0.091
	ljn	0	0	0	0	0	0	0.394	0.378	0.815	0	0.038	0	0.136	0.120	0.271
	pjn	0.244	0	0.171	0.237	0.105	0	0.068	0.019	0.196	0.018	0.417	0.282	0.022	0.203	0.199
	mdg	0	0	0.042	0	0	0	0	0	0	0	0	0	0.951	0	0.030

Table A8-18 – Vehicle delay

		Data														
	Driver	drb	vw	rsw	sgp	mcw	rdm	cjb	ac	ljn	acm	pjn	dmh	mdg	hhp	cdb
Function	drb	0.912	0	0	0	0	0	0	0	0	0	0	0	0	0	0
	rsw	0.112	0	0.372	0	0.264	0	0.259	0.231	0	0	0	0	0	0.207	0.149
	sgp	0.365	0.194	0.346	0.976	0	0.185	0.353	0.371	0	0.150	0.038	0	0.032	0.258	0.338
	ndv	0.181	0.068	0.471	0.282	0.325	0.461	0.471	0.404	0.393	0.308	0.235	0.292	0.350	0.320	0.412
	cjb	0.144	0.016	0.359	0	0	0	0.669	0.187	0.122	0.299	0	0.118	0.438	0.173	0.283
	ljn	0.324	0.295	0.398	0.193	0.123	0.327	0.415	0.373	0.587	0.378	0.360	0.361	0.384	0.372	0.403
	pjn	0.185	0	0.140	0.163	0.154	0	0.085	0.015	0.169	0.021	0.476	0.402	0.006	0.256	0.100
	mdg	0.073	0	0.121	0.347	0.148	-10	0.155	0.296	0.453	0	0.072	0.352	0.663	0.285	0.413
	cdb	0.011	0.042	0.370	0	0.125	0.084	0.232	0.365	0.152	0.188	0	0	0	0	0.520

Table A8-19 – Init_accel

		Data														
	Driver	drb	vw	rsw	sgp	mcw	rdm	cjb	ac	ljn	acm	pjn	dmh	mdg	hhp	cdb
Function	drb	0.452	0	0.008	0	0	0.052	0.025	0	0	0	0	0	0	0	0
	vw	0.282	0.929	0	0	0	0	0.053	0	0.052	0	0	0	0	0	0
	rsw	0.190	0	0.656	0.032	0	0.127	0.173	0.207	0	0	0	0	0.252	0	0
	rdm	0.359	0	0.355	0.353	0	0.901	0.225	0.391	0.321	0.340	0.189	0.298	0.355	0.375	0.394
	cjb	0.018	0	0.139	0	0	0	0.935	0.372	0	0	0.038	0	0	0	0
	ac	0.077	0	0.222	0	0	0.176	0.199	0.707	0	0	0	0	0	0	0
	ljn	0.032	0.013	0.191	0.379	0.093	0.050	0.081	0.166	0.421	0.185	0.219	0.265	0.299	0.145	0.211
	hhp	0.148	0.095	0.346	0.391	0.450	0.220	0.303	0.387	0	0	0.027	0	0.260	0.420	0.079

Table A8-20 – Accel_prog

		Data														
	Driver	drb	vw	rsw	sgp	mcw	rdm	cjb	ac	ljn	acm	pjn	dmh	mdg	hhp	cdb
Function	rsw	0.242	0	0.482	0.308	0.293	0	0.201	0.223	0	0	0.170	0.055	0.226	0.150	0.020
	mcw	0.076	0.065	0.214	0.078	0.812	0.071	0.112	0.199	0.146	0.131	0.224	0.162	0.129	0.226	0.220
	rdm	0.213	0.024	0.075	0	0	0.672	0.092	0	0	0	0	0	0	0	0
	cjb	0.081	0	0.154	0.308	0.002	0.011	0.521	0.040	0.058	0.200	0.125	0.006	0.315	0.039	0.144
	ljn	0.121	0.128	0.365	0.065	0	0.154	0.295	0.366	0.852	0.140	0.309	0.319	0.364	0.333	0.240
	acm	0.323	0.203	0.284	0.365	0.077	0.243	0.454	0.300	0.228	0.498	0.123	0.314	0.496	0.316	0.356
	pjn	0.024	0	0.388	0.340	0.211	0	0.178	0.250	0.159	0.123	0.626	0.125	0.342	0.440	0.272
	mdg	0	0	0	0.172	0.003	0	0.063	0.245	0.256	0	0	0.317	0.582	0.037	0.359

Table A8-21 – Performance

		Data														
	Driver	drb	vw	rsw	sgp	mcw	rdm	cjb	ac	ljn	acm	pjn	dmh	mdg	hhp	cdb
Function	drb	0.389	0	0.269	0	0.450	0	0	0	0	0	0	0	0	0	0
	rsw	0.034	0	0.423	0	0.468	0	0	0	0	0	0	0	0	0	0
	rdm	0.289	0.402	0.377	0.158	0	0.920	0.362	0.366	0.153	0.475	0.254	0.105	0.366	0.342	0
	cjb	0	0	0.177	0.219	0.428	0	0.551	0.342	0.504	0.476	0.500	0.386	0.350	0.564	0.420
	ac	0.381	0.305	0.415	0	0.331	0.138	0.269	0.398	0.002	0	0	0	0	0	0
	ljn	0	0	0	0	0	0	0	0	1.000	0	0	0	0	0	0
	acm	0.301	0.319	0.303	0.039	0.080	0	0.462	0.238	0.192	0.506	0.113	0.172	0.190	0.118	0.172

Acceleration and jerk metric subset, LS fit

Table A8-22 – Smoothness

		Data														
	Driver	drb	vw	rsw	sgp	mcw	rdm	cjb	ac	ljn	acm	pjn	dmh	mdg	hhp	cdb
Function	drb	0.368	0.000	0.340	0.000	0.401	0.000	0.000	0.000	0.000	0.000	0.000	0.000	0.000	0.000	0.000
	rsw	0.000	NaN	0.517	0.021	0.000	0.000	0.296	0.040	0.000	0.000	0.000	0.000	0.000	0.000	0.000
	mcw	0.048	0.000	0.331	0.159	0.656	0.090	0.095	0.151	0.048	0.008	0.164	0.062	0.071	0.018	0.073
	cjb	0.213	NaN	0.209	0.019	0.000	0.000	0.044	0.041	0.171	0.000	0.000	0.000	0.042	0.000	0.176

Table A8-23 – Engine delay

		Data														
	Driver	drb	vw	rsw	sgp	mcw	rdm	cjb	ac	ljn	acm	pjn	dmh	mdg	hhp	cdb
Function	rdm	0.521	0.011	0.331	0.000	0.494	0.166	0.039	0.000	0.000	0.000	0.000	0.000	0.000	0.000	0.000
	cjb	0.000	NaN	0.187	0.058	0.000	0.048	0.321	0.028	0.018	0.006	0.000	0.030	0.091	0.029	0.191
	ljn	0.202	0.200	0.411	0.000	0.078	0.230	0.258	0.304	0.575	0.004	0.127	0.105	0.230	0.183	0.300

Table A8-24 – Vehicle delay

		Data														
	Driver	drb	vw	rsw	sgp	mcw	rdm	cjb	ac	ljn	acm	pjn	dmh	mdg	hhp	cdb
Function	cjb	0.000	NaN	0.441	0.554	0.239	0.000	0.146	0.199	0.329	0.146	0.149	0.076	0.286	0.301	0.295
	ljn	0.178	0.105	0.377	0.185	0.371	0.142	0.237	0.333	0.581	0.000	0.022	0.128	0.295	0.316	0.186

Table A8-25 – Init_accel

		Data														
	Driver	drb	vw	rsw	sgp	mcw	rdm	cjb	ac	ljn	acm	pjn	dmh	mdg	hhp	cdb
Function	rdm	0.348	0.000	0.116	0.015	0.000	0.823	0.034	0.092	0.054	0.000	0.000	0.018	0.010	0.061	0.077
	cjb	0.046	0.000	0.332	0.412	0.401	0.000	0.585	0.513	0.500	0.402	0.329	0.388	0.381	0.267	0.311

Table A8-26 – Accel_prog

		Data														
	Driver	drb	vw	rsw	sgp	mcw	rdm	cjb	ac	ljn	acm	pjn	dmh	mdg	hhp	cdb
Function	rsw	0.242	NaN	0.482	0.308	0.293	0.000	0.201	0.223	0.000	0.000	0.170	0.055	0.226	0.150	0.020
	mcw	0.020	0.000	0.314	0.407	0.707	0.008	0.138	0.244	0.383	0.176	0.187	0.389	0.372	0.312	0.251
	rdm	0.228	0.039	0.093	0.000	0.038	0.514	0.105	0.037	0.000	0.000	0.000	0.000	0.000	0.000	0.000
	ljn	0.181	0.187	0.396	0.147	0.038	0.230	0.319	0.383	0.815	0.137	0.300	0.219	0.293	0.392	0.308

Table A8-27 – Performance

		Data														
	Driver	drb	vw	rsw	sgp	mcw	rdm	cjb	ac	ljn	acm	pjn	dmh	mdg	hhp	cdb
Function	drb	0.389	0.000	0.269	0.000	0.450	0.000	0.000	0.000	0.000	0.000	0.000	0.000	0.000	0.000	0.000
	rdm	0.345	0.074	0.073	0.000	0.000	0.785	0.052	0.006	0.000	0.000	0.000	0.000	0.000	0.000	0.000
	cjb	0.000	0.000	0.177	0.219	0.428	0.000	0.551	0.342	0.504	0.476	0.500	0.386	0.350	0.564	0.420
	ljn	0.181	0.186	0.393	0.013	0.000	0.243	0.301	0.367	0.618	0.075	0.228	0.150	0.126	0.264	0.235

Acceleration and jerk metric subset, LWS fit

Table A8-28 – Smoothness

		Data														
	Driver	drb	vw	rsw	sgp	mcw	rdm	cjb	ac	ljn	acm	pjn	dmh	mdg	hhp	cdb
Function	rsw	0.019	0.000	0.271	0.153	0.158	0.037	0.053	0.072	0.061	0.006	0.038	0.032	0.048	0.048	0.319
	mcw	0.018	0.000	0.252	0.146	0.567	0.045	0.058	0.104	0.031	0.000	0.124	0.041	0.055	0.003	0.071
	cjb	0.000	NaN	0.354	0.050	0.000	0.000	0.094	0.020	0.067	0.034	0.004	0.000	0.092	0.000	0.243

Table A8-29 – Engine delay

		Data														
	Driver	drb	vw	rsw	sgp	mcw	rdm	cjb	ac	ljn	acm	pjn	dmh	mdg	hhp	cdb
Function	rdm	0.382	0.000	0.333	0.000	0.482	0.088	0.029	0.000	0.000	0.000	0.000	0.000	0.000	0.000	0.000
	cjb	0.000	NaN	0.054	0.018	0.000	0.000	0.334	0.080	0.000	0.000	0.000	0.000	0.072	0.000	0.149
	ljn	0.368	0.410	0.458	0.000	0.000	0.465	0.309	0.419	0.555	0.000	0.084	0.104	0.134	0.085	0.264

Table A8-30 – Vehicle delay

		Data														
	Driver	drb	vw	rsw	sgp	mcw	rdm	cjb	ac	ljn	acm	pjn	dmh	mdg	hhp	cdb
Function	cjb	0.000	NaN	0.338	0.386	0.000	0.288	0.080	0.128	0.097	0.081	0.012	0.000	0.153	0.073	0.319
	ljn	0.179	0.105	0.378	0.185	0.372	0.144	0.239	0.336	0.596	0.000	0.023	0.129	0.305	0.324	0.188

Table A8-31 – Init_accel

		Data														
	Driver	drb	vw	rsw	sgp	mcw	rdm	cjb	ac	ljn	acm	pjn	dmh	mdg	hhp	cdb
Function	rdm	0.314	0.000	0.081	0.000	0.000	0.806	0.006	0.032	0.000	0.000	0.000	0.000	0.000	0.000	0.000
	cjb	0.000	0.000	0.394	0.354	0.215	0.000	0.672	0.489	0.311	0.201	0.257	0.320	0.244	0.011	0.208

Table A8-32 – Accel_prog

		Data														
	Driver	drb	vw	rsw	sgp	mcw	rdm	cjb	ac	ljn	acm	pjn	dmh	mdg	hhp	cdb
Function	mcw	0.000	0.000	0.236	0.000	0.843	0.012	0.000	0.000	0.000	0.000	0.000	0.000	0.000	0.000	0.000
	rdm	0.210	0.031	0.098	0.000	0.032	0.479	0.112	0.043	0.000	0.000	0.000	0.000	0.000	0.000	0.000
	ljn	0.181	0.188	0.397	0.144	0.042	0.231	0.321	0.384	0.819	0.140	0.299	0.222	0.292	0.392	0.305

Table A8-33 – Performance

		Data														
	Driver	drb	vw	rsw	sgp	mcw	rdm	cjb	ac	ljn	acm	pjn	dmh	mdg	hhp	cdb
Function	rdm	0.341	0.073	0.074	0.000	0.000	0.783	0.052	0.006	0.000	0.000	0.000	0.000	0.000	0.000	0.000
	cjb	0.000	0.000	0.101	0.077	0.437	0.000	0.394	0.200	0.436	0.350	0.299	0.213	0.392	0.430	0.372
	ljn	0.137	0.137	0.361	0.000	0.060	0.164	0.286	0.340	0.682	0.024	0.243	0.154	0.278	0.311	0.238

Appendix IX – Driver auto-correlations

The following tables show the auto-correlations for the driver subsets (that is the results produced by applying the correlation equation to the data with which it was produced). These are therefore an accurate representation of the trends for the various drivers' data.

Table A9-34 – Driver subset autocorrelations
using full metric set, least squares fit correlation to all drivers

Driver	smoothness	eng_delay	vehicle_delay	init_accel	accel_prog	performance
ac	0	0	0	0	0	0
acm	0	0	0	0	0.513	0.906
cdb	0	0.992	0.497	0	0	0
cjb	0.336	0.582	0.638	0.908	0.618	0.726
dmh	0	0	0	0	0	0
drb	0	0	0.945	0.307	0	0
hhp	0	0	0	0	0	0
ljn	0	0.814	0.654	0.428	0.852	0.974
mcw	0.674	0.624	0	0	0.823	0
mdg	0	0	0.733	0	0	0
ndv	0	0	0	0	0	0
pjn	0	0	0	0	0.468	0
rdm	0.964	0.088	0	0.857	0.667	0.694
rsw	0.702	0	0	0	0	0
sa	0	0	0	0	0	0
sgp	0	0	0.998	0	0	0
vw	0	0	0	0.980	0	0

Table A9-35 – Driver subset autocorrelations
using full metric set, LWS fit correlation to all drivers

Driver	smoothness	eng_delay	vehicle_delay	init_accel	accel_prog	performance
ac	0	0	0	0.707	0	0.398
acm	0.417	0	0	0	0.498	0.506
cdb	0.530	0	0.520	0	0	0
cjb	0.627	0.666	0.669	0.935	0.521	0.551
dmh	0	0	0	0	0	0
drb	0.368	0.300	0.945	0.452	0	0.389
hhp	0.469	0	0	0.420	0	0
ljn	0	0.815	0.587	0.421	0.852	1.000
mcw	0.656	0.637	0	0	0.812	0
mdg	0.618	0.951	0.663	0	0.582	0
ndv	0	0.992	0.828	0	0	0
pjn	0	0.417	0.476	0	0.626	0
rdm	0.964	0.166	0	0.901	0.672	0.920
rsw	0.445	0	0.372	0.666	0.482	0.423
sa	0	0	0	0	0	0
sgp	0	0.487	0.976	0	0	0
vw	0	0	0	0.929	0	0

Table A9-36 – Driver subset autocorrelations

using acceleration and jerk metric set, least squares fit correlation to all drivers

Driver	smoothness	eng_delay	vehicle_delay	init_accel	accel_prog	performance
ac	0	0	0	0	0	0
acm	0	0	0	0	0	0
cdb	0	0	0	0	0	0
cjb	0.460	0.534	0.440	0.672	0	0.394
dmh	0	0	0	0	0	0
drb	0	0	0	0	0	0
hhp	0	0	0	0	0	0
ljn	0	0.555	0.596	0	0.819	0.682
mcw	0.567	0	0	0	0.843	0
mdg	0	0	0	0	0	0
ndv	0	0	0	0	0	0
pjn	0	0	0	0	0	0
rdm	0	0.088	0	0.806	0.479	0.783
rsw	0.271	0	0	0	0	0
sa	0	0	0	0	0	0
sgp	0	0	0	0	0	0
vw	0	0	0	0	0	0

Table A9-37 – Driver subset autocorrelations

using acceleration and jerk metric set, LWS fit correlation to all drivers

Driver	smoothness	eng_delay	vehicle_delay	init_accel	accel_prog	performance
ac	0	0	0	0.817	0	0
acm	0	0	0	0	0	0
cdb	0	0	0	0	0	0
cjb	0.521	0.548	0.461	0.585	0	0.551
dmh	0	0	0	0	0	0
drb	0.368	0	0	0	0	0.389
hhp	0	0	0	0	0	0
ljn	0	0.575	0.581	0	0.815	0.618
mcw	0.656	0	0	0	0.707	0
mdg	0	0	0	0	0	0
ndv	0	0	0	0	0	0
pjn	0	0	0	0	0	0
rdm	0	0.166	0	0.823	0.514	0.785
rsw	0.526	0	0	0	0.482	0
sa	0	0	0	0	0	0
sgp	0	0	0	0	0	0
vw	0	0	0	0	0	0

Appendix X – Correlation Results

Test function and data from same group of vehicles

Train using all vehicles

Table A10-38 - Full metric set LS fitting

Data subset	accel_prog	eng_delay	init_accel	performance	smoothness	vehicle_delay
All data	0.296	0.297	0.407	0.333	0.366	0.396
25% pedal	0.102	0.147	0.112	0.030	0.110	0.125
50% pedal	0.110	0.042	0.063	0.001	0.183	0
75% pedal	0.034	0.085	0.006	0.130	0.130	0.102
100% pedal	0.271	0.212	0.387	0.281	0.158	0.269
0 kph	0	0	0	0	0	0
2 kph	0.240	0.413	0.613	0.483	0.482	0.591
12 kph	0.209	0.153	0.253	0.260	0.278	0.284
40 kph	0.104	0.194	0.098	0.110	0.130	0.195
60 kph	0.196	0.127	0.319	0.208	0.260	0.278
Launch Feel	0	0	0	0	0	0
Performance Feel	0.278	0.175	0.402	0.266	0.156	0.262
Traffic Crawl	0.215	0.237	0.245	0.171	0.294	0.244
BMW	0.171	0.223	0	0.108	0.228	0.197
Me	0.007	0.034	0.024	0.077	0.003	0.023
Ms	0.092	0.102	0.092	0.199	0.041	0.307
Omega	0.048	0.045	0.079	0.015	0.122	0.006
PRIUS	0	0	0	0	0	0
CVT Mondeo	0	0	0	0	0	0

Table A10-39 - Full metric set LWS fitting

Data subset	accel_prog	eng_delay	init_accel	performance	smoothness	vehicle_delay
All data	0.343	0.144	0.403	0.387	0.408	0.371
25% pedal	0.200	0.110	0.090	0.097	0.186	0.048
50% pedal	0.109	0.094	0	0	0.130	0.013
75% pedal	0.168	0.036	0.102	0.151	0.161	0.155
100% pedal	0.341	0.110	0.382	0.358	0.288	0.249
0 kph	0	0.063	0	0	0	0
2 kph	0.165	0.054	0.634	0.536	0.489	0.543
12 kph	0.193	0.158	0.311	0.266	0.312	0.325
40 kph	0.324	0.213	0.109	0.085	0.298	0.276
60 kph	0.353	0.095	0.266	0.304	0.387	0.259
Launch Feel	0	0.052	0	0	0	0
Performance Feel	0.332	0.110	0.362	0.338	0.283	0.231
Traffic Crawl	0.240	0.181	0.232	0.234	0.341	0.169
BMW	0.346	0.201	0.158	0.176	0.230	0.122
Me	0.268	0.008	0.095	0.138	0.108	0.122
Ms	0.181	0.042	0.148	0.189	0.103	0.276
Omega	0.023	0.044	0	0.008	0.134	0.087
PRIUS	0	0.005	0	0	0	0
CVT Mondeo	0	0.004	0	0	0	0

Table A10-40 - Acceleration and jerk metrics, LS fitting

Data subset	accel_prog	eng_delay	init_accel	performance	smoothness	vehicle_delay
All data	0.167	0.224	0.266	0.274	0.266	0.345
25% pedal	0.048	0.053	0.108	0.100	0.064	0.051
50% pedal	0.015	0.082	0.019	0.053	0.071	0.032
75% pedal	0.213	0.257	0.314	0.282	0.209	0.376
100% pedal	0.136	0.149	0.230	0.229	0.141	0.257
0 kph	0.084	0.170	0.151	0.175	0.152	0.285
2 kph	0.226	0.336	0.440	0.378	0.332	0.552
12 kph	0.165	0.176	0.300	0.281	0.250	0.282
40 kph	0.148	0.177	0.228	0.236	0.252	0.316
60 kph	0.123	0.062	0.155	0.219	0.286	0.145
Launch Feel	0.052	0.143	0.144	0.155	0.106	0.256
Performance Feel	0.144	0.084	0.209	0.228	0.147	0.168
Traffic Crawl	0.097	0.154	0.153	0.171	0.209	0.199
BMW	0.028	0.069	0.022	0.045	0.111	0.057
Me	0.144	0.127	0.112	0.149	0.097	0.118
Ms	0.194	0.173	0.186	0.244	0.084	0.249
Omega	0.078	0.078	0.048	0.118	0.182	0.064
PRIUS	0	0	0	0.047	0.123	0
CVT Mondeo	0	0	0	0	0	0

Table A10-41 - Acceleration and jerk metrics, LWS fitting

Data subset	accel_prog	eng_delay	init_accel	performance	smoothness	vehicle_delay
All data	0.236	0.239	0.315	0.309	0.242	0.399
25% pedal	0.092	0.098	0.108	0.142	0.021	0.045
50% pedal	0.004	0.085	0.038	0.064	0.005	0
75% pedal	0.183	0.267	0.339	0.304	0.234	0.387
100% pedal	0.187	0.151	0.269	0.255	0.176	0.319
0 kph	0.176	0.173	0.202	0.195	0.125	0.319
2 kph	0.299	0.377	0.487	0.460	0.402	0.627
12 kph	0.204	0.205	0.343	0.331	0.249	0.361
40 kph	0.264	0.201	0.264	0.270	0.215	0.375
60 kph	0.196	0.088	0.153	0.261	0.432	0.354
Launch Feel	0.059	0.145	0.171	0.169	0.118	0.286
Performance Feel	0.250	0.088	0.207	0.263	0.371	0.375
Traffic Crawl	0.127	0.192	0.204	0.217	0.160	0.275
BMW	0.036	0.079	0.002	0.068	0.083	0.106
Me	0.287	0.107	0.098	0.162	0.094	0.142
Ms	0.181	0.163	0.176	0.269	0.350	0.360
Omega	0.058	0.116	0.129	0.127	0.159	0
PRIUS	0.325	0	0	0.077	0.150	0
CVT Mondeo	0	0	0	0	0	0

Only the AT equipped vehicles

Table A10-42 - Full metric set, LS fit

Data subset	accel_prog	eng_delay	init_accel	performance	smoothness	vehicle_delay
All data	0.437	0.527	0.371	0.573	0.570	0.650
25% pedal	0.134	0.398	0.147	0.307	0.419	0.370
50% pedal	0.203	0.265	0.125	0.305	0.396	0.480
75% pedal	0.213	0.022	0.393	0.001	0.034	0.080
100% pedal	0.358	0.383	0.288	0.407	0.358	0.500
0 kph	0	0	0.186	0	0	0
2 kph	0.222	0	0.461	0	0	0.110
12 kph	0.444	0.434	0.408	0.468	0.436	0.563
40 kph	0.376	0.540	0.375	0.516	0.596	0.640
60 kph	0.407	0.318	0.359	0.368	0.494	0.508
Launch Feel	0	0	0.202	0	0	0
Performance Feel	0.371	0.338	0.326	0.420	0.379	0.423
Traffic Crawl	0.203	0.472	0.171	0.425	0.483	0.513
BMW	0.017	0.090	0.033	0	0.134	0.143
Me	0.141	0	0.199	0.089	0.026	0.011
Ms	0.265	0.052	0.267	0.146	0.116	0.208
Omega	0	0	0.045	0.187	0.108	0

Table A10-43 - Full metric set, LWS fit

Data subset	accel_prog	eng_delay	init_accel	performance	smoothness	vehicle_delay
All data	0.569	0.533	0.542	0.584	0.585	0.624
25% pedal	0.207	0.475	0.332	0.279	0.404	0.413
50% pedal	0.331	0.446	0.354	0.397	0.391	0.383
75% pedal	0.021	0	0.027	0.040	0	0
100% pedal	0.531	0.359	0.507	0.497	0.348	0.490
0 kph	0	0	0	0	0	0
2 kph	0	0	0.110	0.048	0	0.059
12 kph	0.567	0.399	0.476	0.578	0.462	0.513
40 kph	0.516	0.572	0.258	0.573	0.057	0.554
60 kph	0.460	0.373	0.327	0.486	0.450	0.527
Launch Feel	0	0	0	0	0	0
Performance Feel	0.382	0.401	0.399	0.413	0.342	0.457
Traffic Crawl	0.372	0.518	0.428	0.442	0.473	0.487
BMW	0.162	0	0.120	0.168	0.156	0.252
Me	0	0	0.058	0.058	0	0
Ms	0.165	0.116	0.165	0.187	0.078	0.326
Omega	0	0.342	0.213	0.082	0.061	0.178

Table A10-44 - Acceleration and jerk metrics, LS fit

Data subset	accel_prog	eng_delay	init_accel	performance	smoothness	vehicle_delay
All data	0.401	0.365	0.371	0.460	0.421	0.510
25% pedal	0.151	0.185	0.147	0.255	0.287	0.241
50% pedal	0.197	0.202	0.125	0.253	0.241	0.296
75% pedal	0.468	0.406	0.393	0.452	0.387	0.543
100% pedal	0.342	0.262	0.288	0.364	0.278	0.398
0 kph	0.303	0.240	0.186	0.316	0.263	0.403
2 kph	0.228	0.157	0.461	0.203	0.393	0.336
12 kph	0.444	0.399	0.408	0.468	0.420	0.483
40 kph	0.321	0.252	0.375	0.397	0.384	0.424
60 kph	0.317	0.293	0.359	0.410	0.442	0.428
Launch Feel	0.314	0.245	0.202	0.314	0.258	0.415
Performance Feel	0.347	0.272	0.326	0.388	0.312	0.367
Traffic Crawl	0.199	0.246	0.171	0.296	0.306	0.323
BMW	0.040	0.048	0.033	0.078	0.062	0.068
Me	0.152	0.112	0.199	0.229	0.154	0.143
Ms	0.283	0.198	0.267	0.318	0.194	0.284
Omega	0.061	0.054	0.045	0.118	0.130	0.067

Table A10-45 - Acceleration and jerk metrics, LWS fit

Data subset	accel_prog	eng_delay	init_accel	performance	smoothness	vehicle_delay
All data	0.434	0.394	0.471	0.514	0.450	0.539
25% pedal	0.242	0.287	0.310	0.397	0.392	0.387
50% pedal	0.300	0.271	0.331	0.425	0.317	0.372
75% pedal	0.503	0.430	0.507	0.458	0.367	0.537
100% pedal	0.371	0.329	0.413	0.450	0.295	0.448
0 kph	0.320	0.255	0.349	0.388	0.279	0.437
2 kph	0.100	0.003	0.188	0.090	0.429	0.251
12 kph	0.496	0.432	0.479	0.520	0.425	0.524
40 kph	0.399	0.432	0.446	0.494	0.542	0.533
60 kph	0.462	0.397	0.328	0.466	0.500	0.493
Launch Feel	0.317	0.247	0.333	0.360	0.248	0.424
Performance Feel	0.453	0.391	0.364	0.386	0.319	0.454
Traffic Crawl	0.317	0.347	0.371	0.460	0.402	0.440
BMW	0.036	0.108	0.059	0.071	0.122	0.147
Me	0.122	0.087	0.114	0.143	0.029	0.061
Ms	0.244	0.262	0.272	0.274	0.127	0.315
Omega	0.135	0.125	0.208	0.277	0.194	0.130

Test function and data from same vehicle

BMW

Table A10-46 - All metrics, LS fit

Data subset	accel_prog	eng_delay	init_accel	performance	smoothness	vehicle_delay
All data	0	0	0.117	0	0	0
25% pedal	0	0	0	0	0	0
50% pedal	0	0	0	0	0	0
75% pedal	0	0	0.036	0	0	0
100% pedal	0	0	0.162	0	0	0
0 kph	0	0	0.132	0	0	0
2 kph	0	0	0	0	0	0
12 kph	0	0	0.145	0	0	0
40 kph	0	0	0	0	0	0
60 kph	0	0	0	0	0	0
Launch Feel	0	0	0.094	0	0	0
Performance Feel	0	0	0	0	0	0
Traffic Crawl	0	0	0	0	0	0

Table A10-47 - All metrics, LWS fit

Data subset	accel_prog	eng_delay	init_accel	performance	smoothness	vehicle_delay
All data	0.216	0	0.251	0	0	0.358
25% pedal	0.311	0	0.375	0	0	0.421
50% pedal	0	0	0	0	0	0
75% pedal	0	0	0	0	0	0
100% pedal	0	0	0	0	0	0
0 kph	0	0	0	0	0	0
2 kph	0	0	0	0	0	0
12 kph	0.011	0	0.024	0	0	0
40 kph	0.353	0	0.370	0	0	0.343
60 kph	0	0	0	0	0	0
Launch Feel	0	0	0	0	0	0
Performance Feel	0	0	0	0	0	0
Traffic Crawl	0.312	0	0.345	0	0	0.434

Table A10-48 – Acceleration and jerk metric subset, LS fit

Data subset	accel_prog	eng_delay	init_accel	performance	smoothness	vehicle_delay
All data	0	0	0.085	0	0	0
25% pedal	0	0	0	0	0	0
50% pedal	0	0	0	0	0	0
75% pedal	0	0	0.025	0	0	0
100% pedal	0	0	0.068	0	0	0
0 kph	0	0	0.102	0	0	0
2 kph	0	0	0	0	0	0
12 kph	0	0	0.096	0	0	0
40 kph	0	0	0.009	0	0	0
60 kph	0	0	0	0	0	0
Launch Feel	0	0	0.051	0	0	0
Performance Feel	0	0	0	0	0	0
Traffic Crawl	0	0	0	0	0	0

Table A10-49 – Acceleration and jerk metric subset, LWS fit

Data subset	accel_prog	eng_delay	init_accel	performance	smoothness	vehicle_delay
All data	0.210	0	0.251	0	0	0.269
25% pedal	0.301	0	0.375	0	0	0.430
50% pedal	0	0	0	0	0	0.035
75% pedal	0	0	0	0	0	0
100% pedal	0	0	0	0	0	0.052
0 kph	0	0	0	0	0	0
2 kph	0	0	0	0	0	0
12 kph	0.002	0	0.024	0	0	0
40 kph	0.342	0	0.370	0	0	0.408
60 kph	0	0	0	0	0	0.138
Launch Feel	0	0	0	0	0	0
Performance Feel	0	0	0	0	0	0.076
Traffic Crawl	0.308	0	0.345	0	0	0.412

AT Mondeo (economy mode)

Table A10-50 - All metrics, LS fit

Data subset	accel_prog	eng_delay	init_accel	performance	smoothness	vehicle_delay
All data	0.159	0	0.221	0.287	0	0
75% pedal	0.097	0	0.121	0.179	0	0
100% pedal	0.176	0	0.265	0.349	0	0
0 kph	0	0	0	0	0	0
2 kph	0	0	0	0	0	0
12 kph	0.047	0	0	0	0	0
40 kph	0	0	0	0.099	0	0
60 kph	0	0	0.434	0.025	0	0
Launch Feel	0	0	0	0	0	0
Performance Feel	0.187	0	0.281	0.346	0	0

Table A10-51 - All metrics, LWS fit

Data subset	accel_prog	eng_delay	init_accel	performance	smoothness	vehicle_delay
All data	0.088	0	0.413	0.460	0	0.235
75% pedal	0.020	0	0.084	0.118	0	0.342
100% pedal	0	0	0.471	0.521	0	0
0 kph	0	0	0	0	0	0.321
2 kph	0	0	0	0	0	0.259
12 kph	0	0	0	0	0	0
40 kph	0	0	0.013	0	0	0
60 kph	0	0	0.346	0.411	0	0
Launch Feel	0	0	0	0	0	0.321
Performance Feel	0.117	0	0.491	0.539	0	0.011

Table A10-52 – Acceleration and jerk metric subset, LS fit

Data subset	accel_prog	eng_delay	init_accel	performance	smoothness	vehicle_delay
All data	0.136	0	0	0.186	0	0
75% pedal	0.174	0	0	0.187	0	0
100% pedal	0.093	0	0	0.167	0	0
0 kph	0	0	0	0	0	0
2 kph	0	0	0	0	0	0
12 kph	0	0	0	0.097	0	0
40 kph	0	0	0	0	0	0
60 kph	0	0	0	0.116	0	0
Launch Feel	0	0	0	0	0	0
Performance Feel	0.077	0	0	0.154	0	0

Table A10-53 – Acceleration and jerk metric subset, LWS fit

Data subset	accel_prog	eng_delay	init_accel	performance	smoothness	vehicle_delay
All data	0.088	0	0.317	0.348	0	0
75% pedal	0.020	0	0.045	0.070	0	0
100% pedal	0	0	0.387	0.063	0	0
0 kph	0	0	0	0	0	0
2 kph	0	0	0	0	0	0
12 kph	0	0	0	0	0	0
40 kph	0	0	0	0	0	0
60 kph	0	0	0	0.445	0	0
Launch Feel	0	0	0	0	0	0
Performance Feel	0.117	0	0.060	0.428	0	0

AT Mondeo (sports mode) function

Table A10-54 - All metrics, LS fit

Data subset	accel_prog	eng_delay	init_accel	performance	smoothness	vehicle_delay
All data	0.166	0	0	0	0	0.208
25% pedal	0	0	0	0	0	0
50% pedal	0	0	0	0	0	0
75% pedal	0	0	0	0	0	0
100% pedal	0	0	0	0	0	0
0 kph	0.078	0	0	0	0	0
2 kph	0.141	0	0	0	0	0.229
12 kph	0	0	0	0	0	0.179
40 kph	0	0	0	0	0	0
60 kph	0	0	0	0	0	0
Launch Feel	0	0	0	0	0	0
Performance Feel	0	0	0	0	0	0.045
Traffic Crawl	0	0	0	0	0	0

Table A10-55 - All metrics, LWS fit

Data subset	accel_prog	eng_delay	init_accel	performance	smoothness	vehicle_delay
All data	0	0.181	0.181	0	0	0.352
25% pedal	0	0	0	0	0	0
50% pedal	0	0	0	0	0	0
75% pedal	0	0	0	0	0	0
100% pedal	0	0	0	0	0	0
0 kph	0	0	0.024	0	0	0
2 kph	0	0	0.156	0	0	0.114
12 kph	0	0	0.097	0	0	0.055
40 kph	0	0	0	0	0	0
60 kph	0	0	0	0	0	0
Launch Feel	0	0	0	0	0	0
Performance Feel	0	0	0	0	0	0.036
Traffic Crawl	0	0	0.039	0	0	0

Table A10-56 – Acceleration and jerk metric subset, LS fit

Data subset	accel_prog	eng_delay	init_accel	performance	smoothness	vehicle_delay
All data	0.085	0	0	0	0	0
25% pedal	0.015	0	0	0	0	0
50% pedal	0.080	0	0	0	0	0
75% pedal	0.033	0	0	0	0	0
100% pedal	0	0	0	0	0	0
0 kph	0.092	0	0	0	0	0
2 kph	0.081	0	0	0	0	0
12 kph	0	0	0	0	0	0
40 kph	0	0	0	0	0	0
60 kph	0	0	0	0	0	0
Launch Feel	0.006	0	0	0	0	0
Performance Feel	0	0	0	0	0	0
Traffic Crawl	0.049	0	0	0	0	0

Table A10-57 – Acceleration and jerk metric subset, LWS fit

Data subset	accel_prog	eng_delay	init_accel	performance	smoothness	vehicle_delay
All data	0	0.122	0	0	0	0
25% pedal	0	0	0	0	0	0
50% pedal	0	0	0	0	0	0
75% pedal	0	0	0	0	0	0
100% pedal	0	0.010	0	0	0	0
0 kph	0	0	0	0	0	0
2 kph	0	0	0	0	0	0
12 kph	0	0	0	0	0	0
40 kph	0	0	0	0	0	0
60 kph	0	0	0	0	0	0
Launch Feel	0	0	0	0	0	0
Performance Feel	0	0.017	0	0	0	0
Traffic Crawl	0	0	0	0	0	0

Appendix XI – Time-series data Fourier analysis

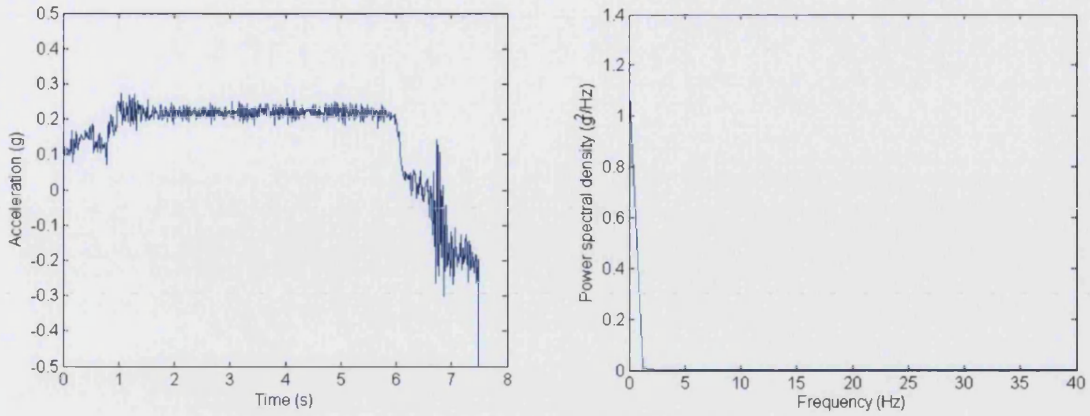

Figure A11-7 – Acceleration data and power spectral density

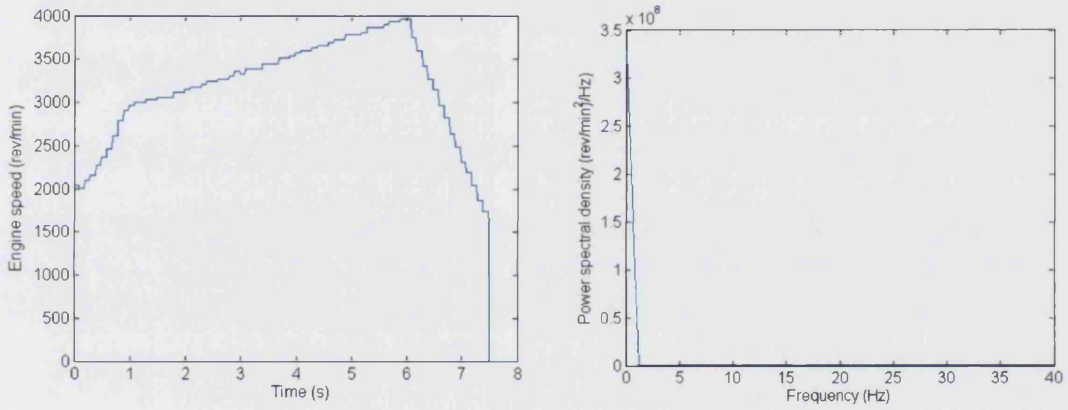

Figure A11-8 – Engine speed data and power spectral density

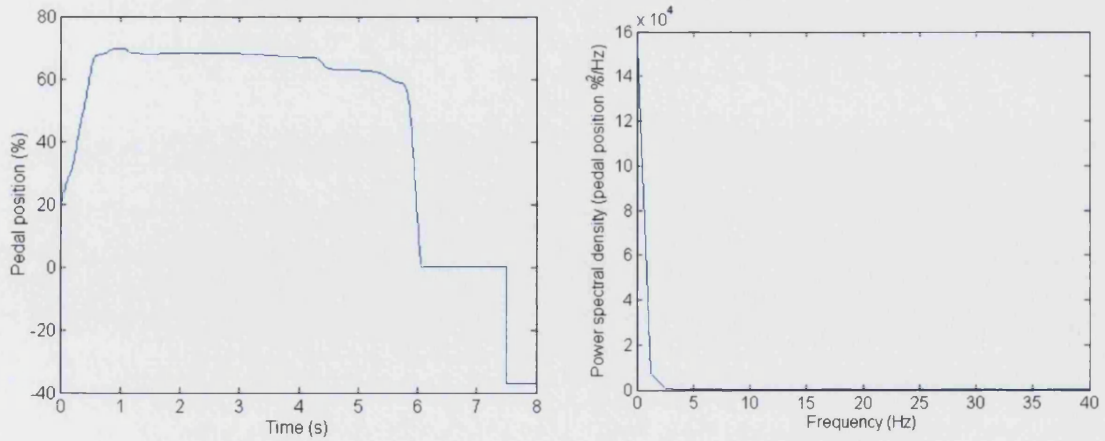

Figure A11-9 – Pedal position data and power spectral density

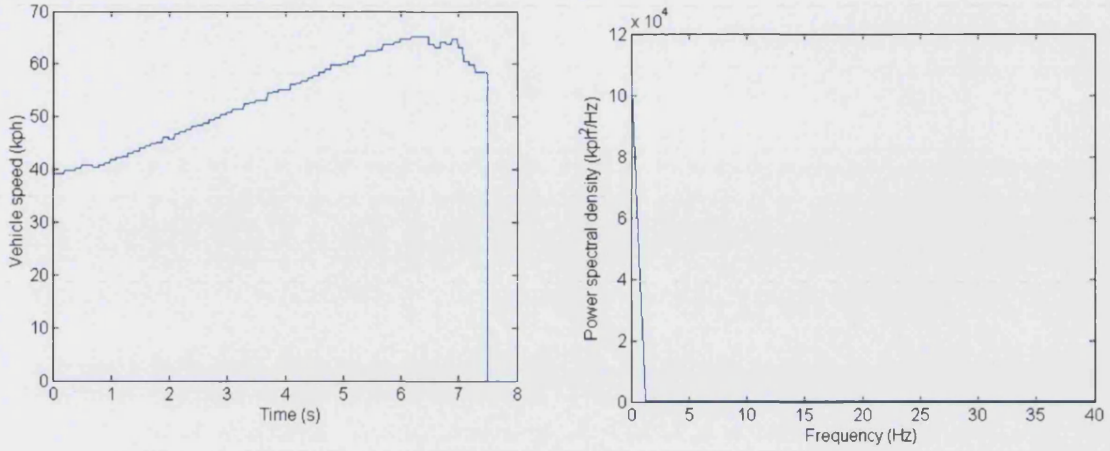

Figure A11-10 – Vehicle speed data and power spectral density

Appendix XII – Actual vs. predicted subjective metrics for AT vehicle data using all objective metrics

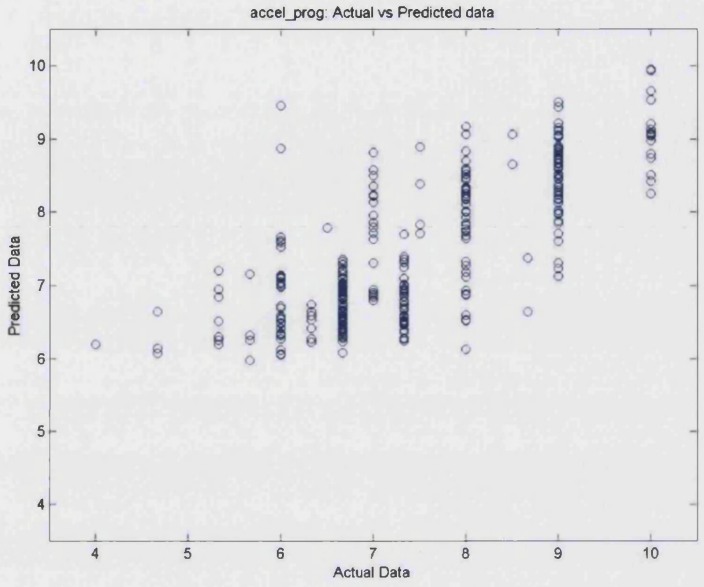

Figure A12-11 – Plot of predicted and recorded *accel_prog* ratings

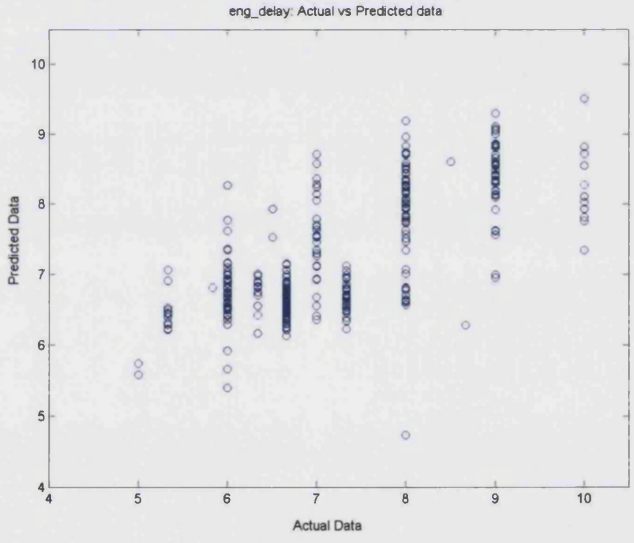

Figure A12-12 - Plot of predicted and recorded *eng_delay* ratings

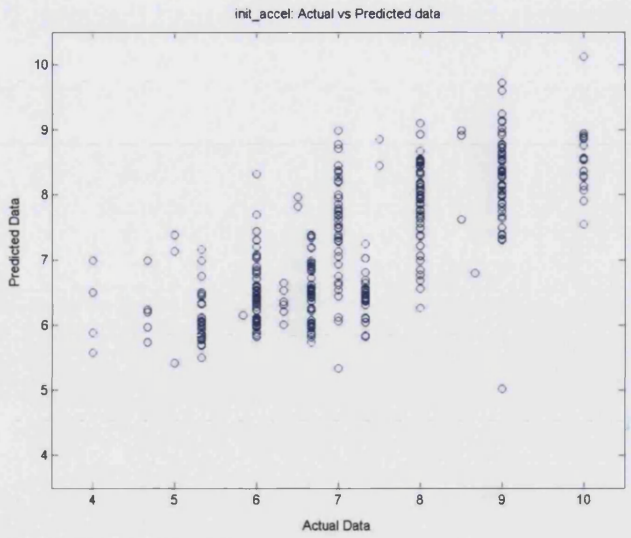

Figure A12-13 – Plot of predicted and recorded *init_accel* ratings

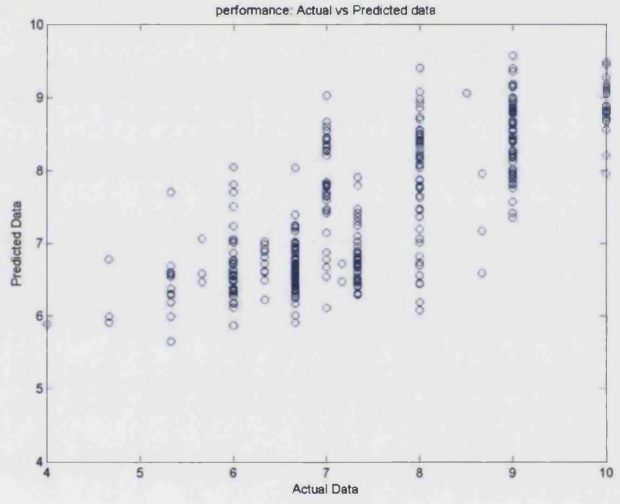

Figure A12-14 – Plot of predicted and recorded *performance* ratings

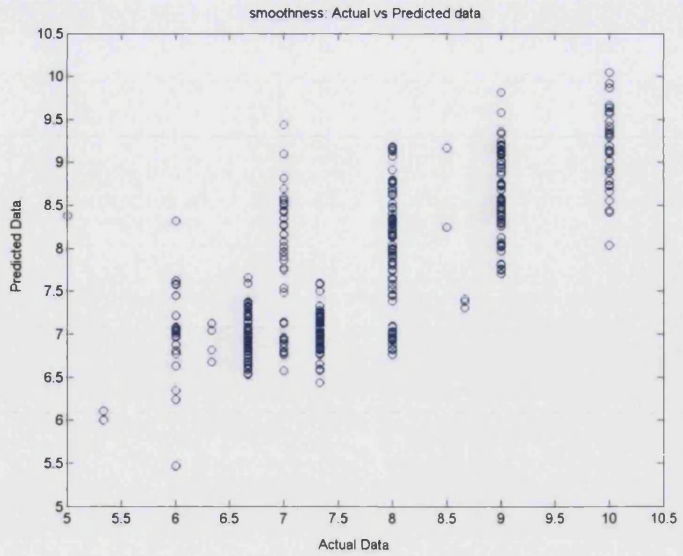

Figure A12-15 - Plot of predicted and recorded *smoothness* ratings

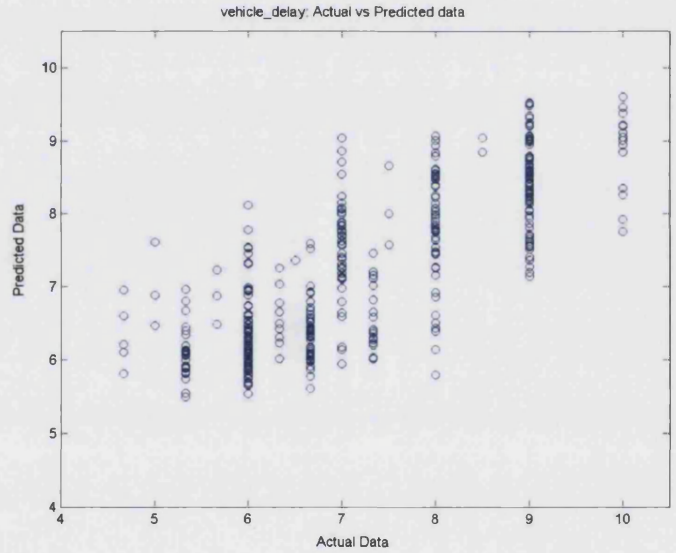

Figure A12-16 - Plot of predicted and recorded *vehicle_delay* ratings

Appendix XIII – AT vehicle correlations – acceleration and jerk metrics

It can be seen from the results presented so far in this Section that the correlation equations contain a mixture of acceleration and jerk terms as well as a variety of engine speed, pedal position and vehicle speed metrics.

It was therefore decided to analyse the results of the best acceleration and jerk subset equation to determine how much of the correlation these metrics were able to explain.

The correlations predicted by the acceleration and jerk LWS equation fitted against various data subsets are shown below in Table A13-58.

Table A13-58 – Acceleration and jerk metric subset, LWS fit

Subset	accel_prog	eng_delay	init_accel	performance	smoothness	vehicle_delay
All data	0.434	0.394	0.471	0.514	0.450	0.539
25%	0.242	0.287	0.310	0.397	0.392	0.387
50%	0.300	0.271	0.331	0.425	0.317	0.372
75%	0.503	0.430	0.507	0.458	0.367	0.537
100%	0.371	0.329	0.413	0.450	0.295	0.448
0	0.320	0.255	0.349	0.388	0.279	0.437
2	0.100	0.003	0.188	0.090	0.429	0.251
12	0.496	0.432	0.479	0.520	0.425	0.524
40	0.399	0.432	0.446	0.494	0.542	0.533
60	0.462	0.397	0.328	0.466	0.500	0.493
Launch feel	0.317	0.247	0.333	0.360	0.248	0.424
Performance feel	0.453	0.391	0.364	0.386	0.319	0.454
Traffic crawl	0.317	0.347	0.371	0.460	0.402	0.440
BMW	0.036	0.108	0.059	0.071	0.122	0.147
AT Mondeo (economy mode)	0.122	0.087	0.114	0.143	0.029	0.061
AT Mondeo (sports mode)	0.244	0.262	0.272	0.274	0.127	0.315
Omega	0.135	0.125	0.208	0.277	0.194	0.130

For these correlation equations, produced using all of the AT vehicles' data, none of the fits was above average for the vehicle subsets. As the differences are not very large, and the correlations are not very high, this may be due to scatter in the data combined with the relatively small amount of data for each vehicle causing the poor correlations. The AT Mondeo (sports mode) and Omega vehicle subsets generally produced better fits than the other vehicles, with the AT Mondeo sports mode set being the best of the two, however considering the relatively low correlations this may simply be a random occurrence related to

the location of the scattered data points rather than a real difference between the behaviours of the vehicles.

The above theory assumes that the vehicles' data do follow the same trend as the correlation equation predicts, albeit with a large amount of scatter. The other possibility, which may be more likely considering the noticeably better correlations found for the pedal and speed subsets, is that the vehicles are actually different from one another and therefore the overall fit equation is fitting to an amalgam of the vehicles whose effective behaviours do not represent any single vehicle. To test whether this is the case, correlations were produced from single vehicle data and the results of this analysis are shown in Section 9.2.

Analysis of correlation equation terms and metrics

Table A13-59 shows the acceleration and jerk subset LWS correlation equations for each subjective metric.

Table A13-59 - Correlation equations for acceleration and jerk subset LWS fit

Metric	Correlation equation
smoothness	1574761.207137 +12751.535817* aMaximumJerk^(1/-2) -19033.036224* aMaximumJerk^(1/-3) -6282.182285* LN(aMaximumJerk) -0.090406* AccelDelayTime^-3
eng_delay	29051.928410 +557.903536* aMaximumJerk^(1/-2) -558.693056* aMaximumJerk^(1/-3) -0.487039* aMaxAccel^-1 -1.710024* aMaximumJerk^3 +0.179795* aAverageAccelToMaxSpeed^-2
vehicle_delay	-3298.411107 +436.402789* aMaximumJerk^(1/-2) -436.837309* aMaximumJerk^(1/-3) -0.357524* aMaxAccel^-1 -1.302969* aMaximumJerk^3 +0.123737* aAverageAccelToMaxSpeed^-3 -0.289839* aAverageAccelToMaxSpeed^3 +0.155508* aInitialJerk^2
init_accel	-527.204817 +40.615953* aMaximumJerk^(1/-2) +40.739600* aMaximumJerk -0.698453* aMaxAccel^-1 +0.399683* aMaxAccel^-3 -0.152239* AccelDelayTime^-2 -1.002189* aMaximumJerk^3 -0.160194* aAverageAccelToMaxSpeed^3
accel_prog	4947.686925 +2.926697* aMaximumJerk^(1/-2) +3.622388* aMaximumJerk^2 -0.872512* aMaxAccel^-1 +0.543683* aMaxAccel^-2

	+0.107270* AccelDelayTime^2 -1.475395* aMaximumJerk^3
performance	27954.567910 +529.835585* aMaximumJerk^(1/-2) -530.227751* aMaximumJerk^(1/-3) -0.608626* aMaxAccel^-1 +0.306539* aMaxAccel^-3 -1.397983* aMaximumJerk^3 -0.155474* AccelDelayTime^-3

It can be seen from the correlation equations that each correlation equation contains similar terms. This may be expected as there are high correlations between the different subjective terms as were seen in Section 7.3, however the strengths of the partial correlation coefficients and the strength of the effect of each term due to that term's coefficient differs between the equations indicating which variables have the most effect on a given subjective metric. The subjective rating equations are analysed in the following sections:

The acceleration progression correlation equation

This section analyses the *acceleration progression* (metric name: *accel_prog*) correlation equation. Figure A13-17 below shows predicted vs. actual ratings for the *accel_prog* rating. A perfect fit would show all of the data points lying on a line stretching diagonally across the graph from the lower left-hand corner to the upper right-hand corner. The coefficient of determination for this dataset is R^2=0.434.

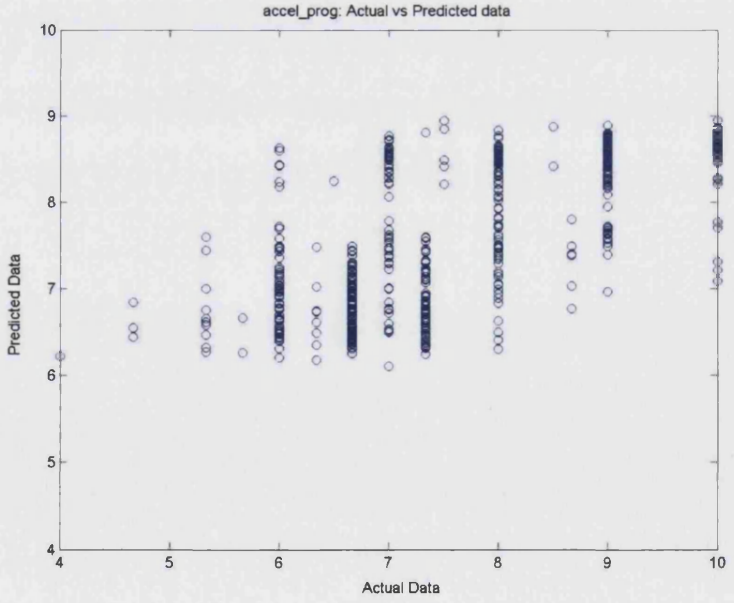

Figure A13-17 - Plot of predicted and recorded *accel_prog* ratings

Figure A13-18, below, shows the behaviour of the individual metrics in this correlation equation.

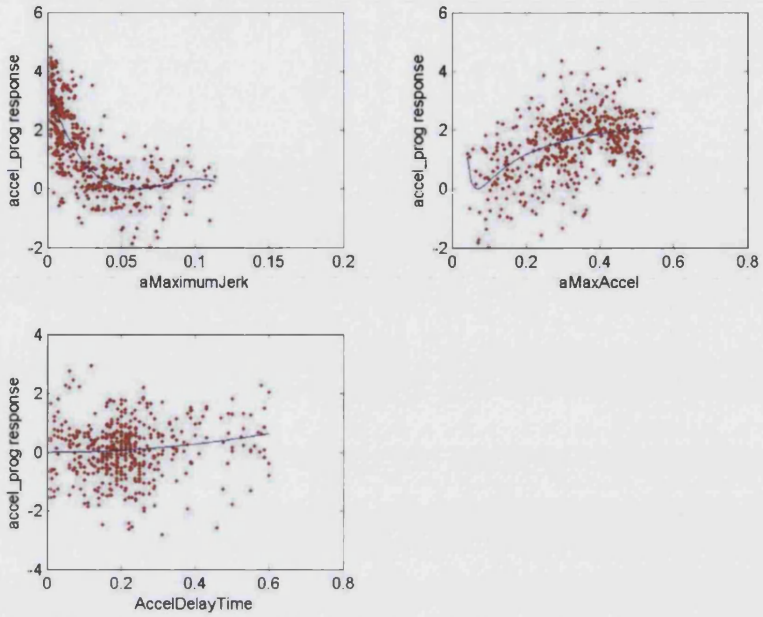

Figure A13-18 - Response for each metric in *accel_prog* prediction equation

It can be seen that an increase in *aMaximumJerk* shows a general downward trend for the *accel_prog* response with a plateau and slight increase as the level reaches a threshold value of 0.05 g/s. This may be an actual trend – whereby the acceleration later in the test is worse for those tests with higher initial jerk – or it may be caused by a high initial jerk overshadowing the later acceleration performance and causing the drivers to rate it poorly. These possibilities are detailed in Section 9.1.2.8.2.

The *aMaxAccel* metric shows a clear positive correlation with *accel_prog* with the exception of an initial downward trend. This initial downward movement is very short and appears to be an artefact of the particular curve fitted to these data and can therefore be safely ignored. Surprisingly, the AccelDelayTime metric shows almost no correlation; the slight upward trend that is present (and is the opposite of what would be expected – a short delay time resulting in a higher rating) appears to the result of the few data points which occur beyond a delay time of about 0.4s.

It should be noted that the partial correlation coefficient for *aMaximumJerk* is greater than for *aMaxAccel* as shown in Figure A13-19 below. This means that the *aMaximumJerk* term(s) of the correlation equation fit the data better than the *aMaxAccel* term(s) and the response of

the *aMaximumJerk* metric also shown a greater range indicating that it will have more effect on the overall prediction of the correlation equation.

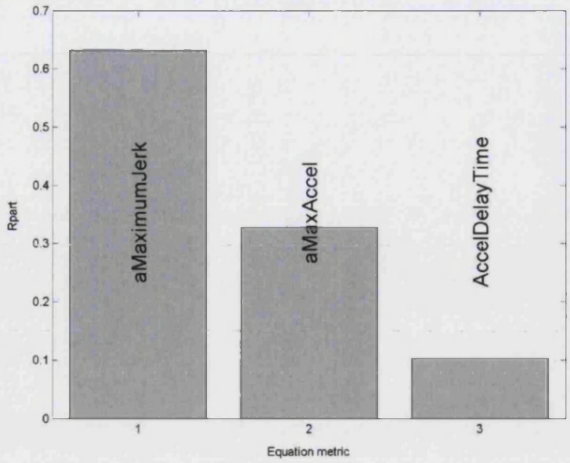

Figure A13-19 - Partial correlations for each metric in *accel_prog* prediction equation

The engine delay correlation equation

This section analyses the *engine delay* correlation equation. Figure A13-20 below shows predicted vs. actual ratings for the *engine_delay* rating. The coefficient of determination for this dataset is R^2= 0.394

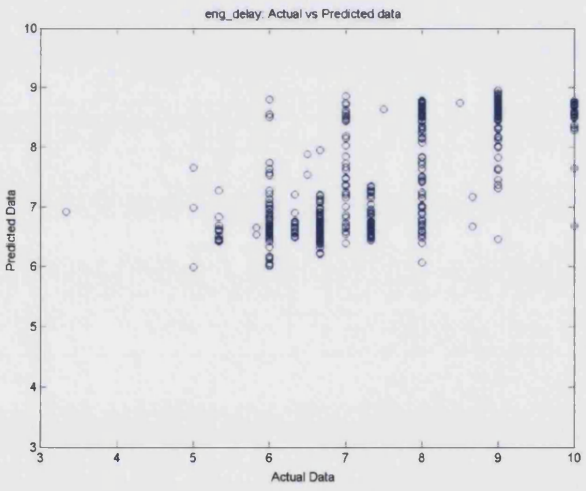

Figure A13-20 - Plot of predicted and recorded *eng_delay* ratings

Figure A13-21, below, shows the behaviour of the individual metrics in this correlation equation.

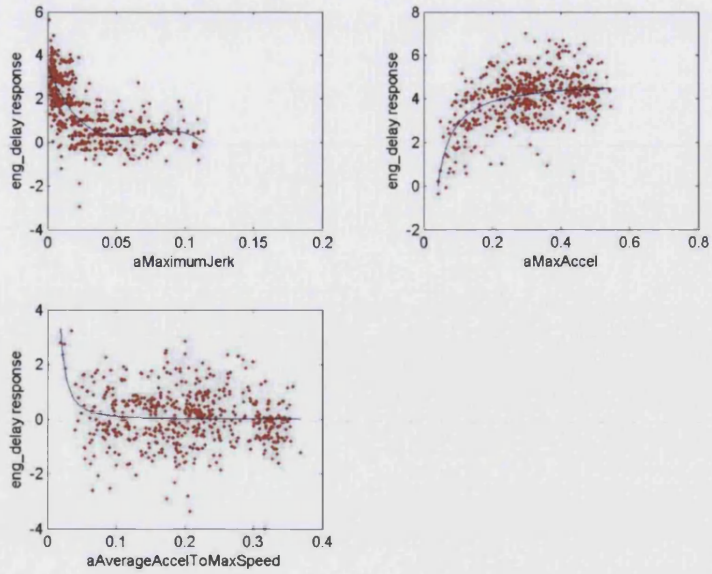

Figure A13-21 - Response for each metric in *eng_delay* prediction equation

The *aAverageJerk* and *aMaxAccel* combination of metrics appears to follow a similar trend to that seen for the *accel_prog* equation. These trends are detailed in Section 9.1.2.8.2. The *aAverageAccelToMaxSpeed* metric is different; however it displays only a very small negative correlation. The initial downward trend at low values of *aAverageAccelToMaxSpeed* appears to be caused by skew from the 5 data points in that location and has little effect on the results of this metric other than to allow it to be included (if the line were almost horizontal its coefficient of determination would be almost zero). It can be seen from Figure A13-22 below, that the partial correlation is quite weak for this metric as can be seen from the scatter in Figure A13-21.

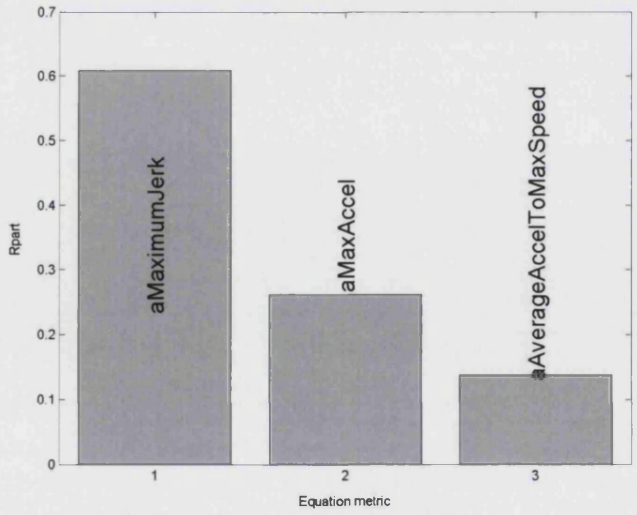

Figure A13-22 - Partial correlations for each metric in *eng_delay* prediction equation

The initial jerk correlation equation

This section analyses the *initial jerk* correlation equation. Figure A13-23 below shows predicted vs. actual ratings for the *init_accel* rating. The coefficient of determination for this dataset is R^2= 0.471

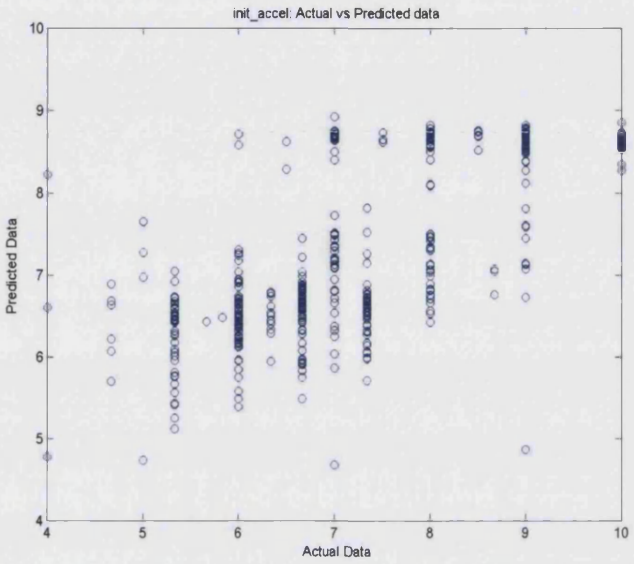

Figure A13-23 – Plot of predicted and recorded *init_accel* ratings

Figure A13-24, below, shows the behaviour of the individual metrics in this correlation equation.

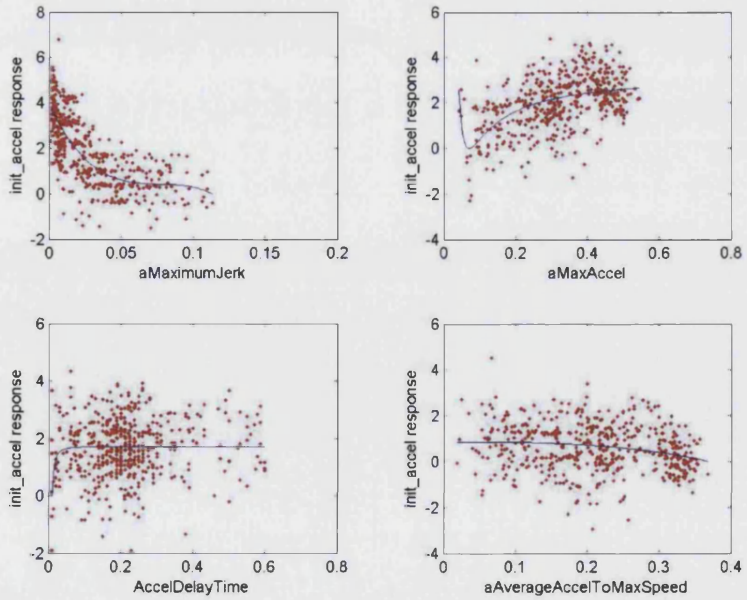

Figure A13-24 - Response for each metric in *init_accel* prediction equation

The *aAverageJerk* and *aMaxAccel* combination of metrics again follows a similar trend to that seen for the *accel_prog* equation. These trends are detailed in Section 9.1.2.8.2. The *AccelDelayTime* metric shows no apparent effect on the *init_accel* rating which is somewhat surprising, as this had been expected to be an important variable. It should be noted that the same effect was also seen in the *accel_prog* equation.

The *aAverageAccelToMaxAccel* metric shows a slight negative correlation, increasing as the average acceleration increases. The effect of this metric is rather small when compared with the amount of scatter in the data points; therefore it may or may not be showing an actual trend. If this were a real trend, it would indicate that the init_accel rating is negatively influenced by high average accelerations. This would make sense as the higher acceleration may overshadow the initial jerk in the drivers' memories.

The overall driveability correlation equation

This section analyses the *overall driveability* correlation equation. Figure A13-25 below shows predicted vs. actual ratings for the *performance* rating. The coefficient of determination for this dataset is R^2= 0.514

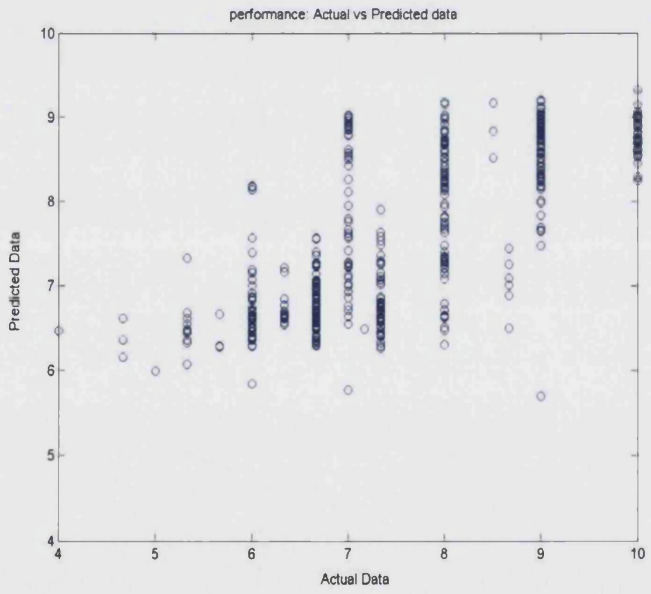

Figure A13-25 – Plot of predicted and recorded *performance* ratings

Figure A13-26, below, shows the behaviour of the individual metrics in this correlation equation.

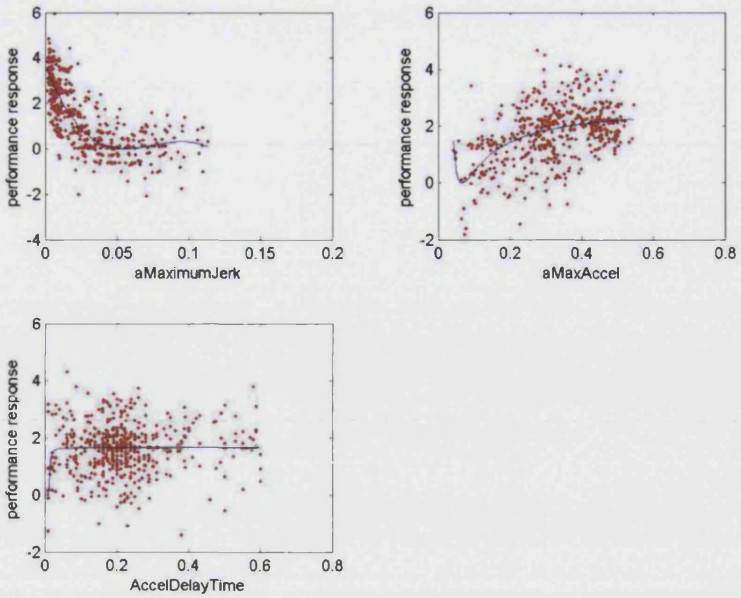

Figure A13-26 - Response for each metric in *performance* prediction equation

The *aAverageJerk* and *aMaxAccel* combination of metrics again follows a similar trend to that seen for the *accel_prog* equation. These trends are detailed in Section 9.1.2.8.2. In this case with the same initial negative correlation for the *aMaxAccel* metric. This is again an artefact caused by the particular curve used to fit the data. In fact, *performance* appears to be very closely related to *accel_prog* as it also contains the *AccelDelayTime* metric, which again does not produce any real contribution to the equation.

The smoothness correlation equation

This section analyses the *smoothness* correlation equation. Figure A13-27 below shows predicted vs. actual ratings for the *smoothness* rating. The coefficient of determination for this dataset is R^2= 0.450

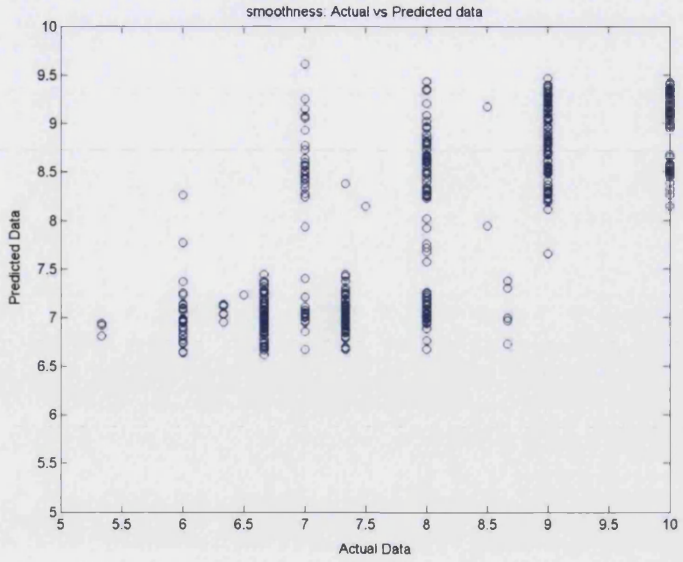

Figure A13-27 - Plot of predicted and recorded *smoothness* ratings

Figure A13-28, below, shows the behaviour of the individual metrics in this correlation equation.

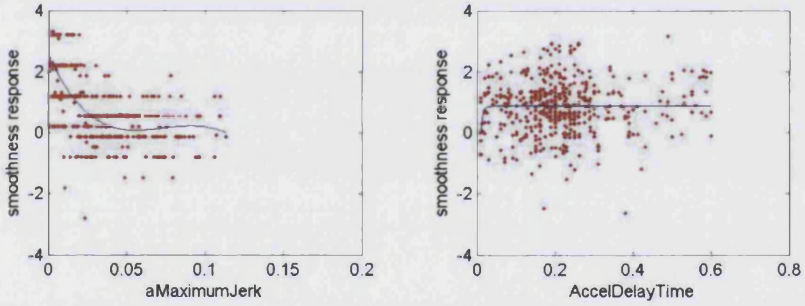

Figure A13-28 - Response for each metric in *smoothness* prediction equation

The *aMaximumJerk* metric shows a clear initial negative correlation which levels off in similar fashion to the other subjective rating equations. The *AccelDelayTime* metric also shows a similar trend to that seen in the other metrics, which is for it to produce almost no effect.

It is curious that the *smoothness* rating shows almost the same response as all of the other rating equations in terms of the *aMaximumJerk* metric. This indicates that the drivers rated *smoothness* poorly for vehicles with high *aMaximumJerk*. However the similarity in behaviour of this term to those in the other subjective rating correlation equations is of some

concern. It may be that the other subjective ratings also partly consider the *smoothness*, or it may simply be that the shapes are coincidentally similar.

The vehicle delay correlation equation

This section analyses the *vehicle delay* correlation equation. Figure A13-29 below shows predicted vs. actual ratings for the *vehicle_delay* rating. The coefficient of determination for this dataset is R^2= 0.539

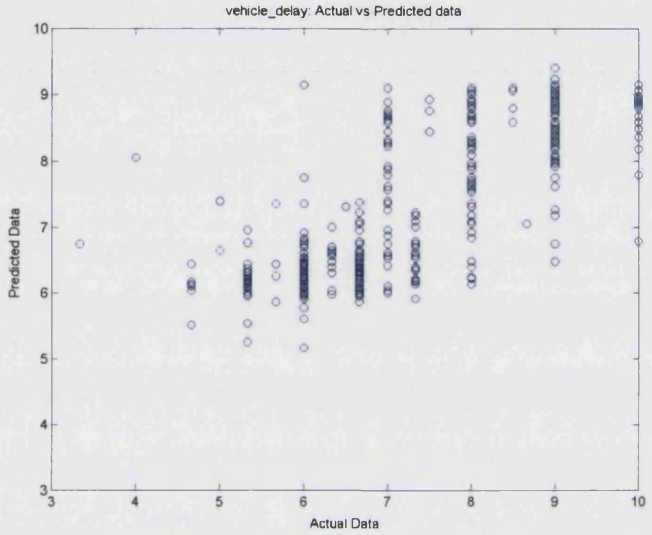

Figure A13-29 - Plot of predicted and recorded *vehicle_delay* ratings

Figure A13-30, below, shows the behaviour of the individual metrics in this correlation equation.

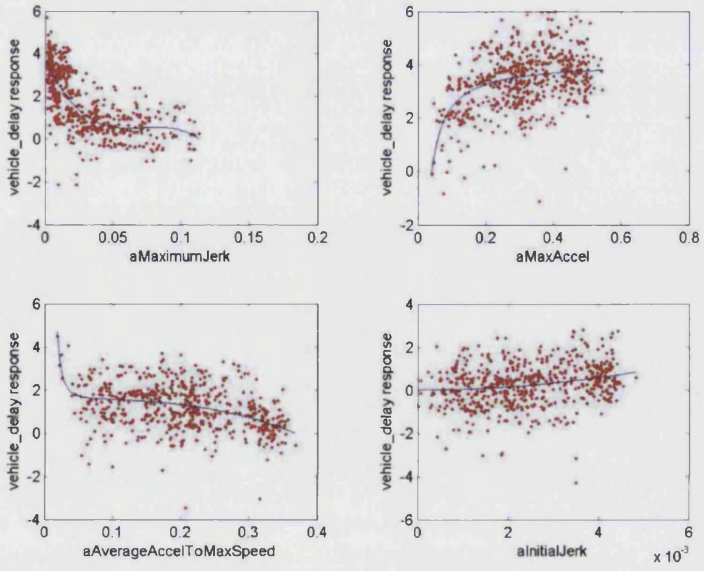

Figure A13-30 - Response for each metric in *vehicle_delay* prediction equation

The *vehicle_delay* response shows a similar response to the other ratings with the *aMaximumJerk* and *aMaxAccel* metrics. These trends are detailed in Section 9.1.2.8.2. In this case, however, the other metrics that are included in the equation appear to produce an effect (they are not simply horizontal or near horizontal for the majority of their range). The *aAverageAccelToMaxSpeed* metric shows an initial high-gradient downward slope, which appears to be a fitting artefact as there is so little data in this region, followed by a lower gradient downward trend. This trend indicates that as average acceleration over the period from the start of the acceleration to the end of the acceleration (maximum vehicle speed) increase, so the *vehicle_delay* rating is reduced.

The physical reason for this trend could be related to two effects – firstly the higher maximum acceleration may highlight any initial delays which occur as the vehicle changes gear or simply starts to accelerate; this would mean that for tests with identical delays, the one with higher average acceleration would appear to have more delay to the driver as the later acceleration highlights the difference. The second possibility is that any initial delays may in fact be greater – the fact that a higher acceleration is experienced indicates that the driver input a larger pedal demand. Although there is a large overlap in the data, this trend can be seen in Figure A13-31 below.

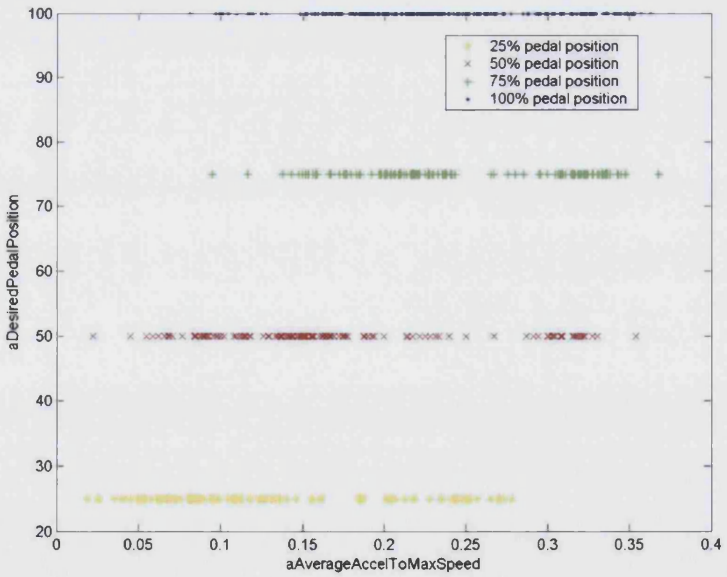

Figure A13-31 – *aDesiredPedalPosition* plotted against *aAverageAccelToMaxSpeed* metric for each pedal position

It was initially thought that this higher pedal demand would alter the gear-shift strategy and may result in a number of downshifts in quick succession which would produce a longer

initial delay though this would probably not be detected by the *AccelDelayTime* metric as this looks for the start of vehicle acceleration and the vehicle would be expected to start accelerating slightly before the first gear shift is performed.

However further investigation produced an interesting picture of the test types which produce the highest average acceleration. It can be seen from Figure A13-32, below, that it is in fact the lower speed tests which produce the highest average acceleration (and which therefore have poor *vehicle_delay* ratings) for all pedal positions.

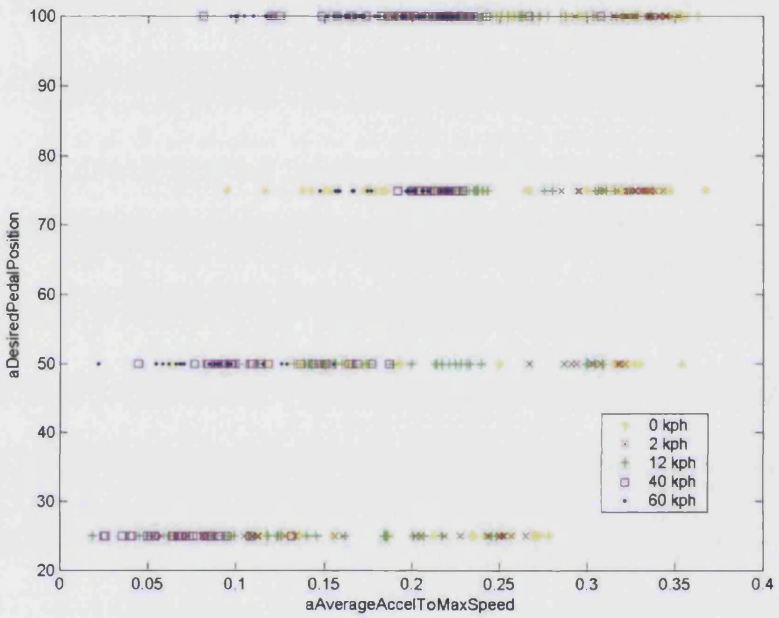

Figure A13-32 - *aDesiredPedalPosition* plotted against *aAverageAccelToMaxSpeed* metric for each initial vehicle speed

This trend is understandable – at lower speeds, the torque converter will not be locked and will produce more torque multiplication due to the large speed difference. This will result in higher accelerations. The question is whether it is the torque converter itself which is causing some physical delay (wind-up for example) which the drivers are rating with the *vehicle_delay* rating, or whether it is simply the fact that the higher acceleration makes any delays more noticeable and therefore the drivers rate them poorly.

The aInitialJerk metric has a slight positive correlation meaning that as the initial jerk (the average jerk over the first second after acceleration is detected) increases so does the *vehicle_delay* rating. This is an expected and understandable result.

Strength of *aMaximumJerk* and *aMaxAccel* responses

Although the shape of the response produced by *aMaximumJerk* remains similar for all of the ratings, the shape of the *aMaxAccel* response has two forms. One is shared by the eng_delay and vehicle_delay equation, and the other by the remaining ratings' equations. These are shown in Figure A13-33 below:

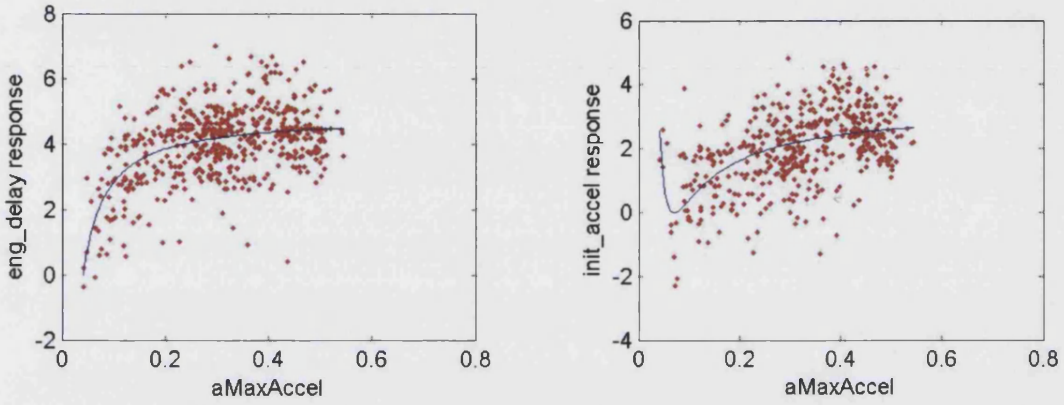

Figure A13-33 – aMaxAccel metric response comparison

Although the actual differences in the predictions are not marked (though there is a slight difference in the shapes of the curves, there is so much scatter that it is difficult to draw any conclusions about this), the initial downward gradient which is an artefact of the fitting curve, indicates that the equations do have a definite significant difference. This difference between the delay ratings and the other ratings confirms the link that was seen in Section 7.3.

There is one other difference between the responses of the *aMaximumJerk* and *aMaxAccel* metrics; despite their similarities in shape, the ranges over which they stretch are all different. These ranges are shown in Table A13-60 and Table A13-61 below:

Table A13-60 - aMaximumJerk metric ranges

Subjective Rating	Minimum (start of approx. zero gradient region)	Maximum	Range
accel_prog	0	3.5	3.5
eng_delay	0.5	4	3.5
init_accel	0.5	4	3.5
performance	0	4	4
smoothness	0	2.5	2.5
vehicle_delay	0.5	4	3.5

Table A13-61 - aMaxAccel metric ranges

Subjective Rating	Minimum (start of approx. zero gradient region)	Maximum	Range
accel_prog	0	2	2
eng_delay	0	4.5	4.5
init_accel	0	2.75	2.75
performance	0	2.5	2.5
smoothness	-	-	-
vehicle_delay	0	3.5	3.5

Therefore, it can be seen that although the equations contain identical metrics with very similar behaviour, the effect of each of the metrics is slightly different for each subjective rating.

The *accel_prog* rating shows that the negative jerk trend is more important that the maximum acceleration – this may indicate the original idea that a large initial jerk colours the drivers' judgement of the later acceleration when rating this aspect. Surprisingly, *init_accel* shows a similar trend, although in this case the *aMaxAccel* metric is even more important. This may indicate that the drivers are not actually rating the jerk here but rather the acceleration, perhaps because they do not know how the differences in jerk will feel. The performance rating shows a split in the importance of the metrics, which is in between those of the *init_accel* and *accel_prog* ratings. As this rating is defined as a combination of the others this is not surprising. Of the vehicle and engine delay metrics, *aMaxAccel* is slightly more important for the engine delay metric. This may be because the *vehicle_delay* metric also includes some other metrics that produce appreciable effects.